



TECHNISCHE UNIVERSITÄT MÜNCHEN

Wissenschaftszentrum Weihenstephan für Ernährung, Landnutzung und Umwelt

Forschungszentrum Weihenstephan für Brau- und Lebensmittelqualität

**Chemical analysis and *in vitro* cytotoxicity studies of limonene and selected ozonolysis products: 4-oxopentanal (4-OPA), 4-acetyl-1-methylcyclohexene (4-AMCH) and 3-isopropenyl-6-oxoheptanal (IPOH) in human lung cells**

Dorelia Simona Lipsa

Vollständiger Abdruck der von der Fakultät Wissenschaftszentrum Weihenstephan für Ernährung, Landnutzung und Umwelt der Technischen Universität München zur Erlangung des akademischen Grades eines

Doktors der Naturwissenschaften

genehmigten Dissertation.

Vorsitzender: Prof. Dr. Michael Rychlik

Prüfer der Dissertation: 1. apl. Prof. Dr. Mehmet Coelhan

2. Prof. Dr. Jörg E. Drewes

Die Dissertation wurde am 28.12.2015 bei der Technischen Universität München eingereicht und durch die Fakultät Wissenschaftszentrum Weihenstephan für Ernährung, Landnutzung und Umwelt am 10.04.2017 angenommen.



**Chemical analysis and *in vitro* cytotoxicity studies of limonene and selected ozonolysis products: 4-oxopentanal (4-OPA), 4-acetyl-1-methylcyclohexene (4-AMCH) and 3-isopropenyl-6-oxoheptanal (IPOH) in human lung cells**

von

Dorelia Simona Lipsa

## Table of contents

---

<b>Chapter Title</b>		
	Acknowledgements	i
	Abbreviations and Symbols	ii
	List of tables and figures	iii
	<b>Summary / Zusammenfassung</b>	<b>iv</b>
<b>1.</b>	<b>INTRODUCTION</b>	<b>1</b>
1.1	<b>Indoor air quality</b>	<b>1</b>
1.1.1	Terpenes	3
1.1.2	Terpenes in consumer products	3
1.2	<b>Limonene</b>	<b>4</b>
1.2.1	Physicochemical properties	4
1.2.2	Production, use, human exposure and regulations	6
1.3	<b>d-Limonene ozonolysis products</b>	<b>7</b>
1.3.1	Selected d-limonene ozonolysis products: 4-oxopentanal (4-OPA), 4-acetyl-1-methylcyclohexene (4-AMCH) and 3-isopropenyl-6-oxoheptanal (IPOH)	12
1.4	<b>Pulmonary toxicity</b>	<b>14</b>
1.4.1	Lung as the target organ - description	15
1.4.2	Defence mechanisms of the lung	17
1.4.3	Respiratory health effects	19
1.4.3.1	<i>In vivo</i> studies	19
1.4.3.2	<i>In vitro</i> studies	26
1.5	<b>Aim of the work</b>	<b>32</b>
<b>2.</b>	<b>MATERIALS and METHODS</b>	<b>33</b>
2.1	<b>Experimental design: Overview</b>	<b>33</b>
2.2	<b>Materials</b>	<b>35</b>
2.2.1	Chemicals and equipment	35

## Table of contents

---

2.2.2	Environmental chambers	38
2.2.3	Human cell lines. <i>In vitro</i> exposure systems	38
2.3	<b>Methods and procedures</b>	39
2.3.1	<b>Generation of controlled d-limonene-ozone gas atmospheres in environmental chambers</b>	39
2.3.1.1	Procedure for the preparation of the environmental chambers before injection of d-limonene and ozone	39
2.3.1.2	Procedure for d-limonene, ozone injection	40
2.3.2	<b>Generation of controlled gas mixture atmospheres with 4-OPA, IPOH, 4-AMCH (in absence or presence of ozone) in Tedlar bags (TBs)</b>	42
2.3.2.1	Clean-up procedure of TBs	42
2.3.2.2	Generation of the gas atmosphere mixture of 4-OPA + IPOH + 4-AMCH in absence of ozone	42
2.3.2.3	Generation of the gas atmosphere mixture of 4-OPA + IPOH + 4-AMCH in presence of ozone	43
2.3.3	<b>Chemical analysis of d-limonene and ozonolysis reaction products: 4-OPA, 4-AMCH, IPOH</b>	44
2.3.3.1	Sampling procedure for d-limonene and d-limonene ozonolysis reaction products: 4-OPA, IPOH, 4-AMCH	44
2.3.3.2	Breakthrough phenomena investigation	44
2.3.3.3	Analytical method (TD-GC-MS) for the quantification of d-limonene and its ozonolysis reaction products: 4-OPA, 4-AMCH, IPOH	45
2.3.3.4	Stability tests of 4-OPA, 4-AMCH, IPOH in the culture medium by GC-FID	47
2.3.3.5	Intracellular glutathione species (GSH, GSSG, GSNO) determination by in house HPLC-UV method	47
2.3.3.6	Metabolomics screening analysis using LC-MS Orbitrap in ad hoc experiment	49
2.3.4	<b>Biological measurements carried out in human cells and blood</b>	50
2.3.4.1	Human alveolar epithelial cell line (A549) description	50
2.3.4.2	Human leukemia cell line (THP-1) description	50
2.3.4.3	Human bronchial epithelial cell line (16HBE14o-) description	51
2.3.4.4	Cryopreserved Human Whole Blood description	52
2.3.4.5	Cell culture maintenance, sub-culturing and counting protocols	54
2.3.4.6	<i>In vitro</i> exposure method: Liquid-Liquid interface (LLI) and its protocols	56
2.3.4.7	<i>In vitro</i> exposure method: Air-Liquid interface (ALI) and its protocols	63
2.3.4.8	<i>In vitro</i> protocols: Cell viability by Neutral Red Uptake assay	73

## Table of contents

---

2.3.4.9	<i>In vitro</i> protocols: Cell viability by Presto blue assay	74
2.3.4.10	<i>In vitro</i> protocols: Cell viability by Lactate dehydrogenase assay	75
2.3.4.11	<i>In vitro</i> protocols: Inflammation by Cytokine/Chemokines assays	75
2.3.4.12	<i>In vitro</i> protocols: Oxidative stress by reactive oxygen species assay	76
2.3.4.13	<i>In vitro</i> protocols: Oxidative stress by glutathione species assay	77
2.4	<b>Data processing and statistical analyses</b>	77
3.	<b>RESULTS AND DISCUSSION</b>	81
3.1	<b>Development/optimisation of chemical and biological methods</b>	81
3.1.1	Determination of secondary reaction products 4-OPA, 4-AMCH, IPOH in cell culture medium (GC-FID) and gas atmospheres (GC-MS)	82
3.1.1.1	Determination of stability of secondary reaction products 4-OPA, 4-AMCH, IPOH solubilized into the culture medium (GC-FID)	82
3.1.1.2	Determination of 4-OPA, 4-AMCH, IPOH in gas atmospheres prepared as a mixture in Tedlar bags	84
3.1.1.3	Results obtained after clean-up procedure of TBs	85
3.1.1.4	Results on the performance of the analytical method for the determination of 4-OPA, 4-AMCH, IPOH in gas atmospheres	87
3.1.1.5	Results regarding the target concentration of the chemical mixture and ozone prepared in Tedlar bags	88
3.1.2	Development and optimisation of the HPLC-UV method for the detection and quantification of intracellular glutathione species	89
3.1.3	Optimisation of extraction procedure of intracellular glutathione species from human cell lines	97
3.1.4	Optimisation of cellular density on different seeding surfaces (24, 96-well plates and transwell porous membranes)	98
3.1.4.1	Optimisation of the <i>in vitro</i> cell cultures seeded on 24-, 96-well plates	98
3.1.4.2	Optimisation of the <i>in vitro</i> cell cultures seeded on transwell porous membrane inserts	99
3.1.5	Evaluation of the performance of an automated cell counting pipette versus traditional cell counting (Trypan blue)	100
3.1.6	Optimisation of the Air-Liquid interface exposure conditions	104
3.2	<b><i>In vitro</i> studies with human lung cells and blood exposed to d-limonene and ozonolysis products 4-OPA, 4-AMCH, IPOH via liquid/liquid interface</b>	107

## Table of contents

---

3.2.1	Evaluation of the cytotoxic effects of d-limonene, 4-OPA, 4-AMCH, IPOH and the binary/ternary mixtures of 4-OPA, 4-AMCH, IPOH via liquid/liquid interface	107
3.2.1.1	Concentration-response relationship for alveolar (A549) and bronchial (16HBE14o-) cells determined by Neutral Red Uptake assay	107
3.2.1.2	Oxidative stress in alveolar (A549) and bronchial (16HBE14o-) epithelial cells measured by reactive oxygen species (ROS) assay	115
3.2.1.3	Oxidative stress in alveolar (A549) and bronchial (16HBE14o-) epithelial cells measured by glutathione content assay	121
3.2.1.4	Inflammatory response in alveolar (A549) and bronchial (16HBE14o-) cells measured by cytokines/chemokines assay	123
3.2.1.5	Assessment of the metabolic profile of A549 cells exposed to the mixture of 4-OPA+IPOH+4-AMCH	131
3.2.2	Potential inflammatory capacity of d-limonene and 4-OPA, 4-AMCH, IPOH in human blood evaluated by <i>In vitro</i> Pyrogen test (IPT)	148
3.3	<b><i>In vitro</i> studies with human lung cells exposed to d-limonene and the mixture of 4-OPA, IPOH, 4-AMCH in presence/absence of ozone via Air-Liquid interface (CULTEX system)</b>	151
3.3.1	Assessment of the cytotoxic effects induced by d-limonene, ozone and d-limonene-ozone gas mixtures on human lung cells	151
3.3.1.1	CULTEX exposure to d-limonene and ozone as individual compounds using A549 and THP-1 cells	151
3.3.1.2	CULTEX exposure to d-limonene-ozone mixture using A549 and THP-1 cells	155
3.3.1.3	Chemical characterisation of generated atmosphere of d-limonene-ozone mixture and verification of target concentration of test compounds	156
3.3.2	Assessment of the cytotoxic effects of the mixture of 4-OPA+4-AMCH+IPOH in presence and absence of ozone on A549 and 16HBE14o-cells	158
4.	<b>CONCLUSION</b>	168
5.	<b>OUTLOOK</b>	172
6.	<b>BIBLIOGRAPHY</b>	173

### Acknowledgements

The work presented here was carried out during 2011-2014 at the former Chemical Assessment Testing unit (CAT unit), Institute for Health and Consumer Protection of the Joint Research Centre (JRC), Ispra, and it was funded by the European Union 7<sup>th</sup> Framework (Agreement 265267) under the Theme: ENV.2010.1.2.2-1.

I would like to express my gratefulness to Dr. Dimitris Kotzias (Head of Unit at the CAT unit until 2012), for giving me the possibility to conduct this interesting research project as a Ph.D. student and for his profound suggestions and encouragement throughout my study.

I am very thankful to Dr. Pilar Aguar (Head of Unit at the CAT unit since 2012), for her fundamental role in my doctoral work, for her encouragement and inspiration. Her share of abstract reasoning, experience and constructive criticism broadened the horizons of my scientific temperament and experience.

I also thank Dr. Josefa-Barrero Moreno (JRC supervisor) for her readiness to supervise my thesis and for assisting me whenever difficult scientific questions and situations arose.

I thank Prof. Dr. rer. nat. Mehmet Coelhan from Technical University of Munich who accepted me as being his Ph.D. student and who provided me with both scientific and administrative support.

Special thanks to Dr. Bo Larsen who shared important ideas and insightful comments during the writing stages of this work.

I am grateful to all my colleagues at CAT unit for their moral support and for providing a kind environment in the lab. In particular, I wish to express my thanks to Paolo Leva for his technical and logistical assistance as well as for his fruitful discussions. Special gratitude goes to Dr. Carmen Cacho for her introduction to the beauty of statistics. I am thankful to Otmar Geiss for sharing his analytical knowledge with me. I acknowledge Dr. Hubert Chassaing for his prompt and excellent assistance in conducting experiments in the metabolomic/proteomic topic. I thank Dr. Pilar Prieto for her time, interest and helpful comments on my manuscript. I would also like to mention Dr. David Asturiol for his help regarding the prediction of harmful effects of my compounds by using quantitative-structure-activity relationship (QSAR models).

Lastly, I wish to express my thankfulness to my parents (Constantin and Aurica) and my brother (Alexandru) who stayed in close contact with me and gave me moral support. A special thanks to my beloved husband (Jean-Michel) for encouraging me throughout this experience and sticking by my side, even when I was irritable.

### Abbreviations and Symbols

#### List of Abbreviations and Symbols:

<b>ALI</b>	Air-Liquid interface
<b>et al.</b>	et alii (and others)
<b>FU</b>	Fluorescence units
<b>GSH</b>	Reduced glutathione
<b>GSSG</b>	Disulfide (oxidized) glutathione
<b>GSNO</b>	Nitroso-glutathione
<b>HPLC</b>	High performance liquid chromatography
<b>IC<sub>50</sub></b>	The half maximal inhibitory concentration
<b>IPT</b>	<i>In vitro</i> Pyrogen Test
<b>LLI</b>	Liquid-liquid interface
<b>LOEC</b>	The lowest-observed-adverse-effect concentration
<b>mAU</b>	Milli absorbance units
<b>mbar</b>	Millibar
<b>MeOH</b>	Methanol
<b>MS</b>	Mass spectrometry
<b>m/z</b>	Mass-to-charge ratio
<b>n</b>	Sample size
<b>n/a</b>	Not applicable
<b>PBS</b>	Phosphate-buffered saline
<b>ppbv</b>	Part per billion by volume
<b>ppmv</b>	Part per million by volume
<b>ROS</b>	Reactive oxygen species
<b>rpm</b>	Revolutions per minute
<b>RPMI 1640</b>	Roswell Park Memorial Institute
<b>SOD</b>	Superoxyde dismutase
<b>SDS</b>	Sodium dodecyl sulphate
<b>T</b>	Temperature
<b>t</b>	Time
<b>TFA</b>	Trifluoroacetic
<b>UV</b>	Ultraviolet
<b>v/v [%]</b>	volume per volume
<b>w/w [%]</b>	weight per weight
<b>λ</b>	Wavelength

**List of tables and figures****List of tables:**

<b>Name</b>	<b>Title</b>	<b>Page</b>
<b>Table 1</b>	Key indoor pollutants and their potential toxic effects on human health	<b>2</b>
<b>Table 2</b>	Summary of the physical/chemical properties of limonene	<b>5</b>
<b>Table 3</b>	Identified d-limonene ozone reaction products	<b>9</b>
<b>Table 4</b>	Physico-chemical properties of selected d-limonene ozonolysis reaction products: 4-acetyl-1-methylcyclohexene, 3-isopropenyl-6-oxo-heptanal, 4-oxopentanal	<b>12</b>
<b>Table 5</b>	Cytokine levels at the lower respiratory tract of both mice and humans	<b>18</b>
<b>Table 6</b>	Data on human health effects of d-limonene-ozone reaction	<b>20</b>
<b>Table 7</b>	Summary of <i>in vivo</i> experiments carried out with animals regarding the health effect of d-limonene-ozone mixture	<b>22</b>
<b>Table 8</b>	<i>In vitro</i> cellular models available to study <i>in vitro</i> toxicity at the pulmonary level	<b>26</b>
<b>Table 9</b>	Determination of the limit of detection (LOD) and quantification (LOQ) of 4-OPA, IPOH, 4-AMCH	<b>88</b>
<b>Table 10</b>	Tested mobile phase composition consisting in water, acetonitrile, trifluoroacetic acid and sodium perchlorate	<b>89</b>
<b>Table 11</b>	Chemical characteristics of glutathione molecule	<b>92</b>
<b>Table 12</b>	Detection, quantification limits and sensitivity obtained for GSH, GSSG, GSNO within the proposed method	<b>96</b>
<b>Table 13</b>	The amount of GSH extracted from the alveolar and bronchial epithelial cells by using each of the above described procedures for the lysis of the cells	<b>98</b>
<b>Table 14</b>	Total cell counts obtained for A549 and 16HBE14o- by Trypan blue and Scepter measurement (n = 3)	<b>102</b>
<b>Table 15</b>	Evaluation of the coefficient variation of both selected methods for total cell counting 16HBE14o- (cells mL <sup>-1</sup> = NOperator*10 <sup>3</sup> , n = 12) executed by well-trained operators	<b>102</b>
<b>Table 16</b>	Comparison of the sensitivity of bronchial (16HBE14o-) and alveolar (A549) cell lines exposed to 4-OPA by one-way analysis of variance (ANOVA) with Tukey's multiple comparison test	<b>109</b>
<b>Table 17</b>	Calculated values of LOEC and IC <sub>50</sub> for both alveolar (A549) and bronchial (16HBE14o-) cell lines based on the concentration-response curves obtained for the individual chemicals	<b>110</b>
<b>Table 18</b>	Total concentration of the tested mixtures expressed as mM	<b>111</b>
<b>Table 19a</b>	Calculated values of LOEC and IC <sub>50</sub> for both alveolar (A549) and	<b>113</b>

	bronchial (16HBE14o-) cell lines based on the concentration-response curves obtained for the mixture of the tested compounds	
<b>Table 19b</b>	Interaction of toxicity response for the binary or ternary mixture's where the <i>Observed effect</i> represents the experimental number of viable cells obtained; the <i>Calculated effect</i> represents the number of viable cells that was calculated based on the Colby's formula	<b>114</b>
<b>Table 20</b>	Evaluation of the most representative fold change of pro-inflammatory cytokines and anti-inflammatory cytokines ratio for both alveolar (A549 cells) and bronchial (16HBE14o- cells) exposed to individual compounds at 50 µM for 24 hours	<b>129</b>
<b>Table 21</b>	Evaluation of the most representative fold change of pro-inflammatory cytokines and anti-inflammatory cytokines ratio for both alveolar (A549 cells) and bronchial (16HBE14o- cells) exposed to the binary/ternary mixture of the tested compounds at 50 µM for 24 hours.	<b>131</b>
<b>Table 22</b>	Quantification of 4-OPA, IPOH, 4-AMCH in the cell culture medium following cell exposure at two concentrations (high and low) over time (24 and 72 h)	<b>133</b>
<b>Table 23</b>	De-regulated metabolites present in the cellular medium and cellular extract [student t-test (p < 0.001) and annotation using the human metabolome database (HMDB)]	<b>147</b>
<b>Table 24</b>	Cellular location indicated in the human metabolome database (HMDB) of the most significant de-regulated metabolites which were found in the cellular medium and cellular extract	<b>148</b>
<b>Table 25</b>	Concentrations of d-limonene, ozone and NO <sub>2</sub> (positive control) used to expose A549 cells in CULTEX exposure module coupled to the environmental test chamber	<b>153</b>
<b>Table 26</b>	Concentrations of d-limonene and ozone used to expose A549 and THP-1 cells in CULTEX exposure module coupled to their mixture generated in the 0.45 m <sup>3</sup> environmental test chamber	<b>158</b>
<b>Table 27</b>	Total amount [µg] of target chemicals IPOH, 4-OPA and 4-AMCH in absence and presence of ozone which was delivered to both A549 and 16HBE14o- cells exposed within CULTEX for 1 and 2 hours (n = 3 ± SD)	<b>161</b>
<b>Table 28</b>	Recovery values obtained from Tenax tubes collected from the inlet line	<b>162</b>

**List of figures:**

<b>Name</b>	<b>Title</b>	<b>Page</b>
<b>Figure 1</b>	Molecular structure of limonene (stereoisomers)	<b>5</b>
<b>Figure 2</b>	Representation of the deposition patterns of the particles in the human respiratory system	<b>14</b>
<b>Figure 3</b>	A. General view of respiratory structures in the body, B. Detailed view of the airways, alveoli (air sacs), and capillaries (tiny blood vessels), C. Specific view of gas exchange (CO <sub>2</sub> and O <sub>2</sub> ) between the capillaries and alveoli	<b>15</b>
<b>Figure 4</b>	The main cell types at the bronchial-alveolar epithelium level	<b>17</b>
<b>Figure 5</b>	General overview of the experimental design	<b>33</b>
<b>Figure 6</b>	Generation of gas atmosphere containing d-limonene-ozone mixture in 1 m <sup>3</sup> environmental chamber	<b>41</b>
<b>Figure 7</b>	Injection of a mixture of water-target compounds 4-OPA, IPOH, 4-AMCH in TBs with the scope to generate gaseous atmosphere. On the left side: the heater and on the right side: the TBs protected from light with aluminium foil	<b>43</b>
<b>Figure 8</b>	Main steps involved in the generation of gas mixture atmospheres in TBs: 1. Ozone generator; 2. Sampling of ozone with the PP syringe; 3. Injection of ozone in the TBs already containing the mixture of 4-OPA+IPOH+4-AMCH	<b>44</b>
<b>Figure 9</b>	Breakthrough phenomena investigation	<b>45</b>
<b>Figure 10</b>	Observation of viable A549 cells done under Nikon optical microscope	<b>51</b>
<b>Figure 11</b>	Observation of viable differentiated THP-1 cells under Nikon optical microscope	<b>52</b>
<b>Figure 12</b>	Observation of viable 16HBE14o- cells under Nikon optical microscope	<b>53</b>
<b>Figure 13</b>	Observation of viable human cryopreserved blood under Nikon optical microscope	<b>54</b>
<b>Figure 14</b>	Schematic illustration of the experimental steps followed in the study where the human bronchial, alveolar cells and blood are exposed to the test chemicals solubilized into the culture media	<b>57</b>
<b>Figure 15</b>	Schematic representation of the biological experimental set-up to measure ROS, cytokines and LDH from the same pool of cells exposed to chemicals by LLI technique	<b>58</b>
<b>Figure 16</b>	Schematic representation of the biological experimental set-up to quantify intracellular glutathione species (GSH, GSSG,	<b>58</b>

	GSNO) from cells exposed to chemicals by LLI technique	
<b>Figure 17</b>	Schematic representation of the biological experimental set-up used for the metabolomics analysis. The negative control (cells untreated) were receiving medium alone, then the same approach was followed for the metabolomics analysis	<b>59</b>
<b>Figure 18</b>	Layout of 96-well plate used to generate concentration-response curves. BG refers to backgrounds (test chemical in the culture medium); NC refers to negative controls (cells grown in the culture medium); PC refers to positive control (cells with sodium dodecyl sulfate added into the culture medium); C1-C10 refers to a serial dilution of chemicals prepared in culture medium and added to cells (where C1 stands for the highest concentration used)	<b>60</b>
<b>Figure 19</b>	Schematic illustration of the experimental steps followed in the study where human bronchial and alveolar cells are directly exposed to the chemicals at the air/liquid interface	<b>63</b>
<b>Figure 20</b>	Schematic representation of the main steps needed for the exposure and endpoints when cells are exposed to chemicals at the air/liquid interface	<b>64</b>
<b>Figure 21</b>	Representation of the CULTEX exposure module (the picture was modified based on images collected from CULTEX website: <a href="http://www.cultex-laboratories.com/Catalog/Modules/cultex-cg-module-24mm.php?p=Images">http://www.cultex-laboratories.com/Catalog/Modules/cultex-cg-module-24mm.php?p=Images</a> )	<b>64</b>
<b>Figure 22 A</b>	Exposure of human lung cells to pollutants such as d-limonene and NO <sub>2</sub> in a gas cylinder using the CULTEX system: A. CULTEX basic scheme (including the exposure modules)	<b>66</b>
<b>Figure 22 B</b>	Exposure of human lung cells to pollutants such as limonene and NO <sub>2</sub> in a gas cylinder using the CULTEX system: B. Gas cylinder set-up scheme	<b>66</b>
<b>Figure 23</b>	Exposure of human lung cells to a generated atmosphere of d-limonene-ozone reaction in 0.45 m <sup>3</sup> environmental chamber connected to the CULTEX system. 1. Environmental chamber; 2. Manifold; 3. Cultex exposure chambers; 4. Mass flow controllers; 5. Vacuum pumps	<b>67</b>
<b>Figure 24</b>	Chamber set-up connected to the CULTEX basic scheme	<b>68</b>
<b>Figure 25</b>	Tedlar bag set-up connected to the CULTEX basic scheme	<b>71</b>
<b>Figure 26</b>	Exposure of human lung cells to gaseous phase of the mixture of 4-OPA, IPOH, 4-AMCH in presence or absence of ozone	<b>71</b>

	generated in TBs connected to the CULTEX system	
<b>Figure 27</b>	Sampling position of Tenax tube on the CULTEX system collected for the recovery test: 1. Tenax tubes added immediately before the gas atmosphere is distributed to the cells; 2. Tenax tubes added immediately after the CULTEX chambers (gas atmospheres already fumigated the cell culture)	<b>72</b>
<b>Figure 28</b>	Stability analysis of 4-OPA, 4-AMCH and IPOH solubilized in culture medium at various concentration of Fetal Bovine Serum (FBS) carried out by GC-FID over time (0, 1, 2, 3, 24 hours) (n=3 ± STD)	<b>83</b>
<b>Figure 29</b>	Chromatogram of a 5-cycles cleaned Tedlar bag still containing DMA (retention time=14) and phenol (retention time=16)	<b>86</b>
<b>Figure 30</b>	Chromatogram of a 10-cycles cleaned Tedlar bag	<b>86</b>
<b>Figure 31</b>	Chromatogram obtained within TD-GC-MSD method for the determination of 4-OPA, IPOH, 4-AMCH among other volatile organic compounds as follows: 1. Toluene (retention time = 13.29), 2. 4-OPA (retention time = 17.8), 3. 6-MHO (retention time = 23), 4. Limonene (retention time = 24.13), 5. Dimetiloctanolo (retention time = 24.97), 6. 4-AMCH (retention time = 26.15), 7. DHC (retention time = 27.14), 8. IPOH (retention time = 28.2)	<b>87</b>
<b>Figure 32</b>	Effect of the mobile phase composition on the chromatographic resolution of reduced, oxidised and nitroso- glutathione forms. Numbers indicated on the x axis correspond to the composition of eluent presented in the table 2 (n = 4)	<b>90</b>
<b>Figure 33</b>	Percentage degradation of GSSG calculated based on sodium perchlorate amount added to the mobile phase (n=3)	<b>91</b>
<b>Figure 34</b>	Separation of the three glutathione forms on the above mentioned columns using glutathione standards: 1. Reduced glutathione; 2. Oxidized glutathione; 3. S-nitroso-glutathione	<b>93</b>
<b>Figure 35</b>	Chromatograms (overlay) obtained under optimum conditions with the YMC ODS-A column representing a mixture of GSH, GSSG and GSNO standards and the intracellular glutathione species determined in A549 exposed to NO <sub>2</sub>	<b>93</b>
<b>Figure 36</b>	Comparison of reduced glutathione (GSH) at various concentrations determined in spiked biological samples and GSH standard solutions	<b>94</b>
<b>Figure 37</b>	Calibration curves of the three glutathione species (reduced –	<b>95</b>

	GSH, oxidised – GSSG, and nitroso – GSNO) where concentrations were plotted against the area units of the peaks within HPLC-UV chromatogram (n = 3 ± SD)	
<b>Figure 38</b>	Linearity range for A549 and 16HBE14o- cell numbers and the Neutral red uptake absorbance level obtained for 3 independent experiments with 3 replicates each (R <sup>2</sup> ≥ 0.978)	<b>99</b>
<b>Figure 39</b>	Linearity range for A549 and 16HBE14o- cell numbers and the Neutral red uptake absorbance level obtained for 3 independent experiments with 3 replicates each (R <sup>2</sup> ≥ 0.988)	<b>99</b>
<b>Figure 40</b>	Illustration of the different cell densities of plated A549 cells. <b>A.</b> Cell density 32 x 10 <sup>3</sup> cells cm <sup>-2</sup> <b>B.</b> Cell density 7.0 x 10 <sup>4</sup> cells cm <sup>-2</sup> <b>C.</b> Cell density 1.0 x 10 <sup>5</sup> cells cm <sup>-2</sup>	<b>100</b>
<b>Figure 41</b>	Viable cells counting of 16HBE14o- using Scepter 2.0 and both sensing tips of 40 and 60 µm	<b>101</b>
<b>Figure 42</b>	Comparison of total cell count obtained by Trypan blue and Scepter 2.0 for both cell lines (R <sup>2</sup> =0.99, n=3, horizontal standard bars stand for counts done by Scepter pipette, while the vertical standard bars for Trypan blue)	<b>103</b>
<b>Figure 43</b>	Evaluation of cellular viability by Scepter pipette of A549 cells exposed to Zero air within CULTEX system (n=25 ± STD) <b>A.</b> Results (% cellular viability) from cells kept in Incubator and cells exposed to Zero air in both CULTEX exposure modules <b>B.</b> Results (% cellular viability) from cells exposed to Zero air in the CULTEX 2 holding the three vessels (insert 4, insert 5, insert 6) <b>C.</b> Results (% cellular viability) from cells exposed to Zero air in the CULTEX 1 holding the three vessels (insert 1, insert 2, insert 3)	<b>105</b>
<b>Figure 44</b>	Comparison of cellular viability data from cells exposed to Zero air under two relative humidity (RH) conditions (50 and 80 %) (n = 3 ± STD)	<b>106</b>
<b>Figure 45</b>	Effects of time exposure on cellular viability of cells exposed to Zero air (n = 9 ± STD)	<b>107</b>
<b>Figure 46</b>	Concentration-response curves obtained from A549 and 16HBE 14o- cells exposed to <b>A.</b> 4-AMCH (0 to 5.8 mM), <b>B.</b> 4-OPA (0 to 115 mM), <b>C.</b> IPOH (0 to 17.5 mM), <b>D.</b> d-limonene (0 to 100 µM)	<b>108</b>
<b>Figure 47</b>	Concentration-response curves obtained from A549 (red line) and 16HBE14o- (purple line) cells exposed to <b>E.</b> binary mixture of IPOH + 4-AMCH, <b>F.</b> binary mixture of 4-OPA + 4-AMCH, <b>G.</b> ternary mixture of IPOH + 4-OPA + 4-AMCH , <b>H.</b> binary	<b>112</b>

	mixture of IPOH + 4-OPA	
<b>Figure 48 A-G</b>	ROS production measured in A549 cells at 60 minutes for all tested compounds. A. 4-OPA; B. 4-AMCH; C. IPOH; D. 4-OPA + 4-AMCH; E. IPOH + 4-AMCH; F. IPOH + 4-OPA; G. 4-OPA + IPOH + 4-AMCH	<b>115</b>
<b>Figure 49</b>	Intracellular ROS levels measured in A549 cells exposed to individual test compounds at 31.2; 125 and 500 $\mu$ M after a treatment of 60, 120, 210 and 1440 min	<b>117</b>
<b>Figure 50</b>	Kinetic measurements of intracellular ROS formation in A549 cells exposed to tested compounds individually and their binary/ternary mixture in the range of 0 to 500 $\mu$ M ( $n = 8 \pm$ SD)	<b>118</b>
<b>Figure 51</b>	ROS production measured in 16HBE14o- cells at 60 minutes for all tested compounds. A. 4-OPA; B. IPOH; C. 4-OPA + 4-AMCH	<b>119</b>
<b>Figure 52</b>	Determination of ROS production in 16HBE14o- and A549 cells exposed to tested compounds at 500 $\mu$ M for 24 hours. ( $n = 8 \pm$ SD)	<b>120</b>
<b>Figure 53</b>	The fold change of GSSG/GSH ratio in both A549 (blue) and 16HBE14o- (red) cells exposed for 2 and 24 hours to the tested compounds compared to GSSG/GSH ratio of untreated cells ( $n = 3 \pm$ SD) B. The fold change of GSNO/GSH ratio in both A549 (blue) and 16HBE14o- (red) cells exposed for 2 and 24 hours to the tested compounds compared to GSNO/GSH ratio of untreated cells ( $n = 3 \pm$ SD)	<b>122</b>
<b>Figure 54</b>	Total production of various cytokines by human pulmonary alveolar epithelial cells after 24-hours stimulation with 4-OPA, IPOH, 4-AMCH at two concentrations [1.5 and 50 $\mu$ M] ( $n = 9 \pm$ SD). A. IL-6 levels in A549 cells treated with test compounds at concentrations of 50 $\mu$ M (left ) and 1.5 $\mu$ M (right); B. IL-8 levels in A549 cells treated with test compounds at concentrations of 50 $\mu$ M (left ) and 1.5 $\mu$ M (right)	<b>124</b>
<b>Figure 55</b>	Evaluation of IL-6 and IL-8 release in the culture medium from 16HBE14o- cells exposed to individual compounds and their binary / ternary mixtures at 1.5 and 50 $\mu$ M ( $n = 3 \pm$ SD). Error bars that are smaller than the symbol size are not visible	<b>125</b>
<b>Figure 56</b>	Total production of various pro-inflammatory cytokines (IL-6, IL-8, TNF-alpha) released by A549 and 16HBE14o- cells after 24-hours stimulation with 4-OPA and IPOH at 1.5 and 50 $\mu$ M. Cells treated with medium (1% FBS) are expressed as "neg	<b>126</b>

	ctrl"=negative control (IL-8=132 pg mL <sup>-1</sup> , IL-6=81 pg mL <sup>-1</sup> , TNF-α=12 pg mL <sup>-1</sup> ) (n = 9 ± SD; *p<0.05, **p<0.01, ***p<0.001)	
<b>Figure 57A</b>	A General view (RT = 0-15) of the LC-MS chromatograms obtained from A549 cellular medium after chemical exposure to the 4-OPA + 4-AMCH + IPOH mixture (negative control corresponds to untreated cells; low concentration corresponds to cells exposed to 25 µg mL <sup>-1</sup> ; while high concentration corresponds to 260 µg mL <sup>-1</sup> of the chemical mixture)	<b>136</b>
<b>Figure 57 B</b>	Detailed cut view (RT = 7-12) referring to the chromatograms presented above (cut view for the negative control – untreated cells)	<b>137</b>
<b>Figure 57 C</b>	Detailed cut view (RT = 7-12) referring to the chromatograms presented above (cut view for the low concentration – cells treated with the mixture prepared at low concentration)	<b>138</b>
<b>Figure 57 D</b>	Detailed cut view (RT = 7-12) referring to the chromatograms presented above (cut view for the high concentration – cells treated with the mixture prepared at high concentration)	<b>139</b>
<b>Figure 58</b>	Score plot of PC1 versus PC2 from principal component analysis of cellular extract after A549 treatment for 72 h with the mixture (significance of dot colours: green corresponds to the negative control, red corresponds to the samples treated with low mixture concentration where 1 % of cells lost their viability, purple corresponds to the samples treated with high mixture concentration, where 10 % of cells lost their viability)	<b>140</b>
<b>Figure 59</b>	Cleavage reaction of 3-isopropenyl-6-oxo-heptanal leading to epoxides and aldehydes	<b>143</b>
<b>Figure 60</b>	Possible pathways of cellular reaction of IPOH leading to formation of radicals, epoxides and aldehydes	<b>143</b>
<b>Figure 61</b>	Possible pathways of cellular reaction of 4-OPA leading to the formation of aldehydes, acids, alcohols	<b>145</b>
<b>Figure 62</b>	Possible pathways of cellular reaction of 4-AMCH leading to the formation of peroxides, alcohols	<b>146</b>
<b>Figure 63</b>	Evaluation of time blood distribution on potential inflammatory capacity of various LPS concentrations [from 0.125 to 2 EU] added to blood (n=9 ± STD)	<b>150</b>
<b>Figure 64</b>	Measurement of IL-1 beta release from blood incubated with LPS concentration in the range of 0.5-2 EU mL <sup>-1</sup> investigated at various incubation times	<b>150</b>

<b>Figure 65</b>	IL-1 beta detected in human blood incubated with individual tested compounds at four concentrations (0-500 $\mu\text{M}$ ). Data represent mean $\pm$ SD, n = 3	<b>151</b>
<b>Figure 66</b>	Cellular viability results obtained after exposure of A549 cells in CULTEX for 1 and 2 hours to gas atmospheres containing A. d-limonene alone at various concentrations 250 $\mu\text{g m}^{-3}$ (approx. 0.02 ppmv), 5800 $\mu\text{g m}^{-3}$ (approx. 0.5 ppmv) and 15000 $\mu\text{g m}^{-3}$ (approx. 2.5 ppmv), relative humidity (RH)=80 % B. d-limonene alone at various concentrations 250 $\mu\text{g m}^{-3}$ (approx. 0.02 ppmv), 5800 $\mu\text{g m}^{-3}$ (approx. 0.5 ppmv) and 15000 $\mu\text{g m}^{-3}$ (approx. 2.5 ppmv), relative humidity (RH)=50 % C. ozone alone 137 $\mu\text{g m}^{-3}$ (approx. 0.07 ppmv), RH=50 %. Mean ( $\pm$ STD) of at least three independent runs are presented. Carrier control (humid Clean/Zero air), negative (incubator) and positive ( $\text{NO}_2$ ) controls are also included in the figures.	<b>154</b>
<b>Figure 67</b>	Glutathione levels in A549 cells after exposure to limonene atmospheres (0.02, 0.5 and 2.5 ppmv). Positive control $\text{NO}_2$ (12 ppmv) and negative controls (clean air and incubator) are shown. The results are expressed as GSH, GSSG and GSNO equivalents, corrected for protein content. Mean ( $\pm$ STD) of three independent runs are presented	<b>156</b>
<b>Figure 68</b>	Membrane damage measured in A549 cells in CULTEX after exposure for 1 and 2 hours to gas atmospheres containing only ozone (0.07 ppmv) and its mixture with 0.02 ppmv of d-limonene. Mean ( $\pm$ STD) of at least three independent runs are presented. Negative (black and light purple colors) and positive controls (red color) are shown	<b>157</b>
<b>Figure 69</b>	Evaluation of cellular viability of pulmonary cells exposed to the mixture of 4-OPA + IPOH + 4-AMCH for 1 and 2 hours. A. 16HBE14o- cells; B. A549 cells (n = 9 $\pm$ SD, significance of t-test, * p < 0.05, ** p < 0.01))	<b>163</b>
<b>Figure 70</b>	Evaluation of cellular viability of pulmonary cells exposed for 1 and 2 hours to the mixture of 4-OPA + IPOH + 4-AMCH in presence of ozone. A. 16HBE14o- cells; B. A549 cells. The effects of (n=9 $\pm$ SD, significance of t-test, ** p < 0.01))	<b>164</b>
<b>Figure 71</b>	Determination of IL-6, IL-8, TNF-alpha, RANTES, IL-15, IL-4 release in the medium of A549 and 16HBE14o- cells exposed to the mixture of 4-OPA + IPOH + 4-AMCH in absence and in presence of ozone (noted in the figure as mix + ozone)	<b>166</b>

### Summary

The prevalence of respiratory diseases in large populations has increased in recent decades. This phenomenon has been associated, among other factors, to poor air quality in indoor environments. Several hundreds of chemicals belonging to various chemical classes, including volatile organic compounds (VOCs), nitrogen oxides (NO<sub>x</sub>) and ozone have been identified in indoor environments. Toxicological information is to some extent missing or incomplete for most of them. The focus of studies on indoor air quality in the past was on the identification and quantification of individual (single) compounds and the evaluation of their toxicological properties with respect to a possible risk for human health. Little attention was paid to mixtures of chemicals and possible reactions between the chemicals accumulated indoors, in analogy with chemical reactions outdoors. Several studies have reported the presence of new chemical substances (reaction products) as the result of indoor air chemistry between reactive volatile compounds, in particular terpenes, and e.g. ozone with not well known toxicological behavior.

d-Limonene, one of the most common terpenes present in indoor environments through its ubiquitous use in fragrances, air-fresheners, cleaning products, food manufacturing etc., is reactive towards ozone (O<sub>3</sub>), hydroxyl radicals ( $\cdot$ OH) and alkylperoxy radicals (RO<sub>2</sub>) leading to various oxidation products.

The aim of this thesis was to evaluate the potentially toxicological impact of the three major limonene oxidation products (LOPs) with ozone: 4-oxopentanal, 4-acetyl-1-methylcyclohexene, and 3-isopropenyl-6-oxoheptanal on human pulmonary cell lines and blood.

Analytical methodologies (e.g. HPLC-UV, GC-MS) were further developed/optimized to analyze the selected chemicals in the air and in the cell culture medium and subsequently to evaluate the possible toxic effects such as cell viability, oxidative stress and inflammation observed when human lung were exposed to the selected chemical products as single compounds or mixtures.

The findings of the present study clearly demonstrate that the selected chemicals caused lung cellular injury characterized by decrease in cell survival, changes in the oxidative balance, inflammation and the metabolic activity of the cells. It should be emphasized, that with the methodology used is possible to obtain information on biological endpoints with *in vitro* experiments and so to avoid/reduce the number of experiments done with animals.

### Zusammenfassung

Die Häufigkeit von Erkrankungen der Atemwege in großen Bevölkerungsgruppen hat in den letzten Jahrzehnten zugenommen. Dieses Phänomen wurde unter anderem auf eine schlechte Luftqualität in Innenräumen zurückgeführt. Mehrere Hunderte von Chemikalien, die zu verschiedenen chemischen Klassen gehören, wie z.B. flüchtige organische Verbindungen (VOCs), Stickoxide (NO<sub>x</sub>) und Ozon, wurden in Innenräumen identifiziert. Toxikologische Informationen für die meisten von ihnen fehlen oder sind unvollständig. Der Schwerpunkt der Studien über die Raumluftqualität in der Vergangenheit lag meistens bei der Identifizierung und Quantifizierung von Einzelverbindungen und bei der Bewertung ihrer toxikologischen Eigenschaften im Hinblick auf ein mögliches Risiko für die menschliche Gesundheit. Es wurde jedoch wenig Aufmerksamkeit auf die Präsenz von Mischungen von Chemikalien und auf mögliche Reaktionen zwischen den akkumulierten in Innenräumen Chemikalien, in Analogie zu chemischen Reaktionen im Freien, gelegt. In diesem Zusammenhang hat man in mehreren Studien auf die Anwesenheit neuer chemischer Substanzen (Reaktionsprodukte) als Ergebnis der Raumluftchemie zwischen reaktiven flüchtigen Verbindungen hingewiesen. Hierbei wurde insbesondere auf die Reaktion von Terpenen mit Ozon hingewiesen, die unter anderem zu Reaktionsprodukten mit nicht bekannten toxikologischen Verhalten führt.

d-Limonen, ein der häufigsten Terpene, das als Duftstoff, biogenes Lösungsmittel und Reiniger in Innenräumen durch die allgegenwärtige Verwendung von Duftstoffen, Lufterfrischungssprays, Reinigungsmitteln, Lebensmittelherstellung etc. verwendet wird, reagiert mit Ozon (O<sub>3</sub>), Hydroxylradikalen (OH<sup>·</sup>) und Alkylperoxyradikalen (RO<sub>2</sub><sup>·</sup>) zu verschiedenen Oxidationsprodukten. Ziel dieser Arbeit war es, die möglichen toxikologischen Auswirkungen der drei Hauptprodukte (LOPs) aus der Reaktion von Limonen mit Ozon: 4-Oxopentanal, 4-Acetyl-1-methylcyclohexen und 3-Isopropenyl-6-oxoheptanal, auf menschliche Lungenzelllinien und Blut auszuwerten.

Analytische Methoden (z.B. HPLC-UV, GC, GC-MS) wurden weiterentwickelt / optimiert, um die ausgewählten Produkte in der Luft, im Zellkulturmedium zu analysieren. Anschließend wurden die biologischen Prüfungen durchgeführt und die möglichen zytotoxischen Auswirkungen, wie oxydativer Stress und Entzündungen, erfasst und bewertet. Die obenerwähnten Hauptprodukte wurden als Einzelverbindungen und als Gemische getestet.

Die Ergebnisse der vorliegenden Arbeit zeigen deutlich, dass die Hauptprodukte aus der Limonen/Ozon Reaktion einen Lungenzellschaden verursachen, der durch die

Abnahme der Lebenszeit, Veränderungen des oxydativen Gleichgewichts, der Entzündung und der metabolischen Aktivität der Zellen gekennzeichnet ist. Es sollte betont werden, dass mit der verwendeten Methodik möglich ist, Informationen über biologische Endpunkte mit Experimenten *in vitro* zu erhalten und somit die Anzahl der Tierexperimente zu vermeiden / zu reduzieren.

# 1. INTRODUCTION

## 1.1 Indoor air quality

Indoor air pollution may substantially contribute to overall human exposure, since people spend nearly 85-90 % of their time indoors [1, 2]. It is also important to consider that air pollutants generally accumulate indoors, thus concentrations of most pollutants indoors are typically 5 times higher than outdoors [3].

The impact of poor indoor air quality on occupant comfort, health and well-being depends on the type of pollutants that are released from various sources (e.g. building materials, furnishings), in settings (e.g. inadequate ventilation, high temperature and humidity levels) and due to human lifestyles and activities (e.g. household cleaning and smoking) [4-6]. The number of people affected by Chronic Obstructive Respiratory Diseases (COPD) is rapidly increasing [7] and it will become the third leading cause of death by 2030, according to the World Health Organisation (WHO) indicators [8]. In spite of the increased prevalence of COPD and evidence that, besides smoking, other risk factors, may be associated to its development, only a limited number of studies have attempted to assess the association between COPD and indoor air pollution in the general adult population [9-12]. In 2004, WHO estimated that asthma sufferers numbered approximately 235 million people, and approximately 20 % of the world population were suffering from allergic diseases [13]. According to the International Study of Asthma and Allergies in Childhood (ISAAC), asthma and rhinoconjunctivitis are among the most common diseases among European children [14]. The contributing factors are thought to be a combination of genetic predisposition and environmental exposure to inhaled substances and particles which induce allergic or irritating reactions [15 - 18].

For example, air pollution in indoor office environments (i.e. chemical irritants in the workplace, indoor allergens) [19 - 22] might initiate or aggravate illness on both respiratory [23] and cardiovascular levels [24 - 26], while the presence of tobacco smoke in indoor air enhances the risk of developing lung cancer in non-smokers [28 - 31]. Cardiovascular disease is the leading cause of death in the industrialized world, accounting for over 4.35 million deaths each year in Europe and over 1.9 million deaths in the European Union [32].

A number of studies revealed that an increased prevalence of asthmatic symptoms among the personnel [33] is related to cleaning activities including the use of cleaning

sprays [34 - 38].

The results offered by Sherriff et al., in a study at Bristol University, suggest that the development of childhood asthma could be related to the use of various cleaning materials and fragrances in the home [39].

The Registration, Evaluation, Authorisation and Restriction of Chemicals (REACH) programme launched by the European Union raised concerns regarding insufficient information on the potential human health risks of many inhaled compounds [40].

A survey of the literature produced a list of key indoor pollutants present in indoor environments together with their demonstrated or hypothesised health and comfort effects and is summarized in the table below.

**Table 1** Key indoor pollutants and their potential toxic effects on human health. The table was adapted from [41].

	Eye/ nose irritation	Respiratory symptoms	Allergies / asthma	Cardiovascular	Inflammation & oxidative stress	Ref.
<b>GAS POLLUTANTS</b>						
VOC <sub>s</sub>	yes	yes		yes		[42 - 44]
NO <sub>2</sub>		yes	yes		yes	[45, 46]
Ozone		yes				[47, 48]
<b>TERPENE REACTION PRODUCTS</b>						
SOA		yes		yes	yes	[46, 47, 49]
Terpenoids	yes	yes				[46, 47]
<b>PARTICULATE MATTER</b>						
PM <sub>2.5</sub>		yes		yes	yes	[50, 51]
PM <sub>1</sub>		yes		yes	yes	[52, 53]
Ultra-fine particles		yes		yes	yes	[54]
<b>BIOLOGICAL POLLUTANTS</b>						
Bioaerosols		yes	yes		yes	[55 - 57]

where VOCs = Volatile Organic Compounds; NO<sub>2</sub> = Nitrogen Dioxide; SOA = Secondary Organic Aerosols; PM<sub>2.5</sub> or PM<sub>1</sub> = Particulate Matter up to 2.5 or 1 micrometers in size

The INDEX project was the first study where a list of air pollutants were prioritised according to their potential effects on human health (irritations, respiratory diseases, cardiovascular diseases, cancer) [58].

Besides indoor air pollutants known for their adverse health effects, concern about indoor chemical reactions has grown over the last few years [59]. This is due to increasing evidence that products from indoor chemical reactions (e.g. ozone-terpenes), may contribute to adverse effects on human health [60 - 64]. As an example of exacerbated potentially harmful health effects due to air chemistry, ozone-terpene reactions produce secondary organic aerosols (SOA), i.e. ultrafine particles, that once inhaled have been linked to lung inflammation and systemic effects, including cardiovascular issues [65 - 67].

### 1.1.1 Terpenes

Terpenes have received considerable attention over the past years, regarding their ability to be rapidly oxidized by ozone thereby forming a broad range of reaction products [68]. Höpfe et al. found that reactions of ozone with terpenes from wood may have produced irritative substances for forestry workers [69]. Epidemiological studies carried out by Groes et al. indicated that chemical reactions between VOCs and ozone (O<sub>3</sub>) may be responsible for the prevalence of increased sick building syndrome (SBS) [70].

Terpenes are organic compounds emitted from both natural sources (e.g. conifers, fruits...) and consumer products (e.g. detergents, perfumes, air-fresheners...). Accordingly, they are among the most abundant indoor air pollutants. Several studies have attempted the quantification of terpene compounds in both indoor and outdoor air. In this regard, typical concentrations of terpene compounds in indoor air range from 6 to 200 µg m<sup>-3</sup>, and can in some cases be greater [71, 72]. Pine wood used as flooring material can account for up to 13 % of the total VOC content in indoor air [73].

### 1.1.2 Terpenes in consumer products

Sarwar et al. analysed the presence of terpenes in various consumer products (e.g. cleaners, air fresheners, perfumes). In the samples analysed by thermal desorption and GC/MSD, d-limonene was detected in all tested products. Content analysis of three air fresheners and three laundry products carried out by static headspace combined with GC/MS analysis indicates the presence of d-limonene (in all six products), α-pinene, β-

pinene (in five products); carene isomer (in four products); and linalool (in three products) [74]. Steinemann, Norgaard et al. examined four kinds of nano-film spray products (NFPs), used in an extensive variety of consumer products such as bathroom tiles, flooring, textiles and windows. An amount needed for coating 1 m<sup>2</sup> surface was sprayed toward a stainless steel target plate placed in a closed aerosol chamber (0.66 m<sup>3</sup>). The authors noticed that a number of VOCs including d-limonene, chlorinated acetones, perfluorinated silane, and nanosize particles were emitted, but some of the VOCs identified in the emissions were not listed in the product safety sheets [75, 76]. Quite recently, Maupetit and Squinazi have presented emission outcomes obtained from 43 incense and scented candle products available in France. The measurements of emissions from eight products showed the presence of d-limonene and five other VOCs (benzene, toluene, xylene, styrene, naphthalene) [77]. In a study carried out in Korea, limonene has been detected at a frequency of 58 % in the headspace phase of twenty-six air freshener gel products [78]. On the other hand, in Nazaroff's study, the levels of terpenes ranged from 0.2 to 26 % in various consumer products [79]. However, the previous studies do not use the collected data to investigate the possible toxic impact on human health which corresponds with the discovered d-limonene levels.

### 1.2 Limonene

Limonene is one of the most common monoterpenes emitted globally [80]. It is also known by a variety of synonyms, including the following: 1-Methyl-4-(1-methylethenyl)-cyclohexene (IUPAC name); 1,8(9)-p-Menthadiene; 1-methyl-4-isopropenyl-1-cyclohexene; alpha-limonene; dipentene; p-mentha-1,8-diene etc.

Limonene has been used for many years as a flavour in foods and beverages but it is also increasingly used as a biogenic solvent to substitute chlorinated hydrocarbons, chlorofluorocarbons (CFCs) and other organic solvents. It is reported to be emitted from different sources such as air fresheners, resins and adhesives and it is also applied as a wetting and dispersing agent or used in insect control [72, 81].

#### 1.2.1 Physicochemical properties

Limonene – a colourless liquid hydrocarbon at room temperature – occurs in two optically active forms: d-limonene ((R)-enantiomer) and l-limonene ((S)-enantiomer). Both isomers (**Figure 1**) are characterized by a different odours: d-limonene has a strong smell of orange/lemon (odour threshold = 1111.29 µg m<sup>-3</sup>) while l-limonene

smells piney (odour threshold = 2778.2  $\mu\text{g m}^{-3}$ ) [82 - 85].

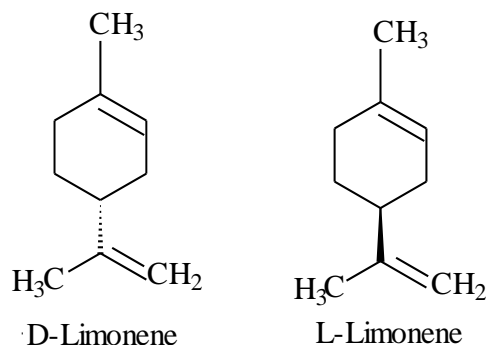


**Figure 1** Molecular structure of limonene (stereoisomers)

The main chemical form found in nature and used in industry is d-limonene [86, 87]. Other physical and chemical properties of limonene are presented in **Table 2**. The information cited in the table below was taken from Concise International Chemical Assessment Document No. 5: Limonene. World Health Organization, Geneva, 1998 [87].

**Table 2** Summary of the physical/chemical properties of limonene

	<b>d-limonene</b>	<b>l-limonene</b>
<b>CAS no.</b>	5989-27-5	5989-54-8
<b>Empirical formula</b>	$\text{C}_{10}\text{H}_{16}$	
<b>IUPAC name</b>	(R)-(+)-para-Mentha-1,8-diene	(S)-(-)-para-Mentha-1,8-diene
<b>Molecular weight</b>	136.23	
<b>Boiling point (<math>^{\circ}\text{C}</math>)</b>	175.5 - 176.0	
<b>Melting point (<math>^{\circ}\text{C}</math>)</b>	-74.35	
<b>Water solubility (<math>\text{mg L}^{-1}</math> at 25 <math>^{\circ}\text{C}</math>)</b>	13.8	-
<b>Vapour pressure (Pa at 200 <math>^{\circ}\text{C}</math>)</b>	190	-
<b>Density (<math>\text{g/cm}^3</math> at 20<math>^{\circ}\text{C}</math>)</b>	0.8411	0.8422
<b>Henry's law constant (<math>\text{kPa m}^3/\text{mol}</math> at 25<math>^{\circ}\text{C}</math>)</b>	34.8 <sup>b</sup>	-
<b>Partition coefficient (Log <math>K_{ow}</math>)</b>	4.23 <sup>c</sup>	-

Where  $K_{ow}$  = Octanol-Water Partition Coefficient;  $\mathbf{b}$  = value from Assessment Tool for the Evaluation of Risk (ASTER) database, Environmental Research Laboratory, US Environmental Protection Agency, Duluth, MN, 1991 and Massaldi et al. [88];  $\mathbf{c}$  = calculated value (ENVIROFATE database, Office of Toxic Substances, US Environmental Protection Agency, and Syracuse Research Corporation) [89].

### 1.2.2 Production, use, human exposure and regulations

In the US (1984), the consumption of d-limonene was 250 tonnes [90], while in Sweden (1994), between 69 and 80 tonnes of d-limonene were used in 48 products, 15 for consumers (according to Swedish National Chemicals Inspectorate). In Japan (1993), the production volume of d-limonene was about 40 000 tonnes [86]. The annual production of limonene in Europe is between 10.000-100.000 tonnes per annum as reported by the European Chemicals Agency (ECHA) [91].

To be able to accurately assess the potential public health impacts of exposure to realistic levels (e.g. indoor environments) of d-limonene and d-limonene ozonolysis reaction products, the content of d-limonene in/and the use of the products and materials used indoors must be well-known. At present, these data are only partially known. However, some information is available about the quantities of production and contents of terpenes in products.

In the review by Holcomb and Seabrook (1995), limonene has been regarded as being one of the volatile organic compounds most frequently measured in indoor air [92]. A number of indoor measurements revealed that typical average indoor d-limonene concentrations range from 2 to 500  $\mu\text{g m}^{-3}$  [93, 94]. However, and due to lifestyle, considerably higher concentrations can be found following different activities. As an example, a concentration of 970  $\mu\text{g m}^{-3}$  of limonene was found after spraying a cleaning wax for 15 seconds [95], or 1950  $\mu\text{g m}^{-3}$  after peeling an orange [96].

In the Bangkok office buildings study conducted by Ongwandee et al. (2011), limonene was found to be one of the most dominant VOCs with concentrations varying from 113 to 241  $\mu\text{g m}^{-3}$ . Air fresheners and cleaning products were assessed to be the main indoor emission sources involved in this measurement. Within this study, the calculated mean of indoor to outdoor ratios of limonene concentrations was greater than 1 [97]. Indoor/outdoor ratios (I/O ratios) may vary significantly, depending on the prevalence of indoor and outdoor sources, geographical regions, and climatic conditions. The determination of differences in I/O ratios helps to monitor the status of indoor concentrations of the chemicals investigated. A ratio of less than 1 indicates that the

concentration of the chemicals investigated is higher outdoors than indoors, while an I/O ratio above 1 indicates a significant accumulation of the chemicals in indoor environments more than outdoors [98].

In Europe, measurement campaigns (in approximately 80 public buildings) were carried out during different seasons to monitor the limonene exposure concentrations among other VOCs (e.g. alpha-pinene), as well as the indoor/outdoor ratios of these chemicals. From the data obtained, the I/O ratio for d-limonene was ranging from 7 to 132 (these values represent average values for all indoor and outdoor measurements) [99].

In a study reported by Jia et al., the measurements carried out in southeast Michigan, USA, identified that limonene was the dominant terpene compound present among nearly 100 VOCs – the detection frequency of limonene in indoor environments based on all 37 indoor samples was around 89 % – which were detected in ten mixed-use buildings (typically an office area and an industrial/commercial area were selected). Remarkable differences were observed in the limonene concentrations monitored in offices (average value =  $5.5 \mu\text{g m}^{-3}$ ) and in ambient air ( $0.01 \mu\text{g m}^{-3}$ ), while the difference in limonene concentrations determined in offices and workplace area was not statistically different (p-values of 0.83 calculated in Wilcoxon signed rank test (n = 9)) [100].

A number of investigations including 47 chemicals inhaled by humans, ranked d-limonene on the 12<sup>th</sup> position of human olfactory detectability [101]. Tamás et al. showed that the perceived air quality in a room with d-limonene and ozone significantly decreased when compared to rooms containing only d-limonene or only ozone, as noted by human subjects [102]. Their study is in agreement with Knudsen et al. [103].

### 1.3 d-Limonene ozonolysis products

High concentrations of ozone are feasible indoors whenever outdoor concentrations are elevated or whenever indoor emissions derive from office equipment [104 - 106] or devices such as portable ion generators [107 - 109]. Potential sources of ozone include electric motors, vent-fog precipitators, copying machines, and laser printers [110 - 114]. Peak outdoor ozone concentrations can reach 120-400  $\mu\text{g m}^{-3}$  in many European regions and its infiltration indoors amounts to 20-70 % of outdoor concentrations [115 - 117]. On the other hand, Allen et al. reported that indoor ozone concentrations were up to 490  $\mu\text{g m}^{-3}$  when generated by electrostatic air cleaners and photocopying machines in poorly ventilated rooms [114]. Moreover, particular attention has been given to indoor ozone levels in aircraft cabins, since indoor air is recirculated during flights [118]. Mean

ozone concentrations in the cabins of aircrafts have been reported to range from 43.1  $\mu\text{g m}^{-3}$  [119] to 392.2  $\mu\text{g m}^{-3}$  [120]. The Environmental Protection Agency (EPA) has established an 8-h national ambient air quality standard (NAAQS) concentration of 0.08 ppmv for ozone [121]. The US Building Assessment Survey Evaluation (BASE) study reinforces the idea of ozone's presence indoors due to its infiltration from outdoors, when the authors correlated the ambient ozone concentrations with indoor concentrations of some aldehydes (e.g. formaldehyde, acetaldehyde) formed during indoor ozone reactions [122]. In 1995, Bernhard et al. confirmed within their study the presence of ozone in 56 European buildings (the European Audit project) [123]. According to Jensen and Wolkoff (1996), the odour threshold of ozone is 100  $\mu\text{g m}^{-3}$  and the threshold of mucous membrane irritation estimate 2  $\text{mg m}^{-3}$  [124].

One of the more important types of indoor ozone gas-phase reactions are those with terpenes (e.g. d-limonene). The presence of d-limonene as a fragrance in many consumer products such as cleaning agents and air fresheners may lead to its abundant occurrence in indoor environments. In such a complex environment, the evaluation of the potential toxic impact of d-limonene on human health requires a complete toxicological evaluation of d-limonene, not only as a single compound but also the effect of the combination of d-limonene and other compounds present in the environment (e.g. ozone,  $\text{NO}_2$ ). This reaction has been reported to form both gaseous reaction products (e.g. formaldehyde) and fine and ultrafine particles [68, 125]. The concentrations of highly reactive free radicals formed during this reaction as intermediates are not well known, even if they are needed to advance in indoor chemistry modelling [126]. The reaction between d-limonene and ozone is initiated by the oxidative cleavage of the C=C double bonds and the consequent formation of the corresponding ozonides. Due to their instability, these ozonides rapidly decompose, forming Criegee biradicals and primary products containing a carbonyl group. Subsequently, the energy-rich Criegee intermediates may rearrange or may be entailed in various reaction steps to generate additional products. The stable oxidation products comprise a number of aldehydes (both saturated and unsaturated) and organic acids (e.g. formic acid, acetic acid) [127, 128]. The intermediate reactions have also been demonstrated to produce highly reactive species such as hydroxyl radicals ( $\text{OH}\cdot$ ) with a yield of 0.86 % [129]. Having higher oxidant ability than ozone, such hydroxyl radicals can further react with either parent d-limonene or more stable compounds that were not oxidized by ozone itself [130 - 133]. In 1999, Calogirou et al. published a paper in which possible decomposition pathways of d-limonene oxidized by OH radicals are proposed [68].

During experiments investigating d-limonene ozonolysis reaction, various chemical products formed have been identified (see **Table 3**) [134 - 138].

**Table 3** Identified d-limonene ozone reaction products

<b>Class of compound</b>	<b>Name of compound</b>	<b>Ref.</b>		
Peroxides	Limonene-1-hydroperoxide	139 – 140		
	Limonene-2-hydroperoxide			
	Limonene-2-methyl-hydroperoxide			
Epoxides	Limonene-1,2-epoxide	141 – 142		
	Limonene oxide			
	Limonene 8,9-epoxide			
Alcohols/diols				
(di) Carbonyls	3-acetyl-7-hydroxy-6-oxoheptanal	142 – 145		
	5-hexene-2-one			
	Methylglyoxal			
	3-oxobutanal			
	<b>4-oxopentanal (4-OPA)</b>			
	6-methyl-5 heptene-2-one			
	<b>4-acetyl-1(+/-) methylcyclohexene (4-AMCH)</b>			
	Formaldehyde			
	<b>3-isopropenyl-6-oxoheptanal (IPOH)</b>			
	3-acetyl-6-oxo-heptanal			
	Hydroxyl/carboxyl		butanedioic acid	146 – 150
			4-oxopentanoic acid	
pentanedioic acid				
hexanedioic acid				
3-acetyl-6-oxo-heptanoic acid				
2-isopropenyl-pentadioic acid				
3-isopropenyl-hydroxy-6-oxo-heptanoic acid isomers				
3-isopropenyl-hexanedioic acid				
3-carboxy hexanedioic acid				
3-isopropenyl-6-oxoheptanoic acid				

As mentioned above, primary and secondary d-limonene products can exist in both gas and condensed phase. The partition between these two phases depends on the vapour

pressure specific to each compound and the surface area of existing airborne particles. The mechanism which contributes to the size and mass growth of particles is directly correlated to the low vapour pressure of the chemicals. These will condense and absorb on pre-existing particles and smaller particles, generally referred as Secondary Organic Aerosols (SOAs) [95, 130, 151 - 153].

Weschler and Shields supported the hypothesis of particles generated during the reaction of d-limonene with ozone, with yields in the region of 10-15 % [130]. The composition of particles - in particular their oxidant potential - is hypothesised to be important in assessing health effects [154]. Lamorena and Lee focused on the formation of secondary gaseous compounds and ultra-fine particles during ozone-initiated oxidations with emitted monoterpenes (d-limonene, alpha-pinene, beta-pinene, p-cymene) from a car air-freshener. Injection of ozone into the Teflon bag chamber containing already the monoterpenes released from the air freshener lead to the formation of ultra-fine particles within a size range of 4.4–160 nm. Formaldehyde, acetaldehyde, acrolein, acetone, and propionaldehyde were some of the secondary gaseous products formed during the ozone-initiated reactions. The authors also concluded that the ozone concentration (98 and 196.1  $\mu\text{g m}^{-3}$ ) and the temperature (30 and 40 °C) significantly influenced the generation of gaseous products and the formation of particles during the ozone-initiated reactions. Teflon chamber studies were also used to investigate the yields of formation of oxygenated organic reaction products for gas-phase reactions of the hydroxyl radical ( $\text{OH}\cdot$ ) and ozone ( $\text{O}_3$ ) with a common cleaning product containing terpenes such as d-limonene, R-terpineol, and geraniol. Several dicarbonyl reaction products such as 4-oxopentanal, glyoxal, methylglyoxal were produced by the selected terpenes in presence of ozone. Total carbonyl yield for limonene-ozone reaction was around 5.1 % [155].

The review by Calogirou et al. may serve as a supplement on this particular topic since a list of oxidation products formed during limonene ozonolysis are presented and discussed (e.g. limonon aldehyde, limona ketone etc.) [68].

In addition to the above described oxidation products in the gas phase, several studies have focused on the formation of particulate matter during terpenes ozonolysis experiments. In this regard, an increase in particulate matter of up to 20-fold was observed both in chamber experiments [130] and real scenarios [95] when mixing different terpenes (e.g. limonene, linalool) with ozone at realistic concentration levels. Special interest should be devoted to the increase in the concentration of ultra-fine particles (ranging from 0.1 to 0.3  $\mu\text{m}$ ) as such particles have the potential to penetrate into the blood stream through the alveoli [156].

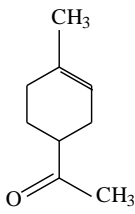
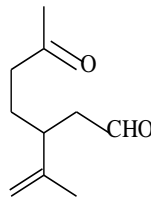
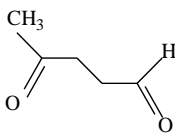
Nazaroff et al. measured the reaction products formed during the oxidation of three consumer products: a cleaner, a degreaser and an air freshener. The studies were conducted in presence of ozone ranging from 58.9 to 490.3  $\mu\text{g m}^{-3}$  and d-limonene ranging between 5.6-170  $\mu\text{g m}^{-3}$ , 560-1280  $\mu\text{g m}^{-3}$  and 3230-4120  $\mu\text{g m}^{-3}$ . The products formed during the consumer products' oxidation were formaldehyde, acetaldehyde, acetone, glycolaldehyde, formic and acetic acid. It had previously been noted that only formaldehyde, formic and acetic acid were formed, when d-limonene was the only VOC present in the mixture. Consecutively, some experiments were conducted by emulating the real use-case of the selected consumer products as follows: approx. 50 g cleaner (1.2 % d-limonene), 4-7 g degreaser (25 % d-limonene) and an air freshener (~ 1.3 % d-limonene) were supplemented with ozone (223.5 - 235.3  $\mu\text{g m}^{-3}$ ). The results indicated the presence of formaldehyde at 7-8 ppbv averaged over a 12-hour period in absence of ozone and 13-20 ppbv in presence of ozone. The number of particles produced by the cleaner and degreaser were about  $7-15 \times 10^8$  times higher when ozone was added when compared to those formed in absence of ozone. Additionally, the number of particles generated by the use of air freshener in presence of ozone was  $3 \times 10^6$  times higher than the number of particles formed by the use of the cleaner without ozone. The results concerning the particle mass concentrations showed that cleaners in presence of ozone were 18 times higher ( $\approx 90 \mu\text{g m}^{-3}$ ) than the particle mass concentration generated in absence of ozone ( $\approx 5 \mu\text{g m}^{-3}$ ) [79].

Formaldehyde, acetaldehyde, formic acid have been measured in many experiments while compounds such as IPOH, 4-OPA, 4-AMCH have been introduced in only a few studies. For example, Clausen et al. demonstrated that reactions between d-limonene (266709.3  $\mu\text{g m}^{-3}$ ) and ozone (7844.4  $\mu\text{g m}^{-3}$ ) formed formaldehyde and formic acid as major products and found the presence of 4-AMCH, IPOH. Also, a 2-fold increase in particles over the background concentration was obtained when d-limonene was added, and a 4-fold increase in particles was measured when ozone was added to d-limonene, compared to the background [159].

### 1.3.1 Selected d-limonene ozonolysis products: 4-oxopentanal (4-OPA), 4-acetyl-1-methylcyclohexene (4-AMCH) and 3-isopropenyl-6-oxoheptanal (IPOH)

Three common d-limonene ozonolysis products [145, 160 – 162]: 4-OPA, 4-AMCH and IPOH were selected in this research, with the scope to assess their potential toxic effects at the respiratory level. Their selection was done on the basis of their stability (e.g. more stable than peroxides), their general abundance with high ozone or hydroxyl radical yields [163] and on the hypothesis that terpene reaction products with multiple oxygen groups such as dicarbonyls may cause inflammatory and respiratory sensitising properties and/or skin irritation [164 – 167].

**Table 4** Physico-chemical properties of selected d-limonene ozonolysis reaction products: 4-acetyl-1-methylcyclohexene, 3-isopropenyl-6-oxo-heptanal, 4-oxopentanal

d-Limonene reaction products	CAS no.	MW	Vapour pressure mmHg	Boiling point °C	Water solub. mg L <sup>-1</sup>	Structure
4-acetyl-1-methylcyclohexene C <sub>9</sub> H <sub>14</sub> O, (4-AMCH)	6090-09-1	138.21	0.568	205-206	811	
3-isopropenyl-6-oxo-heptanal C <sub>10</sub> H <sub>16</sub> O <sub>2</sub> , (IPOH)	7086-79-5	168.23	1.3	80.5-82/ 1 mm Hg	2920	
4-oxopentanal C <sub>5</sub> H <sub>8</sub> O <sub>2</sub> , (4-OPA)	626-96-0	100.12	1.3	100-105/ 20 mm Hg	50000	

Only scarce quantitative information is available on the formation of the d-limonene ozonolysis reaction products in indoor air, referring to 4-oxopentanal (4-OPA) and 3-isopropenyl-6-oxo-heptanal (IPOH). Data from a recent study have identified the formation of IPOH, 4-OPA and 4-AMCH, when a kitchen cleaning agent (KCA) and a plug-in air freshener were used in the presence of low (19.6 µg m<sup>-3</sup>) and high (98 µg m<sup>-3</sup>) ozone. The KCA was mostly containing d-limonene and dihydromyrcerol

while the plug-in air freshener contained dihydromyrcerol, terpineol and linalool as most abundant VOCs. At high concentration of ozone, IPOH, 4-OPA and 4-AMCH was determined to be around 17 and less than  $3 \mu\text{g m}^{-3}$  (for 4-OPA and 4-AMCH) when KCA was used, while in the case of the use of air freshener only 4-OPA was detected (around  $70 \mu\text{g m}^{-3}$ ). Using KCA in presence of low ozone concentration, only IPOH was determined at around  $2 \mu\text{g m}^{-3}$ , while for the air-freshener none of the selected d-limonene ozonolysis products was detected [168]. A current study carried out by Nørgaard et al. extends the measurement by investigating the concentrations of 4-OPA, IPOH and 4-AMCH before and after the replacement of the regular floor cleaning agent in the offices of 4 European countries: France, Greece, Hungary, Italy. After the use of regular cleaning agents, the offices were characterised by limonene, ozone and their ozonolysis products levels, as follows: limonene levels in France were around  $13 \mu\text{g m}^{-3}$ , ozone was below the limit of detection (LOD) and 4-OPA, IPOH and 4-AMCH were below LOD; in Greece, limonene was  $32 \mu\text{g m}^{-3}$ , ozone was  $7 \mu\text{g m}^{-3}$ , IPOH was found to be around  $1.3 \mu\text{g m}^{-3}$  while 4-OPA was  $10 \mu\text{g m}^{-3}$ ; in Hungary, limonene concentrations were  $0.1 \mu\text{g m}^{-3}$ , ozone was  $4 \mu\text{g m}^{-3}$  and IPOH in the order of  $0.5 \mu\text{g m}^{-3}$  while in Italy, limonene was present at a concentration of  $9 \mu\text{g m}^{-3}$ , ozone was  $1.5 \mu\text{g m}^{-3}$ , IPOH was present at the concentration of  $10 \mu\text{g m}^{-3}$ , 4-OPA at  $18 \mu\text{g m}^{-3}$  and 4-AMCH at  $0.1 \mu\text{g m}^{-3}$ . After the replacement of the regular floor cleaning agents with a common lower total volatile organic compounds, the outcomes showed a reduction of 4-OPA, IPOH and 4-AMCH which was in line with the lower limonene levels, as follows: in France, limonene level was almost 10-fold lower than before replacement of the floor cleaning agent, while ozone and the selected limonene ozonolysis products were below LOD; in Greece, the limonene levels were about  $1 \mu\text{g m}^{-3}$ , the average ozone level was about 2-fold elevated (e.g.  $19 \mu\text{g m}^{-3}$ ), 4-OPA was below  $\mu\text{g m}^{-3}$  while IPOH disappeared; in Hungary, ozone was elevated at about 2-fold, IPOH disappeared while 4-AMCH appeared (e.g.  $0.9 \mu\text{g m}^{-3}$ ) probably due to its outdoor presence; in Italy, a low level of limonene was measured of  $1.7 \mu\text{g m}^{-3}$ , 4-OPA was observed at the same order as before, while IPOH levels were drastically reduced to  $0.4 \mu\text{g m}^{-3}$ , the ozone levels increased at  $8 \mu\text{g m}^{-3}$ . One of the author's conclusion was that the formation of limonene ozonolysis reaction products is closely related to the presence of ozone, since in France for example, the concentration of the selected limonene ozonolysis reaction products was low in line with the absence of ozone. On the other hand, in Greece, the measured high levels of 4-OPA were in consonance with elevated ozone level. However, the high levels of 4-OPA were associated also to the presence of other precursors such as geraniol, linalool or squalene [169].

### 1.4 Pulmonary toxicity

The main sites of exposure of a noxious agent's entry into the human body are the lungs, skin and the gastro-intestinal tract via inhalation, dermal and oral routes, respectively. When insoluble gases, droplets or small solid particles contained in the inhaled air (a 70 kg adult is assumed to inhale 20 m<sup>3</sup> of air per day [170]) penetrate the respiratory tract, they often accumulate on the deep lung areas. The deeper parts of the lung (the smallest airways and the alveoli) constitute a favorable situs for the accumulation of contaminants due to their narrow diameter characteristics and the low air flow velocity. Moreover, the tendency for accumulation increases with the decrease in water solubility of the toxicants and the decrease of particle size (see **Figure 2**) [171 - 173].

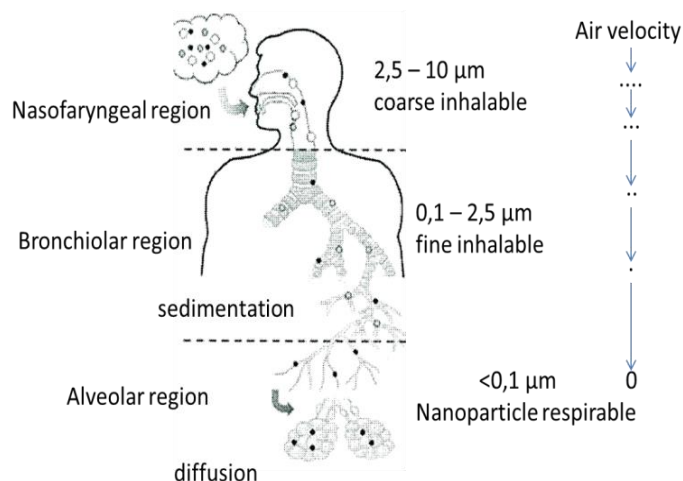


**Figure 2** Representation of the deposition patterns of the particles in the human respiratory system (the picture was adapted after [171])

Severe health disorders may result during the respiratory process - inhalation phase, when fresh air containing various gaseous components, aerosols and particulate matter is moved into the lung through the upper respiratory tract and the conducting airways into the terminal respiratory units. When the clearance activity (natural defence mechanism of the lung) at this level is not efficient, the potentially toxic agents will be diffused from the alveolar membrane into the flow of blood that surrounds the alveoli. Once the chemicals are distributed in the blood, they may elicit toxic responses in the heart (70 to 80 cm<sup>3</sup> of blood per heartbeat irrigates the lung) or they can be distributed throughout the whole body [174]. For example, very insoluble gases such as carbon monoxide will be absorbed at the pulmonary blood supply level, while gases that are

very soluble in water such as formaldehyde will be absorbed nearly completely at the nose or upper airways level [175]. However, studies on particle deposition patterns indicate that gaseous compounds absorbed on particles surface will follow the deposition patterns of the particles [176].

### 1.4.1 Lung as the target organ – description

The upper respiratory part includes the nose and pharynx while the conducting airways consist of the trachea divided in two main bronchi, which progressively decrease their internal diameter and lead into bunches of tiny round air sacs called alveoli, where the gas-exchange occurs. Each of these alveoli is surrounded by tiny blood vessels called capillaries which are connected to the arteries and veins that move blood through the whole body (see **Figure 3**, taken from National Heart Lung and Blood Institute website [177]).

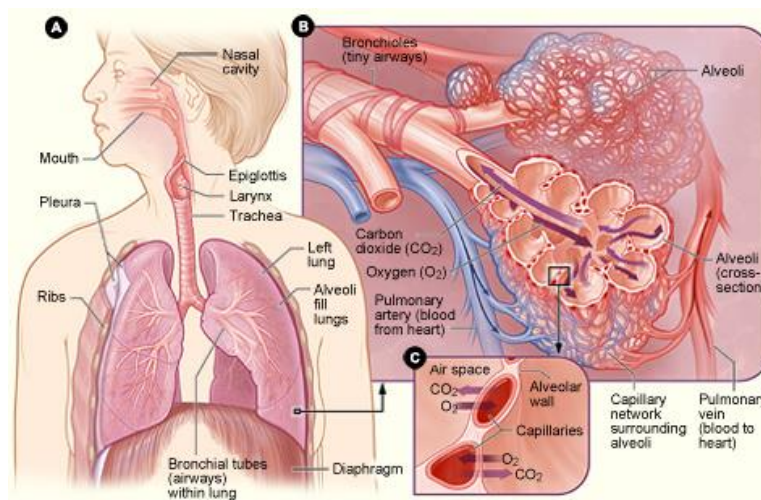


**Figure 3** A. General view of respiratory structures in the body, B. Detailed view of the airways, alveoli (air sacs), and capillaries (tiny blood vessels), C. Specific view of gas exchange (CO<sub>2</sub> and O<sub>2</sub>) between the capillaries and alveoli

Concerning the histological constituents of the lung (see **Figure 4**), the conducting airways (upper and lower part) are covered by a mucosal epithelium – formed by tight apical junctions between epithelial cells – that protects the respiratory tract from injury produced by chemicals, microbes, and biogenic agents.

Concerning the morpho-histological characteristics of the bronchial epithelium in the case of a normal mammalian lung, this consists of many morphologically distinct cell types (basal cells, goblet cells and ciliated columnar cells) which have an active role in

airway immune function and mucociliary clearance. Morphological or functional alterations in the bronchial epithelium have been associated with airway irritation, carcinogenesis, chronic bronchitis and cystic fibrosis [178, 179].

The gas-exchange region represents approximately 480 million alveoli which are irrigated by the pulmonary artery capillaries that permit air-blood contact. Alveoli are tiny structures with a very large surface area (approx. 100 m<sup>2</sup>) and their epithelium is made of two main cell types: the epithelial type I and II cells and occasional brush cells [180]. The type I cells are extremely squamous and have an attenuated cytoplasm; they totalize only 40 % of the entire alveolar lining cells and cover a large surface area of the alveolar surface (about 95 %). On the other hand, the type II cells – cuboidal cells with large nucleus and vacuolated cytoplasm – comprise 60 % of the alveolar lining cells. They produce surfactant with a bactericidal effect, prevent the alveoli from collapsing upon expiration and replace damage type I cells after lung injury [181, 182].

Differently from the bronchial epithelium, the alveolar epithelium is not protected by mucus and cilia, but by alveolar macrophages which are located at the inter-phase between air and lung tissue. The alveolar macrophages or phagocytotic cells are derived from blood monocytes. Since monocytes respond slowly to infection, they develop into macrophages which become the first defensive line against inhaled constituents of the air (being the only macrophages in the body exposed to air). Their main role, as a defensive activity, is to keep the alveoli's surface sterile, to kill and ingest the intruders (e.g. phagocytosis of bacteria) and to clean-up the cell debris (e.g. phagocytosis of cell debris). When macrophages interact with proteins - released by lymphokines - the tumoricidal and microbicidal activity of macrophages is activated [183]. They also play an important role in immune response reactions by stimulating lymphocytes and other immune cells to respond to the pathogen [184, 185].

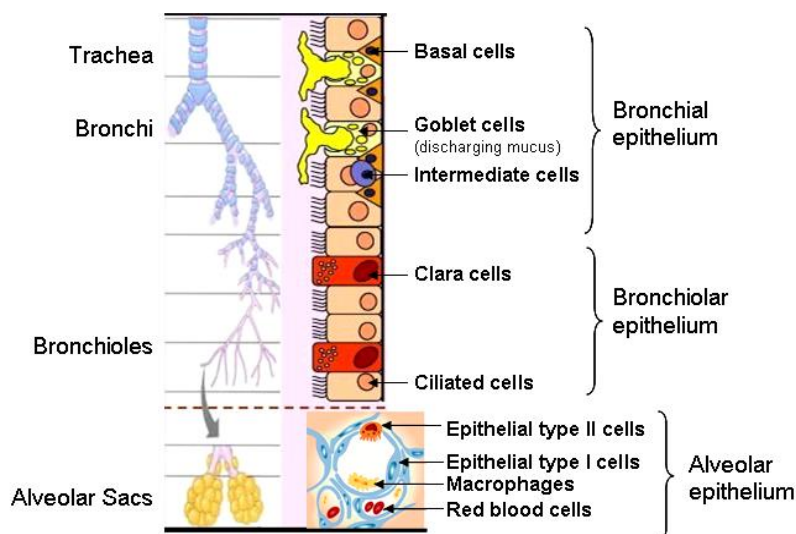


**Figure 4** The main cell types at the bronchial-alveolar epithelium level (figure was modified based on representation of [181] and the drawings prepared by [186])

### 1.4.2 Defensive mechanisms of the lung

The inhalants can cause reversible or irreversible harm to the lung or to the extra-pulmonary sites depending upon several factors such as: physicochemical characteristics and concentration of the toxicants, frequency and type of exposure (i.e. occupational, accidental or prolonged) and their reaction/interaction with other toxicants [187]. Thus, each of the lung cell types – over 40 different cell types – and their function can become a potential target for the toxic action of the inhaled chemicals.

Several studies have revealed that the lung has a great capability to metabolise many xenobiotics because of a high number of lung enzymes involved in xenobiotic metabolism [188, 189]. These enzymes facilitate the elimination of lipophilic chemicals by introducing new functional groups (Phase I reaction), or by conjugating with internal cell molecules such as glutathione, amino acids (Phase II) to increase water-solubility and further be eliminated in bile and urine [190]. Even though the lung has a great capability to biotransform such compounds, there are situations in which the biotransformation reactions can transform a harmful/harmless substance into toxic metabolites. The lung defends itself from various groups of noxious gases, particulates as well as infectious agents by:

1. Initiating the *cytokine host defence mechanism*, that plays an important role in maintaining the balance in both the immune and inflammatory response. Cytokines are a group of protein signal molecules, which act simultaneously to detect and classify the injurious and harmless agents. When the cytokine-controlled network of cells has to

combat the foreign substance (activation versus tolerance), cytokines act in different ways, e.g. to initiate and amplify inflammation, to induce T-cell independent macrophage activation etc. [191, 192]. Alveolar macrophages produce pro-inflammatory cytokines such as interleukin (IL)-1beta and tumor necrosis factor (TNF-alpha) which activate alveolar epithelial cells to produce chemokines such as IL-6, IL-8 [193 - 196].

A considerable amount of literature has been published on the use of cytokines/chemokines as biomarkers in studies with mice and humans to investigate the immune-pathological profile of the respiratory tract, in particular of asthma (that inflames the lung airways) and (COPD) associated with damage to proximal bronchial airways (bronchitis) and to distal airways and airspaces [197 – 202]. Inflammatory diseases are dictated by a dysregulation of the ratio between pro and anti-inflammatory cytokines. In several studies a series of pro- and anti-inflammatory cytokines have been selected to be considered as indicators for the assessment of the inflammatory process's status after the exposure of humans or animals to different contaminants (see **Table 5**).

**Table 5** Cytokine levels at the lower respiratory tract of both mice and humans (table adapted from [203])

Type of cytokines		Asthma	COPD	Ref.
Pro-inflammatory	Anti-inflammatory	Cytokine levels		
IL-6		High	High	[207 – 211]
IL-8		High	High	[213 – 220]
TNF- $\alpha$		High	High	[221 – 225]
IL-1 $\beta$		High	High	[226, 227]
	IL-4	High	High	[205, 206]
IL-10	IL-10	High	High	[204, 229-234]
	IL-5	High	High	[232, 233]
IL-9	IL-9	High	High	[234 – 238]
	IL-13	High	-	[239 – 243]
IL-17		High	High	[244 – 248]

Pro-inflammatory cytokines including IL-1beta, TNF-alpha, IL-6, IL-8 etc. are acting to induce inflammation, while a series of anti-inflammatory cytokines such as IL-4, IL-10, IL-13 act to reduce inflammation and to promote healing [249 – 252]. Thus, a higher ratio of TNF-alpha / IL-10 that might be determined in the lung shows an upward trend of the pro-inflammatory cytokine TNF-alpha and a downward trend of the anti-inflammatory cytokine IL-10, which can lead to severe lung diseases such as asthma.

2. To reduce oxidant damage to biological molecules, the human lung has several *antioxidant defense mechanisms* (e.g. superoxide dismutase, glutathione peroxidase and catalase), which participate to the detoxification of reactive products [253 – 256]. The over-production of reactive oxygen species (ROS) or reactive nitrogen species (RNS) may decrease or inactivate the antioxidant defence. Therefore, it is essential for normal cell growth to maintain ROS or RNS balance [257 – 268]. A misbalance in cell redox reactions can lead to severe damages of different cellular components such as DNA, cell membrane and cytoskeleton damage which are indirectly responsible for injuries such as inflammation and tissue damage [269 – 275]. According to current knowledge, intracellular glutathione (reduced GSH, oxidized GSSG, nitroso GSNO) plays a key role in detoxification, immune modulation, apoptosis, mitochondrial respiration etc. [276 - 282]. Furthermore, GSH deficiency has been suggested to play a significant role in the pathophysiology of a number of lung diseases: COPD [283 – 287], acute respiratory distress syndrome (ARDS) [288, 289], and asthma [290 – 294].

### 1.4.3 Respiratory health effects

The human health effects caused by inhalable air pollutants as individuals or mixtures have been assessed by carrying out different studies: cohort, *in vivo* (exposure tests using humans or animals: mice, rats) and *in vitro* (where many different cell types can be employed in toxicological tests).

As mentioned in the literature, due to various inconvenients such as unpredictable human health risk, long term exposure (years), diverse human diets, a limited number of cohort studies have been carried out regarding people exposed to various consumer products containing terpenes such as d-limonene. During 1993-1997, a cohort study reported by Rosenman et al. showed 12 % of work-related asthma cases associated with human exposure to cleaning products containing d-limonene [33].

#### 1.4.3.1. *In vivo* studies

*In vivo* toxicological studies have demonstrated associations between ambient chemicals and numerous pulmonary diseases (e.g. asthma, lung cancer, bronchitis) [295 – 297]. Accordingly, several publications are suggesting that certain terpene oxidation products can behave as carcinogens (e.g. formaldehyde), asthma promoters and irritants (e.g. acetic acid) [298 – 304]. At concentration levels typical for indoor environments, toxicological data has linked an increased prevalence of asthmatic

symptoms and an increase of eye blinking frequency associated with humans exposed to d-limonene-ozone (see **Table 6**).

**Table 6** Data on human health effects of d-limonene-ozone reaction

Humans	Pollutant – concentration	Exposure time (hrs)	Human health effects	Ref.
Men	d-Limonene = 511.2 $\mu\text{g m}^{-3}$ Ozone = 198 $\mu\text{g m}^{-3}$	20 min	-increase of blinking frequency by 17% (LOEL of the d-limonene-ozone mixture)	[306]
Women	VOCs (23 compounds) = 26 $\text{mg m}^{-3}$ d-Limonene = 825.5 $\mu\text{g m}^{-3}$ Ozone = 78.4 $\mu\text{g m}^{-3}$	140 min	-lung function and neurobehavioral was not compromised -no significant response of eye blinking	[305]

Acute effects of d-limonene and ozone mixtures on the human lung function do not seem to occur at concentration levels typical for indoor environments, as demonstrated in a study with 130 young women exposed for 140 minutes to a mixture of 23 VOCs (26  $\text{mg m}^{-3}$ ) containing both d-limonene (833.5  $\mu\text{g m}^{-3}$ ) and  $\alpha$ -pinene (0.15 ppmv), in presence or absence of  $\text{O}_3$  (78.4  $\mu\text{g m}^{-3}$ ) [305]. On the other hand, studies have given some evidence of inflammatory reactions at these concentration levels in the respiratory system and significant eye irritation.

Detailed examination of nasal lavage of healthy men exposed to a mixture of VOCs (total, ca. 25  $\text{mg m}^{-3}$ ) carried out by Koren et al., showed that a significant increase of neutrophils - an indicator of inflammatory response - was observed even after 24 h [307].

Data from whole-body human exposures found that 1.8, 40 and 81 ppmv d-limonene concentrations did not produce sensory irritation [308]. However, it has later been demonstrated that a mixture of d-limonene (1222.4  $\mu\text{g m}^{-3}$ ) and ozone (722.3  $\mu\text{g m}^{-3}$ ) did cause eye irritation and increased blinking frequency of male subjects exposed for 20 minutes [306]. In agreement with this, the impact of d-limonene ozonolysis products was confirmed in a human eye exposure study, in which significantly increased eye blink frequency was demonstrated at concentrations below 511.2  $\mu\text{g m}^{-3}$  of d-limonene and 196.1  $\mu\text{g m}^{-3}$  of ozone. In each d-limonene ozonolysis products mixture, the d-

limonene/ozone ratio was 1 and the residual ozone was about  $7.8 \mu\text{g m}^{-3}$  [309]. In another study, nasal inflammation was confirmed as a result of 130 non-smoking women exposed to a mixture of  $694.6 \mu\text{g m}^{-3}$  d-limonene and  $78.4 \mu\text{g m}^{-3}$  ozone (including the reaction products). However, the study failed to link the effect with markers of nasal inflammation (interleukin-6, interleukin-8) [310].

Quite recently, noticeable attention has been paid to secondary pollutants, suspected to be more likely responsible for eyes and airways irritation rather than primary pollutants. To support this hypothesis, a considerable amount of *in vivo* studies (see **Table 7**) were directly looking to the health effects of d-limonene or its oxidative products by exposing mice under different experimental conditions such as time exposure, humidity level, or by varying the concentration of both d-limonene and ozone. The parameters investigated in the majority of the studies were sensory irritation at the upper airway level, bronchoconstriction and pulmonary irritation.

For example, Clausen and co-workers used a mouse bioassay to study the irritancy of products resulting from the reaction between d-limonene and ozone. Parameters such as sensory irritation, bronchoconstriction and pulmonary irritation were used as bio-indicators of chemicals airway irritancy. The 16s reaction mixture of ozone ( $7844.4 \mu\text{g m}^{-3}$ ) with large excess of d-limonene ( $266709.3 \mu\text{g m}^{-3}$ ) produced reductions in the respiratory rate of 33 % in mice during 30-min acute exposures. Based on the irritancy test outcomes, the investigators concluded that "One or more strong airway irritant(s) of unknown structure(s) were formed" that might be responsible for the irritancy effects, since neither the reactants (e.g. d-limonene and ozone alone) nor the identified GC-MS stable reaction products (e.g. formaldehyde) were satisfactory to clarify the irritancy results of the d-limonene-ozone mixture reaction (human sensory irritation of d-limonene has been measured at  $444515.5 \mu\text{g m}^{-3}$  [311]). As an extension of previous study, Rohr et al., has conducted a similar study with slightly modified concentrations for d-limonene ( $18891.9 \mu\text{g m}^{-3}$ ) and ozone ( $100015.9 \mu\text{g m}^{-3}$ ). Apart from the similar effects observed in the former study on the upper airways, the Rohr's study demonstrated a moderate-lasting adverse effect of d-limonene/ozone reaction products in the pulmonary regions [312]. Although the studies of Clausen, Rohr and co-workers have been conducted at concentration levels several orders of magnitude higher than those typical for average indoor environments, these studies point to potential adverse effects that should be addressed in studies at more realistic concentration levels.

**Table 7** Summary of *in vivo* experiments carried out with animals regarding the health effect of d-limonene-ozone mixture (n.p. = not present; NM = not measured)

d-Limonene <sub>i</sub> ppmv	O <sub>3i</sub> ppmv	RH %	T <sup>0</sup> C	Reaction time (s)	d-Limonene ppmv	O <sub>3</sub> ppmv	Species (animals)	Exposure time (min)	Endpoints	Summary of results	Ref.
80	4.0–6.0	20 ± 10	21 ± 2	16	48	0.3 – 0.4	Balb/c mice	30	Sensory irritation	34.% reduction in respiratory rate	[313]
48	4	-1	23 ± 2	162	44	0.03	Balb/c mice	30	Sensory irritation, pulmonary irritation, broncho-constriction	33% reductions in respiratory rate Several d-limonene ozonolysis products identified, eg. 1-methyl-4-acetylcyclohexane, 3-isopropenyl-6-oxoheptanal, formaldehyde, formic acid	[159]

51	3.4	N.p.	N.p.	N.p.	Considered -same as admixing	<0.35	Balb/c mice	60+30min with air or terpene alone	Sensory irritation, pulmonary irritation, broncho- constriction	65% reductions in respiratory rate Airflow limitation was aggravated with d-limonene immediately following exposure to d- limonene/ozone mixture	[312]
46	0.5, 1.2 or 3.5	2% or 32%	N.p.	16 or 30	N.p.	45	Balb/c mice	30	Sensory irritation	Irritation effect was exacerbated at low humidity/short reaction mixtures. The lowest O <sub>3</sub> conc. gave the same result as d- limonene alone. Residual ozone did not cause irritation as NOEL for	[314]

---

									sensory irritation is >1ppmv
6	0.8	21 ± 5	25,5 ± 2 N.p.	NM but 5.2 predicted	0.06	F344 rats	180	Broncho- alveolar lavage fluid biomarkers and lung histeo- pathology	Increased levels of [315] TNF-α, COX-2, SOD in macrophages, Type II cells were induced by the reaction products. The effect on older rats were attenuated compared with younger rats

---

40	4	21 ± 1 2	16	0,5-0,8 (no denuder)	<0.05	Balb/c mice	30	Sensory irritation, pulmonary irritation, broncho- constriction	>30% reduction in respiratory rate and effects in conducting airway without denuder. Denuder employed to remove gaseous reaction products	[316]
52	0.5, 2.5 or 3.9	-5 23 ± 16 2	16	N.p.	-0.05	Balb/cA mice	1h/day for 10 consecutive days	Sensory irritation, pulmonary irritation, broncho- constriction broncho- alveolar lavage	Sensory irritation and airflow limitation was observed. No cumulative effect with increasing exposures and pulmonary inflammation. No effect level of -0,3 ppmv ozone (extrapolated)	[317]

### 1.4.3.2 *In vitro* studies

The conduction of human *in vivo* studies at toxic concentration levels is highly problematic for ethical reasons and there are additional ethical and scientific arguments against animal *in vivo* studies. For example, exposure of mice to carcinogens by the inhalation route produced cancer at the nasal level [318], rather than developing it at the bronchi level, which is commonly observed in humans [319]. Moreover, strong evidence of differences in biotransformation enzymes between humans and animals is reinforcing the idea that animal data may not be appropriate to predict what actually might occur in human lung [320].

The EU directive on animal testing (directive 2010/63/EU) promotes the development and validation of alternative *in vitro* methods that could greatly contribute to better assess the biochemical and metabolic routes and parameters of chemicals, since the first sign of a potential toxic effect occurs at the cellular level. However, there are some limitations when running *in vitro* studies, such as limitations of a wide variety of human cell lines that are not recapitulate the phenotype characteristics, the extrapolation of *in vitro* toxic effects to the *in vivo* situation is not straight forward and there are several aspects, e.g. *in vitro* pharmacokinetics, that need to be understood and considered.

The first approach by scientists to simulate the respiratory epithelia was to use organ slices or isolated organs [321], but experiments of this type have been limited by the lack of reproducibility [322] and functional breakdown of the tissue [323]. Clemedson et al. [324] observed differences in sensitivity between human cells and other mammalian cells. Supporting this observation, Ekwall et al. ran cytotoxicity tests to show that human cell lines predict human toxicity more accurately than nonhuman mammalian cell lines [325, 326]. In comparison to this approach, various cell cultures gained importance by proving to be suitable models of the human bronchio-alveolar epithelium (see **Table 8**).

**Table 8** *In vitro* cellular models available to study *in vitro* toxicity at the pulmonary level

Location	Name	Origin	Characteristics	Ref.
<b>Bronchial</b>	NHBE	Primary cells, not from tumor or being transformed	Differentiated and polarized, form cilia, mucous, limited life span	[327 – 329]
	Epi Airway	Commercially available primary culture	Differentiated polarized model of ciliated and goblet cells, form cilia and secrete mucous, limited life span	[330, 331]
	Mucil Air	Commercially available primary culture	Differentiated polarized model of ciliated and goblet cells, cilia, mucous	[332]
	Calu-3	Bronchial adenocarcinoma	metabolic capacity, mucous production, no clear evidence of mature cilia	[333, 334]
	BEAS-2B	Derived from normal epithelial cells (immortalized by adenovirus 12-simian virus 40 hybrid virus)	Secrete cytokines, used for studying inflammatory response and metabolism, no functional tight junctions, mucous secretion, and cilia	[335]
	16HBE 14o-	Transformed bronchial epithelium (SV40 large T-antigen)	Polarized monolayer, basal cell like morphology, cilia, no mucous secretion	[336, 337]
	HAEPc (Alveolar type I and type II)	Primary human alveolar epithelium, isolated from resected lung	Type II to type I transdifferentiation, presence of lamellar bodies	[338]
<b>Alveolar</b>	A549 (Alveolar type II)	Derived from adenocarcinoma	Features of alveolar type II cells, mucin gene expression, no surfactant protein A, lack of functional tight junctions	[339, 340]
	H441	Derived from the pericardial fluid of a patient with papillary lung adenocarcinoms	considered as a model for alveolar or bronchial level, express mRNA and protein of surfactant protein A	[341]

The THP-1 cell line has been used extensively as a suitable *in vitro* model for primary human monocytes/macrophages to study macrophages polarisation, potential inflammatory effects of various chemicals, or immune diseases [342, 343].

The use of primary cells is not indicated since they reach senescence easily due to a finite life span. To re-establish fresh cultures from explanted tissue implies a significant variation from one cell culture to another. Thus, immortalized cell lines are preferred, since they offer the advantage of indefinite proliferation and good reproducibility within toxicological studies. For the implementation of cell cultures in human pulmonary toxicological studies it is necessary for the cell lines chosen to have similar characteristics with the cells of the human epithelium lung.

Mechanism-derived information (e.g. cellular and molecular mechanism of toxicity) can be provided by running various biological assays. Cytotoxicity assays are used to better understand the normal/abnormal biological processes that control cell growth, division and death but also to give indications on which compounds might have safety concerns in humans.

The first and most easily observed effect succeeding a cell's exposure to chemicals is based on morphological alteration in the cell shape or size which can be checked by using a light microscope. Therefore, the effect of chemicals on the capability of cells to survive or to replicate is another indicator of toxicity that can be measured by various parameters including cell viability investigated by methods such as dye exclusion (e.g. trypan blue or neutral red). This process is normally performed by the exposure of cells to a dye followed by counting in a hemocytometer [344 – 346]. Coloured and transparent cells are counted with the aid of an optical microscope, and their amount is correlated with the amount of dead and viable cells in the cell culture [347]. Generally, one analysis takes at least 5 minutes per sample [348, 349]. A substantial amount of research is currently being oriented towards the development of automatic methods of cell counting such as Coulter counting or flow cytometers [350].

Recent studies have focused on the validation of automatic cell counting instruments for different cell lines [351 – 353], instruments which are based on the Coulter technique and to which sensing tips are attached [354]. Nonetheless, work still needs to be done in order to determine the general validity of these instruments, since the most difficult part to validate is the selection of the appropriate sensing tip, especially when the cell diameter is not known.

Toxicants can alter the cell membrane or the organelles membrane which can further lead to irreversible processes, such as cellular death. In order to distinguish between the

effects of chemicals on specific organelles (e.g. lysosomes, mitochondria) it is recommended to apply a combination of several endpoints within the same *in vitro* experiment [355].

The most frequent cytotoxic method for determining plasma membrane damage induced by chemical compounds is by measuring lactate dehydrogenase (LDH). LDH is a cytosolic enzyme that is released into the cell culture medium upon cell damage or lysis. This process can occur either by apoptosis or by necrosis [356]. The release of LDH into the culture supernatants has been measured for several years by a coupled enzymatic reaction using tetrazolium salts in conjunction with diaphorase [357]. Initially, LDH catalyzes the conversion of lactate to pyruvate via reduction of NAD<sup>+</sup> to NADH. Therefore, diaphorase uses NADH to reduce tetrazolium salt to formazan product (red), which absorbs strongly at 490-520 nm. The amount of colour formed is proportionate to the amount of LDH released in the medium.

One of the most common methods applied to quantify the number of viable cells after their exposure to toxic substances is the Neutral Red Uptake Assay [358]. This cell survival/viability technique is assumed to be universal among cell types, independently of their nature, and is based on the ability of viable cells to incorporate and bind the supravital neutral red dye in lysosomes [359, 360]. Neutral red dye diffuses through the plasma membrane, staining the living cells; therefore the decreased amount of neutral red retained by the cell culture corresponds to cell death.

The detection of toxic effects of chemicals at cellular level can also be investigated by the identification of changes in cell replication/proliferation (e.g. protein content by Bradford assay, bicinchoninic acid assay), cell metabolism (e.g. lysosome and Golgi body activity- Neutral red uptake, mitochondrial integrity) or by the loss of intracellular enzyme (e.g. lactate dehydrogenase – LDH) [361].

On the other hand, new screening methods to predict early biological responses to potential toxic chemicals have been developed with various biomarkers representatives of inflammation response (e.g. cytokines or chemokines) [362, 363] and cellular oxidative stress (e.g. glutathione, reactive oxygen species, caspases) [364, 365].

The most widely used *in vitro* screening method for studying inflammatory reactions is based on the Enzyme-Linked Immuno-Sorbant Assay (ELISA) principle. Considering the high sample volume required by ELISA method, recent technology developments to quantify multiple cytokines (up to 25 different cytokines) in the same sample at the same time has been achieved by multiplex arrays. The most commonly used format is based on the utilization of flow cytometry, but there are multiplex array formats also for

chemiluminescence or electrochemiluminescence.

Molecular oxygen is vital for mammalian cells, since it is participating in the generation process of metabolites such as adenosine triphosphate (ATP). On the other hand, O<sub>2</sub> can also be destructive for the cells, in situations when lung cells activated by exposure to environmental particulates, oxidants (e.g. ozone, carcinogens) start to release chemicals that cause inflammation or produce excessive amounts of ROS or reactive nitrogen species (RNS) [366, 367].

Due to their high instability and reactivity, many ROS are difficult to measure directly. However, three main approaches can be used for *in vitro* methods: i) electron spin resonance for relatively stable radicals, ii) spin trapping methods (isolation of the radical and reaction with the trapping molecule to form a stable radical adduct) and iii) fluorescence based methods (incubating cells with a non-fluorescent probe which, oxidised by intracellular ROS, will convert into a highly fluorescent molecule).

To reduce deleterious effects of oxidative stress (ROS or RNS), there are many redox couples in cells that work together to maintain their homeostasis status.

The most abundant glutathione species are: (1) Reduced glutathione, GSH, which is the active species participating in cell protection; (2) Oxidized glutathione, GSSG, which is formed due to the antioxidant activity of glutathione, and therefore increases in the presence of oxidative stress caused by e.g. free radicals or peroxides; (3) S-nitroso glutathione, GSNO, which is formed due to the conjugation of the thiol group in GSH with nitric oxide and peroxynitrite formed during cell metabolism [281]. Generally, the impairment in GSSG / GSH or GSNO / GSH ratio indicates an alteration of the cellular redox balance which can lead to pathological conditions of the immune or detoxification system [368, 369].

Several methods have been described in the literature to measure reduced and oxidized glutathione. These methods are either based on ELISA tests using commercially available kits [370], or on their separation with HPLC using either fluorescence [371, 372] or UV detection [373]. ELISA kits usually require a high amount of cells (~10<sup>6</sup> cells) to do the analysis [370].

Fluorescent determination, on the other hand, generally provides a considerably higher sensitivity, but presents the drawback of requiring a derivatization step in order to form fluorescent compounds. Derivatization is normally carried out by the reaction with dansyl chloride [371] or with o-phthalaldehyde [372]. Such a derivatization step implies not only a longer and more complex sample treatment, but also that the simultaneous determination of GSH and GSSG is not possible due to the fact that the derivatization reaction is

selective either towards thiol groups or disulphide bonds.

Today's availability of human cell lines poses obvious advantages for *in vitro* studies on the human toxicology of the d-limonene-ozone system. However, only a few of the available methodologies that are described above have been employed for *in vitro* studies of human toxicology of d-limonene-ozone mixtures [374]. At high concentration levels ( $111128.9 \mu\text{g m}^{-3}$  limonene /  $7844.4 \mu\text{g m}^{-3}$  ozone) these authors reported toxic effects of d-limonene ozonolysis reaction products in a human pulmonary cell line (A549) as well as in primary human cells isolated from the nasal cavity, the trachea and the bronchus (Mucil Air). The study evaluated the variation of the cell proliferation and diverse cytokines such as IL-6, IL-8, monocyte chemotactic protein-1 (MCP-1) released from the cells exposed to d-limonene, ozone and the unidentified d-limonene-ozone reaction products.

A statistically significant decrease in cell proliferation was found for A549 cells exposed to the limonene-ozone reaction products compared to control cells exposed only to d-limonene or ozone. An increase of IL-8 and MCP-1 amount was observed in cells exposed to d-limonene for 1 hour. On the other hand, the authors noticed a decrease of MCP-1 levels and cell proliferation when cells were exposed to the limonene-ozone reaction.

The same cell line (A549) exposed to limonene and limonene-ozone reaction for 4 hours increased the amount of IL-8 and MCP-1 when compared to cells untreated.

When human airway epithelium (MucilAir) was exposed to limonene at a concentration of  $2778.2 \mu\text{g m}^{-3}$  for 1 hour / day / 5 days per week during 4 weeks, the inflammation outcomes showed an increase of IL-6. The addition of ozone ( $196.1 \mu\text{g m}^{-3}$ ) to limonene caused the release of both IL-6 and IL-8.

Such results indicate that even if limonene alone does not induce cell death (as they had not observed any significant difference on cell proliferation) it poses an inflammatory effect which renders the production of cytokines by the cells. Limonene-ozone reaction products, on the other hand, are not only inflammatory agents but also may have a role in cell death as demonstrated by the decreased cell proliferation.

They unfortunately did not go further in the chemical characterization of the generated atmosphere during the reaction between limonene and ozone, and were thus unable to identify the compound(s) responsible for the increased cell death.

### 1.5 Aim of the work

Considering the fact that to date, only one *in vitro* study using human cells has addressed the potential toxic effects of the d-limonene-ozone mixture and that their individual reaction products have not been tested as individual compounds and mixtures, more research in this area is needed to be carried out for a complete human risk analysis covering these chemicals.

In the present thesis, the potential human health impact of the three selected d-limonene ozonolysis reaction products: 4-oxopentanal (4-OPA), 3-isopropenyl-6-oxoheptanal (IPOH) and 4-acetyl-1-methylcyclohexene (4-AMCH) as individuals compounds as well as their binary and ternary mixture on human lung cells [bronchial (16HBE14o-), alveolar (A549), activated macrophages (THP-1)] and blood was evaluated in a wide concentration range (including realistic environmental conditions) by using various *in vitro* exposure methods.

With the scope to provide accurate biological outcomes, new methodological approaches for the separation and quantification of the targeted chemicals in gas mixtures and cell culture media based on GC-MSD, GC-FID, HPLC-UV and LC-Orbitrap-MS have been developed/optimized and applied.

*In vitro* toxicological effects have been determined and evaluated through:

- (i) Liquid/Liquid interface exposure (LLI), where the human alveolar cells (A549) and human bronchial cells (16HBE14o-) cultured in plastic wells were exposed to various concentrations of the target chemicals solubilized into the culture media.
- (ii) Air/Liquid interface exposure (ALI), where the apical surface of the selected human cells seeded on transwell inserts were directly exposed to various concentrations (covering also realistic concentrations found in living environments) of the target chemicals prepared as gas phase, by the use of *in vitro* device (CULTEX).
- (iii) *In vitro* PyrogenTest (IPT), where the cryo-preserved human blood in suspension was exposed to various concentrations of the selected chemicals with the aim to investigate the potential inflammatory capacity of the test chemicals which might pass through the alveolar barrier and get in close contact with human blood.

## 2. MATERIALS AND METHODS

### 2.1 Experimental design - Overview

A general experimental design was defined as presented below:

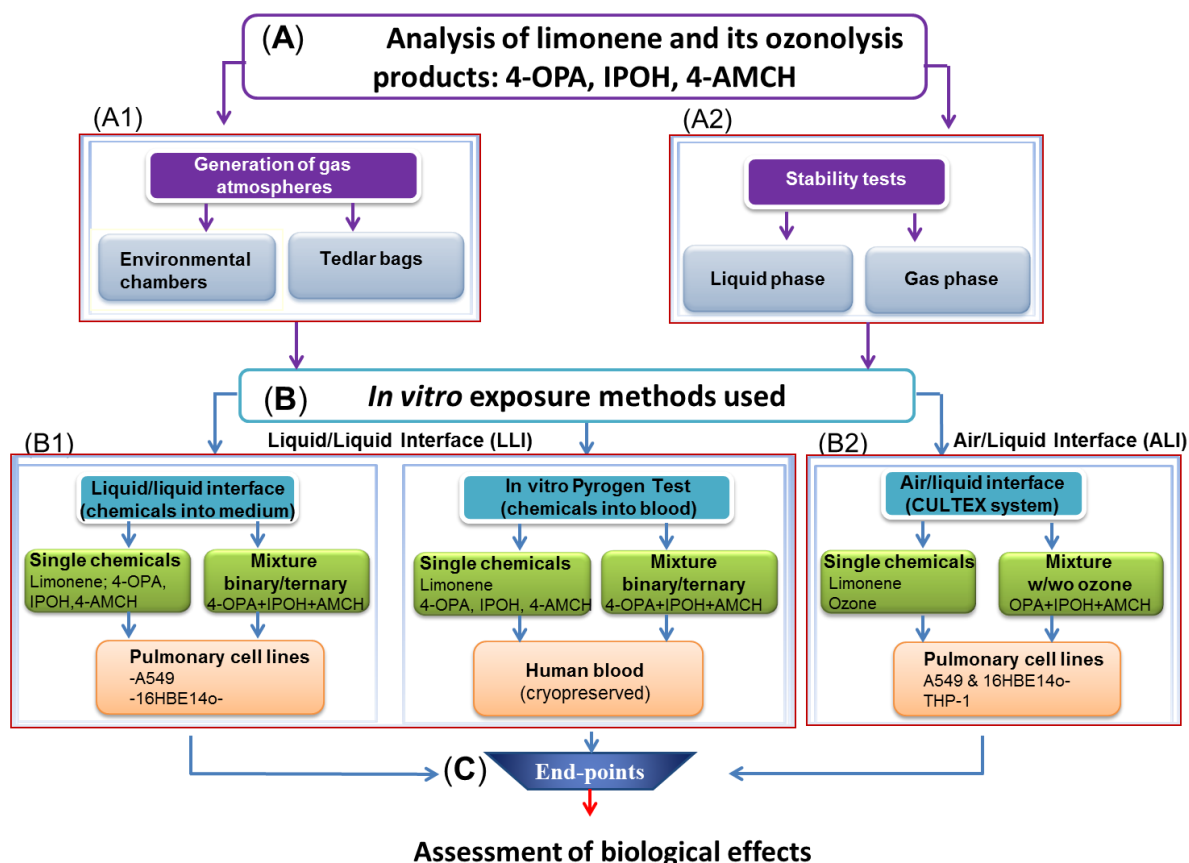


**Figure 5** General overview of the experimental design

#### (A) Analysis of *d*-limonene and its ozonolysis products 4-OPA, IPOH, 4-AMCH

Before studying the *in vitro* cytotoxic effects of the targeted chemicals, new methodological approaches for the separation and quantification of the tested chemicals in gas mixtures and culture media based on gas and liquid chromatography with mass detection (GC/MSD and Orbitrap LC/MS) were developed /optimized and applied.

#### (A1) Generation of gas atmospheres:

In order to gain the most information on the cytotoxic effects of *d*-limonene, ozone, 4-OPA, IPOH, 4-AMCH when human lung cells were exposed to the gas phase of the targeted chemicals, specific techniques and new set-up of the instruments used to generate gas atmospheres (e.g. environmental chambers) were applied.

## Materials and Methods

---

### (A2) Stability tests:

The stability over time exposure of the human lung cells to the above mentioned chemicals prepared both in gas and liquid phase were considered as a pre-requisite for reliable toxicological studies.

Therefore, *in vitro* toxicological studies were carried out through various exposure techniques:

#### (B) *In vitro* exposure methods used

Several *in vitro* experiments were performed by directly exposing the human lung cells and blood to the test chemicals individually and as mixtures added into the cell culture medium (liquid/liquid interface) or prepared as gas phase (air/liquid interface).

#### (B1) Liquid/Liquid interface (LLI)

Individual test compounds (d-limonene, 4-OPA, IPOH, 4-AMCH) and the mixture of (4-OPA + IPOH), (4-OPA + 4-AMCH), (IPOH + 4-AMCH), (4-OPA + 4-AMCH + IPOH) were added to the cells by solubilizing them into the cell culture medium. Additionally, the above mentioned chemicals were added to human blood samples where their potential inflammatory capacity was measured by the *In vitro* Pyrogen Test (IPT).

#### (B2) Air/Liquid interface (ALI):

*In vivo* human inhalation scenarios were simulated with the use of the CULTEX system, where the human lung cells are directly exposed to the gas atmospheres of individual pollutants (d-limonene, ozone) and the mixture of d-limonene/ozone as well as the mixture of (4-OPA + IPOH + 4-AMCH) in presence/absence of ozone.

#### (C) *End-points*

A series of end-points such as cell viability, inflammatory response and oxidative stress were assessed with the scope of ranking all the compounds tested according to their *in vitro* potential toxicity.

Schematic figures of the different biological experiments (including the selected end-points) carried out within this research are described in detail in the following sections.

### 2.2 Materials

#### 2.2.1 Chemicals and equipment

<i>Chemicals</i>	<i>CAS no.</i>	<i>Company</i>
Acetonitrile, 99.8 %	75-05-8	Sigma-Aldrich, USA
4-acetyl-1-methylcyclohexene I, ≥ 95 %	6060-09-1	Sigma-Aldrich, USA
Antibiotic, antimycotic solution		Invitrogen, USA
Bradford reagent		Sigma-Aldrich, USA
Bicinchoninic acid (BCA) protein assay		Thermo Scientific, USA
Collagen solution, 3 mg mL <sup>-1</sup>		Sigma-Aldrich, USA
Cytotoxicity detection kit (LDH)		Roche Life Science, USA
Dichloro-dihydro-fluorescein diacetate (DCFH-DA)		Sigma-Aldrich, USA
Dimethyl sulfoxide	67-68-5	Sigma-Aldrich, USA
E-Toxate water (pyrogen free)	7732-18-5	Sigma-Aldrich, USA
Fetal bovine serum (FBS)		Invitrogen, USA
Fibronectin, lyophilized powder	86088-83-7	Sigma-Aldrich, USA
Human cryopreserved blood		Merck Millipore, USA
3-isopropenyl-6-oxo-heptanal, ≥ 95 %	7086-79-5	Sigma-Aldrich, USA
Isopropyl alcohol	67-63-0	Sigma-Aldrich, USA
(+) Limonene oxide, mixture of cis and trans	203719-54-4	Sigma-Aldrich, USA
d-limonene (liquid form) , ≥ 97 %	5989-27-5	Sigma-Aldrich, USA
d-limonene (gas cylinder)		Air Liquide, Italy
L-Glutathione reduced, ≥ 98 %	70-18-8	Sigma-Aldrich, USA
L-Glutathione oxidized, ≥ 98 %	27025-41-8	Sigma-Aldrich, USA
Methanol, ≥99.9 %	67-56-1	Sigma-Aldrich, USA
Metaphosphoric acid, purum, ~65 % HPO <sub>3</sub> basis	37267-86-0	Sigma-Aldrich, USA
MILLIPLEX MAP Kit		Merck Millipore, USA
Monocyte Activation Test kit		Merck Millipore, USA
Mammalian Protein Extraction Reagent (M-PER)		Thermo Scientific, USA
Minimum Essential Medium (MEM)		Invitrogen, USA
Nitric dioxide (gas)	10102-44-0	Air Liquide, Italy
4-oxopentanal, ≥95 %	626-96-0	Sigma-Aldrich, USA

## Materials and Methods

---

Phosphate buffered saline (PBS)		Invitrogen, USA
Picric acid, ≥98 %	88-89-1	Sigma-Aldrich, USA
Protein standard set (bovine serum albumin)		Sigma-Aldrich, USA
RPMI 1640 medium		Invitrogen, USA
Recovery cell culture freezing medium		Invitrogen, USA
S-nitrosoglutathione, ≥97 %	57564-91-7	Sigma-Aldrich, USA
Sodium Perchlorate monohydrate	7791-07-3	Sigma-Aldrich, USA
Sodium dodecyl sulfate, ≥99 %	151-21-3	Sigma-Aldrich, USA
Trypsin/EDTA solution		Invitrogen, USA
Trifluoroacetic acid	76-05-1	Sigma-Aldrich, USA
Trypan blue solution	72-57-1	Sigma-Aldrich, USA

### *Equipment*

### *Company*

Adsorbent Tube Injector System	Sigma-Aldrich, USA
Amicon ultra- centrifugal filters	Merck Millipore, USA
Analytic balance	Gibertini Crystal 100, Italy
Biopur tips	Eppendorf, Germany
Centrifuge, 5840 R	Eppendorf, Germany
Centrifuge polypropylene tubes	Eppendorf, Germany
Centrifuge plates (96-, 6-well plates)	Eppendorf, Germany
Column YMC ODS-A	YMC Europe GmbH
Column HP5	J&W Scientific, USA
Column Kinetex C18	Phenomenex, USA
Column Synergy Fusion	Phenomenex, USA
CULTEX system	CULTEX, Germany
Data loggers (ESCORT DLS)	Cryopak, USA
Environmental chamber (1m <sup>3</sup> )	Customer made, Italy
Gas chromatography systems used:	Agilent, USA
-Flame ionization detector AGILENT 6890N GC	
-DANI Master TD thermal desorber coupled to a Agilent 7890 GC equipped with a 5975 Mass selective Detector	Agilent, USA
-Perkin Elmer Turbomatrix TD650 thermal desorber coupled to a Agilent 7890 GC equipped with a 5975 Mass selective Detector	Agilent, USA
Fluorescence spectrometer	Perkin Elmer, USA

## Materials and Methods

---

HPLC-UV, 1100	Agilent, USA
Incubator, water jacket CO2	Thermo Scientific, USA
LC-Orbitrap MS	Thermo Fischer, USA
Mass flow controlers (MFC)	Brooks Instrument, LLC
pH meter, 913	Metrohm, Switzerland
Plates culture (6-, 24-, 96-well plates)	Eppendorf, Germany
Polipropylene syringe	Sigma-Aldrich, USA
Scepter pipette	Merck Millipore, USA
SKC pumps (Pocket Pump)	SKC Inc., USA
Sterile filters, PVDF	Merck Millipore, USA
Tenax TA tubes	Supelco, USA
Tedlar bags	SKC Inc., PA, USA
Teflon tubes	Garotti, Italy
Transwells (6-well plate)	Sigma-Aldrich, USA
UV generator Thermo 49	Thermo Fischer, USA
Water bath 285, digital	Thermo Scientific, USA

### 2.2.2 Environmental chambers

Environmental test chambers – normally made of glass or stainless steel, materials that show little sink effects – simulate an environment in which controlled conditions such as temperature, humidity, light, the behavior of a chemical or a chemical reaction can be studied [375].

Before each experiment, the glass walls of the environmental chambers were cleaned with a detergent and washed with clean water. Subsequently, a purge phase with clean air (filtered pre-compressed outdoor air) dried the chamber for approximately 24 hours. In this thesis, experiments were conducted in controlled environmental glass chambers at various sizes from 0.45 and 1m<sup>3</sup>, in which the reaction between d-limonene and ozone was monitored.

### 2.2.3 Human cell lines. *In vitro* exposure systems

Three different human cell lines, representatives of the upper and lower airways of the lung, are being studied in order to assess the cytotoxic potential of the selected test chemicals, as follows: pulmonary alveolar epithelial cell line (A549), bronchial epithelial cell line (16HBE14o-) and human leukemia cell line (THP-1) which was further differentiated in human macrophages. Additionally, human cryopreserved blood was considered within the present study for the detection of the tested chemicals that can induce a fever or inflammation response when they enter into the body.

Two different *in vitro* exposure systems, the conventional liquid/liquid exposure (6-, 24-, 96-well plates) and the air/liquid exposure (transwell porous membranes) were the tools used to expose the cells to the test compounds. The liquid/liquid interface system (LLI) offers the advantage to simultaneously test multiple concentrations of the test chemicals, including negative and positive controls as well as a large number of replicates, while the air/liquid exposure system (CULTEX device), closely simulates the *in vivo* inhalation situation by allowing the direct exposure of the apical surface of the cell culture to the chemicals.

### 2.3 Methods and procedures

#### 2.3.1 Generation of controlled d-limonene-ozone gas atmospheres in environmental chambers

For these experiments, a concentrated (10 ppmv) stream of d-limonene from a commercial cylinder was injected into the air line of the environmental chamber. Ozone was generated by an UV generator (Thermo 49C) and injected into the environmental chamber which was further connected to the *in vitro* CULTEX system.

##### 2.3.1.1 Procedure for the preparation of the environmental chambers before injection of d-limonene and ozone

Before generating controlled atmospheres containing the d-limonene ozone mixture, preliminary preparation of the glass environmental chambers (0.45 and 1 m<sup>3</sup>) was executed as follows:

1. Chambers were operated with Zero air at 0.5 air exchange per hour (ACH). Zero air is supplied by an oil free compressor with a line treatment system composed of a double molecular sieve dryer (mean dew point < -75 °C), a treatment for chemicals removal with an activated charcoal column and pre/post filters for particles removal.
2. The total air flow was set at 3.75 L min<sup>-1</sup>. The total air flow of collected samples was set to be not above 80 % of the total incoming zero air flow. The air flows were controlled and monitored with the use of electronic driven mass flow controllers (MFCs).
3. Air inside the chamber was mixed continuously by an electric fan to ensure homogeneity.

The air exchange rates in the test chamber were controlled at the beginning of the experimental activity using the sulphur hexafluoride decay technique (according to American Society for Testing and Materials (ASTM E741)). Homogeneity was simultaneously controlled with the use of multiple sampling points in the evaluation of air exchange rates.

4. Both temperature and relative humidity were monitored continuously in the experimental chamber by the use of data loggers. The temperature was conditioned by the laboratory temperature, which was set at 23 °C with an observed fluctuation within 1.5 °C. The humidity level, set at 50 %, was achieved by the mixing of dry and humidified air. Humidified air was obtained by bubbling dry air into ultrapure grade

purified MilliQ water. The dry air flow was regulated accordingly to keep relative humidity under control.

5. Background and sink effects were controlled and monitored in the chamber before the test execution. Background controls for VOCs are performed on regular basis. They were performed by sampling and analysing VOCs and carbonyl compounds with sorbent tubes and analysed with the methods reported hereafter.

6. Background VOCs level in the chamber was monitored, resulting to be below  $20 \mu\text{g m}^{-3}$  for TVOCs and  $2 \mu\text{g m}^{-3}$  for single targeted VOC. For this type of test, sink effects were tested separately for terpenes and ozone, in order to estimate their steady state concentration. In the case of terpenes, reversible effects could take place, while for ozone, given its high reactivity, the sink effect test was also included in the passivation step. Passivation was obtained when all possible "reactivity" of the materials in the chamber was saturated and only reversible sinks were left to happen. In the dynamically operated chamber (with a continuous flow of zero air), with a continuously feeding of the chamber with the chemical under investigation at the targeted level, several samples were taken at different points in time to profile the concentration. Operating the chamber in a dynamic mode resulted in the stabilization of the concentration at a steady state value that corresponded to the targeted value for the test.

7. Before running the reaction test of d-limonene-ozone mixture, the chambers were cleaned by passivating them with a mean concentration of 10000 ppmv of ozone over one day.

### 2.3.1.2 Procedure for d-limonene, ozone injection

The experimental set-up used to generate controlled atmospheres of d-limonene ozonolysis reaction products (see **Figure 6**) included the following steps:

1. Standard d-limonene was delivered to the experimental chambers from commercially available concentrated gas cylinders (10 ppmv). Injection into the chambers was made into the flow of Zero air just before it enters the chamber itself. The flow of concentrated d-limonene in dry air was regulated by the use of mass flow controllers. Injection of d-limonene was started and maintained overnight to reach a stable steady state. The time required to reach the steady state concentration depends directly on the air exchange rates: the higher the air exchange rate, the faster the steady state concentration is reached. In this experiment, a 0.5 ACH (Air Change per Hour) was set up, therefore the steady state was reached after approximately 9 hours.

2. Once the target concentration of d-limonene was confirmed by preliminary TD-GC-MSD analysis, ozone was injected into the chamber. Ozone was produced by the use of a UV-light generator in a flow of Zero dry air. A blank test in the chamber with the injection of ozone and without the presence of d-limonene was carried out as well and the ozone concentration reached was around 70 ppbv (this target ozone concentration was selected since is comparable with the ozone concentration normally found indoors). Ozone concentration was monitored with the use of a UV photometric Ozone Analyser.

3. After 24 hours from the ozone injection, a steady state system was reached for the reaction between ozone and d-limonene. Thereafter, the air inside the chamber was collected for VOCs and carbonyls analysis. Sampling of air inside the chambers was made at regular intervals to monitor the concentration evolution. The following time-scheme was applied to sample the VOCs and carbonyl compounds: sampling after 30', 60', 120', 180', 240', 360', and 24h from starting ozone injection.

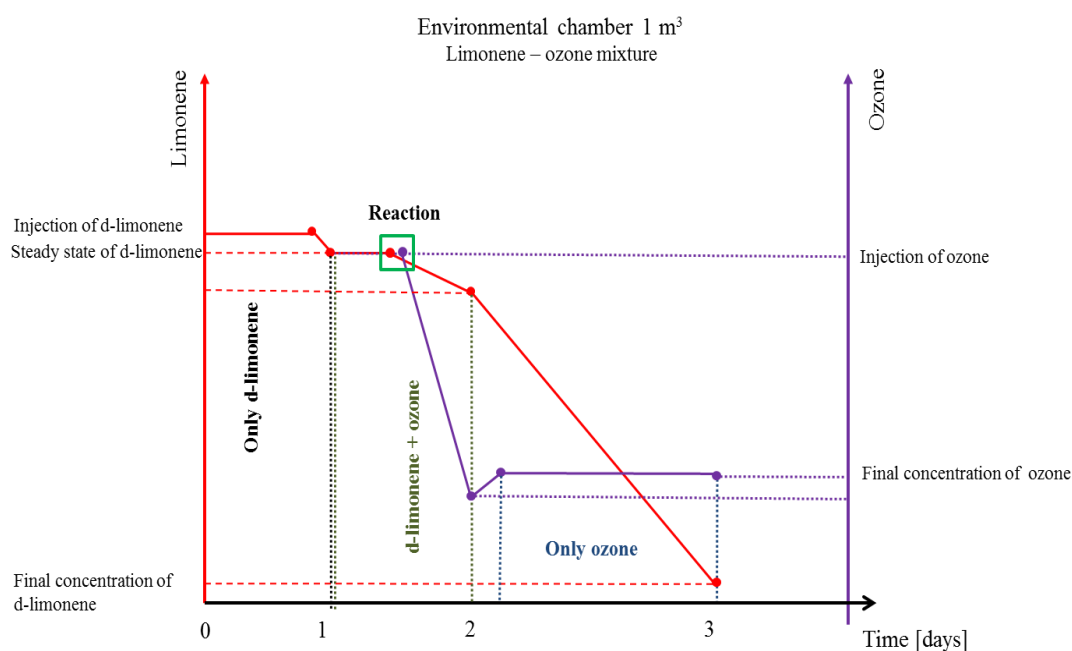


**Figure 6** Generation of gas atmosphere containing d-limonene-ozone mixture in 1m<sup>3</sup> environmental chamber

After the experiments were carried out, the chamber was cleaned by flushing it with humidified Zero air for at least 72 hours. Then background samples were evaluated in order to assure the cleanliness of the environmental chamber.

### 2.3.2 Generation of controlled gas mixture atmospheres with 4-OPA, IPOH, 4-AMCH (in absence or presence of ozone) in Tedlar bags (TBs)

Considering that the target chemicals 4-OPA, IPOH, 4-AMCH are not commercially available in concentrated compressed gas cylinders, the use of Tedlar bags (TBs) were considered to be an effective and reasonable approach for the generation of a controlled atmosphere containing the above mentioned compounds (e.g. less consumption of chemical reagents), atmosphere that was further delivered to the *in vitro* CULTEX system.

In order to comply with the total volume required by the continuous *in vitro* exposures experiments (e.g. 1 and 2 hours), TBs with a capacity of 50 L were prepared following the next steps:

#### 2.3.2.1 Clean-up procedure of TBs

Brand new TBs need several cleaning cycles before they can be used due to the presence of a high level of chemical contaminants (see Results and Discussion chapter), mainly composed of phenol and dimethylacetamide (CAS number 127-19-5), reported also in the literature [376, 377].

The TBs cleaning procedure was executed by several washing cycles consisting in filling and emptying the TBs with dry and humid air. Between the washing cycles, (e.g. at least 10 washing cycles), the TBs were kept in an oven at 100 °C for 2 hours.

The efficacy of the cleaning process was monitored by sampling inner air over TENAX TA tubes followed by qualitative analysis carried out by TD-GC-MS analysis.

#### 2.3.2.2 Generation of the gas atmosphere mixture of 4-OPA + IPOH + 4-AMCH in absence of ozone

Once the TBs were cleaned, test atmospheres were prepared by vaporization of the selected chemical compounds (4-OPA, IPOH, 4-AMCH) in a flow of dry air. The flow of dry air was controlled with the use of MFC which it was set to be at around 2 L min<sup>-1</sup>.

The vaporization of the target liquid chemicals was realized using a glass chamber heated to 100°C through which both water and the selected chemicals were injected into the TBs. The utilized Teflon tube was protected from light (see **Figure 7**). By this procedure, a level of 50 % of relative humidity was reached. The amount of test

compounds to be injected was calculated from the vapor pressure data of each single compound and adjusted accordingly after the evaluation of sink effects inside the TBs. To aid vaporization and to prevent possible degradations, the injection of chemical compounds into the ATIS system was done over the injection of the amount of water needed.

The total duration of a TBs filling (at 80 % of its whole capacity) was around 20 minutes, which sufficed for complete vaporization.



**Figure 7** Injection of a mixture of water-target compounds 4-OPA, IPOH, 4-AMCH in TBs with the scope to generate gaseous atmosphere. On the left side: the heater and on the right side: the TBs protected from light with aluminium foil

### 2.3.2.3 Generation of the gas atmosphere mixture of 4-OPA+IPOH+4-AMCH in presence of ozone

For the preparation of TBs with an atmosphere that includes both the selected d-limonene ozonolysis reaction products 4-OPA, IPOH, 4-AMCH and ozone, the steps described below were executed:

1. Initially, a TB of 5 L volume containing ozone at a very high concentration (ca. 100 ppmv) was prepared by attaching the TB directly to the UV-generator (see **Figure 8**).

Approximately 30 mL of ozone (this final amount was determined experimentally by injecting different volumes (mL) of concentrated ozone from the TB of 5 L to the TB of 50 L) was aspirated from the TB by using a polypropylene (PP) syringe and then injected in the TB (50 L) which was already containing the target mixture of 4-OPA, IPOH, 4-AMCH prepared as described above.



**Figure 8** Main steps involved in the generation of gas mixture atmospheres in TBs: 1. Ozone generator; 2. Sampling of ozone with the PP syringe; 3. Injection of ozone in the TBs already containing the mixture of 4-OPA+IPOH+4-AMCH

In order to avoid light degradation of the chemical mixture in the TBs, the bags were covered with aluminum foil and used for the *in vitro* exposure experiments within the same day of preparation. Furthermore, both d-limonene ozonolysis reaction products concentration and background contamination was checked in the gaseous mixture created in TBs, by collecting various samples with a flow/low volume setup [ $50 \text{ mL min}^{-1}$ ].

For the CULTEX reference line a second TB was prepared and filled only with humidified zero air.

### 2.3.3 Chemical analysis of d-Limonene and ozonolysis reaction products: 4-OPA, 4-AMCH, IPOH by TD-GC-MS

#### 2.3.3.1 Sampling procedure for d-limonene and d-limonene ozonolysis reaction products: 4-OPA, IPOH, 4-AMCH

Prior to sampling, the flow rate of the pump was calibrated by pumping laboratory air through a representative Tenax TA tube and measuring the flow by means of a primary calibrator. Additionally, Tenax tubes were preconditioned by pumping an inert gas (helium or nitrogen) at  $300 \text{ }^\circ\text{C}$  for two hours at a flow rate of  $50 \text{ mL min}^{-1}$  and the blank background chromatogram of each tube was recorded by thermal desorption-GC-MS. The preconditioned tubes were tightly closed with Swagelock caps and stored at room temperature away from any sources of VOCs until they were used for air sampling. For quality assurance purposes, a blank Tenax tube was stored together with the Tenax TA tubes in the same box in order to use it as field blank.

Duplicate air samples containing VOCs were collected from variously sized environmental chambers ( $0.45$  and  $1 \text{ m}^3$ ) by pumping the air through Tenax TA

sorbent tubes using commercial portable SKC pumps. Samples were collected by connecting the bottom entrance of the Tenax tube to the calibrated pump. In the case that samples were collected from the inside of environmental chambers or from tubes in the stream of air, the tubes were inserted directly through the sampling port and attached by Swagelok fittings. When TBs were in use, it was also possible to sample without using fittings, by the means of Teflon tubes  $\frac{1}{4}$  internal diameters. In all cases it was ensured that the sample procedure was leak tight.

### 2.3.3.2 Breakthrough phenomena investigation

In order to ensure data quality, any breakthrough phenomena was evaluated by placing in-line a second tube after the sampling tube, as represented in **Figure 9**. In this way, any pollutant that was not retained by the primary tube would be adsorbed in the second one. Thus, considering that the amount of pollutants on the secondary tube was below the detection limits in all cases it can be excluded that the primary tube suffered from breakthrough and thus, the amount adsorbed on such tube was representative of the amount of pollutant present in the sampled air.

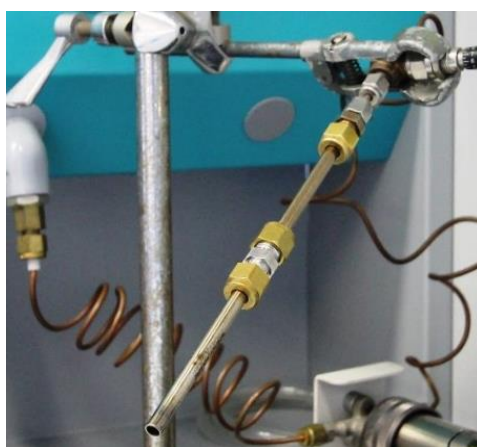


**Figure 9** Breakthrough phenomena investigation

Unless otherwise stated, air sampling was carried out at  $100 \text{ mL min}^{-1}$ . However, the flow rate was lowered to  $50 \text{ mL m}^{-1}$  whenever a high concentration of chemicals was expected (e.g.  $150 \mu\text{g m}^{-3}$ ) to avoid breakthrough phenomena that would lead to a false result. The collected sample volume varied according to the chemicals' concentration in the sampled air spanning from 250 milliliters (concentrated TBs and gas cylinder flows) up to a maximum of 7.2 L (real environment for high sensitivity detection of very low concentrated chemical species).

### 2.3.3.3 Analytical method (TD-GC-MS) for the quantification of d-limonene and its ozonolysis reaction products: 4-OPA, 4-AMCH, IPOH

The Tenax TA tubes were analysed using a Perkin Elmer Turbo Matrix 650 thermal desorber (TD) coupled to an Agilent 7890 GC-MS system. Desorption was carried out at 280 °C for 10 min followed by introduction of the sample into the GC. The column was a 60 m x 0.25 mm with 0.25 µm film thickness (J&W HP5-MS UI, 5 % Phenyl Methyl Siloxane). The GC oven programme was as follows: 10 °C for 1 min, ramp 1: 2 °C min<sup>-1</sup> to 50 °C, and ramp 2: 12 °C min<sup>-1</sup> to 300 °C hold for 2 min. Helium was used as carrier gas at an inlet pressure of 0.97 bar (ca. 1.5 mL min<sup>-1</sup>). The mass spectrometer was operated in TIC/Scan mode from 30 to 550 amu. Transfer line and source were kept at 220 °C. Diluted reference standards were prepared in methanol or acetonitrile solutions and were spiked into Tenax TA tubes, dried under a low flow stream of Helium and then analyzed with the TD-GC-MSD system. Three points calibration were applied ( $R^2 > 0.995$ ) using authentic standards in methanol for 4-OPA. Analysis duration takes approx. 44 minutes.

The method was adapted for the analysis of samples collected at high (ppmv) and low (ppbv) concentrations: (i) direct injection of the collected air sample into the column to achieve the maximum sensitivity; (ii) split injection mode of the collected air sample in order to avoid the saturation of the chromatographic system and to enable evaluation of highly concentrated samples. The direct injection was performed using a Perkin Elmer Turbo Matrix 650 TD, directly connected with the analytical column, while the split injection was performed using a DANI Master TD Thermal Desorber connected with the split/splitless injector of the GC. The parameters used for split injection mode are the following: The column was a 30 m x 0.25 mm with 1 µm film thickness (J&W HP5-MS UI, 5 % Phenyl Methyl Siloxane). The injector was in split mode set at 250 °C with a split ratio of 1:50. The detector 5975 Mass Selective Detector was operating from 30 to 530 amu scan range. T-line at 280 °C, source at 250 °C. The GC oven temperature was initially set at 40 °C hold for 7.5 min, with rate 1 at 4 °C min<sup>-1</sup> to 90 °C and rate 2 at 15 °C min<sup>-1</sup> to 300 °C, hold for 2 min.

### 2.3.3.4 Stability tests of 4-OPA, 4-AMCH, IPOH in the culture medium by GC-FID

The potential interaction of selected chemicals with the cellular medium components (e.g. proteins) was investigated before running any *in vitro* toxicological test. The reason behind is that this interaction of the test chemicals with the culture medium would lead to an uncontrolled environment exposure for cells, since the target chemical concentration would be continuously modified over time. Therefore, qualitative tests were prepared and performed for the evaluation of the stability of 4-OPA, IPOH, 4-AMCH solubilized into cell culture medium. The stability of chemicals was assessed for diverse culture medium formulation covering 24 hours – the maximum exposure time used – as indicated below:

- (i) Target chemicals were solubilized at a concentration of  $0.6 \text{ mg mL}^{-1}$  into the culture medium, which was containing two different concentrations of fetal bovine serum: one with 10 % and the other with 1 %.
- (ii) The glass vials containing aliquots of chemicals prepared in culture medium were kept at  $37 \pm 1 \text{ }^{\circ}\text{C}$  for 24 hours (incubator temperature and time conditions used during cell exposure) and aliquots were analyzed at given time intervals 1, 2 3 and 24 hours (after their solubilization into the culture medium).

The chromatographic peak areas of the target chemicals solubilized into culture medium was compared to the corresponding peak areas of the standards prepared in acetonitrile.

The stability of chemicals prepared in the culture medium was analyzed using an Agilent GC 6890 with a liquid injection autosampler. The injector was set up in split mode at  $250 \text{ }^{\circ}\text{C}$ , with a split ratio of 1: 20. The flame ionization detector (FID) was at  $250 \text{ }^{\circ}\text{C}$ . The column used was a J&W HP-5MS, 5% Phenyl Methyl Siloxane, 30 mt x 0.25 mm i.d. with  $1 \text{ }\mu\text{m}$  film thickness. The GC oven temperature was initially at  $40 \text{ }^{\circ}\text{C}$  hold for 7.5 min, then rate 1 at  $4 \text{ }^{\circ}\text{C min}^{-1}$  to  $90 \text{ }^{\circ}\text{C}$ , rate 2 at  $15 \text{ }^{\circ}\text{C min}^{-1}$  to  $300 \text{ }^{\circ}\text{C}$ , hold for 2 min. Helium was used as carrier gas at  $1.5 \text{ mL min}^{-1}$ . The injection volume used was  $1 \text{ }\mu\text{l}$ .

### 2.3.3.5 Intracellular glutathione species (GSH, GSSG, GSNO) determination by in house HPLC-UV method

#### *Instrumental:*

#### HPLC-UV equipment:

The separation and determination of GSH, GSSG and GSNO molecules was carried out using an Agilent 1100 Series HPLC system composed of binary pump, autosampler and diode array detector (Agilent, Santa Clara, USA). Their separation was achieved on a ODS-A C18 column (YMC, Japan.YMC-Pack, 150 mt x 4.6 mm) with a 5  $\mu\text{m}$  particle size, coupled to a Guard-c precolumn (YMC-Pack, 10 mt x 1-4,0 mm). Data were processed with ChemStation software (version A.08.03, Agilent).

The HPLC analysis was performed using isocratic elution with a mobile phase's composition of water/acetonitrile ( $\text{H}_2\text{O}$  / AcN: 95 / 5, v / v), trifluoroacetic acid (TFA : 0.1%) and sodium perchlorate ( $12 \text{ mg mL}^{-1}$ ) and a flow rate that was adjusted to  $1 \text{ mL min}^{-1}$ . The detection wavelength was set at 215 nm by UV detector. The column oven temperature was kept at room temperature, while the auto-sampler temperature was maintained at  $4^\circ\text{C}$ . A volume of  $10 \mu\text{L}$  of standards or sample solutions (e.g. the cell culture lysate) was directly injected to the HPLC equipment and further analysed. Under these conditions the three selected glutathione species were simultaneous determined in less than 6 minutes.

Different chromatographic conditions such as mobile phase ratio, injection volume, flow rate were optimised before the validation of the method. In-house validation was evaluated by linearity, limits of detection (LODs), limits of quantification (LOQs), reproducibility, repeatability and recovery.

In order to avoid degradation of glutathione, standard solutions and samples were prepared in amber vials and cooled to  $4^\circ\text{C}$  on the auto sampler well plate. A fractional factorial design was applied for the optimisation of the mobile phase composition used in the chromatographic separation of GSH, GSSG and GSNO. Moreover, their stability during the analysis was checked at the beginning and the end of analysis. Additionally, the potential degradation of standards stored under different conditions ( $4, -20, -80^\circ\text{C}$ ) was verified. These temperatures were selected to interrupt any enzymatic activity in the cells, thereby minimizing the risk of any species inter-conversion from the moment of exposure to the target pollutants finishes and the analysis of intracellular glutathione species in the cells takes place.

#### Extraction equipment:

The ultrasonic water bath (Starsonic 35, 28-34 Hz) was supplied by Liarre, Italy. A 5417R centrifuge (Eppendorf, Germany) was used to separate the supernatant from

the cellular debris. Microcentrifuge tubes (Amicon filters, Millipore, USA) were used to collect, filtrate and concentrate the cellular extract. The protein quantification from the cellular debris was performed by using an EnSpire Multimode Plate Reader with integrated software (Perkin Elmer).

### Exposure equipment for human lung cells:

Direct exposure of the human lung cell lines (A549) at the air/liquid interface was performed by using an *in vitro* cell culture exposure device named CULTEX (Germany).

Chemical liquid treatment of the selected cell lines was carried out in cell culture plates under a biological fume hood (Steril-CTH, Angelantoni Life Science) and then placed in an incubator Forma Series II 3110 Water-Jacketed CO<sub>2</sub>, (Thermo Scientific, USA).

### Preparation of glutathione standard solutions:

Stock solutions containing 20 mM GSH (MW 307.3), GSSG (MW 612.6), GSNO (MW 336.3), were prepared in the same buffer as was used for the intracellular extraction of glutathione (e.g. 0.5 % picric acid + 25 mM ammonium sulfate added to the mobile phase). Since picric acid has been shown to be an explosive compound [378], safety guidelines (e.g. working under a well-ventilated fume hood, wearing protective equipment etc.) were applied during all the experiments to prevent inherent dangers of picric acid use.

### Stability test:

Glutathione stability in standards solutions and biological samples was done in order to check their decomposition or oxidation of glutathione molecules over time. Aliquots of the standard solutions (GSH, GSSG, and GSNO) were stored at -80 °C for 10 months (weekly verification tests were performed by quantifying diluted aliquots of selected glutathione species).

### 2.3.3.6 Metabolomics screening analysis using LC-MS Orbitrap in ad hoc experiments

LC-MS analyses were performed on a Ultimate 3000 micro flow-liquid chromatography system (Dionex) coupled on-line with a LTQ Orbitrap XL Fourier Transform high-resolution mass spectrometer (Thermo Scientific) equipped with an electrospray ionisation source (ESI). The LC-MS system was operated using XCalibur 2.0.7 software (for the MS) and Chromeleon 6.8 software (for the LC).

A 96-well plate containing samples was placed on the auto-sampler of the LC system. Samples were loaded and pre-concentrated on a Waters Atlantis T3 guard cartridge (2.1 mm x 10 mm, 3 µm). Metabolites were separated on a Waters Atlantis T3 column

(1.0 x 150 mm, 3 µm). The micro LC pump was operated at a flow rate of 40 µl min<sup>-1</sup>. The eluents used were (A) 0.1 % HCOOH in Milli-Q H<sub>2</sub>O, (B) 0.1 % HCOOH in CH<sub>3</sub>CN and (C) 0.1% HCOOH in CH<sub>3</sub>OH.

The linear gradient used to achieve the analytes separation was as follows: 0-1.5 min: 95 % A, 5 % C; 10 min: 2 % A, 48 % B, 50 % C; 10-11 min: 2 % A, 48 % B, 50 % C; 11.1 min: 2 % A, 98 % B; 11.1-12 min: 2 % A, 98 % B; 12 min: 2 % A, 98 % B; 12.1 min: 98 % A, 2 % C; 12.1-17 min: 98 % A, 2 % C.

The LTQ Orbitrap instrument was operated in the MS mode using the Orbitrap analyser.

Optimised settings were as follows: Capillary voltage, 45V; Tube lens voltage, 135 V; Spray voltage, +3.5 kV; Transfer capillary temperature, 200 °C. The FTMS (Orbitrap) analyser was calibrated using a solution of caffeine, MRFA (L-methionyl-arginyl-phenylalanyl-alanine aceate x H<sub>2</sub>O) and Ultramark 1621 in the range m/z 50-1000.

MS acquisition was performed over the full m/z range with a scan time of 0.7s. The resolution was 30,000 FWHM and mass accuracy was in the range 1-5 ppm. LC-MS data were generated in the continuum mode.

Analysis design for metabonomics involves the analysis of quality controls (QCs) to establish the repeatability and intermediate precision of the LC-MS method, analytical blanks (for possible contamination) and randomised study samples (negative control and treated cell extracts). A batch of analysis corresponds to a biological replicate (6 independent experiments) including untreated (C = control or negative control) and treated with low dose (L), which represents the chemical concentration that is generally selected based on the toxic effect that it has on the cellular viability of the selected cell cultures (e.g. inducing a reduction of 1 % loss of cellular viability) and with high dose (H), that corresponds to the chemicals concentration which reduces the cellular viability by 10 %). Samples were run in a randomized order with the analytical blanks and QCs analyzed 9 times during the sequence.

### **2.3.4 Biological measurements carried out in human cells and blood**

#### 2.3.4.1 Human alveolar epithelial cell line (A549) description

The human tumour alveolar epithelial cell line (ATCC #: CCL-185™) established in 1972 derived from an alveolar carcinoma and in accordance with toxicology literature, it has been characterized as a type II pulmonary epithelial cell model for drug absorption and metabolism (see **Figure 10**).

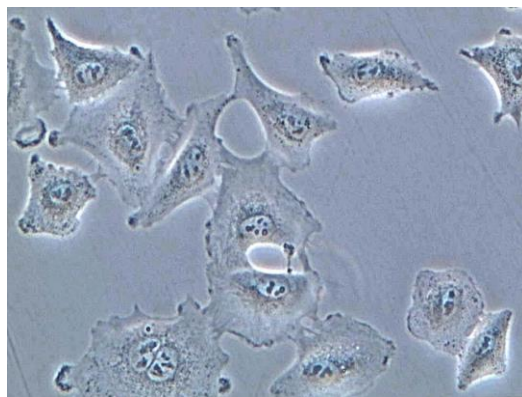


**Figure 10** Observation of viable A549 cells done under Nikon optical microscope

As reported by Foster et al., the A549 cell line forms a confluent monolayer with a morphology characteristic of type II cells that have preserved their polarity and their ability to transport elements out of the basolateral side. Additionally, Lieber et al. observed the presence of short and small microvilli on the surface of A549 cells and the lamellar body was within cytoplasm, those characteristics closely matching the type II alveolar cell phenotype [379]. Also, it has been reported that A549 cells have conserved expression and functionality of some of the P450 isoenzymes involved in xenobiotics metabolism: CYPs 1A1, 1B1, 2B6, 2C, 2E1 [380].

The main functions of type II alveolar cells (also called Type II pneumocytes) are as follows: 1) to synthesise and secrete the pulmonary surfactant, 2) to control the alveolar fluid levels by water recapture using active sodium transport to return excess alveolar surface water to the interstitial fluid, and 3) to be the progenitor cell which can proliferate to restore both type I and type II cells after an alveolar disorder produced by harmful inhaled xenobiotics.

Reported as being a valuable model for studies of lung epithelial structure and the occurrence, development, and treatment of lung cancer [381, 382 ], A549 cells were used in the present research to assess the toxic effects of inhaled chemicals at the pulmonary epithelium level.

### 2.3.4.2 Human leukemia cell line (THP-1) description

The human monocytic leukemia cell line THP-1 (ATCC #: TIB-202™) was isolated by Tsuchiya et al. from the blood of a boy suffering from acute monocytic leukaemia (see **Figure 11**) [384].

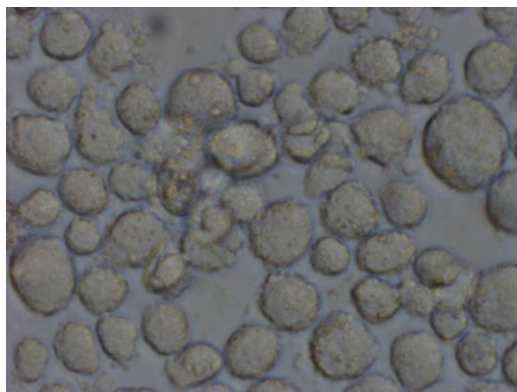


**Figure 11** Observation of viable differentiated THP-1 cells under Nikon optical microscope

The THP-1 cell line can be stopped from proliferating and activated to differentiate into functional macrophages cells, after treatment with phorbol esters (PMA). Previous studies attempted to identify a more natural inducer of differentiation in THP-1 cells, but none of the tested compounds (vitamin D, retinoic acid or cytokines: IL-1, IL-2, TNF, GM-CSF) had the capacity to completely induce the differentiation [383 – 386].

The criteria for selecting the THP-1 cell line for this research were: (1) it should possess an enzymatic activity typical of monocytes [387] and (2) it should not have prominent chromosomal abnormalities as other lines of human leukemia cells [388].

The THP-1 differentiated macrophages cells are considered as a valuable *in vitro* model for the investigation of human macrophages involvement in inflammatory disease since they can release a series of pro-inflammatory cytokines which further can secrete cytokines such as IL-8, IL-6, and MCP-1, leading to lung inflammation [389, 390].

#### 2.3.4.3 Human bronchial epithelial cell line (16HBE14o-) description

The 16HBE14o- cells (see **Figure 12**) were a gift from Dr. Dieter C. Gruenert (Cardiovascular Research Institute at the University of California, San Francisco, California, USA).

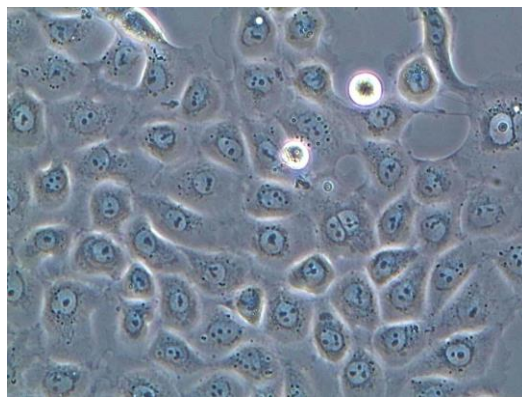


**Figure 12** Observation of viable 16HBE14o- cells under Nikon optical microscope

It has been reported by Cozens et al. that this cell line was generated by the transformation of normal bronchial epithelial cells obtained from a one-year-old male heart-lung transplant patient [337]. As mentioned by the same author, the 16HBE14o- cells retain differentiated epithelial morphology by forming polarized cell layers with cilia and microvilli [391]. Other studies have demonstrated that the 16HBE14o- has the potential to be used in drug absorption models [392, 393] and has the capacity to react to inflammatory stimuli like the primary human bronchial epithelial cells [394]. Much of the recent literature has been using polarized 16HBE14o- cells to study drug transport [393], gene delivery [395], and the barrier function of the airway epithelium [396].

Major factors that promote the differentiation of 16HBE14o- cells in culture are the extracellular matrix (collagen-fibronectin coated supports), the growth medium containing retinoic acid and culture at an air-liquid interface [397]. It has been demonstrated that by maintaining these conditions, the cells retain the properties of differentiated airway epithelial cells, including the formation of tight junctions, regulated ion transport and morphological features, including apical microvilli and cilia [398].

16HBE14o- has been used for toxicity studies with diesel exhaust ultrafine particles [399], with biodegradable nanoparticles [400] and cigarette smoke [401].

#### 2.3.4.4 Cryopreserved Human Whole Blood description

Controlled cryopreserved human whole blood (**Figure 13**) was purchased from Merck, (Darmstadt, Germany) and used according to the manufacturer's instructions.

The alveolar regions are an attractive site for absorption into systemic circulation. Therefore, some of the inhaled chemicals (depending on their physical-chemical

characteristics) which enter the respiratory tract can be deposited in peripheral lung tissue. At this point, they can easily cross the pulmonary blood barrier and gain access to the blood circulation, further being transferred to the liver and other tissues/organs.

Reliable *in vitro* tests designed to predict unexpected harmful effects of various chemicals/drugs are highly requested in immunologic diagnosis. In order to improve assay reproducibility, researchers have compared the reactivity of the cryopreserved blood with that of fresh blood, since fresh blood poses various problems such as high variability between samples, short time for analysis after blood collection and problematical continuous availability of fresh blood samples. The cryopreservation procedure proposed by Schindler et al., demonstrates that fresh blood can be substituted with cryopreserved blood without affecting the viability and functionality of monocytes and lymphocytes and it offers several advantages such as a homogeneous batch of blood, preliminary tests to certify the absence of blood infections such as HIV or hepatitis and the reduction of variability of inter- and intra-aliquot blood. In the execution of *In vitro* Pyrogen Test (IPT), the reaction of cryopreserved blood to different pyrogenic and non-pyrogenic substances showed a similar performance to fresh blood [402].

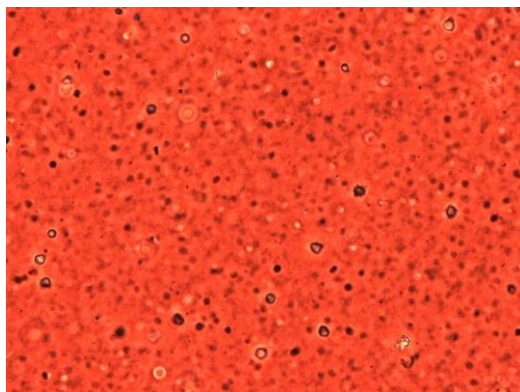


**Figure 13** Observation of viable human cryopreserved blood under Nikon optical microscope

### 2.3.4.5 Cell culture maintenance, sub-culturing and counting protocols

#### Cell culture maintenance

The derived human cell lines A549 and THP-1 were routinely cultivated in RPMI 1640 medium, supplemented with 10 % fetal bovine serum (FBS), 2 mM L-glutamine, 100 unit mL<sup>-1</sup> penicillin and 100 µg mL<sup>-1</sup> streptomycin at 37 °C under humidified atmosphere containing 5 % CO<sub>2</sub>.

The human bronchial epithelial cell line (16HBE14o-) was cultured in flasks in-house coated with a solution containing LHC basal medium, 1 mg mL<sup>-1</sup> human fibronectin, 3 mg mL<sup>-1</sup> bovine collagen type I, and 1 mg mL<sup>-1</sup> BSA. The composition of the cell culture medium was prepared by mixing MEM and 10 % fetal bovine serum supplemented with penicillin (100 units mL<sup>-1</sup>) and streptomycin (100 µg mL<sup>-1</sup>). Once the solution was prepared, the distribution across the surface was carried out immediately to make sure that the entire surface was wetted. Subsequently, all the coated materials were dried overnight under laminar air flow and neutralised by washing twice with PBS before seeding the cells.

In order to keep a good reproducibility between experiments by avoiding variations of their phenotype, the cells were used only between the 3rd and 15th passage after thawing. Additionally, all cell cultures were tested monthly for the presence of mycoplasma.

### Cell sub-culturing procedure

Prior to sub-cultivation, the cell culture conditions (e.g. confluence, fungi contamination) were examined under a light microscope. The following steps of the subculture procedure were executed:

1. The culture media was aspirated and the cell culture monolayer was washed twice with 5 ml of PBS;
2. 5 ml of 0.25 % trypsin-EDTA was added to the adherent cells (A549 and 16HBE14o-) and incubated with cells for a maximum of 5 minutes. THP-1 rounded floating cells were harvested by transferring a certain amount of cells into a new flask containing new fresh media;
3. A549 and 16HBE14o- cell suspension was transferred to a 15 ml Falcon tube and centrifuged at 1200 rpm for 5 minutes;
4. the supernatant was aspirated and the pellet was re-suspended in fresh complete media;
5. cell viability was assessed by an automatic cell counter, Scepter pipette;
6. an adequate amount of cells was added to the new culture flasks already containing 15 mL of complete media preconditioned at 37 °C in a humidified 5 % CO<sub>2</sub> incubator.

### Cell counting protocol

The number of all types of cells was determined by using the automatic cell counter, Scepter 2.0 pipette. The sceptor counting procedure was applied using manufacturer instructions (Millipore). Briefly, the cellular suspension was counted, as follows:

1. Sample preparation was carried out by taking an aliquot from the mother cellular-suspension and diluted in phosphate PBS to a total minimum volume of 100  $\mu$ L
2. The sensor tip was selected based on the cell diameter
3. The Scepter pipette was turned on, and the sensor tip was attached
4. The pipette was fixed inside the Eppendorf tube with the cellular suspension and by pressing the plunger of the pipette, 50  $\mu$ L of the cell suspension was drawn into the sensor channel.
5. Once counting was complete, the sensor was detached and with the displayed histogram, the viable/dead cell number was calculated based on cell volumes or cell sizes indication.

### 2.3.4.6 *In vitro* exposure method: Liquid-Liquid interface (LLI) and its protocols

The cytotoxic effects of the selected chemicals were investigated by, on the one hand, exposing *in vitro* cultures of human pulmonary epithelial cells (A549 and 16HBE14o-) and human blood to the compound which was previously solubilized into the culture medium (liquid/liquid interface exposure method); and, on the other hand, exposing *in vitro* cultures of human pulmonary epithelial cells (A549 and 16HBE14o-) to the chemicals prepared in gas atmospheres (air/liquid interface exposure method applied by the use of CULTEX system).

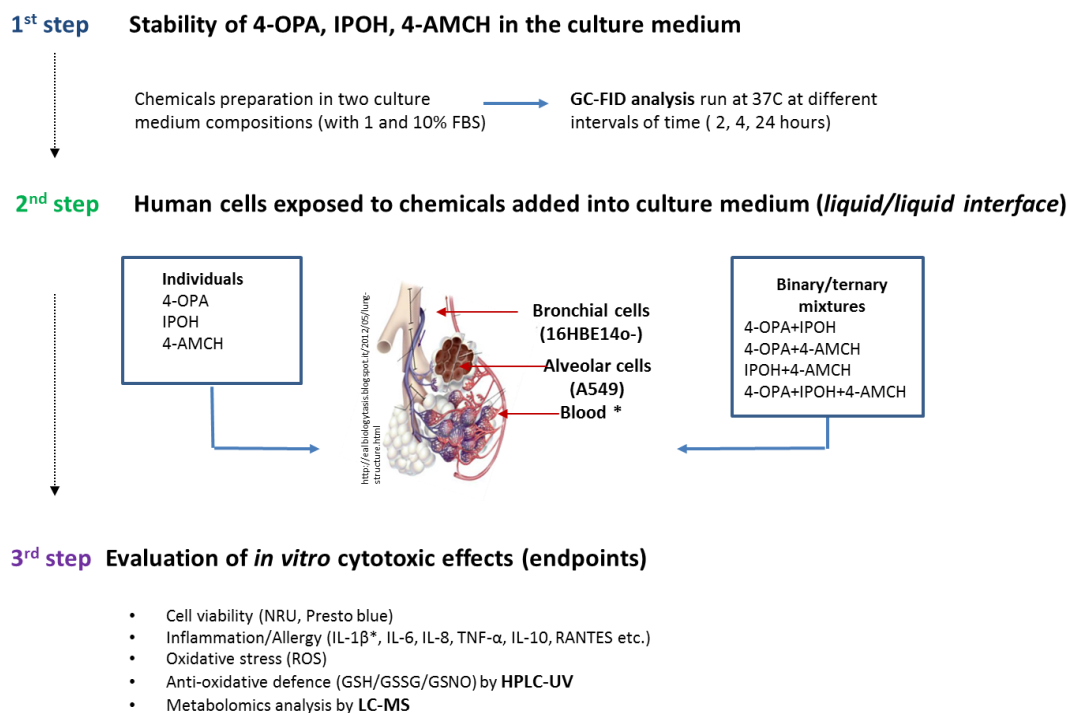


**Figure 14** Schematic illustration of the experimental steps followed in the study where the human alveolar, bronchial cells and blood are exposed to the test chemicals solubilized into the culture media

Before exposure of the cells to the multiple concentrations of the selected chemicals (in 96-well plates), the stability of the above mentioned chemicals prepared in different composition of the culture medium (e.g. 1 % and 10 % of FBS) was determined over time.

### *Preparation of test chemicals*

Stock solutions were freshly prepared by dissolving the chemicals in the cell culture medium (DMEM supplemented with 1 % FBS). Serial dilutions from the stock solution were freshly prepared and used within the same experiment day. For NRU assay, where the cytotoxic effects of chemicals was tested on cellular viability, the stock solutions of the mixtures (binary and ternary) were also prepared in the DMEM supplemented with 1 % FBS. The initial concentration of the mixtures was based on the IC<sub>50</sub> calculated from the concentration-response experiments with the individual chemicals. Then 10 different concentrations were prepared by serial dilution with a dilution factor of 2.

To assess the cytotoxic potential of chemicals on human lung cells, various biomarkers were selected and measured via different biological assays, as follows:

- (i) Neutral red uptake, Presto blue assays and Scepter counting pipette were performed to detect the chemical's cytotoxicity impact on the cellular viability.
- (ii) Lactate dehydrogenase (LDH) assay was used to measure the amount of LDH released into the culture medium, being an indicator of cellular membrane damage.
- (iii) Reactive oxygen species (ROS) and intracellular glutathione content (reduced -GSH, oxidised - GSSG, nitroso - GSNO) were determined to investigate the involvement of test compounds in the oxidative stress process.
- (iv) Cytokines/chemokines levels released in the culture medium were quantified to explore the potential inflammatory/allergenic capacity of the tested chemicals.
- (v) In addition, perturbation of the cellular metabolic activity was investigated in cells exposed to a well-defined mixture of 4-OPA, IPOH and 4-AMCH.

A simultaneous measurement of the selected endpoints was possible to be executed from the same experiment (biological samples) according to the next figure:

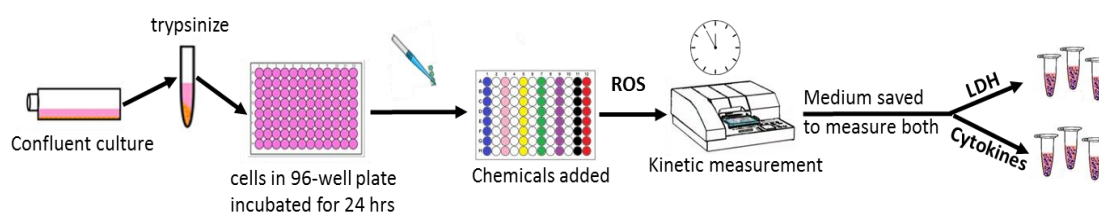


**Figure 15** Schematic representation of the biological experimental set-up to measure ROS, cytokines and LDH from the same pool of cells exposed to chemicals by LLI technique

More details on the execution of each step will be presented in the next paragraphs. As presented in the chart below, a 24-well plate was used to quantify all three intracellular glutathione species (reduced GSH, oxidized GSSG and nitroso GSNO). For control purposes, aliquots from the cellular medium were taken to measure the cytokines levels.

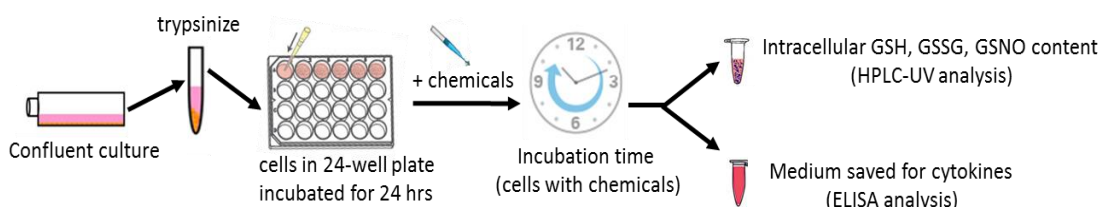


**Figure 16** Schematic representation of the biological experimental set-up to quantify intracellular glutathione species (GSH, GSSG, GSNO) from cells exposed to chemicals by LLI technique

A general flow chart designed to measure the perturbation in the metabolism activity of cells exposed to the mixture of 4-OPA, IPOH, 4-AMCH compared to negative control (untreated cells) is presented in **Figure 17**. As a first step, concentration-response curves were built, from which both Lowest-Observed-Adverse-Effect Concentration (LOAEC) and No-Observed-Adverse-Effect Concentration (NOAEC) were calculated. Afterwards (2<sup>nd</sup> step), cell culture medium and cells treated with LOAEC and NOAEC were prepared for chemical analysis (e.g. quantification of chemicals in the culture medium, metabolomics analysis, as described in **section 2.3.4.3.2**).

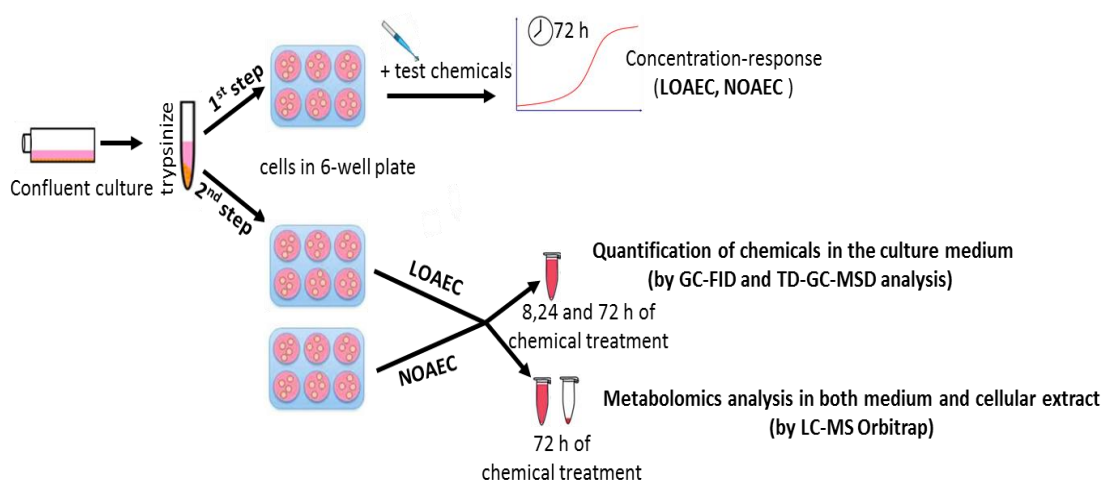


**Figure 17** Schematic representation of the biological experimental set-up used for the metabolomics analysis. The negative control (cells untreated) were receiving medium alone, then the same approach was followed for the metabolomics analysis

A 96-well plate layout used to obtain concentration-response curves by Neutral Red Uptake assay (NRU) is presented in **Figure 18**. The assay was done as described in the **section 2.3.4.8**.

	1	2	3	4	5	6	7	8	9	10	11	12
A	NC	NC										
B	BG	C1	C2	C3	C4	C5	C6	C7	C8	C9	C10	PC
C	BG	C1	C2	C3	C4	C5	C6	C7	C8	C9	C10	PC
D	BG	C1	C2	C3	C4	C5	C6	C7	C8	C9	C10	PC
E	BG	C1	C2	C3	C4	C5	C6	C7	C8	C9	C10	PC
F	BG	C1	C2	C3	C4	C5	C6	C7	C8	C9	C10	PC
G	BG	C1	C2	C3	C4	C5	C6	C7	C8	C9	C10	PC
H	NC	NC										

**Figure 18** Layout of 96-well plate used to generate concentration-response curves. BG refers to backgrounds (test chemical in the culture medium); NC refers to negative controls (cells grown in the culture medium); PC refers to positive control (cells with sodium dodecyl sulfate added into the culture medium); C1-C10 refers to a serial dilution of chemicals prepared in culture medium and added to cells (where C1 stands for the highest concentration used)

### Conditions for cell culture exposed to the liquid form of tested chemicals

Conventional culture conditions were applied for the exposure of A549 and 16HBE 14o- cells to the individual chemicals: d-limonene, 4-OPA, IPOH and 4-AMCH and their selected binary/ternary mixtures.

For NRU, LDH, cytokine/chemokine and ROS experiments, cells were seeded at a culture density of 30.000 cells/ well in culture medium (DMEM w/o phenol red, supplemented with 1% FBS) and grown as a monolayer in Nunc 96 well-plate at 37 °C and 5 % CO<sub>2</sub>. After reaching 90-100 % confluence, cells were incubated for 24 hours with varying concentrations of selected chemicals. After treatment, aliquots of the culture medium were saved for cytokine/chemokine analysis.

For the intracellular glutathione determination, the A549 and 16HBE14o- cells were plated in a Falcon 24 well-plate at the density of 100.000 cells / well and grown as monolyer in complete culture medium. After reaching 90-100 % confluence, cells were treated with the same chemical concentrations that were applied in ROS experiments. Accordingly, for the NRU assay, ten different concentrations as high as 115 mM of 4-OPA, 17.5 mM of IPOH 5.8 mM of 4-AMCH and 100 µM of d-limonene, corresponding to their maximum solubility in the culture media, were added to the cells. In the case of ROS, cytokines and GSH determination, cells were incubated with the lowest observed concentration (LOEC) of the chemicals, which caused statistically significant loss of the cellular viability when compared with the negative control.

### Controls

For each plate, negative, positive and background controls were included. The negative control wells received medium alone (untreated cells) and the background control consisted of culture medium containing the tested chemicals. The positive control wells, in the case of NRU assay, received 1 % of sodium dodecyl sulphate (SDS), while for the ROS assay, 55  $\mu$ M of tert-Butyl hydroperoxide (TBHP). Both SDS and TBHP were added to the cells to demonstrate their capability to respond to chemicals, the negative control (untreated cells) was used as reference for the treated cells, while the background control was included to confirm that no reaction occurred during the assay due to the chemical itself.

### Sampling and sample preparation protocol for metabolomics analyses

#### *Cell cultures and chemical treatment:*

A549 cells at a density of  $3 \times 10^5$  were seeded in 3 mL complete culture medium (6-well plate, Falcon). Cells were maintained in a sub-confluent state (80 %) under standard cell culture conditions (37 °C, 5 % CO<sub>2</sub>, 95 % humidity). For each experimental condition six biological replicates have been performed. Cells were harvested at 72 h for metabolomics experiments.

#### *Cell lysate and culture medium sampling:*

- (1) After 72 hours of chemical treatment of the A549 cells, the cell culture medium was removed (3 mL) and transferred into a 15 mL falcon tube, then stored at -80 °C.
- (2) Cells from each well were washed twice with a volume of 1 ml PBS (this step was done by working on ice).
- (3) Cell lysates (metabolites) were obtained by re-suspending each well in 500  $\mu$ l of ice-cold methanol. Cells were mechanically harvested with a sterile plastic disposable cell scraper. The cells were transferred into a 1.5 mL Eppendorf tube. Each well was washed with an additional 250  $\mu$ l ice-cold methanol and collected into the respective Eppendorf.
- (4) The recovered cell lysate was sonicated at 50 W for 5 min and further centrifuged at 15.000 x g for 15 min at 4°C. The supernatant was stored in a new 1.5 mL Eppendorf tube at -80 °C.

#### *Sample preparation for metabolomics experiments:*

- (1) Cell culture medium:

50  $\mu$ l of the culture medium sample was transferred into an Eppendorf tube. Then the tubes were vortexed and centrifuged at 15.000 x g for 10 min at 4°C. The medium

samples were diluted 1:10 in Milli-Q water. The samples were transferred into 96-well plates. The plates were covered with a suitable cover mat prior to LC-MS analyses.

(2) Cell lysates:

The methanol solution was evaporated to dryness using the speed vacuum system (30 min, cooling system at 10 °C). Then the samples were re-suspended in 100 µl of the LC-MS mobile phase (0.1 % formaldehyde in a solution of milli-Q water: Methanol, 95: 5) and centrifuged at 15.000 x g for 10 min at 4 °C.

The samples were transferred into 96-well plates and covered with a suitable cover mat prior to LC-MS analyses.

### Incubation of human blood via the *In vitro* Pyrogen Test (IPT)

The IPT test is based on the human fever reaction after incubation of blood with a sample followed by analysis with enzyme-linked immunosorbent assay (ELISA) to measure the level of cytokine released, if any. The test detects all kinds of pyrogens present in the sample and is specific for humans since it is based on the reaction with human whole blood. The main steps of the *In vitro* Pyrogen method are: (i) incubation of the blood with the test chemicals; (ii) the measurement by ELISA of the amount of a biomarker of inflammation, which in this case is the interleukin 1-beta (IL-1 β).

### *Procedure for the cryo-blood incubation with test chemicals*

1. The cryo-preserved blood stored in liquid nitrogen was thawed at 37 °C. Homogenization of the blood was done by gently inverting the closed glass vials. In order to avoid variation between samples due to different aliquots of blood, a blood pool was obtained by combining different blood vials into one pyrogen-free reservoir.
2. Six parts of RPMI 1640 (pyrogen-free) and one part of cryo-preserved blood were gently mixed and distribute it to the samples (e.g. test chemicals at various concentrations).
3. Samples were then incubated for 18 h (the optimal time identified in these experiments) at 37 °C ± 1 °C and 5 % CO<sub>2</sub>. Also, optimization of the blood distribution over time it was taken into consideration (see Results and Discussion).
4. Before adding the samples into the coated 96-well plate, the samples containing blood with chemicals were carefully mixed to assure their homogeneity.
5. ELISA analysis (reading at an absorbance wavelength of 450 nm) was done immediately, or the plate with the samples was stored for later use. For storage, sealed plates were frozen at – 20 °C for no longer than 1 week or at – 70 °C for no longer than 8 weeks.

The manufacturer's instructions were followed for the preparation of standard curves (LPS and IL-1 $\beta$ ) as well as for the quantification of the inflammatory response released from blood incubated with airborne contaminants.

### Controls

For each plate, negative, positive and background controls were included. The negative control wells contain medium with only blood, the positive control was prepared at various concentrations of the lipopolisaccharide (LPS) from *Escherichia coli* strain O113 (WHO reference material), while the background control consisted of test chemicals prepared in the culture medium.

#### 2.3.4.7 *In vitro* exposure method: Air-Liquid interface exposure method and its protocols

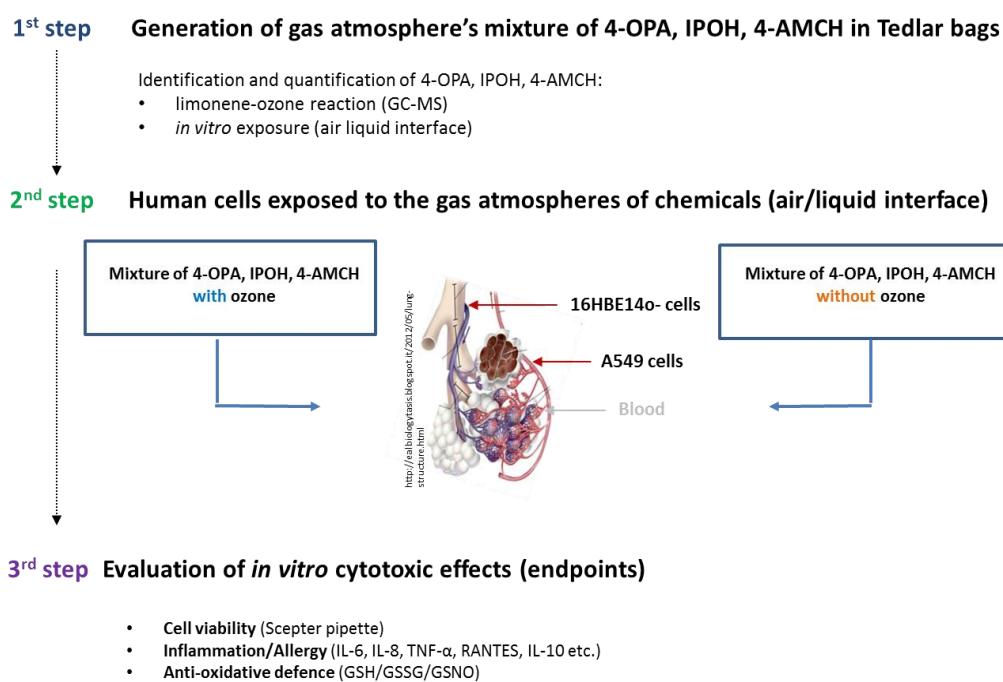


**Figure 19** Schematic illustration of the experimental steps followed in the study where human bronchial and alveolar cells are directly exposed to the chemicals at the air/liquid interface

The *in vitro* studies performed with selected chemicals as gas vapours were accompanied by a series of analytical methods and techniques, which were developed and adapted to quantify and prepare the chemicals as gas atmospheres:

-GC-MS method for the quantification of 4-OPA, IPOH and 4-AMCH collected during air sample.

-CULTEX system set-up was adapted to operate with Tedlar bags filled with the generated vapors of 4-OPA, IPOH, 4-AMCH in presence/absence of ozone.

Various end-points such as cell viability, inflammation response were evaluated following the main steps presented in the figure below.

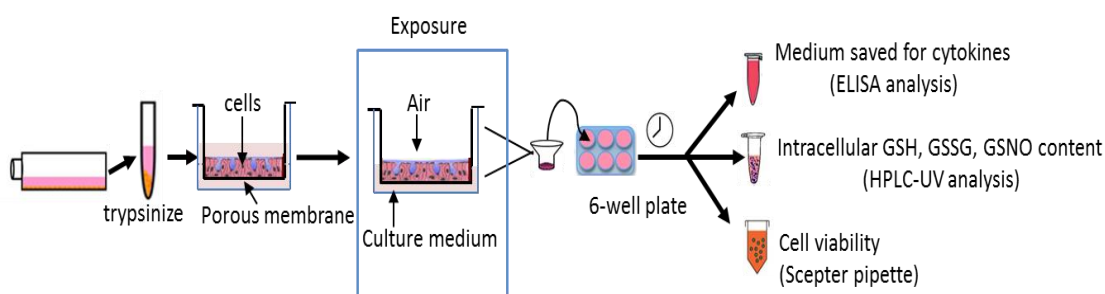
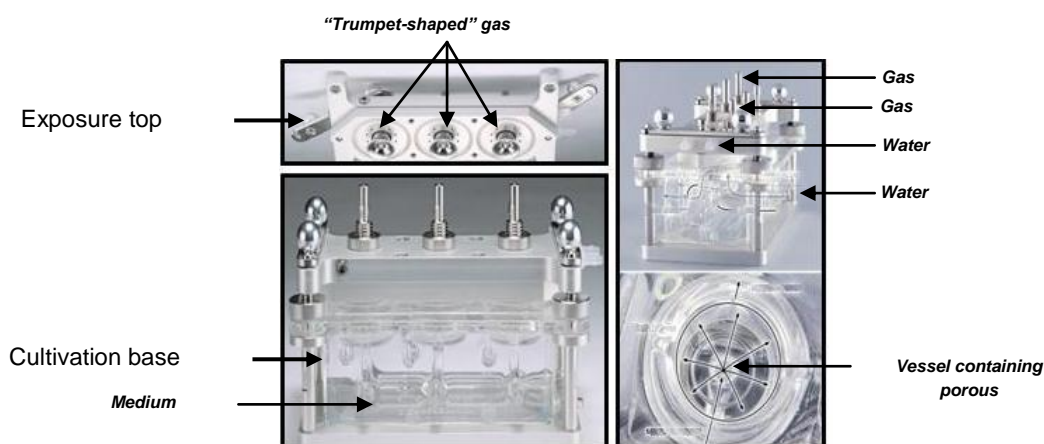


**Figure 20** Schematic representation of the main steps needed for the exposure and endpoints when cells are exposed to chemicals at the air/liquid interface.

In order to simulate a near-realistic inhalation exposure, the cell exposure at air/liquid interface was carried out by using an *in vitro* aerosol exposure device called CULTEX, which allows a direct contact of the apical side of the air-lifted cells with the gaseous phase containing the volatile compounds.

The whole CULTEX system (shown in **Figure 21**) is composed of two exposure modules integrated in an air circuit system which are used as explained below.



Picture modified by D. Lipsa

**Figure 21** Representation of the CULTEX exposure module (the picture was modified based on images collected from CULTEX website: <http://www.cultex-laboratories.com/Catalog/Modules/cultex-cg-module-24mm.php?p=Images>. **Gas inlet** – exposure atmosphere is pulled across the apical surface of the cells. **Gas outlet** –

the atmosphere is removed from the chamber by a vacuum pump at a constant flow rate for all chambers. **Water inlet** tube – the connection of the 1<sup>st</sup> module with the water bath is done by a silicone tube. **Water outlet** tube – makes the connection with the silicone tube of the 2<sup>nd</sup> module

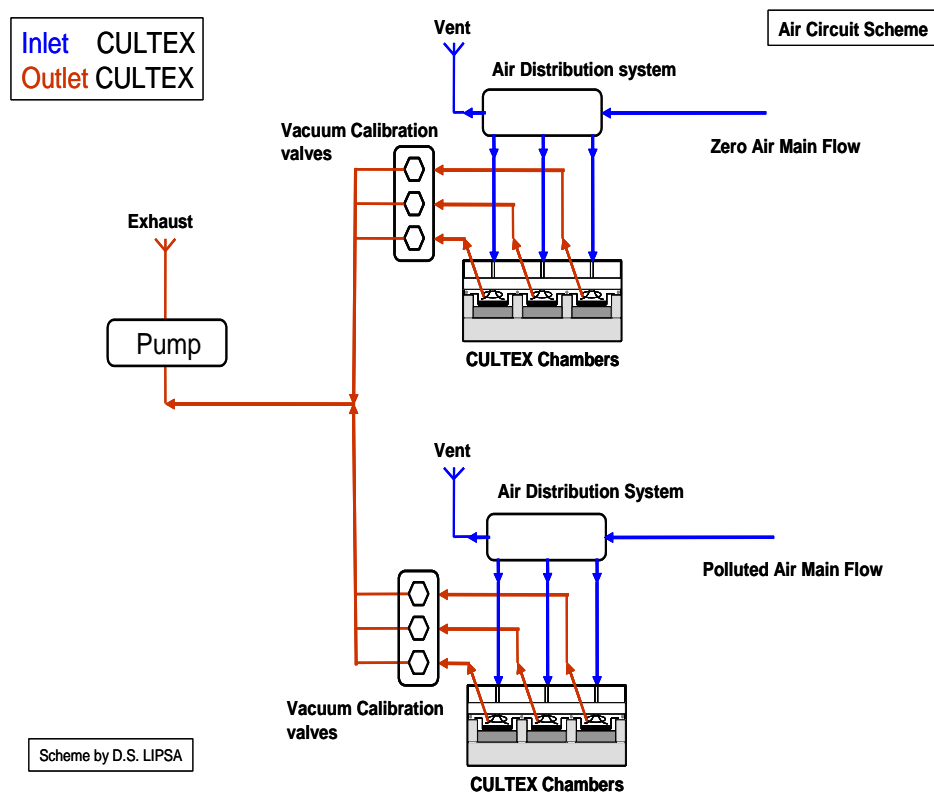
One of the exposure modules was used to have the functionality of the system under control during the experiment during cell exposure to Zero Air. The other module was used to study the biological effects during cell exposure to the selected chemicals. Prior to this selection, both chambers were tested under control conditions and after establishment of their equivalence one of them was dedicated to Zero Air (negative control of the system) while the other was selected for actual exposure measurements.

The lower part of each exposure module housed three vessels filled with medium and specially designed for cells cultured on porous membrane inserts. The optimal temperature of the nutrient medium (37 °C) was controlled by an external water bath which circulated a regulated flow of water (37 °C) through the system. The exposure top part of the modules was constituted of three Teflon trumpets through which the gaseous and particulate pollutants are delivered in a continuous flow to the apical side of the cells. The test atmosphere was entering and leaving the module sucked via negative pressure. The lower base of the trumpets inlet was located 2 mm above the apex cells during exposure. This space was checked before each experiment using a stainless steel washers of 1 mm.

### Exposure experiments executed with CULTEX by using standard chemicals prepared in gas cylinder

In the experiments where cells were exposed to commercially available concentrated pollutants prepared in a gas cylinder, such as d-limonene and nitrogen dioxide, the mainstream flows were obtained with a positive flow given by the gas cylinders (the measurement line) and by the compressed zero air (the reference line). The mainstreams were started 12 hours before the actual experiment took place (the flows of Zero Air and of concentrated gas cylinder were open and left to stabilize overnight). Samples for concentration and background controls purposes were taken by the means of T shaped swagelok systems placed on the mainstream tubes before the deviation for the CULTEX feed. Samples (both VOCs and carbonyl type) were collected at convenient times before and after the execution of a series of test, on a daily basis.

A.



B.

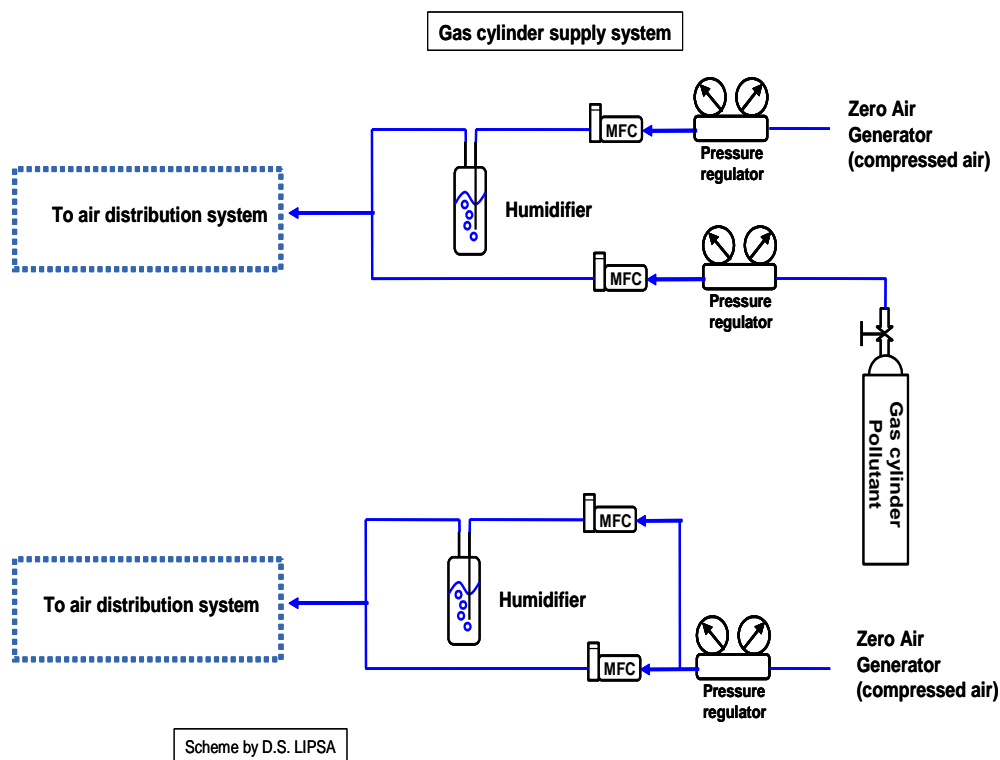


**Figure 22** Exposure of human lung cells to pollutants such as d-limonene and NO<sub>2</sub> in a gas cylinder using the CULTEX system: **A.** CULTEX basic scheme (including the exposure modules). **B.** Gas cylinder set-up scheme

### Exposure experiments executed with CULTEX for d-limonene-ozone mixture prepared in 0.45 m<sup>3</sup> environmental chamber

In the experiments where the cells were exposed to the generated atmosphere from d-limonene-ozone reaction, the measurement line was modified with the use of a pump to realize the mainstream flow (see **Figure 23**). For background control purposes, VOCs and carbonyl samples were taken from the chamber before the injection of d-limonene.

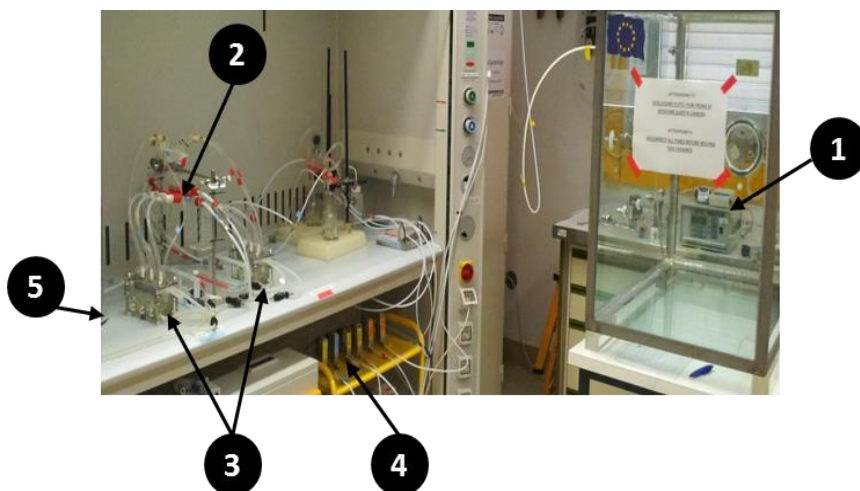


**Figure 23** Exposure of human lung cells to a generated atmosphere of d-limonene-ozone reaction in 0.45 m<sup>3</sup> environmental chamber connected to the CULTEX system. 1. Environmental chamber; 2. Manifold; 3. Cultex exposure chambers; 4. Mass flow controllers; 5. Vacuum pumps

Technical approaches to generate the *d*-limonene-ozone reaction in 0.45 m<sup>3</sup> chamber  
A scheme overview of the environmental chamber set-up connected to the CULTEX system is presented below:

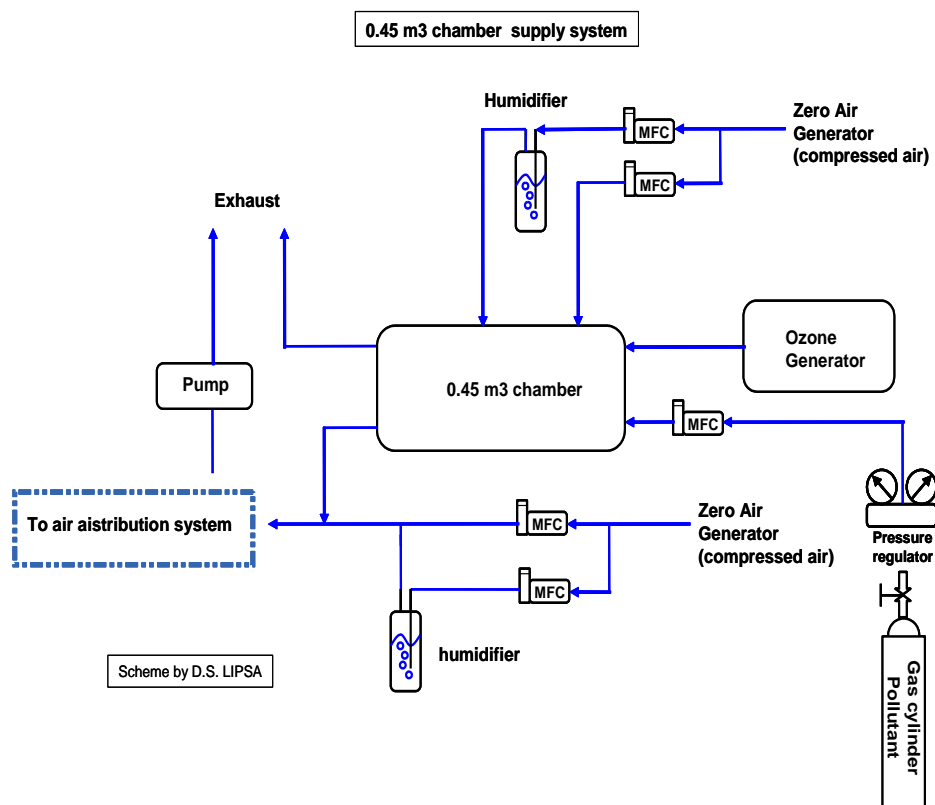


Figure 24 Chamber set-up connected to the CULTEX basic scheme

At the beginning of the test, a steady state concentration of d-limonene was built and maintained for at least 16 hours in the glass chamber. The glass environmental chamber was continuously fed from a concentrated gas cylinder, from which the concentrated stream was injected in the humidified Zero Air just before entering the chamber.

The pump for generating the mainstream of air for the CULTEX system was then started and, after a suitable stabilization time of not less than two hours, also the CULTEX flow pump was started.

VOCs and carbonyls samples were taken at regularly intervals of time.

1. At the end of the d-limonene CULTEX test, the ozone injection was started and maintained for 24 hours in the chamber. At this stage a new steady state situation was achieved in which both chemicals and secondary reaction products were at a constant concentration. VOCs and carbonyls were monitored during the reaction.

The pump for generating the mainstream of air for the CULTEX system was then started and, after a suitable stabilization time of not less than two hours, also the CULTEX flow pump was started.

2. At the end of the test, the d-limonene supply was stopped and ozone maintained overnight in order to achieve the steady state concentration of ozone alone. Samples of VOCs and carbonyls were taken to check for background residual concentration of chemicals (either d-limonene or secondary reaction products).

The pump for generating the mainstream of air for the CULTEX system was then started and, after a suitable stabilization time of not less than two hours, also the CULTEX flow pump was started.

At the end of the CULTEX ozone test, ozone generation was stopped and the test chamber was flushed with humidified Zero Air for cleaning.

### Controls used for the Air-Liquid interface (CULTEX system)

Two different negative controls were considered for this exposure approach. One negative control (Incubator) refers to the control cultures that were left unexposed and kept in a CO<sub>2</sub> incubator for 1 or 2 hours, time that corresponds to the exposure duration of cells exposed to air/liquid interface by the use of CULTEX. These cell cultures were both apically and baso-laterally supplemented with complete culture medium. The second negative control (Zero Air or Clean air) refers to the cell cultures that were left in the CULTEX system for 1 and 2 hours, being exposed to Zero Air. The Zero Air control was used as control of the system reproducibility (for the optimisation of exposure conditions) as well as a control for all gas tested compounds as individuals or mixtures.

As positive control, nitrogen dioxide (NO<sub>2</sub>) generated in a distribution line starting from a gas cylinder was applied to the cultures in the CULTEX exposure system, due to its capacity to induce cytotoxic effects such as oxidative stress, membrane damage etc. Additionally, cell cultures grown on inserts were exposed to a medium containing lipopolysaccharide (LPS), with the scope to verify their capacity to secrete cytokines. The resulting cellular responses confirmed the validity of the experimental setup for the cell exposure system.

### *Zero Air (also called Clean air) preparation procedure*

Compressed air delivered to the system (Zero Air) is dried with molecular sieves to achieve a dew point below -45 °C. Afterwards, the air was treated with activated charcoal to remove residual content of volatile organic compounds (VVOCs, VOCs, SVOCs) and filtered to remove particles.

### *Preparation of various levels of relative humidity*

Humidified air was obtained by bubbling dry Zero Air into Milli-Q grade water. A second empty bubbler was placed after to remove water droplets and to stabilize humidity in the flow up to a 85-95 % RH level. Humid air was then proportionally mixed with dry Zero Air to obtain the desired level of Relative Humidity (50 or 80 %). The final value of Relative Humidity was controlled by placing a T/RH data logger at the exit/exhaust of the CULTEX system. The role of the humidifier device (bubbler) was to keep the good physiological conditions of the cell in order to avoid cell dryness.

### Exposure experiments executed with CULTEX by using Tedlar bags

In the experiments where cells were exposed to the selected d-limonene ozonolysis products in gas phase prepared in TBs, the reference line of the system was modified (see **Figure 25**). Air from the TBs was drawn by the use of membrane pumps and the flow was controlled by the use of mass flow controllers.

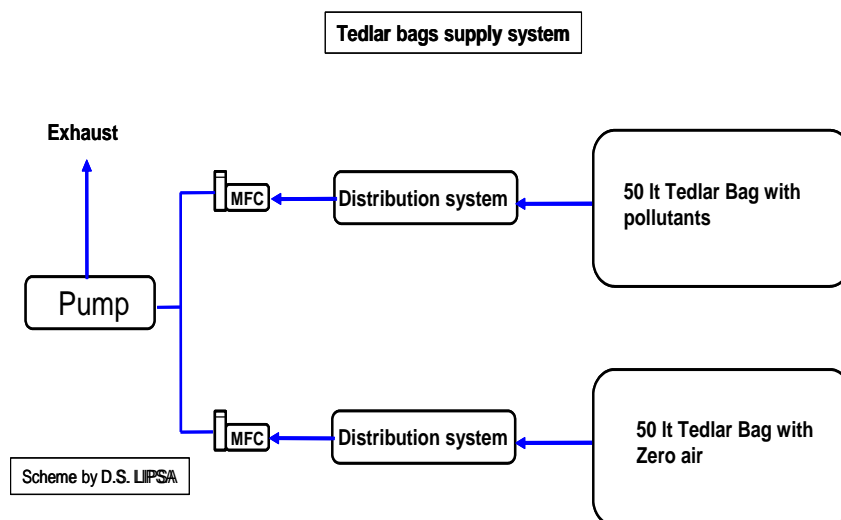


**Figure 25** Tedlar bag set-up connected to the CULTEX basic scheme

The main flow and flow through the CULTEX system, both for the atmosphere under investigation and for the reference Zero Air, were maintained in all experiments at around  $120 \text{ mL m}^{-1}$  (main flow) and  $2 \text{ mL m}^{-1}$  (flow through apical side of the cells) respectively with a maximum allowed deviation from the set point of 5 %.

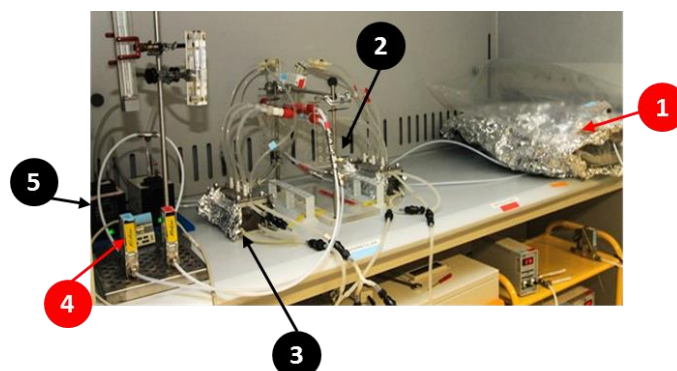


**Figure 26** Exposure of human lung cells to gaseous phase of the mixture of 4-OPA, IPOH, 4-AMCH in presence or absence of ozone generated in TBs connected to the CULTEX system

*Recovery tests for 4-OPA, IPOH, 4-AMCH within CULTEX system*

Preliminary recovery tests were conducted on the CULTEX system connected to the tedlar bags, in order to verify possible loss of chemical compounds before arriving at the cells (between Tedlar bag supply and the system line of CULTEX). Therefore, two different sampling positions were applied, as can be observed in **Figure 27**: in the first position Tenax TA tubes were placed in the inlet (before the gas is distributed to the

CULTEX exposure chambers) and in the second position, Tenax TA was placed at the “end of the inlet”. The “end of the inlet” represents the point where the gas flow is sucked out of the exposure chamber by the pump. This “in-out” process assures the continuous fumigation of the cells by the gas flow.

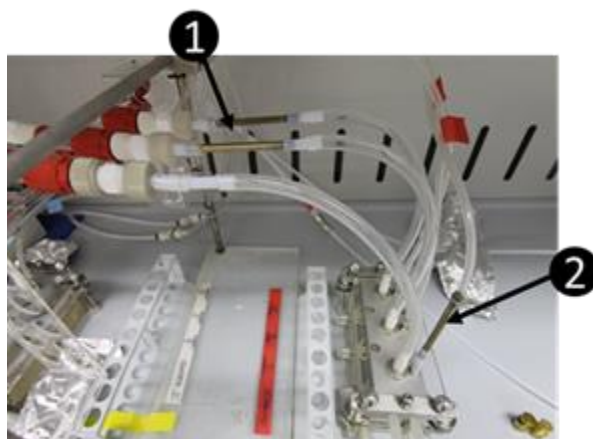


**Figure 27** Sampling position of Tenax tube on the CULTEX system collected for the recovery test: **1.** Tenax tubes added immediately before the gas atmosphere is distributed to the cells; **2.** Tenax tubes added immediately after the CULTEX chambers (gas atmospheres already fumigated the cell culture)

The sampling flow was determined by the actual CULTEX flow, set at  $2 \text{ mL min}^{-1}$ ; the samples were collected for one hour. The analysis was performed with TD-GC-MSD and splitted injection as described in chemical analysis section.

### Cell culture differentiation of THP-1 and 16HBE14o- cells

For the experiments where differentiation was needed, the following protocols were applied:

(a) Differentiation of THP-1 cells into attached macrophages-like cells was performed on Park's protocol. Based on his findings,  $5 \text{ ng mL}^{-1}$  PMA treatments in the THP-1 cells were inducing their differentiation without undesirable gene up-regulation and with a good reaction response to secondary stimuli such as  $10 \text{ ng mL}^{-1}$  LPS [403]. Before their differentiation, the THP-1 cells were centrifuged for 5 min at 1200 rpm, and resuspended in fresh culture medium. Subsequently, the THP-1 cells ( $1 \times 10^6$ /well/1.5 mL) were seeded into porous membrane inserts in presence of  $5 \text{ ng mL}^{-1}$  PMA and incubated overnight to differentiate them into macrophage phenotype (e.g. flat in shape, with well-developed Golgi apparatuses increased size, granularity, and decreased division) [403].

(b) Differentiation of 16HBE14o- involves growing cells on porous supports at an air-liquid interface (ALI) which will enable cells to undergo mucociliary differentiation [336]. The media used to support growth and differentiation on porous membrane inserts was prepared as follows: 50 : 50 mixture of DMEM and LHC basal medium supplemented with retinoic acid which was added to suppress or reverse squamous metaplasia in culture [396].

### Protocol for culturing human cells on porous membrane

Prior to seeding the cells on the porous membrane, the transwells were preconditioned in an incubator for 1 h with culture media (RPMI 1640) supplemented with FBS (10 %; v/v) and antibiotic mixture (1 %; v/v) to both sides (bottom 2.5 mL; top 1.5 mL) in order to improve cell attachment.

Thereafter, the following procedure was applied:

1. The adherent subcultures cells (A549 and 16HBE14o-) were harvested with trypsin, counted and seeded at a density of  $70 \times 10^4$  cells  $\text{cm}^{-2}$  for A549 cells, and  $110 \times 10^4$  cells  $\text{cm}^{-2}$  for 16HBE14o-. The cellular suspension containing THP-1 cells was added directly into inserts at their optimal density ( $100 \times 10^4$  cells/insert).
2. Cells were allowed to attach to the porous membrane as follows: 24 h for A549 cells and THP-1 cells, and 72 h for 16HBE14o-.
3. Complete culture medium was added below (2.5 mL) and above (1.5 mL) the cells.
4. Once cell confluence was achieved (> 85 %), the upper layer of culture media was removed, the membranes were washed twice with warmed PBS from both sides and then transferred to CULTEX holders
5. CULTEX holders were filled with serum free medium supplemented with HEPES buffer used to maintain a constant pH of the medium

At the end of exposure time, inserts were removed and replaced in their six well plates, where fresh serum (1 %) culture media was added to both sides. After this, cytotoxic effects were investigated using different assay endpoints.

### Preparation of the CULTEX system for the air-lifted exposure experiments

Before exposing the cells to the gas atmospheres, several actions were considered as preliminary preparatory steps: (i) The water bath was switched on to reach the optimal temperature ( $37^\circ\text{C}$ ) for the cell culture; (ii) The confluence of the cell culture and possible microbial contamination were checked; (iii) The pump was switched on; the total flow rate as well as the flow rate which are distributed in each Teflon trumpet was measured; (iv) The CULTEX chambers were filled with approximately 10 ml of serum

free culture medium; (v) Meanwhile, the apical cellular medium from the inserts was discarded and the cells were washed twice with PBS; (vi) Then the 6 inserts containing the cell culture monolayer were added into the CULTEX chambers; (vii) The medium level was checked for each of the 6 exposure holders with the aim to ensure that it moistened the insert's membrane only from the basal side (the cells will be fed from the basal side and exposed to volatile chemical at their apical side for 1 or 2 hours - optimal time for exposure without loss of cellular viability); (viii) after exposure, the inserts were taken out and placed into a 6-well plate already containing complete fresh medium. The 6-well plates were added into the incubator; (ix) after a pre-established time of incubation, various bioassays were run (e.g. cell viability, inflammation etc.).

### 2.3.4.8 *In vitro* protocols: Cell viability by Neutral red uptake assay

Neutral red uptake assay is based on the protocol described by the National Institute of Health (NIH) [404] and it was used to quantify the number of viable cells after their exposure to different chemicals [405].

#### *NRU assay procedure*

- (1) After exposure to the tested compounds, cells were rinsed with pre-warmed PBS
- (2) 250  $\mu\text{l}$  of pre-warmed 25  $\mu\text{g mL}^{-1}$  neutral red (NR) solution (in medium) was added to each well and then incubated at 37  $^{\circ}\text{C}$  for 3 h to enable the uptake of the neutral red dye by the cells
- (3) The NR solution was aspirated and the plates were washed with pre-warmed PBS
- (4) 200  $\mu\text{l}$  of a solubilisation solution (acetic acid / water / ethanol) was added to the cells
- (5) The plates were protected from light and gently shaken for 20 min; then left to incubate for 30 min at room temperature
- (6) Subsequently, the plates were added to the plate reader (Perkin Elmer) where the absorbance was recorded at 540 nm.

#### *NRU reagents preparation:*

- Neutral red solution was obtained by mixing Neutral Red in dye in DMEM medium containing 5 % FBS, 4mM glutamine and penicillin and streptomycin. The solution was filtered through 0.2  $\mu\text{m}$  Nylon filters.
- The lysis solution contained acetic acid / water / ethanol (1: 49 : 50, v/v/v).

### 2.3.4.9 *In vitro* protocols: Cell viability by Presto blue assay

The Presto blue reagent (resazurin-based solution) was applied according to the manufacturer's protocol, in order to assess the viability of A549 cells exposed to chemicals that were used in the metabolomics analysis. The Presto blue reagent was added to the wells (1:100) and then, the plate (cells+medium+Presto blue) was incubated at 37 °C for 15 minutes. After this period of incubation, the plates were added to the plate reader, where fluorescence (Excitation/Emission = 560/590) was recorded.

### 2.3.4.10 *In vitro* protocols: Cell viability by Lactate dehydrogenase assay

Loss of membrane integrity was assessed by measuring lactate dehydrogenase (LDH) released into the cellular medium. The quantity of LDH released in the medium was determined using a commercially available kit, Cytotoxicity detection Kit (LDH) (Roche Molecular Biochemicals, Lewes, UK) and following the manufacturer's instructions.

Briefly, cells were cultured on porous membrane inserts and exposed to gaseous chemical atmospheres for 1 or 2 h. Following exposure, a new culture media containing 1 % FBS was added to the cells and then cells were incubated for 24 hrs. Aliquots of culture media and the reagent mixture provided by the kit were mixed in a 96-well plate followed by 30 minutes incubation at room temperature, in the dark. Stop solution was added and the plate was read at 490 nm.

### 2.3.4.11 *In vitro* protocols: Inflammation by Cytokine/Chemokines assay

Cell culture supernatants were used to quantify the production of cytokines using a MILLIPLEX MAP Kit (HCYTOMAG-60K, Millipore, Billerica, MA), according to the manufacturer's protocol. This approach allowed for the simultaneous measurement of the following Human Cytokines/Chemokines: EGF, IL-1 $\beta$ , IL-4, IL-6, IL-8, IL-10, IL-12(p40), IL-13, IL-15, RANTES, TNF $\alpha$ , VEGF. Briefly, supernatants were centrifuged for 10 minutes to remove debris and 25  $\mu$ l were added to 25  $\mu$ l of assay buffer. Then, 25  $\mu$ l of magnetic beads coated with specific antibodies were added to this solution and incubated for 2 hours at RT with shaking. At the end of the incubation, the plate was washed twice in buffer and incubated for 1 hour with 25  $\mu$ l of biotinylated detector antibody at room temperature. Then, the plate was incubated for 30 min at RT with Streptavidin-Phycoerythrin, washed twice, and incubated with 150  $\mu$ l of sheath fluid

for 5 minutes at RT. The plate was run immediately on a Luminex® 100™/200™ platform (Luminex Corporation) with xPONENT 3.1 software. Standard curves for each cytokine (in duplicate) were generated by using the reference cytokine concentrations supplied. The assay was performed in a 96-well plate, using all the assay components provided in the kit. All incubation steps were performed at room temperature and in the dark to protect the beads from light.

### 2.3.4.12 *In vitro* protocols: Oxidative stress by reactive oxygen species assay

The production of ROS was measured using a cell permeant reagent 2', 7'-dichlorofluorescein diacetate (DCFH-DA) that can passively enter the cells and be deacetylated by cellular esterase to a non-fluorescent compound (DCFH) which can later be oxidized by ROS into a highly fluorescent compound, 2', 7' -dichlorofluorescein (DCF) [406].

#### *Procedure for ROS measurement*

After the cells were seeded on a dark 96-well microplate and allowed to attach overnight, on the day of the experiment, cells are washed once with PBS. Subsequently, cell cultures were stained with DCFDA 25  $\mu$ M for 45 minutes at 37 °C. Cells were then washed once with PBS and incubated with 200  $\mu$ l/well of selected chemicals for the desired period of time. The fluorescent plate reader was set at an excitation wavelength of 485 nm, and emission wavelength 535 nm.

#### *ROS reagents preparation:*

The stock solution of DCFH-DA (200 mM in DMSO) was prepared and stored at -20 °C, protected from light. On the day of experiment, a diluted 10 mM stock solution was prepared in complete medium and was used for the preparation of 20  $\mu$ M DCFH-DA working solution. 50  $\mu$ M Tert-butyl hydroperoxide is used as the positive control compound.

### 2.3.4.13 *In vitro* protocols: Oxidative stress by glutathione species assay

#### Extraction procedure of GSH, GSSG, GSNO species from human cells

For the cells exposed to the test chemical solubilized into the culture media, initially the supernatant was discarded; then the same steps were applied as for the air-lifted exposure conditions, as follows:

(i) culture medium was discarded from the cells exposed to the test chemicals solubilized into the culture media; (ii) cells were washed twice with cold PBS (200  $\mu$ L for 24-well plate and 300  $\mu$ L for 6 well plate); (iii) 300  $\mu$ L or 600  $\mu$ L of ammonium sulfate (25 mM) dissolved in 0.5 % picric acid - prepared in mobile phase - was added to the cells (during this step, cells were kept on ice); (iv) After incubation at -18  $^{\circ}$ C for 10 minutes, the cellular homogenates were mechanically scraped for approximately 5 minute and transferred to an Amicon 3K Ultra Millipore filter; (v) the cellular suspension was sonicated in icy water for 2 minutes; (vi) then it was centrifuged for 15 minutes at 4  $^{\circ}$ C (12.000 g) in order to remove proteins and high molecular weight compounds prior to HPLC analysis; (vii) finally, the supernatant was immediately transferred to a pre-chilled dark amber vials and injected into the HPLC or stored at -80  $^{\circ}$ C for further analysis of GSH, GSSG and GSNO. The pellet (containing proteins) was collected from the Amicon 3K Ultra Millipore filter and further quantified by Bradford method according to the manufacturer's recommended protocol.

### 2.4 Data processing and statistical analyses

#### (i) *Dose-response relationships by NRU assay*

Background subtraction was applied for all the measurements, thereafter the obtained measurements of the absorbance of NRU assay - the optical densities (ODs) - were normalized by dividing the OD of each well to the average OD of the negative control (cells untreated). Then the data was further expressed as percentage, according to the formula:

$$\% \text{ cell viability} = \left( \frac{\text{absorbance of exposed cells}}{\text{mean absorbance of untreated cells}} \right) * 100$$

Concentration values represented on X-axis were log transformed, thereafter a nonlinear regression curve fit (four parameter sigmoidal curve) was plotted versus cellular viability values (y axis) using the GraphPad Prism v.5.0. IC50 values are a direct output of GraphPad based on the function

$$Y = \text{Bottom} + \frac{(\text{Top} - \text{Bottom})}{(1 + 10^{(\log \text{IC}_{50} - x) * \text{HillSlope}})}$$

while LOEC was calculated for each cell line by running ANOVA-Dunnett's multiple comparison post-test. Differences were considered to be statistically significant when p values were less than 0.05.

### *(ii) Metabolomics analysis*

Data input and handling: An experimental design table was created for each of the 6 batches of analysis. To each batch was associated a .csv file containing the following information on the analysis sequence: sample name (QC, blank, sample), sample code, file name (unique name in a sequence), treatment (C, L H), sample type (supernatant medium or cell extract). Raw data files were converted into Network CommonData Form (NetCDF) format using the "File Converter" tool of XCalibur software and placed on a server ready for data processing.

Data processing: LC-MS data processing was performed using the open-source XCMS software package (<http://masspec.scripps.edu/xcms/xcms.php>) (version 1.14.1 running under R version 2.8.1) that uses several algorithms written in R language. An R package, so-called "MCG" was developed in-house. The MCG package facilitates the systematic data processing of LC-MS data through a systematic workflow. MCG extracts, nonlinearly aligned retention time and accurate mass of LC-MS produced peaks, in a time range of 2-16 min. The basic output of the MCG programme consists of a table of intensities for detected peaks in each sample with peaks labelled by m/z and rt values (where m/z is the mass-to-charge ratio and rt the retention time in s).

Data pre-processing: The first step was to filter and detect the peaks. In this step, the ion chromatograms were extracted and the "matched filter" algorithm [407, 408] was applied. The peak detection algorithm is based on cutting the LC-MS data into slices, a fraction of a mass unit wide, and then operating on those individual slices in the chromatographic time domain. Extraction was performed using parameters of the extraction method as follows:  $rtcut = c(2,15)*60$ ,  $profmeth = "bin"$ ,  $fwhm = 30$ ,  $max = 10$ ,  $snthresh = 6$ ,  $step = 0.01$ ,  $steps = 2$ ,  $mzdiff = 0.025$ .

After detecting peaks in individual samples, the peaks were matched across samples to allow calculation of retention time deviations and relative ion intensity comparison. This is accomplished using the density algorithm for chromatographic data. Optimized settings were:  $mzppm = 10$ ,  $mzabs = 0$ ,  $minsamp = 1$ ,  $minfrac = 0.5$ ,  $bw = 5$ ,  $minfrac = 0.7$ ,  $minsamp = 2$ ,  $mzwid = 0.013$ ,  $mzVsRTbalance = 10$ ,  $mzCheck = 0.2$ ,  $rtCheck = 15$ ,  $kNN = 10$ . For the function `Groupval`, parameters were as follows:  $GMeth = c("medret","maxint")$ ,  $GVal = "into"$ ,  $GInt = "into"$ ,  $DiffClass = "AllBinaries"$ ,  $KEGGComplete = 0$ ,  $UseDiff = c(p = 0.01, fc = 5, camera = 0.05)$ .

These groups were then used to identify and correct drifts in retention time from run to run. Chromatograms were aligned using the "Obiwarp" algorithm [409]. For every group, the median retention time and the deviation from median for every sample in that group was calculated. The method parameters were as follows:  $GroupBW = 1$ ,

NumPass = 1, missing = 1, smooth = "loess", extra = 1, span = 0.2, profStep = 1, response = 1, factorDiag = 2, factorGap = 1, localAlignment = 0, initPenalty = 0.

Missing peaks can occur because they could be missed during the peak detection step or because an analyte was not present in a sample. An additional step, so-called fill peak, was used. To account for the missing peak data, a mathematical function is used to approximate the difference between deviations and interpolate in sections where no peak groups are present.

Normalization was applied to correct for changes in the sensitivity of the detector across the analytical sequence or changes in the sample concentration [410]. In the case of cell culture medium, the data matrix obtained from XCMS was then normalized to a common MS total useful signal (MSTUS): i.e. the sum of the areas of the peaks that are found in all the chromatographic runs in the set. This method forces all samples in a set of experiments to have equal total intensity.

In the case of cell extracts, normalization of the signal was performed using the Probabilistic Quotient Normalization method "PQ". It is based on the calculation of a most probable dilution factor by looking at the distribution of the quotients of the amplitudes of a test spectrum by those of a reference spectrum.

A peak intensity table (m/z, rt, intensities) was generated for each of the 6 batches of analysis and submitted to statistical treatment.

Statistical data analysis for metabolomics: A statistical data analysis was performed to identify differentially regulated metabolites in the whole experiment in pairwise comparisons of high (H) and low (L) exposure doses vs control (C) for each of the 6 biological replicates.

In order to identify differentially regulated features, a paired t-test was used for comparison of treated cell lines (L, H) against untreated cells (C). The programme calculated a fold change and carried out the test between samples from two nominated groups (H or L vs C) and ranked the m/z, rt values in order of the t-statistic (or p value). The features that failed to have an adjusted p-value < 0.05 for the test were rejected.

A fold change was calculated between experiment groups (H or L vs C) for each feature. The fold-changes (FC) were computed from the average values across biological replicates. This method assessed formally whether the true differential expression is greater than a predefined FC criterion (threshold = 2). Metabolites are considered to be differentially expressed if they show a fold-change of at least 2 (up- or down-regulated) and also satisfy  $p < 0.05$ .

Further peak redundancy removal (de-isotoping and de-adduction) was carried out by auto-correlating intensity feature values across quality control samples into the pc

group windows calculated by the CAMERA open source package, identifying adducts and isotopes occurring from the parent molecular ions.

Data from the 6 independent analysis batches (corresponding to the 3 biological replicates) were combined for processing. The m/z features retained after statistical analysis were then submitted to database search for annotations.

Mass-based metabolite identification: METLIN and the Human Metabolite DataBase (HMDB, <http://www.hmdb.ca>) were used for mass-based metabolite identification. METLIN is a web based database developed by the Scripps Research Institute to facilitate the identification of metabolites using accurate mass data. It includes an annotated list of structural information for known metabolites. HMDB focuses on metabolites found in human body fluid. These databases have links to other public databases such as the Kyoto Encyclopedia of Genes and Genomes (KEGG).

Public database annotations were performed of the processed datasets with putative metabolites matching these queries. A local copy of the HMDB data base was used for the query for speed reasons, whereas the standard KEGG API (KEGGSOAP package) was used to query the METLIN online database. Annotations were carried out by matching the measured accurate masses  $\pm 0.01$  amu with theoretical ones.

### *(iii) Cytokines/chemokines analysis*

Background controls were subtracted from all fluorescence values obtained after measurement. Cytokine/chemokines concentrations in sample were determined with a 5-parameter logistic curve. Final concentrations were calculated from the mean fluorescence intensity and expressed in  $\text{pg mL}^{-1}$ .

### *(iv) Intracellular glutathione analysis*

The peak area of the glutathione standards are plotted (concentration vs. area) on a regression linear curve that is fitting through these points. The peak area of the glutathione biological samples was normalised based on the protein content of each biological sample. Thereafter, the concentrations of the unknown samples are determined from the standard fit and any specified dilution factors are applied.

### 3. RESULTS AND DISCUSSION

This chapter focuses on the *in vitro* biological effects obtained from individual and mixtures of chemicals: d-limonene, ozone, and their reaction products 4-OPA, IPOH, 4-AMCH, tested on human pulmonary cell lines (bronchial-16HBE14o-, alveolar-A549 and macrophages-THP-1) and human blood. In order to provide accurate biological outcomes, various chemical and biological methods/techniques were developed or optimized.

#### 3.1 Development/optimisation of chemical and biological methods

In order to reach the thesis objectives, both chemical and biological methods were developed and/or optimized, as listed below:

- Analytical methods (TD-GC-MSD and GC-FID) were optimized for the analysis of the test compounds in air and cellular medium with high resolution and high precision (RSD < 8 %);
- Analytical method (HPLC-UV) was optimized for the quantification of three intracellular glutathione species (RSD < 5 %) applied to evaluate the oxidative stress in human pulmonary cells exposed to selected compounds;
- *In vitro* exposure CULTEX device was adapted to study the biological effects of 4-OPA, IPOH, 4-AMCH as mixtures in presence/absence of ozone and d-limonene in presence/absence of ozone on human pulmonary cell lines (e.g. exposure time, relative humidity etc.);
- The seeding procedure of human cell culture was optimised for both liquid/liquid and air/liquid exposure conditions taking into consideration parameters such as well surface, type of cell, incubation time etc.;
- Sensitive and reproducible biological methods were optimised for the analysis of cell death and determination of inflammatory response in human blood.

3.1.1 Determination of secondary reaction products 4-OPA, 4-AMCH, IPOH in cell culture medium (GC-FID) and gas atmospheres (GC-MS)

3.1.1.1 Determination of stability of secondary reaction products 4-OPA, 4-AMCH, IPOH solubilized into the culture medium (GC-FID)

Outcomes from the compounds solubilized in culture medium containing 10% fetal bovine serum (FBS) showed different stability between chemical compounds over time, as indicated in **Figure 28**.

The 4-OPA is the least stable compound, showing a significant degradation, more than 50 %  $\pm$  2.9 after 24 hours, followed by IPOH which shows a significant degradation, around 50 %  $\pm$  5.58, after 24 hours.

The 4-AMCH compound is the more stable compound showing no degradation during the whole incubation with the culture medium (24 hours).

On the other hand, outcomes from analysis where the compounds were solubilized into the culture medium containing only 1 % FBS, showed that 4-OPA is slightly degraded, around 6 %  $\pm$  0.16 after 24 hours, while both IPOH and 4-AMCH are the more stable compounds showing no degradation after 24 hours. Under these conditions (e.g. where to the culture medium was added 1 % FBS) the kinetic analytical measurements covering the intervals of time exposure 0, 1, 2, 3 and 24 hours confirmed the stability of each tested compounds involved in the toxicological studies on human lung cells.

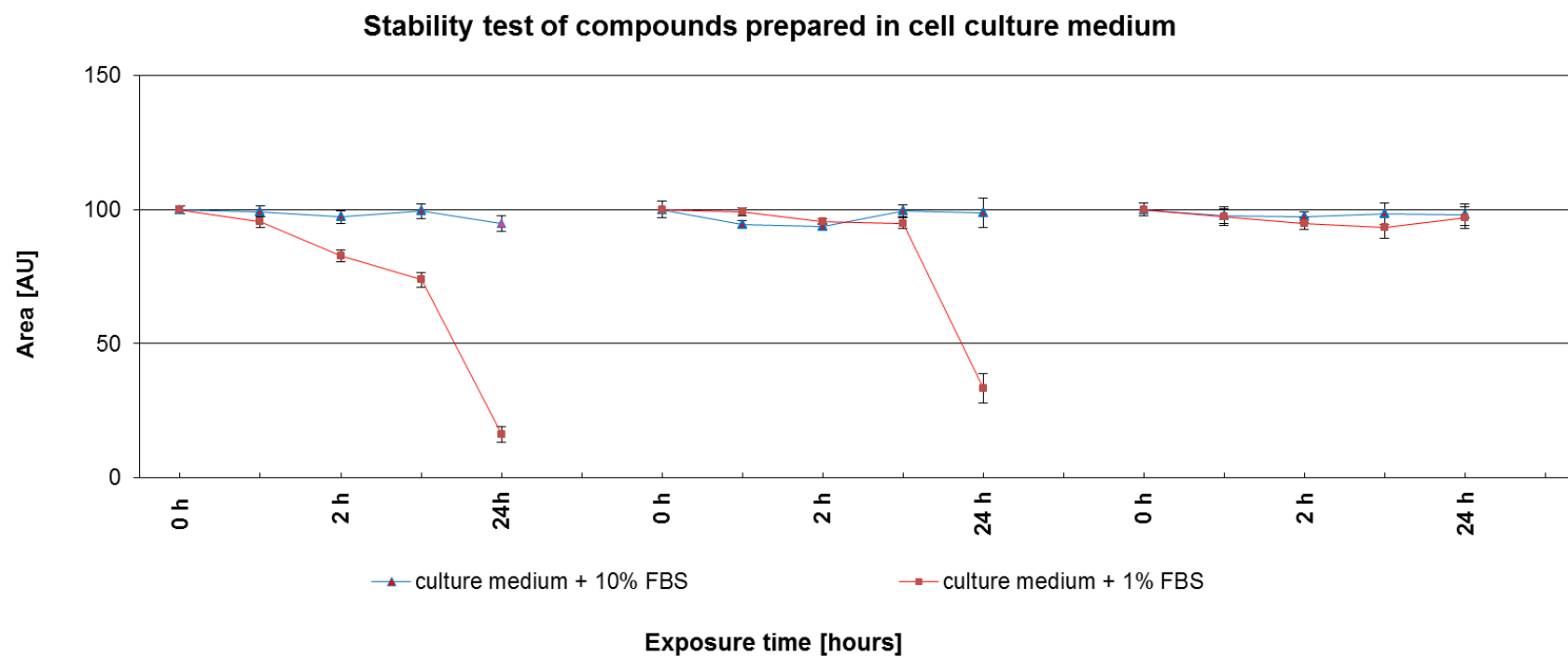


**Figure 28** Stability analysis of 4-OPA, 4-AMCH and IPOH solubilized in culture medium at various concentration of Fetal Bovine Serum (FBS) carried out by GC-FID over time (0, 1, 2, 3, 24 hours) (n=3 ± STD)

In the comparison of the results obtained when varying the concentration of FBS in the culture medium, it can be seen that, in particular, the concentration of measured 4-OPA in 10 % FBS is about 16-fold lower than the concentration of tested compounds prepared in 1 % FBS, measured after 24 hours incubation. The higher concentration of serum (e.g. 10 % FBS) added as cellular nutrient in the cell culture medium influenced the stability of the chemicals 24 hours after their preparation in culture medium, especially for 4-OPA and IPOH. The degradation that occurs under high serum conditions might be explained by the interaction of the aldehyde compounds and the residual  $\text{NH}_2$ -groups of the FBS leading to the formation of a Schiff base.

Additional tests (e.g. Presto blue assay) on cell culture growth under the selected culture medium conditions (1 % FBS) showed that the reduction of FBS did not influence the metabolism activity of the cells. Therefore, in order to keep the concentrations of 4-OPA, IPOH, 4-AMCH as stable as possible during the selected exposure times of human pulmonary cells to the compounds, the concentration of FBS added to culture medium was reduced from 10 % to 1 %.

### 3.1.1.2 Determination of 4-OPA, 4-AMCH, IPOH in gas atmospheres prepared as a mixture in Tedlar bags

The potential cytotoxic effects of the selected chemicals 4-OPA, IPOH, 4-AMCH derived from the gas phase reaction of d-limonene with ozone were investigated on human pulmonary cell lines by the use of an air/liquid exposure system. Considering that humans are exposed to mixtures, rather than individual chemicals, an atmosphere mixture of the selected d-limonene ozonolysis products was thus considered.

In order to simulate a real world setting, the chemicals were mixed in Tedlar bags in a ratio of 13 % (4-OPA): 1 % (4-AMCH): 86 % (IPOH), that reflect those found in an exposure scenario identified in specific settings (e.g. after using an indoor cleaning kitchen product) [168]. Moreover, the mixture of these chemicals was tested both in presence and in the absence of ozone.

An estimation of the total mass of each chemical potentially inhaled by an adult (approx. 70 kg) was made by assuming a breathing volume of  $20 \text{ m}^3/\text{day}$  [170] multiplied by the concentration of each chemicals measured in a real environment (e.g.  $50 \mu\text{g}$  for 4-OPA;  $4 \mu\text{g}$  for 4-AMCH,  $340 \mu\text{g}$  for IPOH).

Thereafter, the human lung cells exposure to the gas mixture of 4-OPA, IPOH, 4-AMCH directly at the air/liquid interface was made possible by adapting the *in vitro* CULTEX system to two Tedlar bags: one filled with the chemical mixture and the other one filled with Zero air (called also Clean air).

### 3.1.1.3 Results obtained after clean-up procedure of TBs

The clean-up procedure applied to Tedlar bags was monitored by pumped sampling of inner air with Tenax TA sorbent tubes followed by thermal desorption-gas chromatography and mass selective detection, as described in the Materials and Methods chapter.

Preliminary *in vitro* exposure experiments with TBs that were not previously cleaned were carried out. Based on the biological outcomes, both contaminants phenol and DMA present in TBs showed a significant role in the pulmonary cells survival. Both bronchial (16HBE14o-) and alveolar (A549) cells were exposed to Zero Air that was refilled in new TBs (without being previously cleaned). After 1 hour exposure, loss of cell viability measured in bronchial cells was determined as being around 25 %, while after 2 hours exposure, more than 40 %. Similar results were observed for alveolar cells after 1 hour and 2 hours exposure (e.g. more than 20 % of cells and 30 %, respectively).

After repeated cleaning cycles of TBs, the abundance of both phenol and N, N-dimethylacetamide (DMA) was drastically reduced. By applying these repeated cleaning cycles, the tedlar bags were considered appropriate to further be used in the *in vitro* exposure experiments since these conditions did not alter the cellular viability of both types of cell lines (bronchial and alveolar). See chromatograms below:

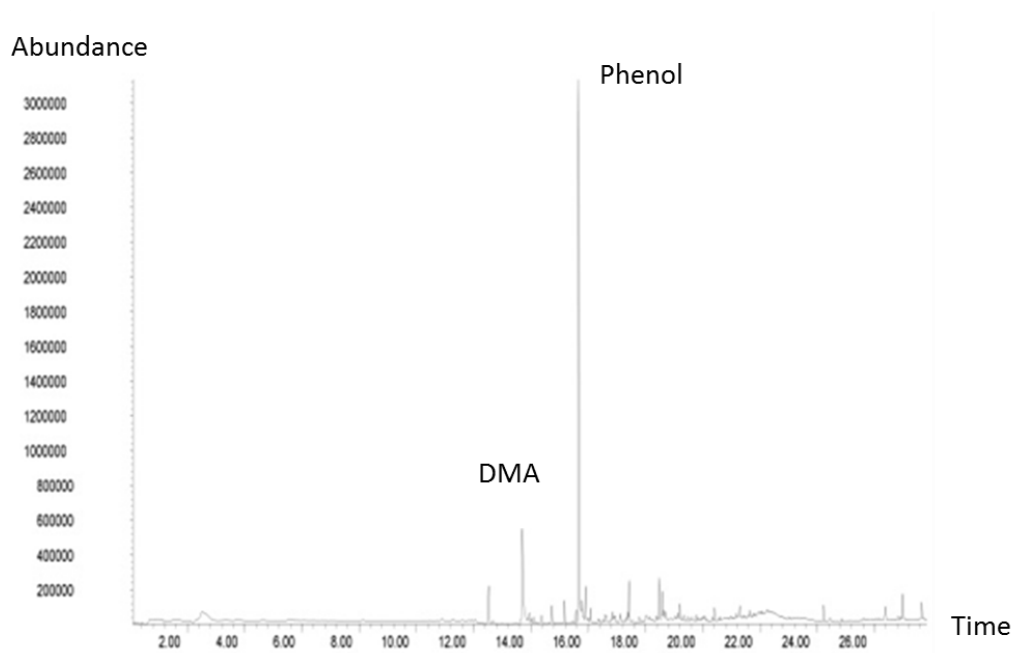


**Figure 29** Chromatogram of a 5-cycles cleaned Tedlar bag still containing DMA (retention time=14) and phenol (retention time=16)

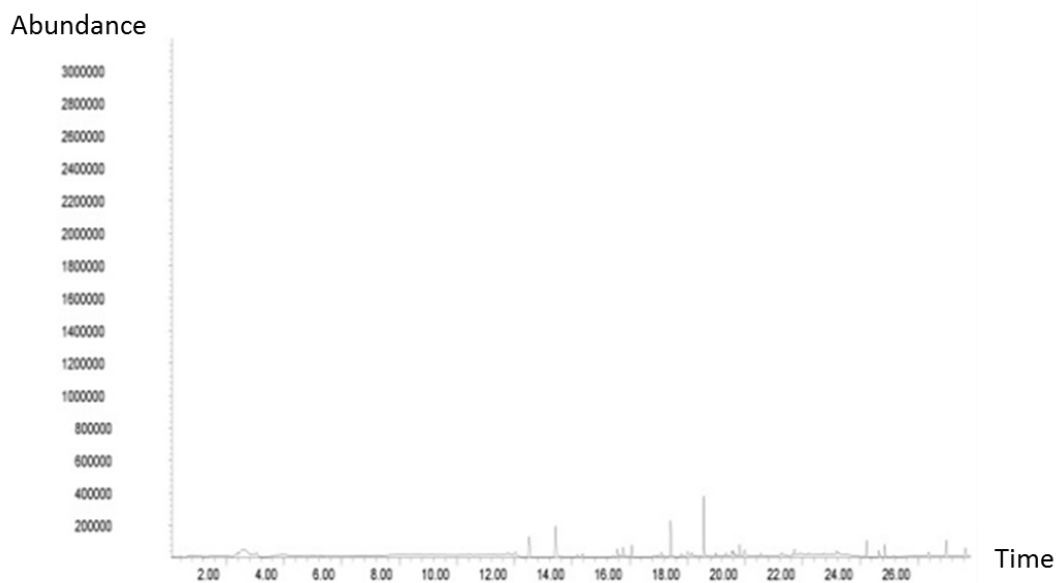


**Figure 30** Chromatogram of a 10-cycles cleaned Tedlar bag

The findings regarding the presence of both phenol and DMA are consistent with findings reported in several papers [376, 377]. Tedlar bags (polyvinyl fluoride) are known to include the above mentioned odorous compounds, latent solvents used in the production of Tedlar film, which have been reported by Ruth et al. at a maximum concentration of  $7200 \mu\text{g m}^{-3}$  and  $1200 \mu\text{g m}^{-3}$  respectively [411].

### 3.1.1.4 Results on the performance of the analytical method for the determination of 4-OPA, 4-AMCH, IPOH in gas atmospheres

The method applied for this case was obtained by slightly adapting the ISO method (ISO 16000-6:2004) based for the identification of VOCs (e.g. limonene, toluene) that did not include the specific compounds 4-OPA, IPOH and 4-AMCH.

Due to the high final concentration of chemicals generated in the TBs, the samples were analysed with Thermal desorption, Gas chromatography, splitted injection and Mass Selective Detection (TD-GC-MSD). Under such conditions, as described in the Materials and Methods chapter, chemical compounds such as d-limonene, 4-oxopentanal, toluene, 4-acetyl-1-methylcyclohexene, 3-isopropenyl-6-oxo-heptanal etc. were separated within 36 minutes.

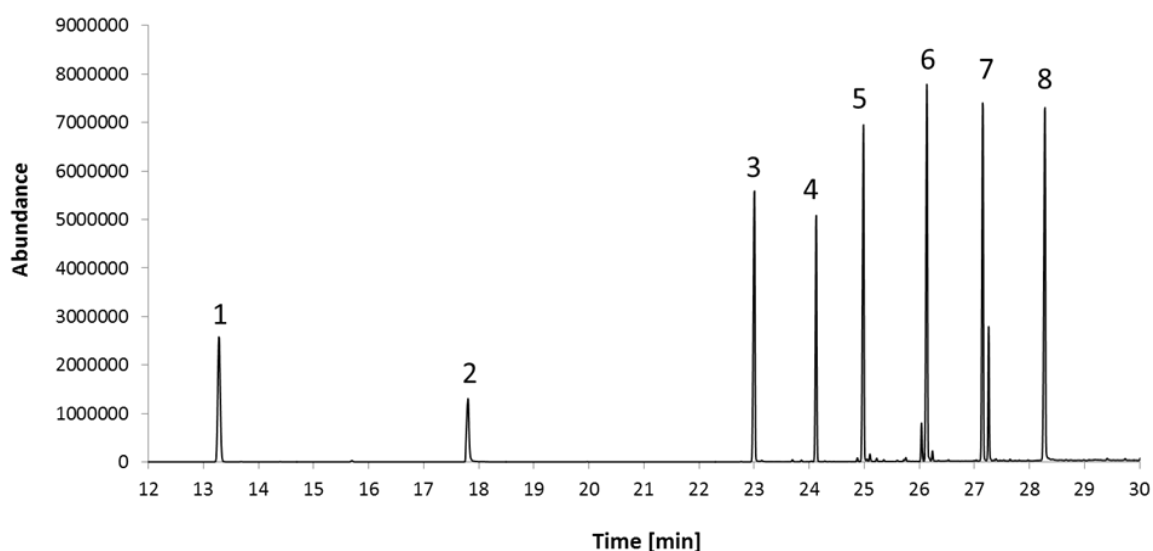


**Figure 31** Chromatogram obtained within TD-GC-MSD method for the determination of 4-OPA, IPOH, 4-AMCH among other volatile organic compounds as follows: 1. Toluene (retention time = 13.29), 2. 4-OPA (retention time = 17.8), 3. 6-MHO (retention time = 23), 4. d-Limonene (retention time = 24.13), 5. Dimetyloctane (retention time = 24.97), 6. 4-AMCH (retention time = 26.15), 7. Dihydrocarbon (DHC) (retention time = 27.14), 8. IPOH (retention time = 28.2)

Selection of the most appropriate column for the GC separation of the target compounds was made according to the suggested columns on the different ISO standards (e.g. ISO 16200- 1:2001 – Workplace air quality, and 16017-1:2000 – Indoor, Ambient and Workplace air) regarding the GC analysis of VOCs. In this sense, the ISO standards

suggest the use of HP5, HP1 or DB624, adapting the most suitable column to the specific set of compounds.

Considering the relatively high polarity of our compounds, either HP5 or DB624 seemed to be the most appropriate ones for the separation. However, DB624 column has the disadvantage of a lower high operating temperature, thus the high temperatures required for the elution of some of the compounds would damage the column in continued use and was thus discarded.

Both limits of detection (LODs) and limits of quantification (LOQs) of the method were determined by spiking 6 Tenax-TA tubes with different volumes of standard solutions containing 1 and 0.1 ng  $\mu\text{L}^{-1}$ . The selection of the sorbent material (a phenylenoxid-polymer that has a good affinity for organic compounds and is thermally stable) is based on the ISO 16017-1:2000 standard. Afterwards, the tube samples were subjected to GC-MS analysis. Triplicate determinations were carried out on each investigated compound. The LODs and LOQs for the selected d-limonene ozonolysis products are calculated as an absolute value (e.g. ng) and are presented in the table below.

**Table 9** Determination of the limit of detection (LOD) and quantification (LOQ) of 4-OPA, IPOH, 4-AMCH

	LOD ng at Signal/Noise = 3			LOQ ng at Signal/Noise = 10		
	4-OPA	4-AMCH	IPOH	4-OPA	4-AMCH	IPOH
<b>ng</b>	7.2	1.6	5.3	24.0	5.2	17.8

### 3.1.1.5 Results regarding the target concentration of the chemical mixture and ozone prepared in Tedlar bags

To calculate the total target amount of chemicals as gas phase in Tedlar bags, two factors were considered:

- The vapour pressure of the most concentrated compound in the mixture, IPOH and
- The possible sink effects of compounds inside the Tedlar bags, including the liquid-vapour equilibrium.

After calculations and preliminary practical evaluation, the following absolute amounts of chemicals were set as target concentrations to be available as mg/40 L in the Tedlar bags for the *in vitro* exposure: 0,27 mg/40 L of 4-OPA; 0,03 mg/40 L of 4-AMCH and 1,91 mg/40 L of IPOH.

The gas mixture of 4-OPA + IPOH + 4-AMCH in absence of ozone showed stability during the whole *in vitro* exposure period (up to 2 hours) since the concentration of the targeted compounds quantified by GC-MS was the same before and after the *in vitro* experiment. When ozone was added to the gas mixture, no other secondary products were observed to be formed when using the GC-MS method.

The stability test of the mixture prepared as gas phase was carried out in triplicate for each exposure experiment.

### 3.1.2 Development and optimisation of the HPLC-UV method for the detection and quantification of intracellular glutathione species

#### (i) Optimisation of the HPLC mobile phase used to separate GSH, GSSG and GSNO

A fractional factorial design was considered for the optimisation of the mobile phase composition used in the chromatographic separation of GSH, GSSG and GSNO. A set of sixteen combinations of the four selected mobile phase compounds (water, acetonitrile, trifluoroacetic acid and sodium perchlorate) was carefully chosen to be tested in a practical way according to the ranges specified in **Table 10**. The mobile phases to be tested were selected to ensure a representative model of all the possible combinations of their four main constituents: water, acetonitrile, trifluoroacetic acid and sodium perchlorate (e.g. 1<sup>st</sup> combination tested was consisting in water (80 %) : acetonitrile (20 %) : trifluoroacetic acid (0 %) : sodium perchlorate (0 mg mL<sup>-1</sup>).

**Table 10** Tested mobile phase composition consisting in water, acetonitrile, trifluoroacetic acid and sodium perchlorate

Mobile phase compositions tested				
H <sub>2</sub> O (%)	80	90	95	100
Acetonitrile (%)	20	10	5	0
	0 / 0	0 / 0	0 / 0	0 / 0
TFA (%) / Sodium perchlorate (mg mL <sup>-1</sup> )	0.05 / 6	0.05 / 6	0.05 / 6	0.05 / 6
	0.1 / 12	0.1 / 12	0.1 / 12	0.1 / 12
	0.15 / 18	0.15 / 18	0.15 / 18	0.15 / 18

### Effects of the water percentage on peak resolution

The dependence of the resolution between the peaks corresponding to GSH, GSSG and GSNO on the composition of the mobile phase was evaluated by both partial least squares regression and multiple linear regression analysis. Subsequently, it was possible to determine the optimum mobile phase that provided baseline separated peaks (that is  $R > 1.5$ ) for all three species in the shortest analysis time (see **Figure 32**). The mobile phase containing higher water/acetonitrile ratios in the mobile phase resulted in considerably longer analysis times and was thus discarded.

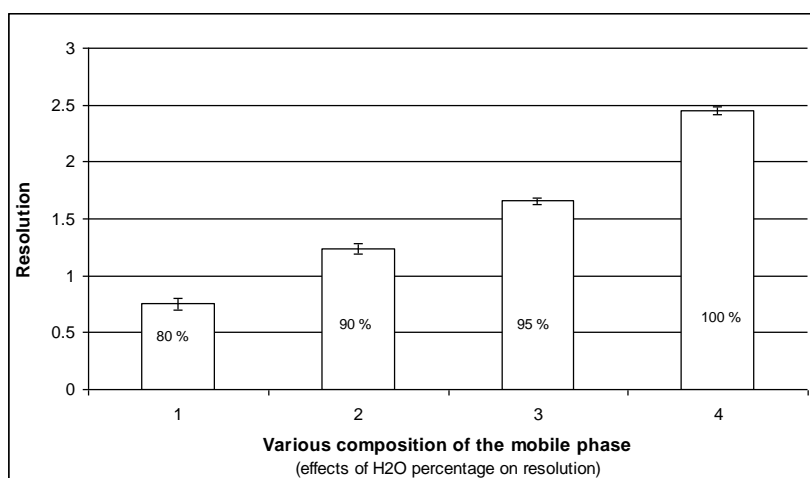


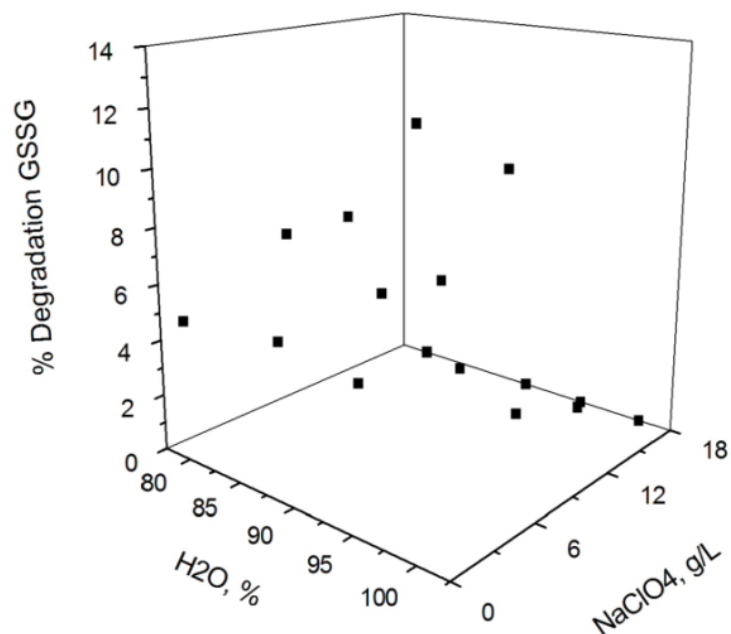
**Figure 32** Effect of the mobile phase composition on the chromatographic resolution of reduced, oxidised and nitroso- glutathione forms. Numbers indicated on the x axis correspond to the composition of eluent presented in the Table 10 ( $n = 4$ )

### Effects of the addition of trifluoroacetic acid to the mobile phase

The addition of a defined amount of TFA to the mobile phase ensured complete protonation of the molecules under investigation and thus symmetric peak shape. An increase in this amount resulted in a poorer reproducibility of the results which was probably due to a poor performance of the chromatographic phase under such acidic conditions. Other acids (e.g. phosphoric or sulfuric) were also evaluated, and showed a similar performance. However, given that TFA was already tested during cell lysis, it was considered as the optimum acid in order to avoid introducing an additional variation into the method that could cause interferences with the sample matrix.

### Effects of sodium perchlorate on GSSG stability

Degradation of GSSG was observed to be negligible during the chromatographic run if at least  $12 \text{ mg mL}^{-1}$  of sodium perchlorate were added into the mobile phase containing water/acetonitrile (95/5, v/v) and 0.1 % trifluoroacetic acid (see **Figure 33**).

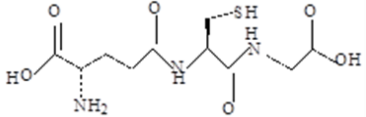
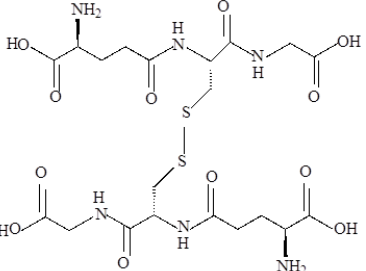
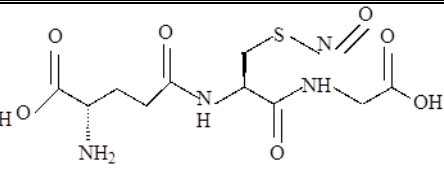


**Figure 33** Percentage degradation of GSSG calculated based on sodium perchlorate amount added to the mobile phase (n=3)

### *(ii) Column effectiveness*

Column selection was based on the solubility and structure of the group of analytes tested (see **Table 11**).

**Table 11** Chemical characteristics of glutathione molecule

Name	Structure	Acidic dissociation constant		Log P
		pKa (most acidic)	pKa (most basic)	
<b>GSH</b>		2.12	9.65	-3.6
<b>GSSG</b>		2	9.61	-4.9
<b>GSNO</b>		2.21	9.28	-2.97

The degree of separation achieved with the selected C18 column was also investigated with two other types of reversed phase C18 columns in order to select the most suitable column for the separation of the three glutathione species.

Columns evaluation was conducted with the aim to identify the best column with which a good separation between selected molecules (resolution), a short time eluting peaks and a good peak shape can be achieved. For this test analysis, columns were selected on the basis of a slight modification in the stationary phase; exploiting the more polar oriented stationary phase, such as the Kinetex, Synergy Fusion column resulted in a confirmation that no overlap with other peaks took place during the optimal separation with the C18 YMC column.

Chromatogram runs obtained for these purposes are reported in **Figure 34**.

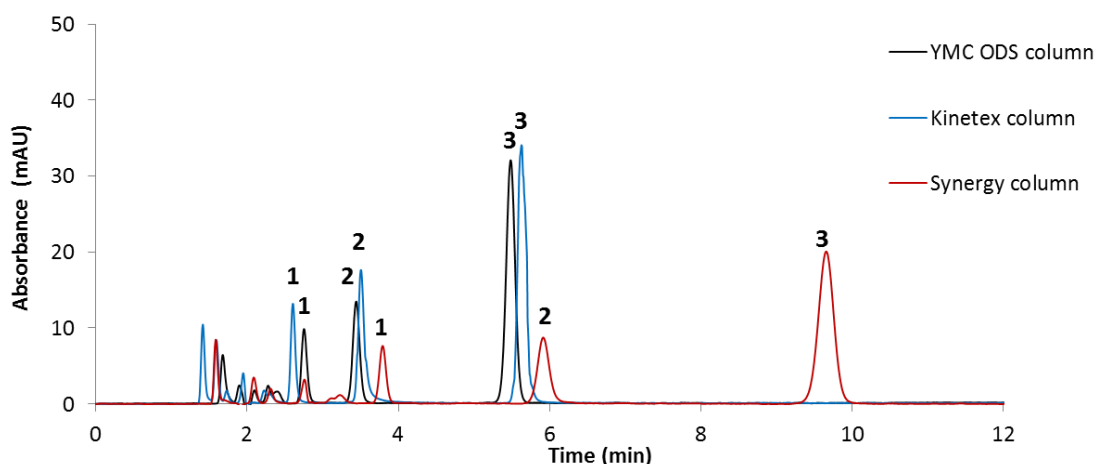


**Figure 34** Separation of the three glutathione forms on the above mentioned columns using glutathione standards: 1. Reduced glutathione; 2. Oxidized glutathione; 3. S-nitrosoglutathione

The YMC ODS-A column was selected as optimum since a shortest analysis time was achieved within 6 minutes, a better peak shape (no peak tailing) of GSSG standard was obtained when compared to the Kinetex column and no overlapping of glutathione species with matrix components was observed when biological samples were analysed. A representative overlay chromatogram of the selected standard glutathiones and intracellular glutathione species determined in A549 cells exposed to  $\text{NO}_2$  is shown in **Figure 35**.

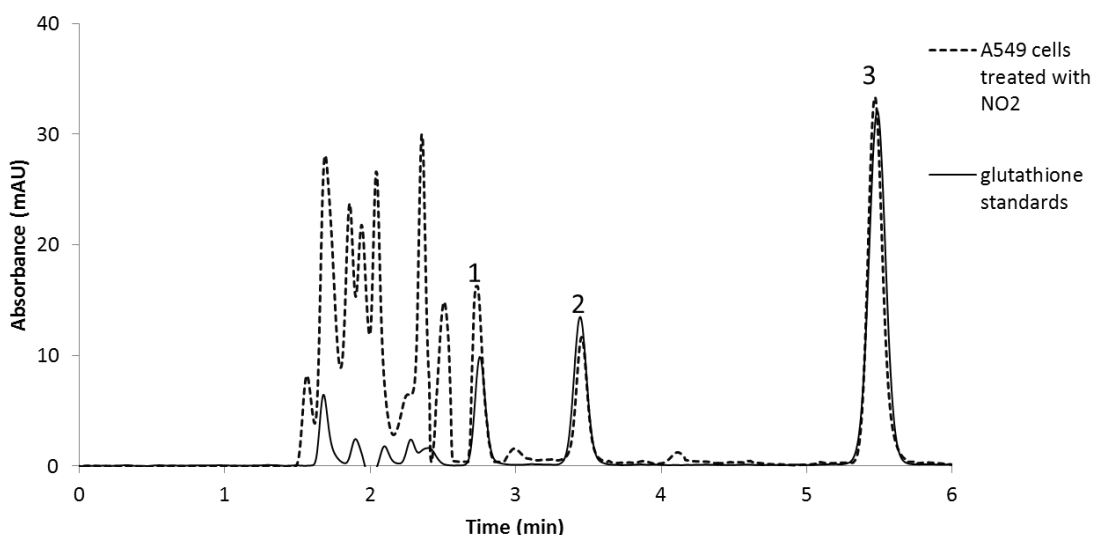


**Figure 35** Chromatograms (overlay) obtained under optimum conditions with the YMC ODS-A column representing a mixture of GSH, GSSG and GSNO standards and the intracellular glutathione species determined in A549 exposed to  $\text{NO}_2$

The presence/absence of ghost peaks or peaks hidden under the main peaks (GSH, GSSG and GSNO) that might appear due to biological samples, (in this case, from the cellular extract of human cells) was investigated by an additional method. The cell extracts were spiked with different concentrations of the selected glutathione standards, as follows: for GSH, 0.25; 0.5; 0.75; 1; 1.25 mM; for GSSG, 0.125; 0.25; 0.325; 0.5; 0.625 mM; and for GSNO, 0.167; 0.333; 0.5; 0.667 mM.

Determination of GSH, GSSG and GSNO under basal conditions (cells that were not treated) from 6 biological replicates, using various number of cells (e.g. 100 000; 290 000; 435 000) was used as reference. Then the same number of cells was spiked with the various concentrations of the glutathione standards mentioned above. In the figure below (e.g. determination of reduced glutathione – GSH in both biological samples (100 000 cells) spiked with GSH standard and GSH standard alone), the results show that there is a correspondence (linearity) between the biological samples spiked with glutathione standards and the glutathione standards injected alone, with  $R=0.995$  (for spiked samples) and  $R=0.997$  (for standard). The same approach was applied for the determination of GSSG and GSNO in spiked samples. A good linearity between the spiked samples and standards ( $R=0.997$  and  $R=0.996$  for spiked samples and GSSG standard, respectively;  $R=0.995$ , and  $R=0.998$  for spiked samples and GSNO standard, respectively) was observed, which confirms the absence of other peaks hidden under the molecules of interest: GSH, GSSG and GSNO.

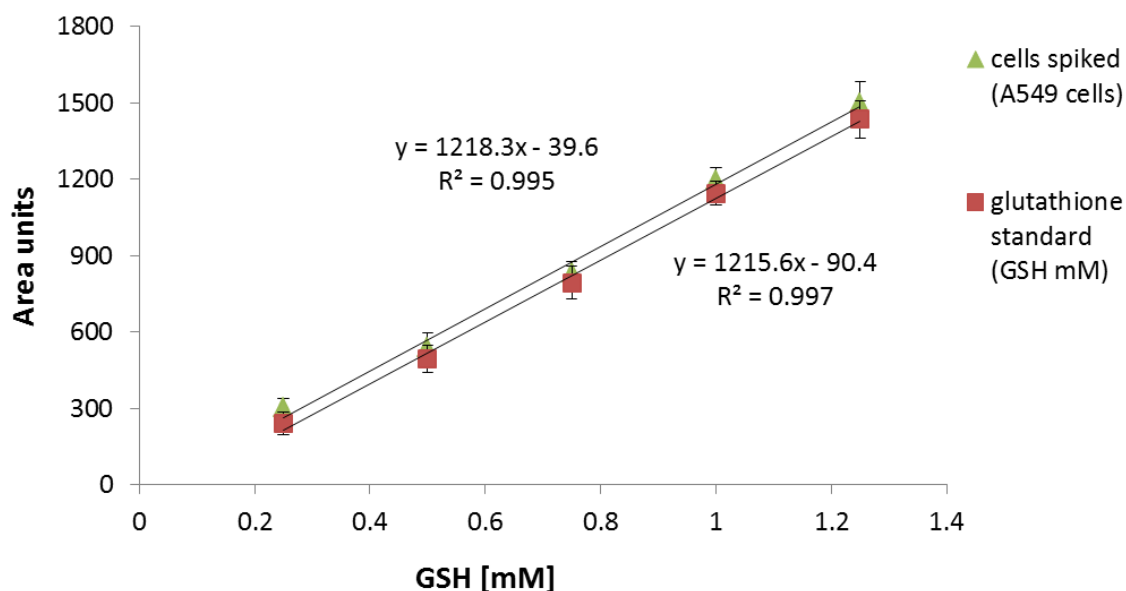


**Figure 36** Comparison of reduced glutathione (GSH) at various concentrations determined in spiked biological samples and GSH standard solutions

(iii) Evaluation of the HPLC-UV method performance

For the in-house validation of this HPLC-UV method, parameters such as limit of detection, limit of quantification, reproducibility and repeatability were evaluated.

Sensitivity detection and quantification limits

With the given mobile phase, the sensitivity, detection and quantification limits for GSH, GSSG and GSNO (standard solutions) were calculated based on the calibration curves generated for each individual analyte (see **Table 12**). Calibration curve correlation coefficients ( $R^2$ ) of 0.998, 0.997 and 0.997 for reduced, oxidized and S-nitroso- glutathione respectively were obtained (see **Figure 37**).

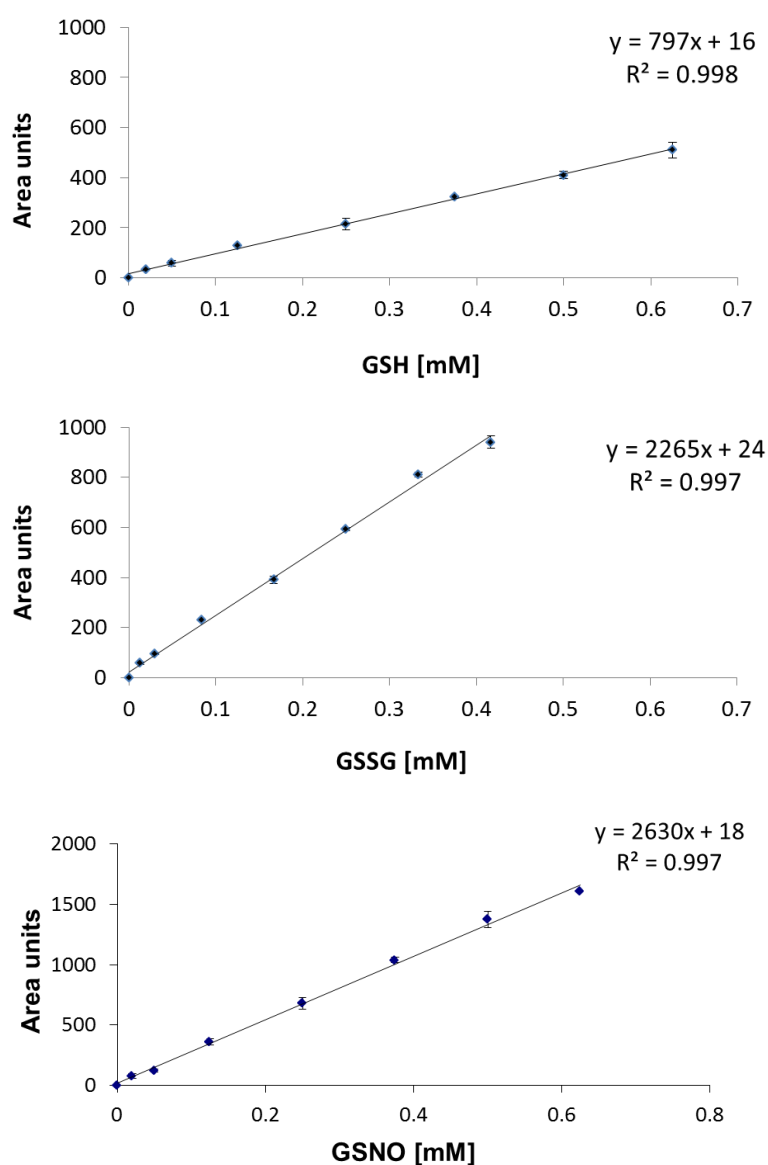


**Figure 37** Calibration curves of the three glutathione species (reduced – GSH, oxidised – GSSG, and nitroso – GSNO) where concentrations were plotted against the area units of the peaks within HPLC-UV chromatogram ( $n = 3 \pm SD$ )

**Table 12** Detection, quantification limits and sensitivity obtained for GSH, GSSG, GSNO within the proposed method

	Detection limit [ $\mu\text{M}$ ]	Quantification limit [ $\mu\text{M}$ ]	Sensitivity [ $\mu\text{M}$ ]
GSH	0.16	0.54	0.02
GSSG	0.08	0.26	0.01
GSNO	0.02	0.05	0.002

### Repeatability and reproducibility

The repeatability of the method (evaluated by the RSD) was assessed from four concentrations of each of the glutathione species and its four replicates. The RSD values for GSH, GSSG and GSNO ranged from 0.05 to 0.16 %; 0.01 to 0.6 % and 0.02 to 0.09 %. Long term reproducibility of the method (2 months) was assessed by the RSD from four different concentrations of freshly prepared standard solutions. The RSD was < 5% for all three glutathione species (0.9–2.7 % for GSH; 0.4-2.9 % for GSSG and 0.2-1.4 % for GSNO).

### Recovery tests

Glutathione recovery was determined by spiking 6 biological replicates of A549 cells with two different concentrations of the standard solutions (GSH, GSSG and GSNO). Following the extraction procedure mentioned in the Materials and Methods section, the cellular extracts were injected immediately in HPLC. The percentage recovery of the present study ranged from 98.7 % to 100.1 %.

### Storage of standard solutions

Standards stored at 4 °C showed stability for up to 3 days (7 % RSD) and for up to 2 months at -80 °C (5 % RSD).

A key objective of the present study was to develop and optimise an analytical method based on liquid chromatography coupled with a UV detector to simultaneously identify and quantify GSH, GSSG and GSNO in human epithelial cells. In this respect, a fast and reproducible method, based on liquid chromatography, coupled to UV detection, was developed and optimised in order to identify and quantify free glutathione species (GSH, GSSG, and GSNO) produced in human cells. The developed method has the advantage of allowing the direct and simultaneous determination of the three most abundant glutathione species in cells, avoiding time-consuming, tedious derivatization steps as

commonly described in the literature [412, 413]. Within this method, intracellular glutathione species were possible to be determined in different experimental set-ups, such as a low number of biological samples ( $\approx 10^4$  cells) and different cell exposure techniques (e.g. direct injection of the chemicals into the culture medium and direct exposure of the cells to the chemicals as a gas atmosphere). This aspect has significant implications in the biological field because it gives the researcher the freedom to choose the best experimental plate design for toxicological studies, without being limited to use a certain number of cells ( $\approx 10^6$ ) as requested by some commercial kits. In comparison with the LC-ES/MS method applied to quantify the three glutathione species (GSH, GSSG, GSNO) content in plants [414] the HPLC-UV method appears to be faster, in terms of both time of analysis and time required for sample preparation.

### 3.1.3 Optimisation of extraction procedure of intracellular glutathione species from human cell lines

As previously published, metal chelators are able to stop enzymatic activities and to prevent the oxidation process of reduced glutathione [415, 416]. Therefore, in order to solve both deproteinization and to prevent oxidation of glutathione, effects of various acids were tested for the extraction of intracellular GSH, GSSG and GSNO from the A549 cell line. This was based on the use of acids, low temperatures and four especially designed lysis buffers: 1) Lysis no.1: Cells were incubated at room temperature with 300  $\mu$ L of Mammalian Protein Extraction Reagent (M-PER) lysis buffer; 2) Lysis no.2: Cells were incubated at -18  $^{\circ}$ C with 300  $\mu$ L of a 5 % trifluoroacetic acid aqueous solution and scrapped using a rubber policeman; 3) Lysis no.3: Cells were incubated at -18  $^{\circ}$ C with 300  $\mu$ L of a 5 % metaphosphoric acid aqueous solution and scrapped; 4) Lysis no.4: Cells were incubated at -18  $^{\circ}$ C with 300  $\mu$ L of a 0.5 % aqueous picric acid solution and scrapped.

On the other hand, it has been demonstrated that in acidic conditions, artifactual formation of GSNO may appear due to the chemical interaction between GSH and nitrite. As demonstrated by Yap et al., treatment of the biological samples with ammonium sulfamate or N-ethylmaleimide resulted in an accurate assessment of GSNO content. Therefore, in order to accurately determine the GSNO content in the cells, nitrite neutralisation under acidic conditions was considered in our work by adding ammonium sulfate to the acidic solution (0.5 % picric acid) prepared to obtain the cellular extract [417].

After the incubation step (5 minutes), the homogenates were transferred to an Amicon 3K Ultra Millipore filter and centrifuged at 12.000 g for 15 minutes in order to remove proteins

prior to HPLC analysis. Finally, the supernatant was directly injected into the HPLC system for the analysis of GSH, GSSG and GSNO.

**Table 13** The amount of GSH extracted from the alveolar and bronchial epithelial cells by using each of the above described procedures for the lysis of the cells.

Lysis procedure	A549 cells GSH [ $\mu$ M]	16HBE14o- cells GSH [ $\mu$ M]
MPER lysis buffer, room temperature	2.8 $\pm$ 1.1	4.0 $\pm$ 1.8
5 % TFA, -18 °C	1.7 $\pm$ 0.5	2.2 $\pm$ 0.61
5 % MPA, -18 °C	0.9 $\pm$ 0.52	1.6 $\pm$ 0.77
0.5 % picric acid, -18 °C	10.3 $\pm$ 0.2	15.3 $\pm$ 0.38

As can be observed, the lysate providing the highest intracellular GSH extraction is that of picric acid, which was thus selected for further analysis of intracellular GSH, GSSG and GSNO in cells exposed to different test compounds.

### 3.1.4 Optimisation of cellular density on different seeding surfaces (24, 96-well plates and transwell porous membrane inserts)

#### 3.1.4.1 Optimisation of the *in vitro* cell cultures seeded on 24-, 96-well plates

Preliminary tests were conducted to find the optimal cell density in 24 and 96-well plates after 24 hours incubation time since the number of cells and exposure time can significantly influence the outcome of the colorimetric assay (false high or false low cell counts). Therefore, both cell lines (A549 and 16HBE14o-) were seeded in the range of 50.000 to 250.000 cells per well tested for 24-well plate and 3.000 to 100.000 cells per well for 96-well plate. Neutral red uptake was selected to evaluate the survival/viability of the cells.

The optimal cell number was selected based on the linearity range of the cell number and absorbance values (see **Figure 38** for results obtained in 96-well plate and **Figure 39** for 24-well plate).

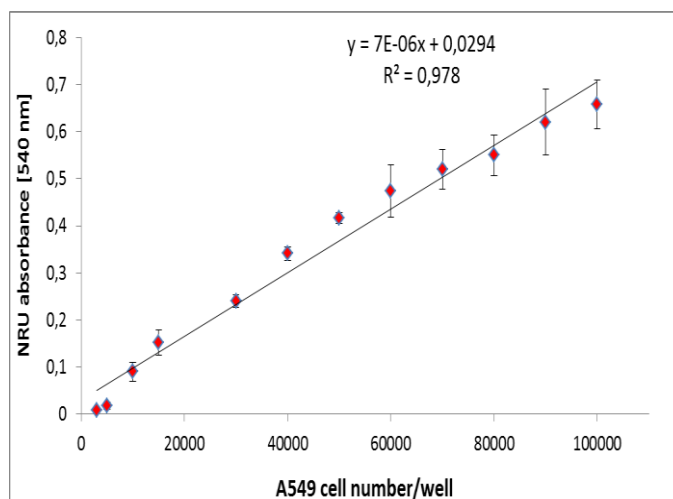


**Figure 38** Linearity range for A549 and 16HBE14o- cell numbers and the Neutral red uptake absorbance level obtained for 3 independent experiments with 3 replicates each ( $R^2 \geq 0.978$ )

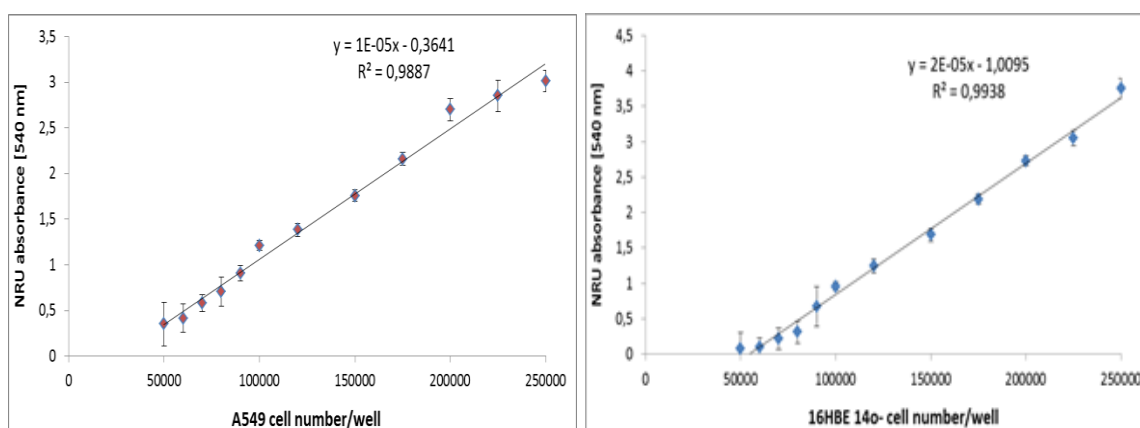


**Figure 39** Linearity range for A549 and 16HBE14o- cell numbers and the Neutral red uptake absorbance level obtained for 3 independent experiments with 3 replicates each ( $R^2 \geq 0.988$ )

### 3.1.4.2 Optimisation of the *in vitro* cell cultures seeded on transwell porous membrane inserts

For the air/liquid interface exposure experiments, cells were seeded onto porous transwell membrane (A549 cells:  $3 \times 10^5$  cells / insert; THP-1 cells  $1 \times 10^6$  cells / insert; 16HBE14o-  $5 \times 10^5$  cells/insert) with a pore diameter of  $0.4 \mu\text{m}$  (Falcon, PET membrane) and were directly exposed to gas atmospheres by the use of an air-lifted CULTEX exposure system in which the cells were fumigated for 1 and 2 hours with a flow of selected gas atmospheres.

The whole procedure regarding the cell culture preparation on permeable microporous membranes was reviewed [418] and optimized (e.g. optimal density).

For example, a range of seeding A549 cell density ( $32 \times 10^3$  cells  $\text{cm}^{-2}$  to  $1.0 \times 10^5$  cells  $\text{cm}^{-2}$ ) was selected to identify the optimum growth onto 0.4  $\mu\text{m}$  porous membranes with a growth area of  $4.27 \text{ cm}^2$ . Thus, the appropriate cell number, which reached a 70-80 % confluence, was further selected based on the observation made by the use of a light microscope (see **Figure 40**). The same approach was studied also for the other cell lines mentioned above.

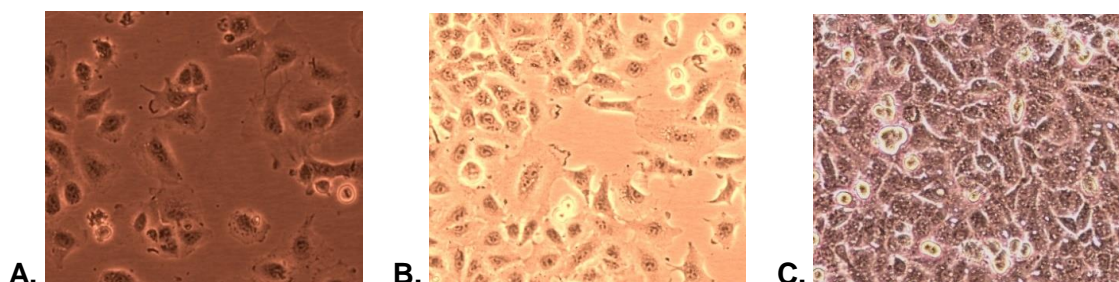


**Figure 40** Illustration of the different cell densities of plated A549 cells. **A.** Cell density  $32 \times 10^3$  cells  $\text{cm}^{-2}$  **B.** Cell density  $7.0 \times 10^4$  cells  $\text{cm}^{-2}$  **C.** Cell density  $1.0 \times 10^5$  cells  $\text{cm}^{-2}$

Microscope observation revealed that a better homogenous monolayer was achieved when transwell porous membranes were pre-incubated for 2 hours prior to seeding with complete medium (bottom = 2.5 ml, top = 0.5 ml). At the moment of cells seeding, the culture medium was removed only from the top and substituted with 1.5 ml of fresh culture media containing the cell suspension at the density mentioned above.

### 3.1.5 Evaluation of the performance of an automated cell counting pipette versus traditional cell counting (Trypan blue)

As commonly used methods used to investigate the status of cellular viability such as Trypan blue are often tedious and time consuming, the objective of this work was to assess the performance of the automatic counting pipette compared to the traditional counting dye exclusion method. The ability of the handy Scepter 2.0 automated microcoulter pipette to count dead, viable and total cells was tested by comparison of the results with those achieved by hemocytometer measurements based on Trypan blue dye. This evaluation was carried out for two human cell lines (A549 and 16HBE14o-).

One of the major challenges in this regard was to hand-pick the sensor tip specific for these cells. An initial screening was applied in order to determine which was the most suitable sensing tip for counting the bronchial cell lines 16HBE14o- (see **Figure 41**).

Therefore, three different cell suspensions were counted using both sensors and Trypan blue for both cell lines.

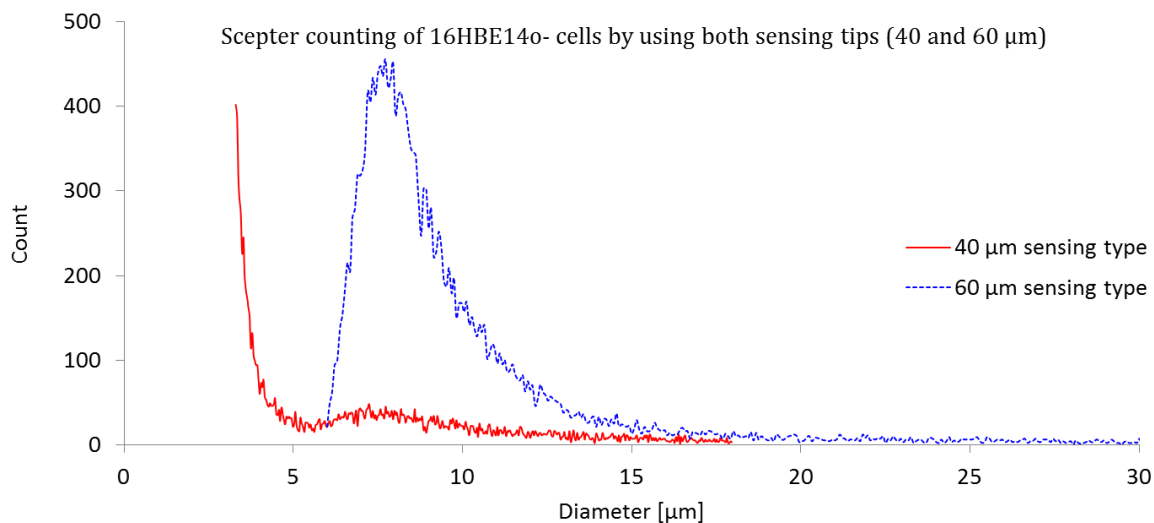


**Figure 41** Viable cells counting of 16HBE14o- using Scepter 2.0 and both sensing tips of 40 and 60 μm

According to the results, the 60 μm sensing tip seems to be the most appropriate for cell counting in both cell lines, as it provides similar results to those obtained with Trypan blue exclusion assay. Using the 40 μm sensor, on the other hand, leads into a slight underestimation of total cell count, and was thus discarded.

The results of the measurements obtained for total cell count of both cell lines in the different cultures, after 24 hours of treatment with 1 % dimethyl sulfoxide (DMSO), are summarized in **Table 14**.

Dilution solutions for A549 cells were prepared with a dilution factor of 1.3 (dilution 1), 1.5 (dilution 2) and 2 (dilution 3), while for 16HBE14o- cells the dilution factors were 2, 1.3, 2.5 respectively.

## Results and Discussion

**Table 14** Total cell counts obtained for A549 and 16HBE14o- by Trypan blue and Scepter measurement (n = 3).

Cell culture samples	A549 cell line			16HBE14o- cell line		
	Trypan blue	Scepter 2.0 cells mL <sup>-1</sup>	Scepter 2.0 cells mL <sup>-1</sup>	Trypan blue	Scepter 2.0 cells mL <sup>-1</sup>	Scepter 2.0 cells mL <sup>-1</sup>
	cells mL <sup>-1</sup>	Tip 40 µm	Tip 60 µm	cells mL <sup>-1</sup>	Tip 40 µm	Tip 60 µm
<b>Initial solution</b>	424 110		416 030	401 380		401360
<b>Dilution 1</b>	309 040	240 540	306 110	214 440	159 310	191 340
<b>Dilution 2</b>	229 200		221 230	158 600		148 060
<b>Dilution 3</b>	115 220	100 160	102 510	61 200	76 550	55 830

**Table 15** Evaluation of the coefficient variation of both selected methods for total cell counting 16HBE14o- (cells mL<sup>-1</sup>= NOperator\*10<sup>3</sup>, n = 12) executed by well-trained operators

N	Trypan blue		Scepter pipette	
	NOperator1	NOperator2	NOperator1	NOperator2
1	237.8	129.5	197.5	197.4
2	211.2	231.4	196.5	205.5
3	239.7	234.6	201.5	211.6
4	231.7	229.8	200.7	186.4
5	202.3	217.4	200.1	157.2
6	214.2	183.7	201.4	221.5
Mean	213.6		198.1	
Stdev	31.234		15.466	
RSD	14.62%		7.81%	

**Figure 42** shows the comparison of the results obtained for the total cell count of 16HBE 14o- cell line achieved by both techniques. A good correlation is obtained, with a slope of 0.98, thus indicating the validity of the Scepter 2.0 procedure, when compared to the analogous cell counts with Trypan blue.

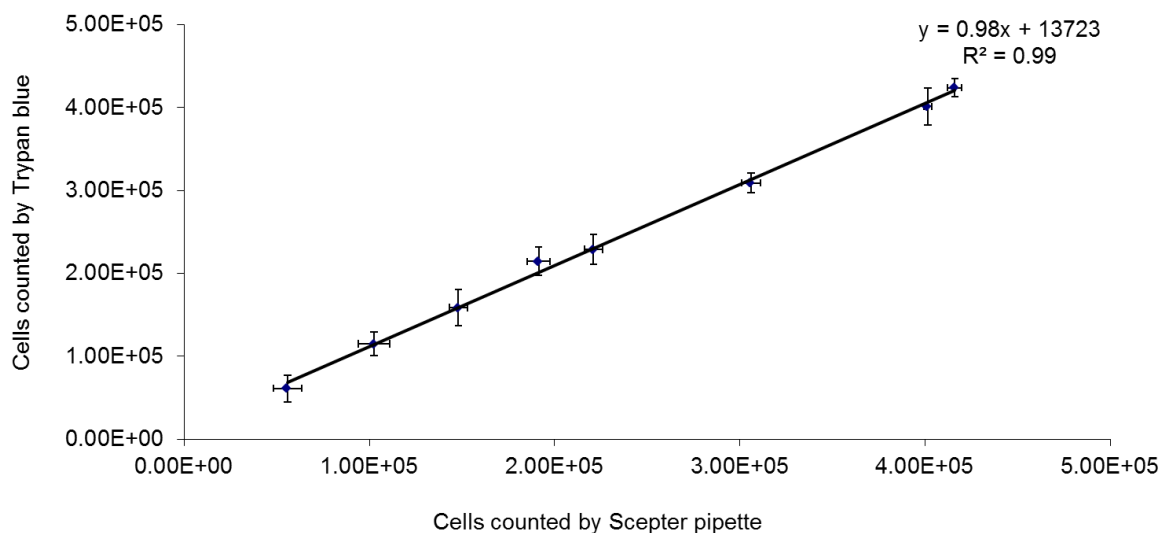


**Figure 42** Comparison of total cell count obtained by Trypan blue and Scepter 2.0 for both cell lines ( $R^2=0.99$ ,  $n=3$ , horizontal standard bars stand for counts done by Scepter pipette, while the vertical standard bars for Trypan blue)

The pipette provides analogous results to those obtained by dye exclusion counting, as demonstrated by the high correlation observed between both counting procedures. In this regard, correlation indexes higher than 0.95 were obtained in all cases, the p-values being below 0.001. Additionally, cell counting with the Scepter 2.0 pipette is considerably faster, requiring only 30 seconds to perform the analysis in contrast to the 5 minutes using a hemocytometer method, and is thus especially interesting for those cases in which a fast and accurate cell count is necessary (for example in case of air / liquid interface exposure). Additionally, Scepter 2.0 enables a more precise and accurate method, with coefficients of variation below 8 % in all cases.

### 3.1.6 Optimisation of the air/liquid interface exposure conditions

#### *Flow rate and pH of the culture medium conditions*

Measurement of the CULTEX system reproducibility was performed by repeated exposure of the A549 cells to Zero Air at a flow corresponding to  $2 \text{ mL min}^{-1}$  for each vessel of the exposure module, as reported in the literature. Another parameter that was considered in the validation of the CULTEX reproducibility was the pH of the culture medium. In order to avoid pH variability during the whole exposure time (maximum 2 hours), 25 mM HEPES was added to the culture medium (RPMI 1640) as suggested in literature [418]. Also, the flow of each Teflon trumpet, through which the compounds as gas phase are delivered into a continuous flow to the apical side of the cells, was adjusted at  $2 \text{ mL min}^{-1}$  each time at the beginning of the experiments.

#### *Performance of the two exposure chambers/modules*

In order to validate the CULTEX device reproducibility under these conditions, cell viability by Scepter pipette was assessed. As shown in **Figure 45**, these exposure conditions proved to give a viability of cells higher than 80 %, close to that of unexposed cell cultures which were maintained in the incubator ( $37 \text{ }^{\circ}\text{C}$ , 5 %  $\text{CO}_2$ ) without medium at the apical side of the cells. For *in vitro* experiments, where cells were exposed to tested compounds, the values of cells exposed to Zero air that were lower than 80 % were considered as outliers, therefore the experiments were discarded.

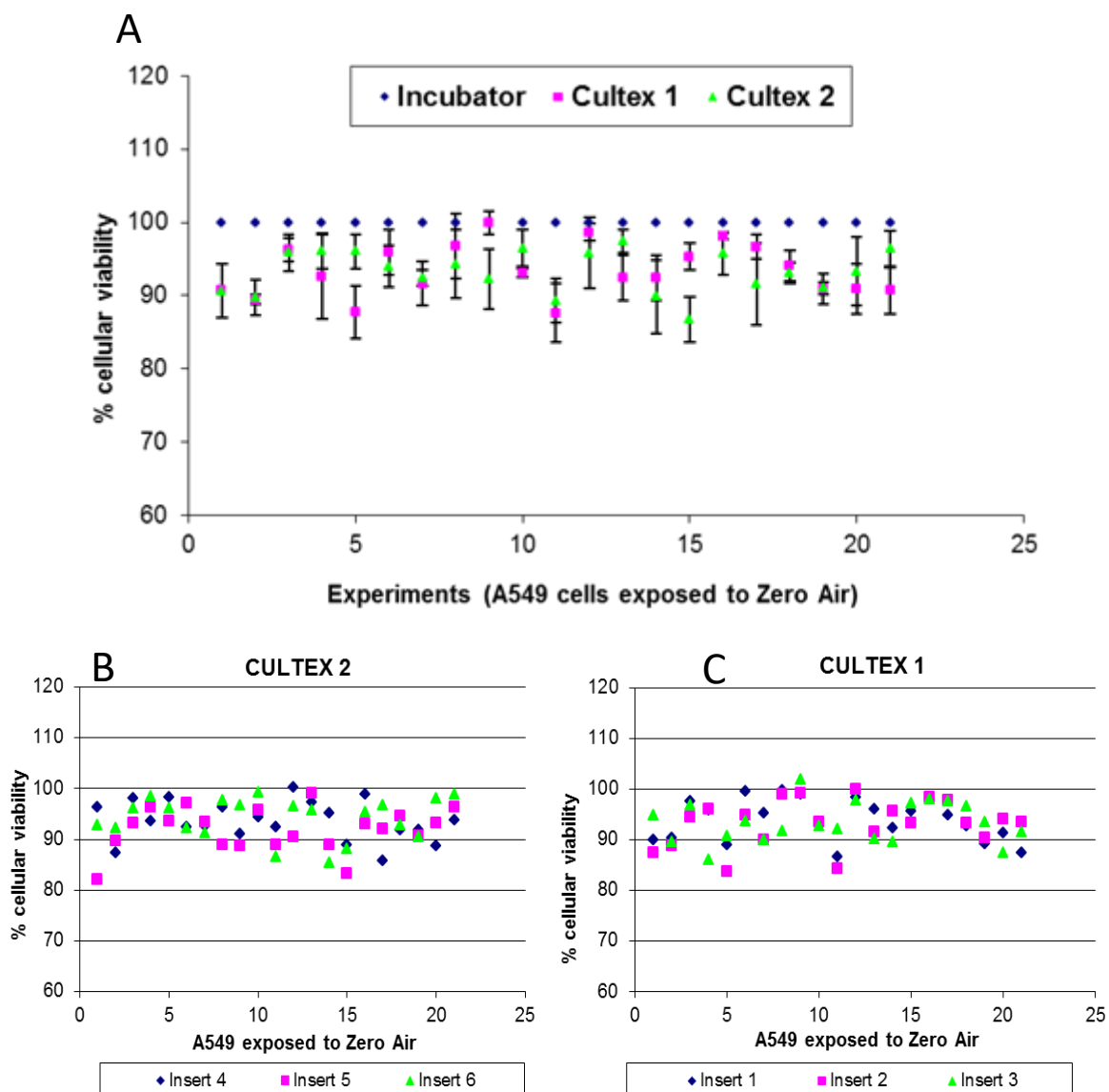


**Figure 43** Evaluation of cellular viability by Scepter pipette of A549 cells exposed to Zero Air within CULTEX system ( $n=25 \pm \text{STD}$ ) **A.** Results (% cellular viability) from cells kept in Incubator and cells exposed to Zero air in both CULTEX exposure modules **B.** Results (% cellular viability) from cells exposed to Zero air in the CULTEX 2 holding the three vessels (insert 4, insert 5, insert 6) **C.** Results (% cellular viability) from cells exposed to Zero air in the CULTEX 1 holding the three vessels (insert 1, insert 2, insert 3)

*Evaluation of two relative humidities of Zero Air on cellular viability*

The impact of the Zero Air at two relative humidities (RH 50 and 80%) was assessed on cellular viability of A549 cells. As shown in **Figure 44**, no statistically significant differences were obtained for A549 cells exposed for 2 hours to Zero Air at both tested relative humidities.

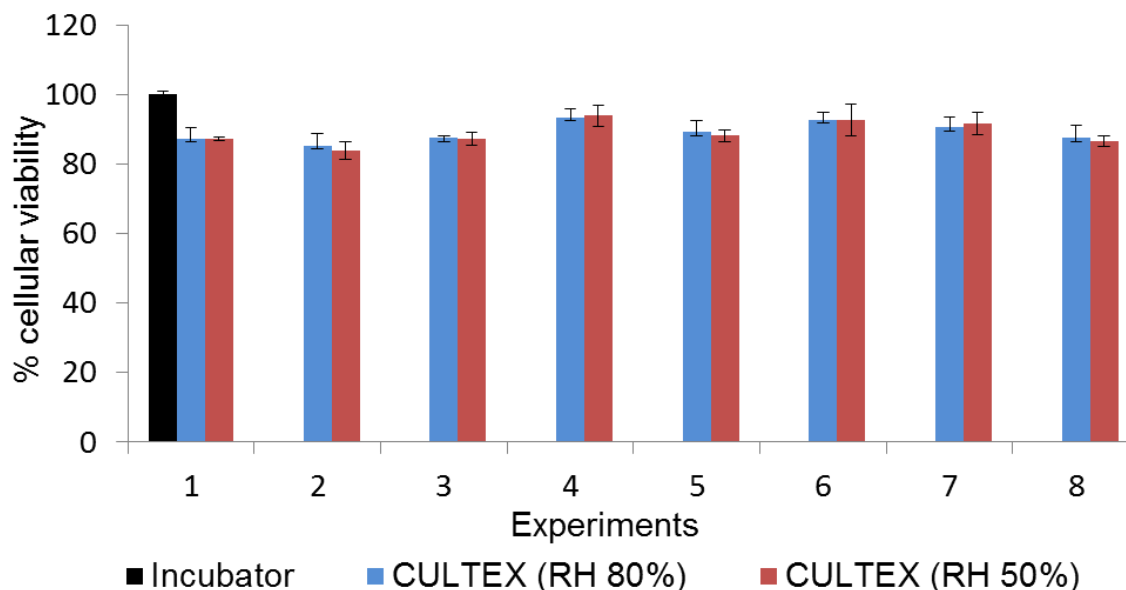


**Figure 44** Comparison of cellular viability data from cells exposed to Zero Air under two relative humidity (RH) conditions (50 and 80 %) ( $n = 3 \pm \text{STD}$ )

*Evaluation of different exposure times on cells exposed to Zero Air*

Different exposure times were performed by exposing A549 cells to Zero Air. The aim of this experiment was to identify the maximum time of exposure at which cell viability is not statistically different from the 80 % value, which was considered as the minimum acceptable value within all experiments.

**Figure 47** shows the effect of Zero Air airflow on the A549 cells at different exposure times: 1 h, 2 h, 2 h 30 min and 3 hours. As can be observed, after 2 hours and 30 minutes of exposure, the cell viability was reduced to around 75 % when compared to the negative control (Incubator) while after 3 hours cell viability reached around 65 %. The linear trend observed between the selected time exposure has a  $R^2$  higher than 0.98. Therefore, in order to avoid a “masking effect” due to Zero Air in the experiments where cells are exposed to test compounds, the maximum exposure time selected was 2 hours.

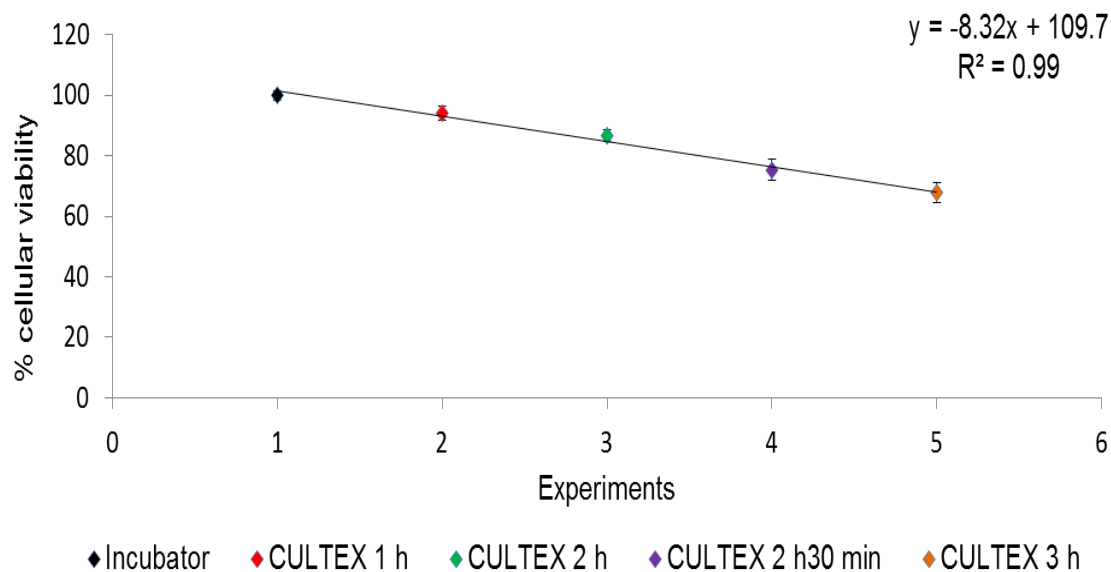


**Figure 45** Effects of time exposure on cellular viability of cells exposed to Zero air (n=9 ± STD).

The main scope of this work was to set up the optimal culture conditions and an *in vitro* exposure system allowing the direct exposure of human pulmonary cells to the test compounds as gas phase.

### 3.2 *In vitro* studies with human lung cells and blood exposed to d-limonene and ozonolysis products 4-OPA, 4-AMCH, IPOH via liquid/liquid interface

#### 3.2.1 Evaluation of cytotoxic effects of d-limonene, 4-OPA, 4-AMCH, IPOH and the binary/ternary mixtures of 4-OPA, 4-AMCH, IPOH via liquid / liquid interface

##### 3.2.1.1 Concentration-response relationship for alveolar (A549) and bronchial (16HBE 14o-) cells determined by Neutral Red Uptake assay

Following chemical treatment for 24 hours, NRU assay was carried out to determine the status of cell viability. As can be observed in the figure below, a concentration dependent decrease in cell viability was observed for both cell lines only when treated with 4-OPA and IPOH. The dash line represents the trend of 4-parametric sigmoidal curve fit. The results were expressed as percentage (%) of control (untreated cells) ± SD of 3 independent experiments (6 replicates each).

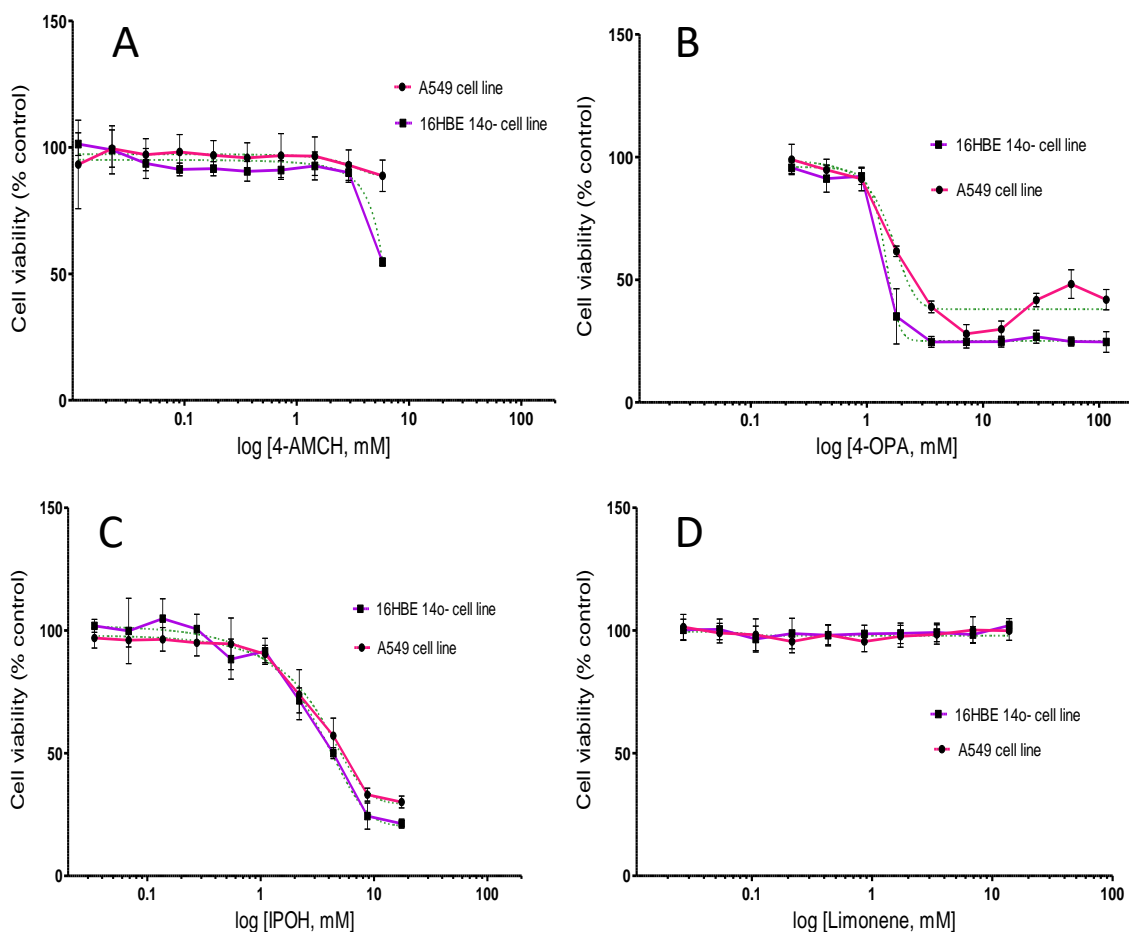


**Figure 46** Concentration-response curves obtained from A549 and 16HBE14o- cells exposed to **A.** 4-AMCH (0 to 5.8 mM), **B.** 4-OPA (0 to 115 mM), **C.** IPOH (0 to 17.5 mM), **D.** d-limonene (0 to 100 μM)

Particular behavior was noticed when A549 cells were incubated with 4-OPA. As depicted in **Figure 46 B**, the shape of the dose response curve changes (the trend changes from decreasing viability to increasing viability). This means that a lower concentration of 4-OPA on adenocarcinomic human alveolar epithelial cells (A549) induces acute damage, rather than at higher concentrations ( $p < 0.05$ ). This type of response has been well recognized in the literature as a hormetic mechanism [419]. Different studies have demonstrated that beneficial biological effects were found when different types of cancer cells (e.g. lung cancer) were exposed to low doses of radiation rather than higher doses [420]. Several studies testing drugs with hormetic mechanism, on both cancer and normal cells, found that some drugs altered cancer cells while normal cells did not induce perturbation on their metabolism [421, 422]. From the outcomes of biological effects of 4-OPA on both selected cell lines, it is possible to conclude that at the highest concentrations (28.7 - 57.5 - 115 mM) 4-OPA had a different effect on bronchial cells when compared to alveolar cells. A plateau effect can be noticed on the bronchial cell line

while a statistically different increased signal of cell viability referring to lysosome integrity is achieved on alveolar cells.

**Table 16** Comparison of the sensitivity of bronchial (16HBE14o-) and alveolar (A549) cell lines exposed to 4-OPA by one-way analysis of variance (ANOVA) with Tukey's multiple comparison test

Cell lines name and 4-OPA [mM]	Mean Diff	Significance	95% CI of diff
A549 vs 16HBE14o- at 115 mM	17	p < 0.005	10 to 24
A549 vs 16HBE14o- at 57.55 mM	23	p < 0.005	17 to 30
A549 vs 16HBE14o- at 28.75 mM	13	p < 0.005	5.7 to 19

As a general view of the potential toxic effects of tested compounds on cellular viability of both pulmonary cell lines, the bronchial (16HBE14o-) cells showed a more sensitive reaction than the alveolar (A549) cells.

However, based on the curves obtained, the concentration of each chemical where 50 % of cells are inhibited was determined by calculating the specific half maximal inhibitory chemical concentration (IC<sub>50</sub>). Additionally, the lowest observable effect concentration (LOEC) which causes statistically significant loss of cellular viability from the untreated cells was determined (see **Table 17**). The aim to estimate the LOEC value is to assure that the potential cytotoxic effects of the tested chemicals on the cell cultures is observed due to their net effect (extracted from bias signals) and not due to their different concentration's effect.

**Table 17** Calculated values of LOEC and IC<sub>50</sub> for both alveolar (A549) and bronchial (16HBE14o-) cell lines based on the concentration-response curves obtained for the individual chemicals (NA = not applicable)

Cell lines	Chemicals	LOEC mM	p value	IC <sub>50</sub> mM	95% confidence interval
A549	4-OPA	0.9	<0.005	1.62	1.47 to 1.78
	IPOH	1.1	<0.005	3.58	3.04 to 4.21
	4-AMCH	2.9	<0.005	NA	NA
16HBE14o-	4-OPA	0.9	<0.005	1.45	1.28 to 1.64
	IPOH	0.6	<0.005	3.36	2.57 to 4.09
	4-AMCH	2.9	<0.005	NA	NA

Based on the consideration above, the tested chemicals 4-OPA and IPOH inhibited cell growth of both cell lines (A549 and 16HBE14o-) in a dose-dependent manner.

Comparison of IC<sub>50</sub> for all tested compounds suggests that the most potent compound to damage the lysosome integrity of both cell lines is 4-OPA, since it has the lowest IC<sub>50</sub>. Its potential toxic effect was similar for both cell lines, with no statistically different p value (95 % confidence interval). The IC<sub>50</sub> of IPOH in A549 cells was approximately 3.6 mM while for 16HBE14o- it was found to be approximately 3.4 mM. However, when their IC<sub>50</sub> was compared based on their 95 % confidence interval, no statistical difference between them was noticed. The IC<sub>50</sub> of 4-AMCH and d-limonene could not be established in the selected concentration range, which was limited due to their maximum water solubility of 811 mg L<sup>-1</sup> at 25 °C and 13.8 mg L<sup>-1</sup>, respectively.

Between the present *in vitro* study and the *in vivo* study described by Wolkoff et al. [423] some common points can be noticed. Strong evidence of severe irreversible lung effects were induced by 4-OPA when mice were exposed to ≤ 100 mg m<sup>-3</sup>, thus limiting their study to establish the concentration that causes 50 % reduction of the respiratory rate (RD<sub>50</sub>) and the lowest observed adverse effect level (LOAEL). According to their toxicity ranking study, IPOH was the second compound which played a substantial role in reducing the respiratory rate of mice, with a RD<sub>50</sub> of 130 mg m<sup>-3</sup>, while for 4-AMCH RD<sub>50</sub> was 3390 mg m<sup>-3</sup> and RD<sub>50</sub> of d-limonene corresponding to 6000 mg m<sup>-3</sup>.

Summing up the results, it can be concluded that most severe effects on human lung cells (A549 and 16HBE14o-) were given by 4-OPA, followed by IPOH, while both 4-AMCH and

## Results and Discussion

d-limonene showed a similar toxic behavior on cellular viability determined by Neutral Red Uptake assay.

In the present study, a similar set of experiments were conducted to investigate the toxic effects of binary (4-OPA + IPOH; 4-OPA + 4-AMCH; IPOH + 4-AMCH) and ternary (4-OPA + IPOH + 4-AMCH) mixtures on the cellular viability of alveolar epithelial cells (A549) and bronchial epithelial cells (16HBE14o-) by means of NRU assay. The experiments were carried out for both cell lines under the same culture medium conditions as previously mentioned.

Because the toxicity of 4-OPA, IPOH and 4-AMCH are very different, their mixtures were prepared based on their individual  $IC_{50}$  calculated above.

Ten different dilutions with a dilution factor of 1.3 were considered to generate their concentration-response curves. The initial concentration of the mixtures was calculated as a total concentration of each  $IC_{50}$  of individual chemical added to the mixture (see **Table 18**).

**Table 18** Total concentration of the tested mixtures expressed as mM

Chemicals	IPOH + 4-OPA	IPOH + 4-AMCH	4-AMCH + 4-OPA	4-OPA + IPOH + 4-AMCH
IPOH				
(%)	66.1	37.7		31.5
4-OPA				
(%)	33.9		76.3	16.2
4-AMCH				
(%)		62.3	23.7	52.3
Total [mM]	5.3	9.3	7.6	11.1

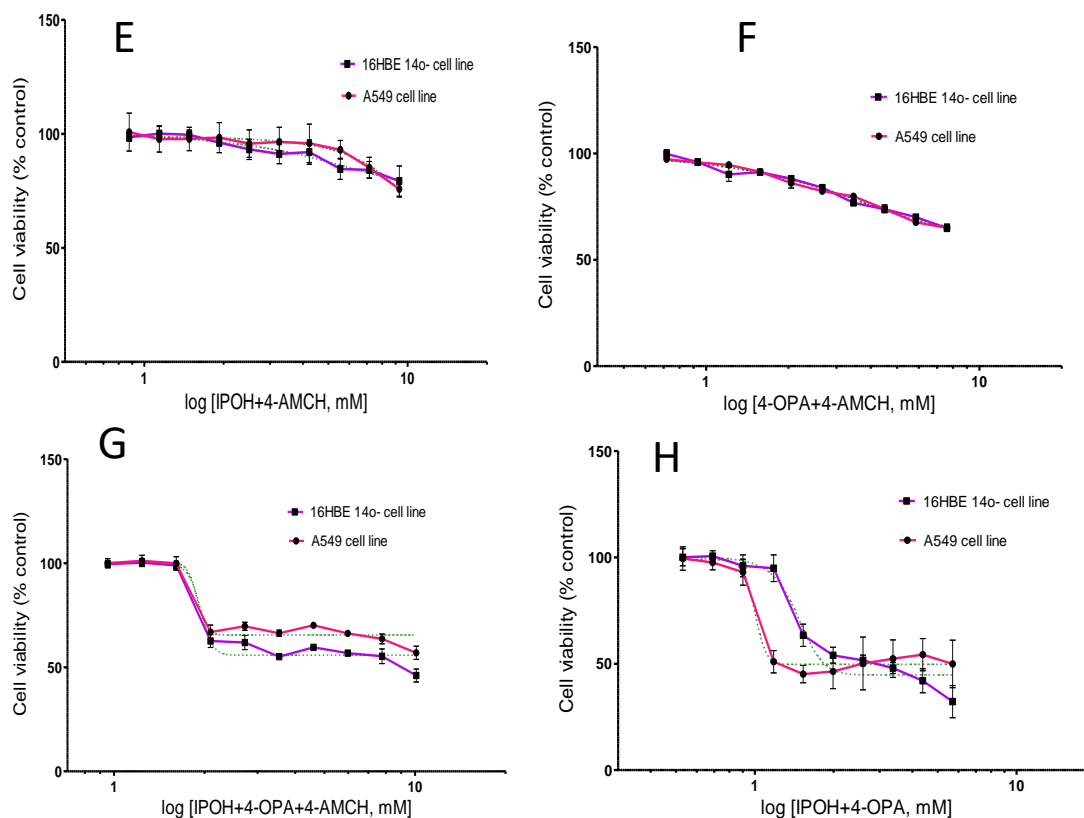


**Figure 47** Concentration-response curves obtained from A549 (red line) and 16HBE14o- (purple line) cells exposed to **E.** binary mixture of IPOH + 4-AMCH, **F.** binary mixture of 4-OPA + 4-AMCH, **G.** ternary mixture of IPOH + 4-OPA + 4-AMCH, **H.** binary mixture of IPOH + 4-OPA

Mixture toxicity of the target chemicals 4-OPA, IPOH, 4-AMCH on A549 and 16HBE14o- cells was evaluated by means of IC<sub>50</sub> and LOEC (see **Table 19a**).

**Table 19a** Calculated values of LOEC and IC<sub>50</sub> for both alveolar (A549) and bronchial (16HBE14o) cell lines based on the concentration-response curves obtained the mixture of the tested compounds (NA = not applicable)

Cell lines	Chemicals	LOEC mM	p value	IC <sub>50</sub> mM	95% confidence interval
<b>A549</b>	IPOH+4-OPA	0.84	< 0.005	0.99	0.90 to 1.09
	4-AMCH+IPOH	1.9	< 0.006	NA	NA
	4-OPA+4-AMCH	0.71	< 0.003	NA	NA
	4-OPA+4-AMCH+IPOH	1.04	< 0.001	1.8	1.68 to 2.06
<b>16HBE14o-</b>	IPOH+4-OPA	0.84		1.49	1.40 to 1.59
	4-AMCH+IPOH	1.4	< 0.005	NA	NA
	4-OPA+4-AMCH	0.71	< 0.0002	NA	NA
	4-OPA+4-AMCH+IPOH	1.04	< 0.005	1.9	1.81 to 2.02

Interestingly, the mixture of 4-OPA + IPOH indicated a different growth effect on A549 cells when compared to the growth effect observed on 16HBE14o- cells. A lower 50 % inhibition concentration (IC<sub>50</sub>) is needed in the case of A549 cells (0.99 mM) than on 16HBE14o- cells (1.49 mM), to obtain a similar inhibitory effect on cell growth. On the other hand, the ternary mixture 4-OPA + IPOH + 4-AMCH has similar inhibitory growth effects on both cell lines (p > 0.05).

*Evaluation of interactive effects of the binary/ternary mixtures*

The interactive toxicity of binary/ternary mixtures was evaluated by applying the method published by A. Hernandez Garcia et al. [424]. This statistical test can predict the mode of action of a mixture as being “additive”, “antagonistic” or “synergistic” by comparing the values obtained from the experimental tests with those calculated. The calculation of toxic effects of the mixtures was based on the Colby’s formula:

Ho: Cell viability<sub>H</sub> (x + y + ...z) = (Cell viability x)\*(Cell viability y)\*....\*(Cell viability z)/100, where Ho is the null hypothesis, x, y and z represent the percentage of cellular viability of each individual compound.

The evaluation of the interactive effects of mixtures was calculated by the difference between the observed response and the null hypothesis (Ho):

Cell viability difference = Cell viability observed – Cell viability hypothesized

## Results and Discussion

If the statistical difference is not relevant, the effect is considered to be “additive”; if the difference is statistically relevant in the positive direction then the compound interaction is considered “antagonistic”; if the difference is negative then the effect is called a “synergetic” effect.

When the method was applied to the tested compounds, the following results were observed:

**Table 19b** Interaction of toxicity response for the binary or ternary mixture’s where the *Observed effect* represents the experimental number of viable cells (expressed as percentage) obtained; the *Calculated effect* represents the number of viable cells (expressed as percentage) that was calculated based on the Colby’s formula. A = antagonistic, S = synergetic and Ad = additive

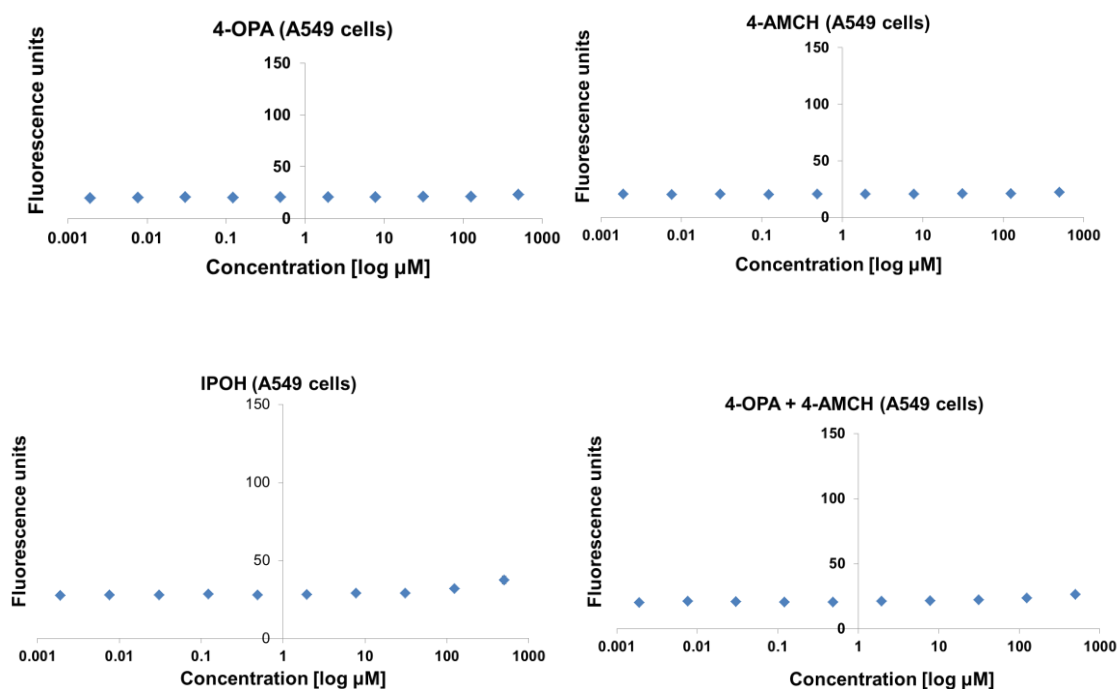
	A549 (% of living cells)				16HBE14o- (% of living cells)			
	IPOH + 4-OPA	IPOH + 4-AMCH	4-OPA + 4-AMCH	Mix all	IPOH + 4-OPA	IPOH + 4-AMCH	4-OPA + 4-AMCH	Mix all
<i>Observed effect</i>	68	75	>65	77	63	75	>65	75
<i>Calculated effect</i>	41	49	66	37	37	39	51	27
Difference	27	26	-1	40	26	36	14	48
Interactive effects	A	A	S	A	A	A	Ad	A

As documented in the table above (based on the cell viability results analysed by comparing data obtained experimentally or from mathematical formula), the mixture of IPOH + 4-OPA interact to produce antagonistic effects on the cellular viability of both cell lines. As a general observation, the effects of the tested mixtures IPOH + 4-AMCH and IPOH + 4-OPA + 4-AMCH were mainly antagonistic. This means that between these chemicals there is a competitive interaction. On the other hand, the mixture of 4-OPA and 4-AMCH interact to produce synergistic effects (an effect which is greater than the sum of each chemical’s effect alone) on A549 cells, while on 16HBE14o-, their interaction produces an additive effect (the effects of 4-OPA and 4-AMCH as individual chemicals were added together).

Taken together, the maximum tolerated concentration for all tested compounds, both as individuals as well as their mixtures, is around 0.5 mM (as indicated by the LOEC value in the tables above) therefore it was selected as being the optimal highest concentration to be further tested in the following cytotoxicity assays: oxidative stress (intracellular reactive oxygen species and glutathione contents measurements) and inflammation / allergy response (various cytokines measurements).

### 3.2.1.2 Oxidative stress in alveolar (A549) and bronchial (16HBE14o-) epithelial cells measured by reactive oxygen species (ROS) assay

Based on the ROS method described in Materials and Methods chapter, both A549 and 16HBE14o- cells were incubated at various times (60, 120, 210 and 1440 minutes) with the individual test compounds 4-OPA, IPOH, 4-AMCH and their binary/ternary mixtures at concentrations ranging from 0 to 500  $\mu$ M. Results showed (see **Figure 48 A-G**) that for the lower concentrations 0-8  $\mu$ M, the fluorescent signal of ROS production is not significantly different from A549 cells untreated, therefore, they were all pooled as an estimation of the background signal ( $S_0$ ) and further treatment was done for the three highest concentrations based upon ( $S-S_0$ ). Moreover, same tendency was seen for all tested compounds (see **Figure 48 A-G**).



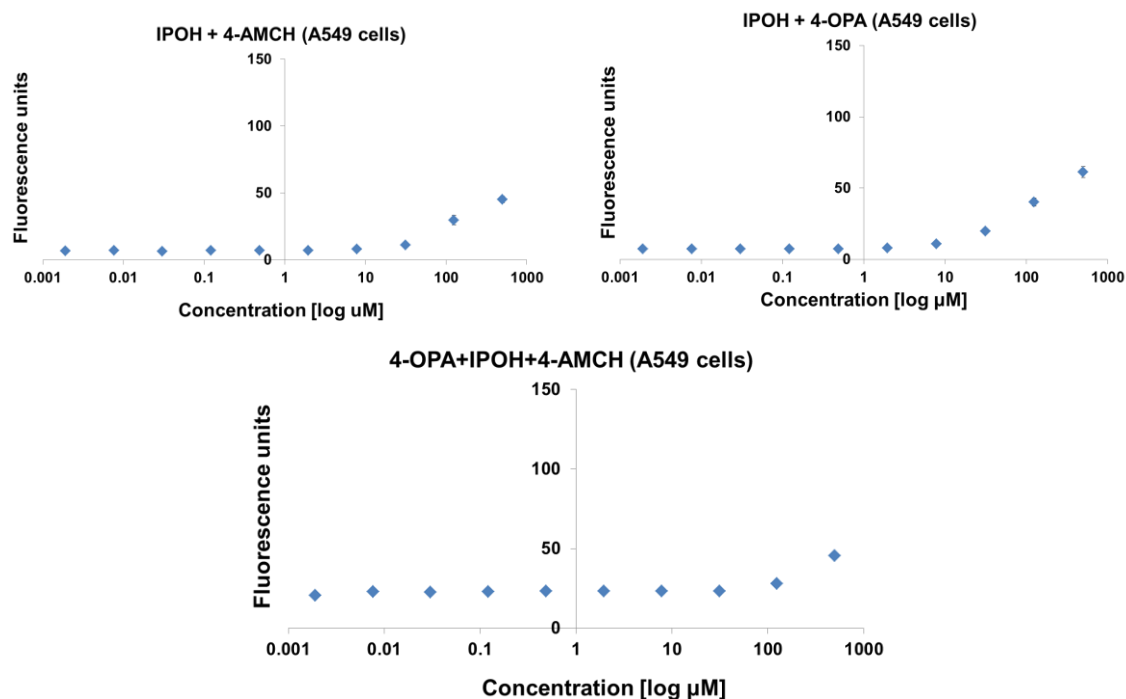


**Figure 48 A-G** ROS production measured in A549 cells at 60 minutes for all tested compounds. **A.** 4-OPA; **B.** 4-AMCH; **C.** IPOH; **D.** 4-OPA + 4-AMCH; **E.** IPOH + 4-AMCH; **F.** IPOH + 4-OPA; **G.** 4-OPA + IPOH + 4-AMCH

Single treatment with IPOH for 24 hours at a concentration of 500 μM, produced 100-times more ROS signal in A549 cells when compared to the ROS signal generated from cells treated with 4-OPA or 4-AMCH. As shown in **Figure 49**, the increased ROS formation is proportionate to the compounds concentration. Only in the case of 4-OPA and 4-AMCH, a significant increase in the amount of reactive oxygen species was measured after 60 minutes (60 min > 120 > 210). When cells were exposed for 24 hours to 4-OPA the ROS production returned to the baseline level (see **Figure 48 A -G**). A possible explanation for IPOH producing the highest levels of ROS on A549 cells when compared to 4-OPA, could be that 4-OPA has no C=C double bond, therefore it is less reactive than both IPOH and 4-AMCH. Moreover, due to its lipophilic character, IPOH is absorbed most efficiently by the cells, via lipid portions of the cellular membrane. The difference in ROS formation between 4-AMCH and IPOH may be due to their chemical structure. IPOH is an open-chain compound (more flexible) while 4-AMCH is a ring compound. All this could mean that IPOH would be able to reach cellular receptors more easily than 4-AMCH. IPOH is also more reactive due to its external C=C double bond compared to the internal C=C double bond in the ring of 4-AMCH. However, more experiments are needed to support this hypothesis.

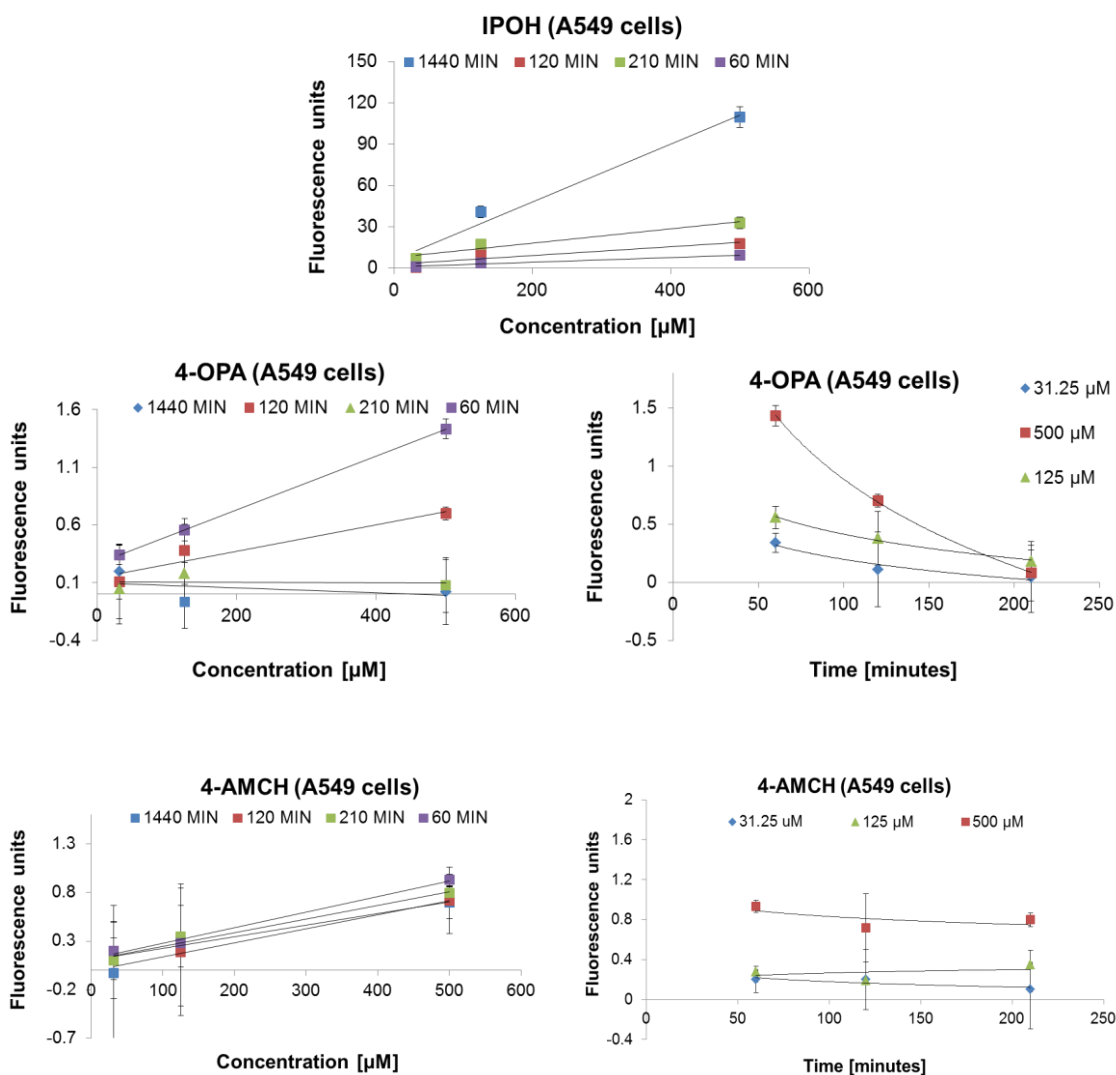


**Figure 49** Intracellular ROS levels measured in A549 cells exposed to individual test compounds at 31.2; 125 and 500 µM after a treatment of 60, 120, 210 and 1440 min

In terms of ROS formation, the most active individual compound IPOH was evaluated in presence of 4-OPA and 4-AMCH, both as a binary and ternary mixture. The binary mixture IPOH + 4-OPA displayed the highest ROS level formation in A549 cells when compared to the other mixtures tested. The addition of 4-OPA to IPOH showed an increased in ROS levels equivalent to a 1.7-fold change than the ROS production obtained with IPOH alone (see **Figure 50**).

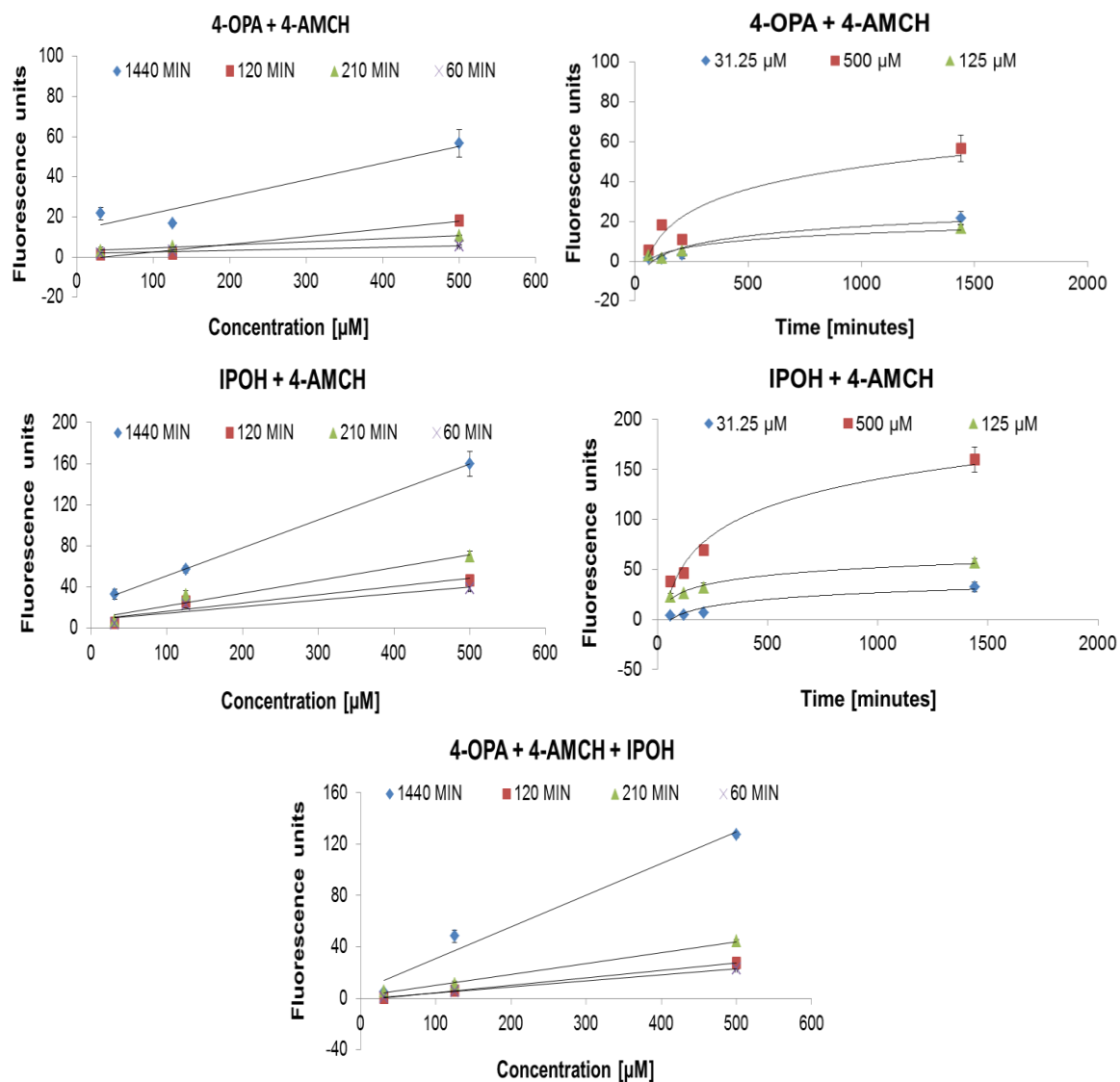


**Figure 50** Kinetic measurements of intracellular ROS formation in A549 cells exposed to tested compounds individually and their binary/ternary mixture in the range of 0 to 500  $\mu\text{M}$  ( $n=8 \pm \text{SD}$ )

In the same way regarding time exposure and concentration, 16HBE14o- cells were treated with the tested compounds.

Results showed that for the lower concentrations 0-8  $\mu\text{M}$ , the fluorescent signal for ROS formation was not statistically different when compared to the control group (see as example **Figure 51**). Therefore, they were pooled and used as an estimation of the background signal which was further used for subtraction.

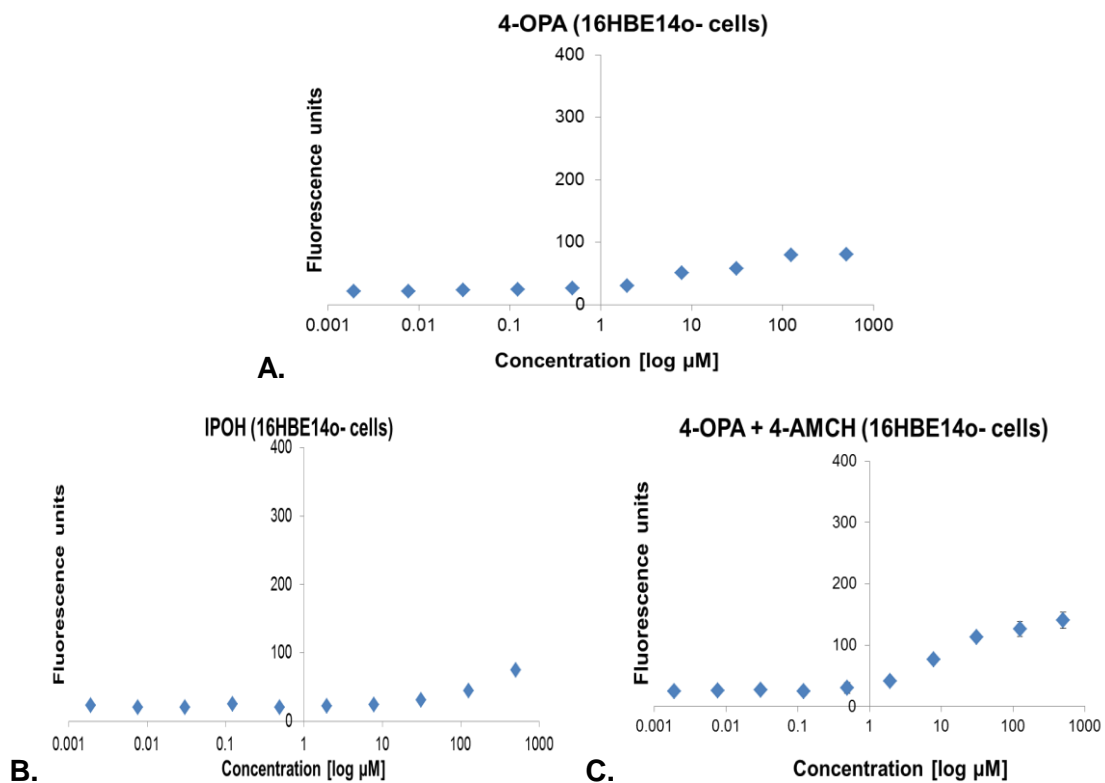


**Figure 51** ROS production measured in 16HBE14o- cells at 60 minutes for all tested compounds. **A.** 4-OPA; **B.** IPOH; **C.** 4-OPA + 4-AMCH;

The obtained results point to a significantly higher sensitivity of 16HBE14o- cells to ROS formation, the amount of ROS formed under similar conditions being 2-fold that of A549 cells. When cells are exposed to the different chemicals on their own, only IPOH presents a significant formation of ROS, while neither 4-OPA nor 4-AMCH seems to have an oxidative effect. Interestingly, however, the mixture of both compounds presents a slight formation of ROS which is nonetheless lower than that formed during exposure to IPOH. As an example, **Figure 52** presents a comparison of ROS formation for both types of cell lines exposed to 500  $\mu\text{M}$  of the different compounds during 24 hours. A similar behaviour was found for any other concentration tested or exposure times.

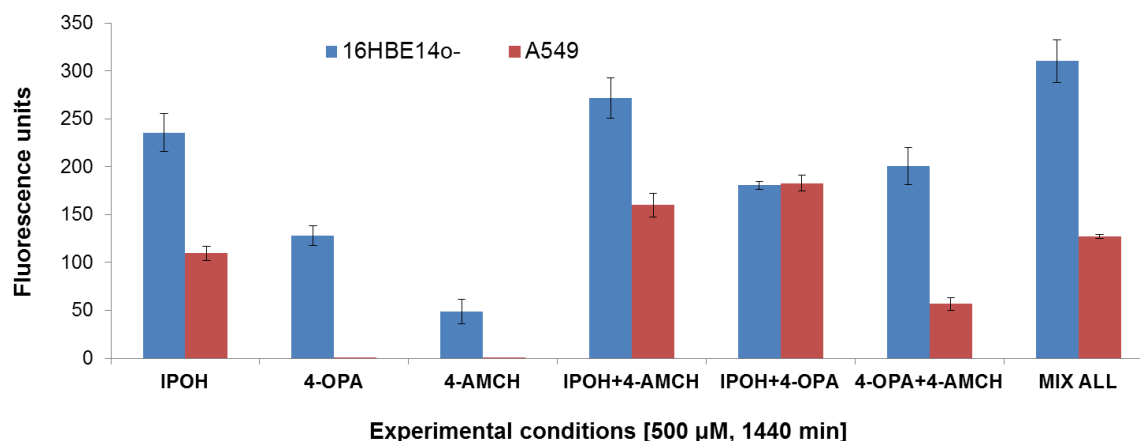


**Figure 52** Determination of ROS production in 16HBE14o- and A549 cells exposed to tested compounds at 500  $\mu$ M for 24 hours ( $n = 8 \pm$  SD)

The difference in ROS levels production detected in the two cell lines may have several causes, such as different esterase activity in the selected cell lines [425], different intracellular localization of fluorochromes [426], differences in the oxidative metabolism between the two cell lines [427], or higher glutathione levels in human lung adenocarcinoma cell line (A549) than in the normal human bronchial cell line (16HBE14o-). The low esterase activity has direct implications in detection of ROS since the non-fluorescent reagent DCFH-DA needs to be hydrolyzed to DCFH which is further oxidized to fluorescent dichlorofluorescein (DCF) by action of free radicals/oxidants [428]. It has been demonstrated that the esterase activity in tumour lung has lower values ( $0.71 \pm 0.09$ ) than in normal lung ( $1.13 \pm 0.19$ ), due to the significant biochemical differences, but no specific data were found in the literature on the selected cell lines investigated in the present study. The results obtained by J.P. Robinson et al., indicated that monocytes and neutrophils stimulated with phorbol myristate acetate (PMA) induce a different increase of the fluorescence signal between the two cell lines, with a higher signal fluorescent ratio for neutrophils than monocytes (5 : 1). The main conclusion of his findings suggests that the differences in the oxidative mechanism of the two cell lines lead to an increased ROS level in neutrophils rather than in monocytes [429]. Numerous publications report that the intracellular glutathione levels in cancer cells are higher than in normal cells, which increase the resistance/defense of A549 in presence of free radicals [430, 431]. This approach can also explain the higher sensitivity of 16HBE14o- cells to ROS production than in A549 cells. In this regard, the intracellular glutathione amount of both selected cell lines was further investigated.

The imbalance between reactive oxygen species (ROS) or reactive nitrogen species (RNS) and their elimination by enzymatic (e.g. superoxide dismutase etc.) or nonenzymatic (e.g. glutathione) antioxidants defines the oxidative stress process which

has been directly linked to cell death, many inflammatory diseases and cancer [432, 433]. In particular, RNS can indirectly induce modifications of proteins and lipids which can increase the risk of mutagenesis [272]. Therefore, the antioxidant protection reaction by glutathione was investigated by measuring the changes that occurred in the intracellular glutathione ratios of GSH / GSSG and GSH / GSNO.

### 3.2.1.3 Oxidative stress in alveolar (A549) and bronchial (16HBE14o-) epithelial cells measured by glutathione content assay

From the observed ROS generation induced by the tested compounds at various concentrations, three concentrations (1.5, 31.2 and 500  $\mu$ M) were further selected to investigate their potential perturbation on the intracellular glutathione level for both alveolar and bronchial cell lines. The compounds concentrations were chosen based on their ROS potency formation: 500  $\mu$ M corresponds to the highest ROS levels generated in the cells, 31.2  $\mu$ M represents the concentration where a minimum ROS level was formed that is statistically different from the ROS levels measured in cells untreated, while 1.5  $\mu$ M is the concentration where the ROS levels induced by the compounds were similar to those observed in cells untreated.

Similarly to the results obtained for ROS formation, 16HBE14o- cells present a significantly higher sensitivity to GSSG and GSNO formation compared to A549 cells when exposed to IPOH, 4-OPA or 4-AMCH, either individually or to their mixtures. Thus, GSH / GSSG ratio in 16HBE14o- cells exposed for 2 and 24 hours to IPOH at 500  $\mu$ M, showed a decrease of 33.2 % and 44.6 % respectively when compared to the GSH / GSSG ratio of untreated cells. On the other hand, IPOH induced changes in the GSH / GSSG ratio of A549 cells of a 31.6 % after 2 hours incubation and 45.1 % after 24 hours. In this case, however, both IPOH and 4-OPA seem to induce GSSG and GSNO formation in both cell lines. It is important to stress that the ratio determined in A549 cells exposed to all tested compounds of GSH / GSNO is higher than that of GSH / GSSG, while for 16HBE14o- cells, GSH / GSSG ratio is higher than GSH / GSNO. These observations might be explained by the great ability of A549 cells to produce higher concentrations of nitric oxide (NO) than the 16HBE14o- cells when treated with the tested compounds. However, in order to prove this hypothesis, specific experiments where NO levels are determined should be carried out, but this was not considered as part of this study. As an example, the GSH / GSSG ratio calculated for 16HBE14o- cells exposed to IPOH at 500  $\mu$ M was approximately 33.2 % (after 2 hours incubation) and 44.6 % (after 24 hours incubation) higher than for unexposed cells, while the GSH / GSNO ratio was found to be 20.0 % and 12.4 % after 2 and 24 hours, respectively.

Intracellular reduced glutathione content in alveolar epithelial cells (A549) were  $34.75 \pm 0.3$  nmole  $\text{mg}^{-1}$  protein ( $n = 8$ ), which is within the concentration range of other published studies [434]. The intracellular glutathione content in bronchial epithelial cells (16HBE14o-) was  $26.3 \pm 1.1$  nmole  $\text{mg}^{-1}$  protein. The GSH / GSSG and GSH / GSNO ratio may be used as a potential indicator of oxidative stress. This view is supported by several studies [435, 436] and it is based on the concept that the intracellular reduced glutathione is typically found as the most abundant state [437]. Owing to extensive studies on the GSH / GSSG ratio steady state level, it was found that a decrease in GSH/GSSG ratio to values of 10 : 1 and even 1 : 1 is an indicator of the oxidative stress [438, 439].

**Figure 53** presents a comparison of GSSG / GSH (**53 A**) and GSNO / GSH (**53 B**) for A549 and 16HBE14o- cells exposed to  $31.2 \mu\text{M}$  of the different chemicals for 2 and 24 hours.

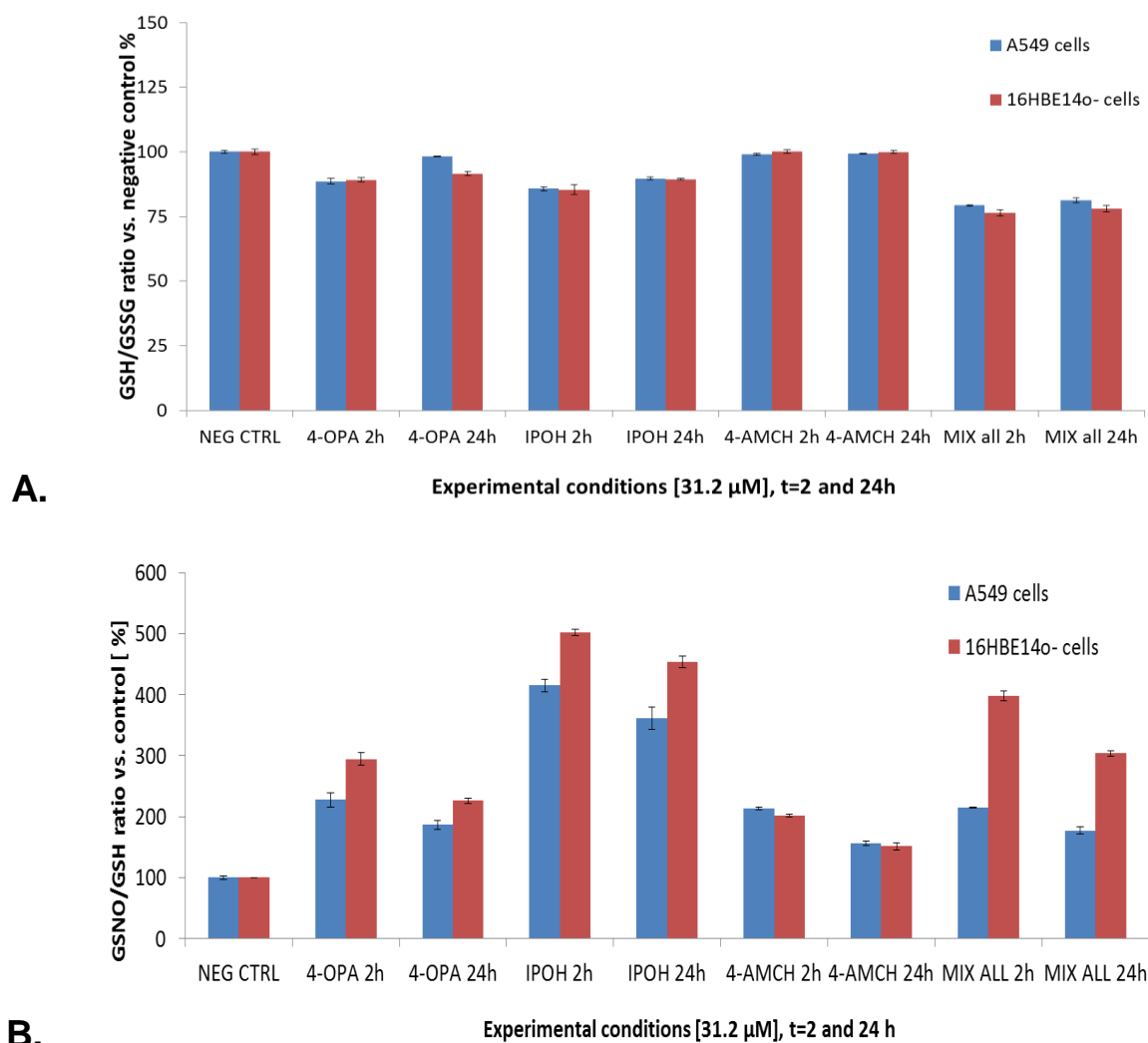


**Figure 53 A** The fold change of GSSG / GSH ratio in both A549 (blue) and 16HBE14o- (red) cells exposed for 2 and 24 hours to the tested compounds compared to GSSG / GSH ratio of untreated cells ( $n = 3 \pm \text{SD}$ ) **B.** The fold change of GSNO / GSH ratio in both

A549 (blue) and 16HBE14o- (red) cells exposed for 2 and 24 hours to the tested compounds compared to GSNO / GSH ratio of untreated cells ( $n = 3 \pm SD$ )

The presence of oxidative stress at the cellular level, identified by an abundant ROS formation followed by reduced antioxidant defenses determined by the depletion of reduced glutathione, is also characterized by high production of pro-inflammatory cytokines. Data from several studies have identified that pro-inflammatory cytokines such as IL-6, TNF-alpha, IL-8 etc. are inducing ROS generation in various types of cells [465, 470]. To evaluate whether there is a potential linkage between ROS formation and inflammation, various pro-inflammatory cytokines (IL-6, IL-8, TNF-alpha, IL-15, RANTES) were evaluated in the culture medium, 24 hours after the exposure of A549 and 16HBE14o- cells to the tested chemicals.

3.2.1.4 Inflammatory response in alveolar (A549) and bronchial (16HBE14o-) cells exposed to test compounds measured by cytokines/chemokines assay

Based on toxic responses observed in previous experiments, three concentrations (1.5, 50 and 500  $\mu\text{M}$ ) were further selected to investigate their potential inflammatory capacity in the alveolar and bronchial cell lines. No pro- or anti-inflammatory effects were observed in both types of cell lines (alveolar and bronchial) when those were exposed to the highest concentration of chemicals (500  $\mu\text{M}$ ). Therefore, only the results that were obtained by exposing the alveolar and bronchial cells to chemicals concentration of 1.5 and 50  $\mu\text{M}$  are reported below.

The results obtained when cells were incubated with IPOH show a concentration-dependent effect as follows: at 1.5  $\mu\text{M}$ , the release of IL-6 levels was 1.3 and 2.3-times higher for A549 and 16HBE14o- cells respectively, while at 50  $\mu\text{M}$ , the amount of IL-6 secreted by A549 cells was found to be 1.5 and for 16HBE14o- cells it increased up to 2.8 higher when compared to the cytokine level determined in untreated cells. A similar behavior, in terms of concentration-dependent effect, was noticed for the IL-8 production in both cell types. However, the amount of this cytokine which plays a role in inflammation (e.g. pathogenesis of bronchiolitis) and wound healing was higher than the determined amounts of IL-6 identified to play a key role in the pathogenesis of asthma, chronic inflammation etc. [208]. For example, when cells were incubated with IPOH at 50  $\mu\text{M}$ , the levels of IL-8 were found to be approximately 1.5 and 7.1-fold change higher than the levels measured in cell controls.

A549 cells incubated with 4-OPA at a concentration of 1.5  $\mu\text{M}$  of 4-OPA expressed up to 1.4-fold higher levels of IL-6 ( $p < 0.01$ ) and 1.3-fold higher levels of IL-8 ( $p < 0.01$ ), while at

## Results and Discussion

a concentration of 50  $\mu\text{M}$  the fold change of IL-6 level was similar to that found at lower tested concentration (1.4-fold higher),  $p < 0.01$ , and slightly increased to 1.3-fold the secretion of IL-8 levels ( $p < 0.05$ ), when compared to negative control (see **Figure 54 A-B**). The total amount of cytokines is expressed as percent of total amount of cytokines released in the cells untreated (negative control).

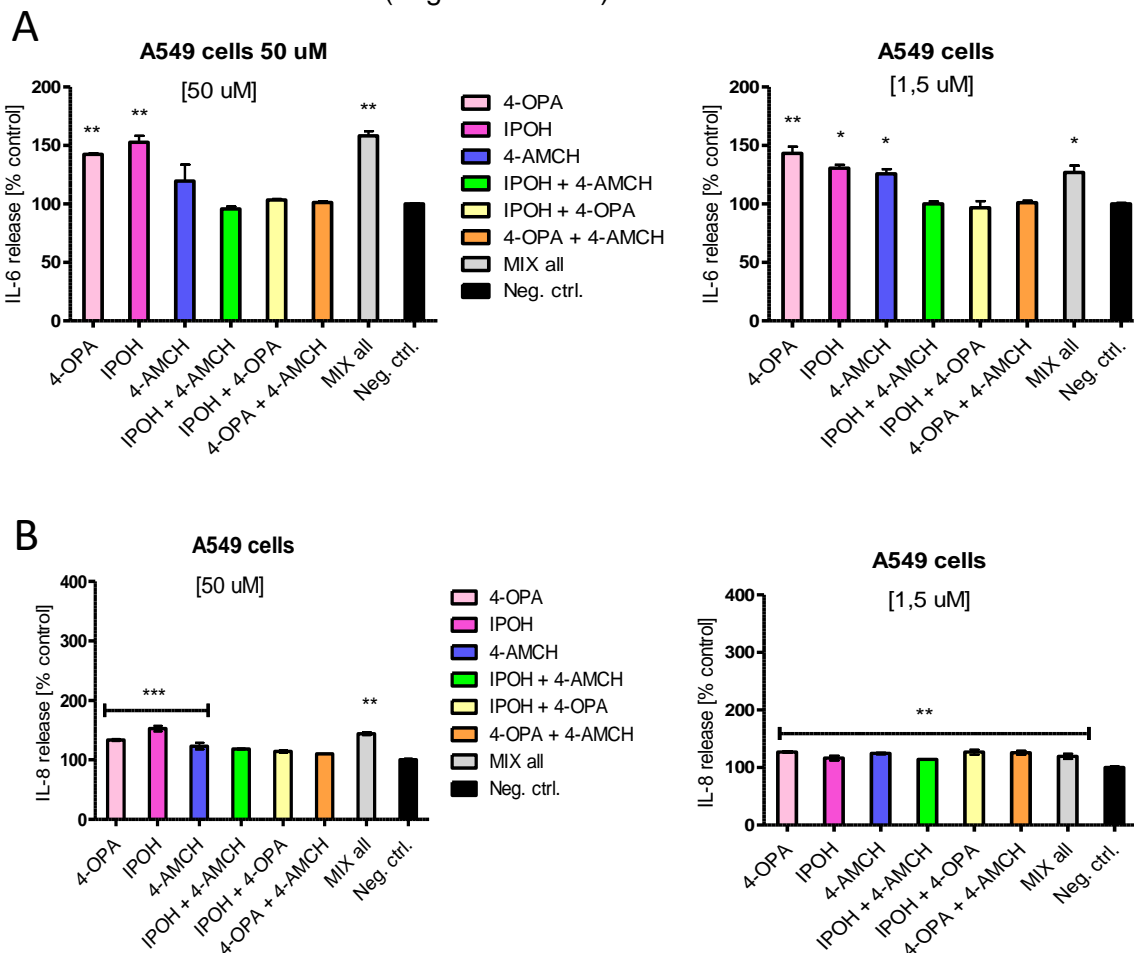


**Figure 54** Total production of various cytokines by human pulmonary alveolar epithelial cells after 24-hours stimulation with 4-OPA, IPOH, 4-AMCH at two concentrations [1.5 and 50  $\mu\text{M}$ ] ( $n = 9 \pm \text{SD}$ ). **A.** IL-6 levels in A549 cells treated with test compounds at concentrations of 50  $\mu\text{M}$  (left ) and 1.5  $\mu\text{M}$  (right); **B.** IL-8 levels in A549 cells treated with test compounds at concentrations of 50  $\mu\text{M}$  (left ) and 1.5  $\mu\text{M}$  (right);

The bronchial cells (16HBE14o-) incubated with 4-OPA at a concentration of 1.5  $\mu\text{M}$  expressed up to 2.4-fold change higher levels of IL-6 ( $p < 0.01$ ), 3.3-fold change higher levels of IL-8 ( $p < 0.05$ ), while at a concentration of 50  $\mu\text{M}$  of 4-OPA, the fold change in the cytokines levels were as follows: 80-fold change down-regulated levels of IL-6 ( $p < 0.01$ ); 61-fold change down-regulated levels of IL-8 ( $p < 0.05$ ), when compared to negative control (see **Figure 55 A-B**).

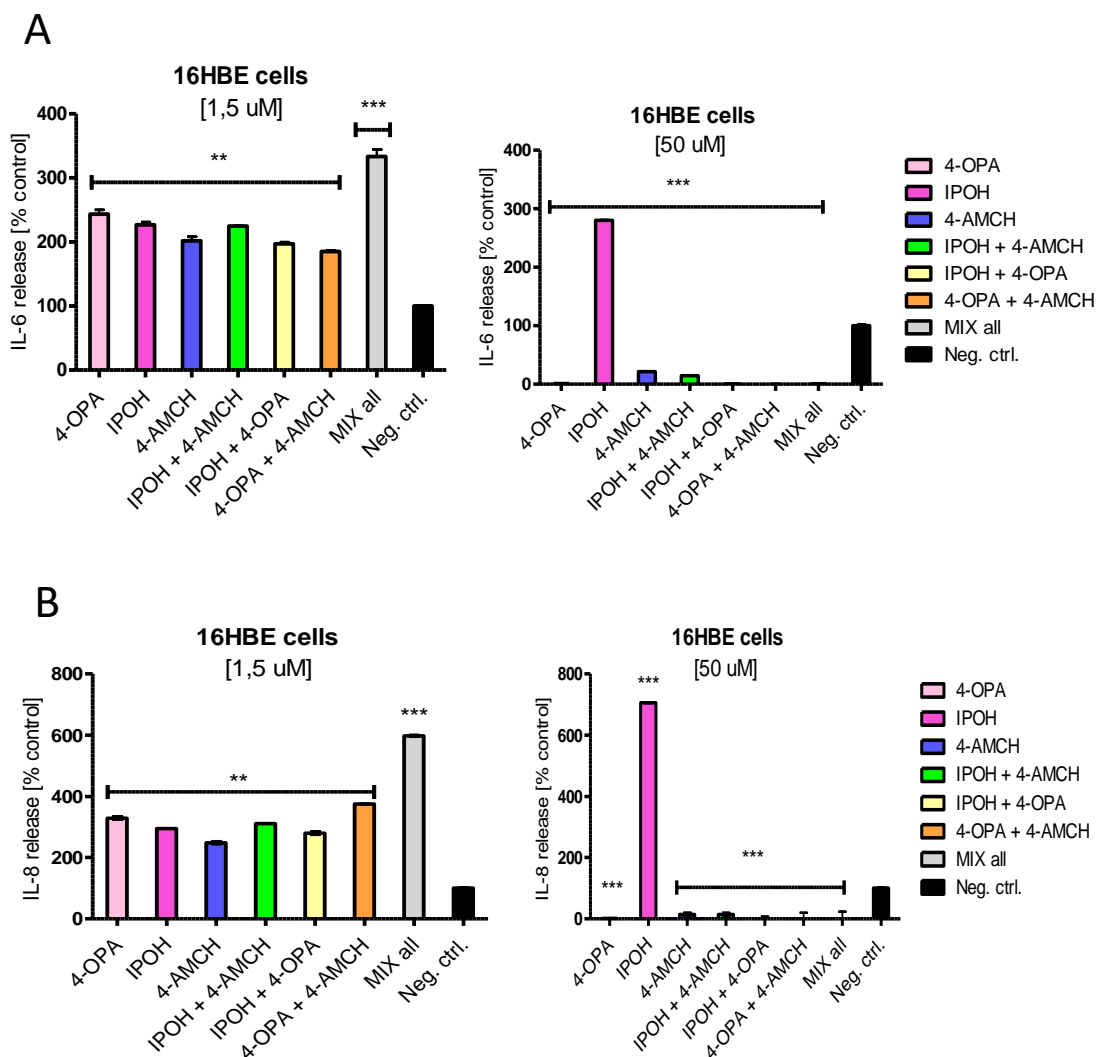
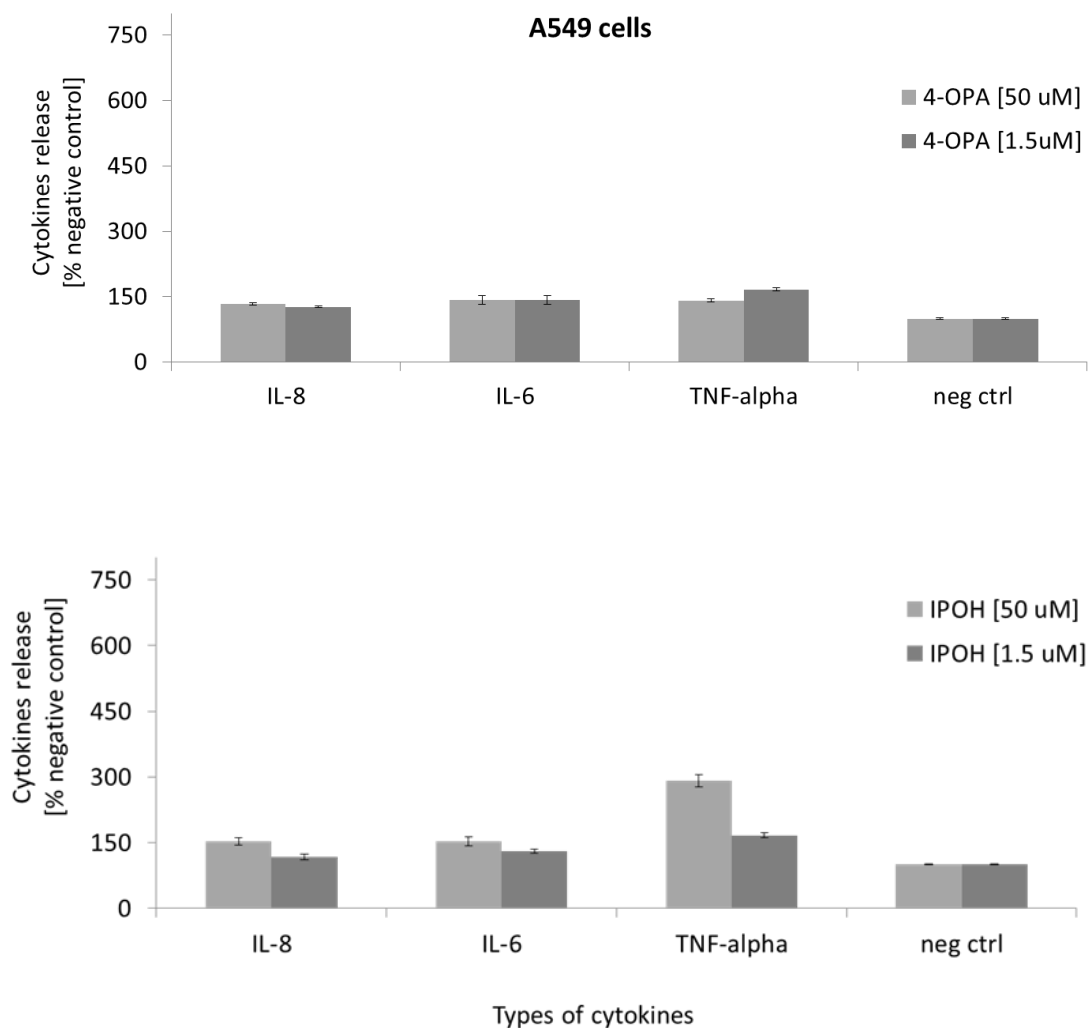


**Figure 55** Evaluation of IL-6 and IL-8 release in the culture medium from 16HBE14o- cells exposed to individual compounds and their binary / ternary mixtures at 1.5 and 50  $\mu\text{M}$  ( $n = 3 \pm \text{SD}$ ). Error bars that are smaller than the symbol size are not visible.

A comparison of IPOH and 4-OPA effects induced in both cells lines reveals that at low tested concentrations (1.5  $\mu\text{M}$ ), the A549 cells treated with IPOH, secreted statistically significant higher amounts of IL-6 and IL-8 than levels measured in A549. On the contrary, at high tested concentration (50  $\mu\text{M}$ ), the inflammatory effects of IPOH investigated by the measurements of IL-6 and IL-8 released from 16HBE14o- cells, were the opposite from the effects induced by 4-OPA. Under the same experimental conditions, IPOH drastically up-regulated the release of both IL-6 and IL-8 (2.8-fold change and 7.0-fold change respectively), while 4-OPA down-regulated IL-6 (80-fold change lower amounts) and IL-8 (61-fold change lower amounts) when compared to the levels of IL-6 and IL-8 identified in cells untreated (see **Figure 56**).

## Results and Discussion

Pro-inflammatory cytokines such as TNF-alpha and RANTES which are involved in the pathogenesis of asthma and in the lung allergic inflammation were also investigated [221]. The results showed that 4-OPA at 1.5  $\mu\text{M}$  stimulated the secretion of TNF-alpha and RANTES up to 1.7-fold higher levels for both cytokines ( $p < 0.01$ ). At a higher concentration, 50  $\mu\text{M}$  of 4-OPA, both cytokines enhanced their amount released into culture medium of A549 cells as follows: 1.4-fold higher levels of TNF-alpha and 11-fold higher levels RANTES ( $p < 0.01$ ). Exposure of 16HBE14o- cells to the same tested compounds, 4-OPA, produced higher TNF-alpha levels (2-fold change at 1.5  $\mu\text{M}$ ) but lower amounts of RANTES (1.3-fold change) when compared to the A549 cells. As presented in the figure below, bronchial cells secreted higher amounts of IL-6, IL-8 than A549 cells for all tested compounds at 1.5  $\mu\text{M}$  while at 50  $\mu\text{M}$  only IPOH was stimulating cells to secrete IL-6 and IL-8.



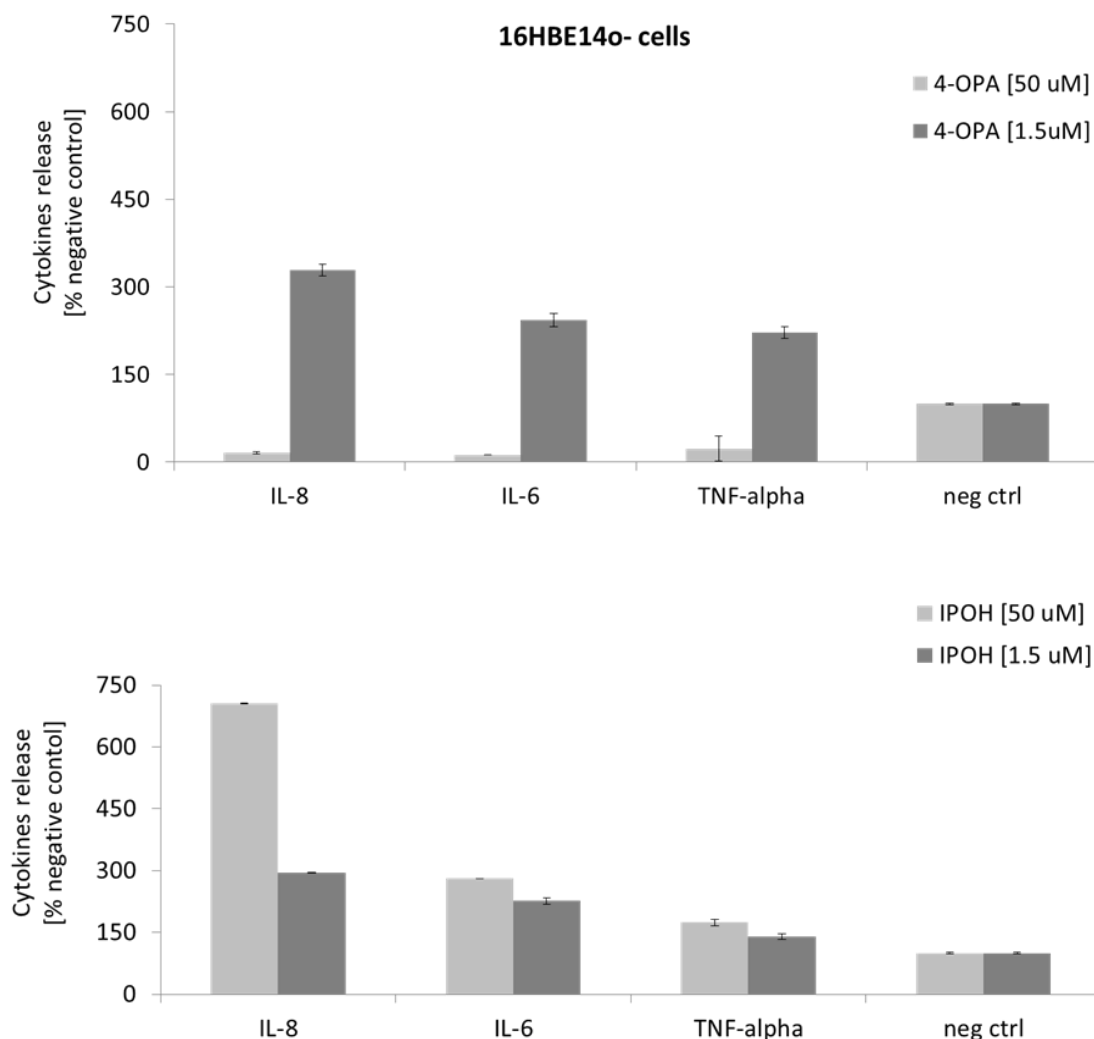


**Figure 56** Total production of various pro-inflammatory cytokines (IL-6, IL-8, TNF-alpha) released by A549 and 16HBE14o- cells after 24-hours stimulation with 4-OPA and IPOH at 1.5 and 50  $\mu\text{M}$ . Cells treated with medium (1 % FBS) are expressed as “neg ctrl”=negative control (IL-8=132  $\text{pg mL}^{-1}$ , IL-6=81  $\text{pg mL}^{-1}$ , TNF- $\alpha$ =12  $\text{pg mL}^{-1}$ ) ( $n = 9 \pm \text{SD}$ ).

There are similarities in the results obtained between the present study regarding the not significant release of IL-10 amount by the A549 cells and the not significant levels of IL-10 measured in mice exposed to 3.4 mM of 4-OPA, which was tested on the mouse ear for dermal sensitisation [423].

Noting that there was a fall in some of the pro-inflammatory cytokines, anti-inflammatory mediators such as IL-10, IL-13 were investigated. Therefore, ratio trends of the pro-inflammatory cytokines to anti-inflammatory cytokines were calculated for all tested compounds and compared as follows: IL-8 / IL-13, IL-8 / IL-10 TNF-alpha / IL-10, TNF-alpha / IL-13, IL-15 / IL-10, IL-15 / IL-13, IL-6 / IL-10, IL-6 / IL-13. A ratio increase (more

than 1) of the pro-inflammatory versus anti-inflammatory cytokines mentioned above was considered to represent an inflammatory response, as dictated by the balance between pro and anti-inflammatory biomarkers [440].

Contrary to the previous experiments, A549 cells seem to be the most sensitive to such compounds, thus their stimulation with the tested compounds showed a response to a considerable broad range of cytokines. However, based on the calculated fold change of each pro-inflammatory and anti-inflammatory ratio mentioned above, the release of cytokines amount in A549 cells seems to be independent from the concentration of the tested compounds.

**Table 20** presents a selection of the most interesting fold change of the ratio of different pro-inflammatory cytokines (e.g. IL-8 or TNF alpha) and anti-inflammatory cytokines (e.g. IL-13 or IL-10) for the exposure of both cell lines to 50  $\mu$ M of the individual tested compounds, in comparison to the corresponding basal ratio of non-exposed cells.

**Table 20** Evaluation of the most representative fold change of pro-inflammatory cytokines and anti-inflammatory cytokines ratio for both alveolar (A549 cells) and bronchial (16HBE 14o- cells) exposed to individual compounds at 50  $\mu$ M for 24 hours

Compounds	Pro-inflam.	Anti-inflam.	Fold change	
			A549 cells [50 $\mu$ M]	16HBE14o- cells [50 $\mu$ M]
<b>IPOH</b>	IL-8	IL-10	1.5	8.5
		IL-13	1.5	6.3
	TNF-alpha	IL-10	2.9	2.1
		IL-13	2.9	1.6
	IL-6	IL-10	2.8	1.8
		IL-13	2.8	1.4
	IL-15	IL-10	1.5	---
		IL-13	1.5	---
<b>4-OPA</b>	IL-8	IL-10	1.3	---
	TNF-alpha	IL-10	1.4	---
		IL-10	1.1	1.6
	IL-15	IL-13	---	2.1
<b>4-AMCH</b>		IL-8	IL-10	1.2
	IL-13		1.2	---
	TNF-alpha	IL-10	1.6	---
		IL-13	1.6	---
	IL-15	IL-13	1.3	---

As can be observed in the table above, a marked increase in the fold change of IL-8 versus IL-10 respectively IL-13 was found in the bronchial cells exposed to IPOH compared with the fold-change ratio of same cytokines released by the A549 cells. In

contrast, both TNF-alpha / IL-10 and IL-6 / IL-10 fold changes were found to be at higher levels in A549 cells than in 16HBE14o- cells. Treatment of cells with 4-OPA indicates that the ratio of cytokines release was in favour of the pro-inflammatory cytokine IL-15 versus IL-10 for both selected cell lines. The secretion of IL-15 was considerably increased in the case of the simultaneous exposure to the mixtures 4-OPA + IPOH or 4-OPA + 4-AMCH (see **Table 21**) for bronchial cells. Such effect is however not observed if the concentration of the chemicals to which cells were exposed is lowered to 1.5  $\mu$ M.

The data on the fold-change ratio calculated for 4-AMCH show that none of the selected pro-inflammatory versus anti-inflammatory cytokines was secreted in bronchial cells. Moreover, there was no statistically significant changes in the ratio of pro versus anti-inflammatory cytokines noted when bronchial cells were incubated with the tested compounds at 1.5  $\mu$ M when compared to the negative control.

When both cell lines were treated with the binary (4-OPA + IPOH, IPOH + 4-AMCH and 4-OPA + 4-AMCH) and ternary (4-OPA + IPOH + 4-AMCH) mixtures of the tested compounds, the most important effect observed was when cells were exposed to the ternary mixture 4-OPA + IPOH + 4-AMCH, whereas a strong pro-inflammatory activity was noted in bronchial cells which is indicated by the high fold-change values of IL-15 / IL-13 (see **Table 21**).

**Table 21** Evaluation of the most representative fold change of pro-inflammatory cytokines and anti-inflammatory cytokines ratio for both alveolar (A549 cells) and bronchial (16HBE14o- cells) exposed to the binary/ternary mixture of the tested compounds at 50  $\mu$ M for 24 hours

Compounds	Pro-inflam.	Anti-inflam.	Fold change	
			A549 cells [50 $\mu$ M]	16HBE14o- cells [50 $\mu$ M]
Mix all	IL-8	IL-10	1.4	---
		IL-13	1.4	---
	TNF-alpha	IL-10	1.9	---
		IL-13	1.9	---
	IL-15	IL-10	1.6	8.1
		IL-13	1.6	129.4
4-OPA+IPOH	IL-6	IL-13	---	9.5
	IL-15	IL-10	---	2.5
		IL-13	---	1.1
4-OPA+4-AMCH	IL-15	IL-10	1.5	3.0
		IL-13	---	4.8
IPOH+4-AMCH	TNF-alpha	IL-10	1.6	---
		IL-13	---	1.9
	IL-8	IL-10	1.2	---
	IL-6	IL-13	---	1.3

The selection of the pro- and anti-inflammatory combination ratio was based on the cytokines characterisation presented in several publications. For example, TNF-alpha has been identified as a key element in various pulmonary diseases such as acute lung injury, asthma, chronic bronchitis [221, 223, 441]. *In vivo* studies found that high levels of TNF-alpha causes necrosis in mice [442] or induces severe pro-inflammatory reactions [224].

Due to its pro-oxidative actions, it has been observed both *in vitro* (on human pulmonary endothelial cells) as well as *in vivo* (transgenic mice) that TNF-alpha depletes cellular glutathione and stimulates the ROS formation [443] in human endothelial cells. Previous research has documented that TNF-alpha induces the synthesis of cytokines such as IL-6 and IL-8.

The existing literature on anti-inflammatory cytokines has suggested that the increased release of IL-10 (a potent anti-inflammatory cytokine) contributed to the reduction of TNF-alpha release in alveolar cells [444] or decreased production of IL-6 in macrophage [445]. The main findings of this study suggest that the balance between pro-inflammatory and anti-inflammatory cytokines caused a relevant increase in the release of pro-inflammatory response. Taken together, the test compounds with a major impact on the inflammatory response were IPOH and the ternary mixture. A similar ratio behaviour was noted for the pro-inflammatory IL-8 versus different anti-inflammatory cytokines (e.g. IL-10 and IL-13) in A549 cells, while in 16HBE14o- cells the ratio of IL-8 / IL-10 higher than IL-8 / IL-13 was noticed. This indicates that IL-10 did not have a significant inhibitory effect on IL-8 secretion compared to IL-13. However, this can be explained by the fact that IL-13 was demonstrated to have a dual role: as pro-inflammatory cytokine, which plays an important role in allergic disease, but it has also been recognized to have anti-inflammatory properties by suppressing cytotoxic and inflammatory functions of monocytes and macrophages [446] or by limiting the production of TNF-alpha-induced IL-8 in a whole blood assay [447]. When cells were treated with the ternary mixture, particularly an increase of IL-15 was noticed in bronchial cells. Data from several studies have identified that IL-15 is directly involved in inflammatory pulmonary disease such as chronic bronchitis, tuberculosis etc. [448].

### 3.2.1.5 Assessment of the metabolism activity in A549 cells exposed to the mixture of 4-OPA+IPOH+4-AMCH

Metabolomics analyses were carried out on A549 cells exposed to 4-OPA+IPOH+4-AMCH as a mixture prepared by taking into consideration their ratios [12 : 86 : 2] that were found in ambient air under certain conditions (e.g. presence of air fresheners) [168].

Studying the profile of metabolites requires, as a first step, information on the mixture's concentration impact on cellular viability and its stability over time. Thus, the A549 cells were incubated with 5 concentrations of the mixture for 72 h, when the cell metabolism (viability) was measured by Presto blue assay. The dilution factor between mixtures was 2.

For all tested concentrations, the results obtained showed that 10 % reduction in cellular viability was achieved when A549 cells were incubated with a mixture containing approximately 40  $\mu\text{M}$  of 4-AMCH, 1535  $\mu\text{M}$  of IPOH and 360  $\mu\text{M}$  of 4-OPA (defined as high mixture), while around 1 % of cells lost their viability when treated with 10-times lower concentration of the mixture (defined as low mixture).

A batch of analysis corresponding to 6 independent biological replicates: untreated (control) and treated A549 cells with both high and low mixture concentrations were used to detect the presence of the test compounds in both cellular medium and cellular extract as well as perturbation in the metabolic activity of the A549 treated cells for 72 h when compared to the control.

### Characterization of the compounds applied as a mixture to A549 cells

The concentration of 4-OPA, IPOH, 4-AMCH prepared as high and low mixture concentration was determined into cell culture medium following cells exposure for 24 and 72 h, by GC-FID and further confirmed by the TD-GC-MSD analysis. Measured concentrations over time are listed in the table below:

**Table 22** Quantification of 4-OPA, IPOH, 4-AMCH in the cell culture medium following cell exposure at two concentrations (high and low) over time (24 and 72 h) The symbol \* refers to the limit of detection, while the symbol \*\* refers to the limit of quantification. Data are shown as mean  $\pm$  SD.

	Low mixture, [] at which 1 % of cells were dead		High mixture, [] at which 10 % of cells were dead	
	24h	72h	24h	72h
4-OPA [ $\mu\text{g mL}^{-1}$ ]	< 0.88*	< 0.88*	< 2.93**	< 0.88*
4-AMCH [ $\mu\text{g mL}^{-1}$ ]	0.27	< 0.06*	0.37	< 0.06*
IPOH [ $\mu\text{g mL}^{-1}$ ]	< 0.45*	< 0.45*	6.02	< 1.5**

As presented in the table above, 4-OPA was detected as being close to the limit of quantification in the medium of cells exposed for 24 h at high mixture concentrations, while at low mixture concentrations, it was detected at trace levels (close to the limit of detection). After 72 h, 4-OPA was detected as being close to the limit of detection in the cellular medium at both low and high concentrations of the mixture. The data obtained for

4-AMCH indicated that after 24 h of cells exposed to the mixture, 4-AMCH was detected for both low and high concentrations, while after 72 h it was detected in the medium samples at trace level (close to the limit of detection). On the contrary, IPOH was identified close to the limit of detection in all incubation times tested at low concentrations but it was detected in all high concentration samples.

In a parallel study, the mixture was incubated with the cell culture medium alone, where the concentrations of each compound were determined. The results showed that IPOH concentration measured into medium without cells was reduced 1.5-times after 72 hours compared to its initial concentration, while both 4-OPA and 4-AMCH were not detected after 72 h, probably due to their evaporation, binding to plastic culturing material, or protein binding contained in the cell culture medium (1 % FBS).

Comparing the identified values of IPOH into the medium without cells with those found in the medium with cells, a decrease in its concentration was observed as being approximately 12-fold change after 24 h and 40-fold change after 72 h. After 24 h cell exposure to 4-OPA and 4-AMCH, a 3-fold change and 7-fold change respectively was observed when compared with their initial concentrations in the medium alone. During chromatogram evaluations, both from GC-FID and TD-GC-MSD analysis, the formation was noticed of unknown compounds or the increase in intensity of unidentified peaks during time, apparently related to the decrease of the IPOH concentration. This evaluation has been made only at a very preliminary stage and could be subject to further studies.

The analysis of cellular extract indicated that 4-OPA was detected neither by the GC-FID technique nor by TD-GC-MSD in none of the exposure conditions (e.g. time and mixture concentrations), while 4-AMCH was detected in all samples by GC-FID at a level close to the limit of detection. Its presence was also confirmed by the Selected Ion Monitoring (SIM) of the TD-GC-MSD data. IPOH presented a similar behavior to the AMCH since it was detectable in all samples at a level close to the limit of detection and confirmed in the SIM evaluation of TD-GC-MSD data.

### Effects of the 4-OPA+IPOH+4-AMCH mixture on the metabolomic profile of A549 cells

Samples were prepared and analyzed by LC and LTQ Orbitrap mass spectrometry, as described in the Materials and Methods chapter. The LC-Orbitrap MS is a multi-analyte detection technique that allows the simultaneous detection of thousands of metabolites in a single run. The untargeted approach is used to screen the metabolome of the cell system (or a sub-metabolome, in this case corresponding mainly to the metabolites extracted from the cytoplasmic compartment of the cell) and to measure the changes in the metabolome induced by exposure to a xenobiotic (individual chemical or chemical mixture) [449]. Relative changes that are measured correspond to de-regulated

metabolites (up- or down regulated). The untargeted metabolomic experiment included 6 analytical batches corresponding to the 6 replicate studies (1 replicate = 1 measurement time, 3 exposure doses).

As presented in **Figure 57 A** (raw plots of LC-MS chromatograms), a different chromatographic profile was observed in treated cells compared to the control (untreated cells). The peak intensity increased in a concentration-dependent manner. Datasets were then analysed using principal component analysis (PCA) to assess differences (de-regulated metabolites) in the whole experiment in pairwise comparison of high and low exposure concentrations versus control.

The PCA was used for dimensionality reduction of the system (or in other words to "simplify the system") by an orthogonal transformation of thousands of variables (m/z, RT, intensity values) that are possibly correlated into a new set of non-correlated variables called principal components (PC1 and PC2 are orthogonal variables). Within this approach, significant differences between groups (cells untreated and cells treated with low and high concentration) can be observed (the formation of clusters). Score plots of the principal component PC1 versus PC2 revealed a statistically significant separation of clusters from cells treated with a high mixture concentration (purple dots represented in the **Figure 58**) when compared to untreated cells (green dots represented in the **Figure 58**). The metabolite profiling obtained for cells treated with low mixture concentration (red dots) was similar to those of cells untreated (see **Figure 58**).

Each spot of the PCA plot corresponds to an observation or, in other words, to a single biological sample. In each of the three groups (control or cells untreated, low dose and high dose) 18 points were displayed on the PCA plot, meaning 6 biological replicates x 3 technical replicates. This first step in data investigation would indicate that more work is needed to highlight the main differences between control and treated samples.

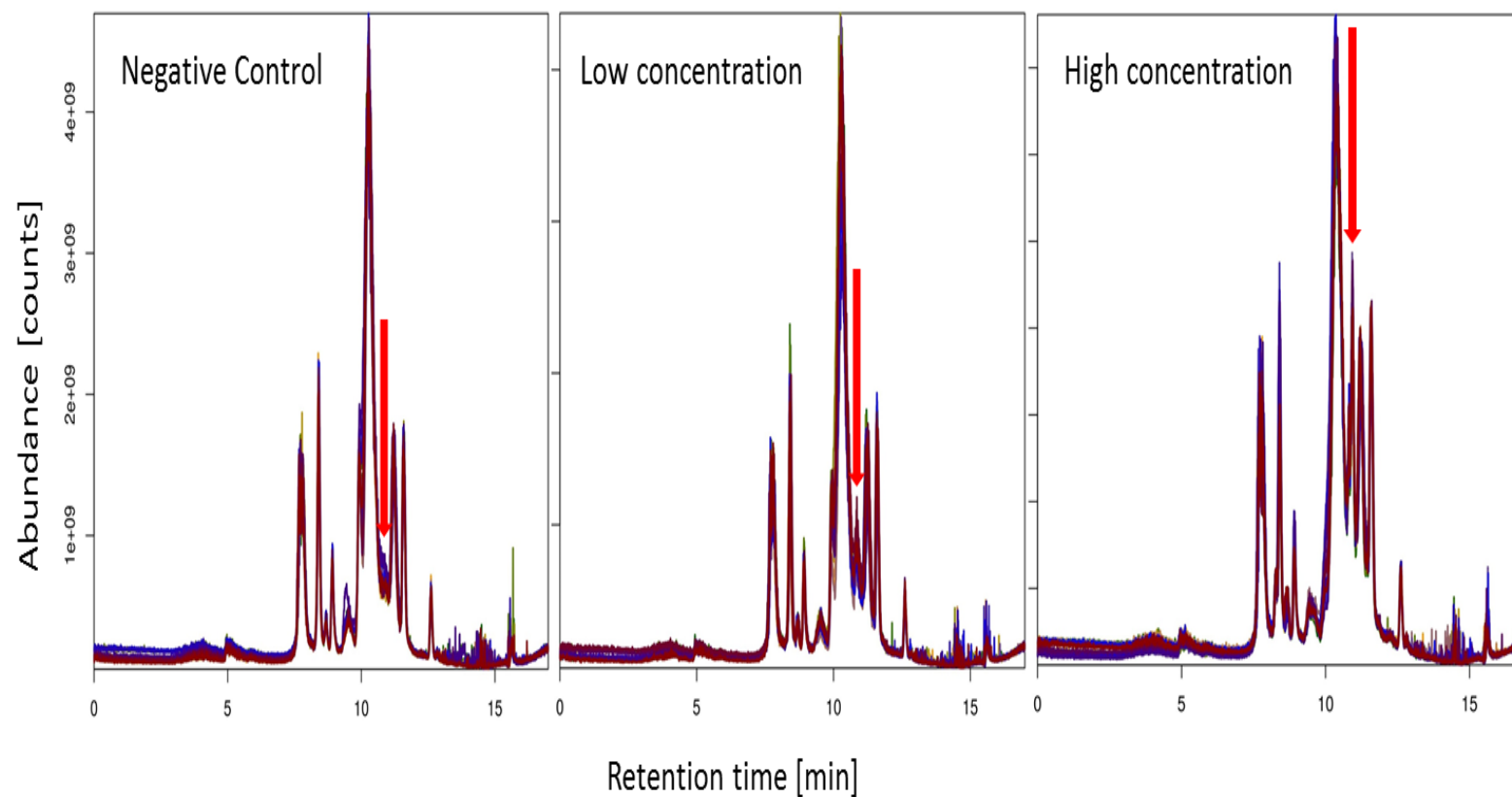


**Figure 57 A** General view (RT = 0-15) of the LC-MS chromatograms obtained from A549 cellular medium after chemical exposure to the 4-OPA + 4-AMCH + IPOH mixture (negative control corresponds to untreated cells; low concentration corresponds to cells exposed to  $25 \mu\text{g mL}^{-1}$ ; while high concentration corresponds to  $260 \mu\text{g mL}^{-1}$  of the chemical mixture).

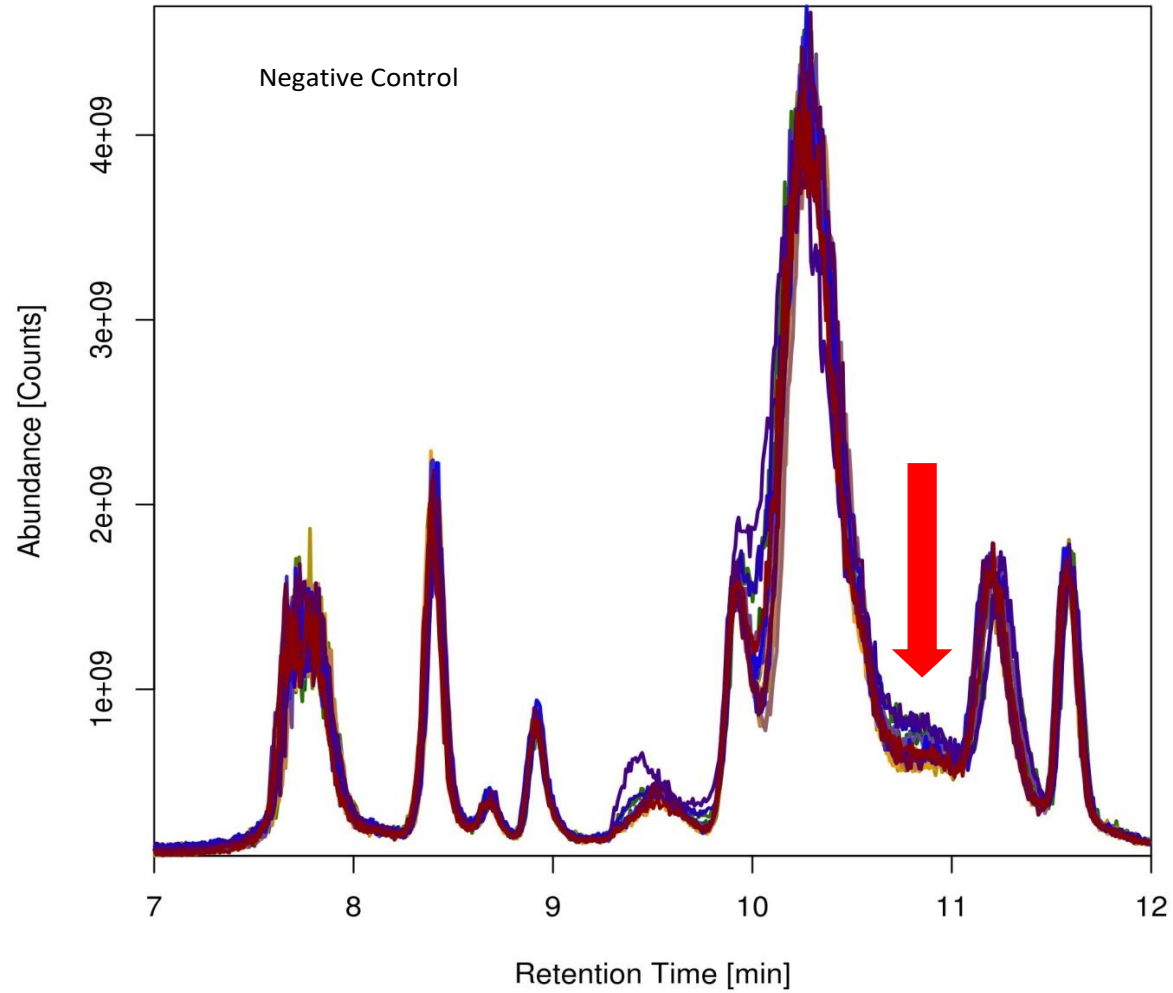


**Figure 57 B.** Detailed cut view (RT = 7-12) referring to the chromatograms presented above (cut view for the negative control – untreated cells)

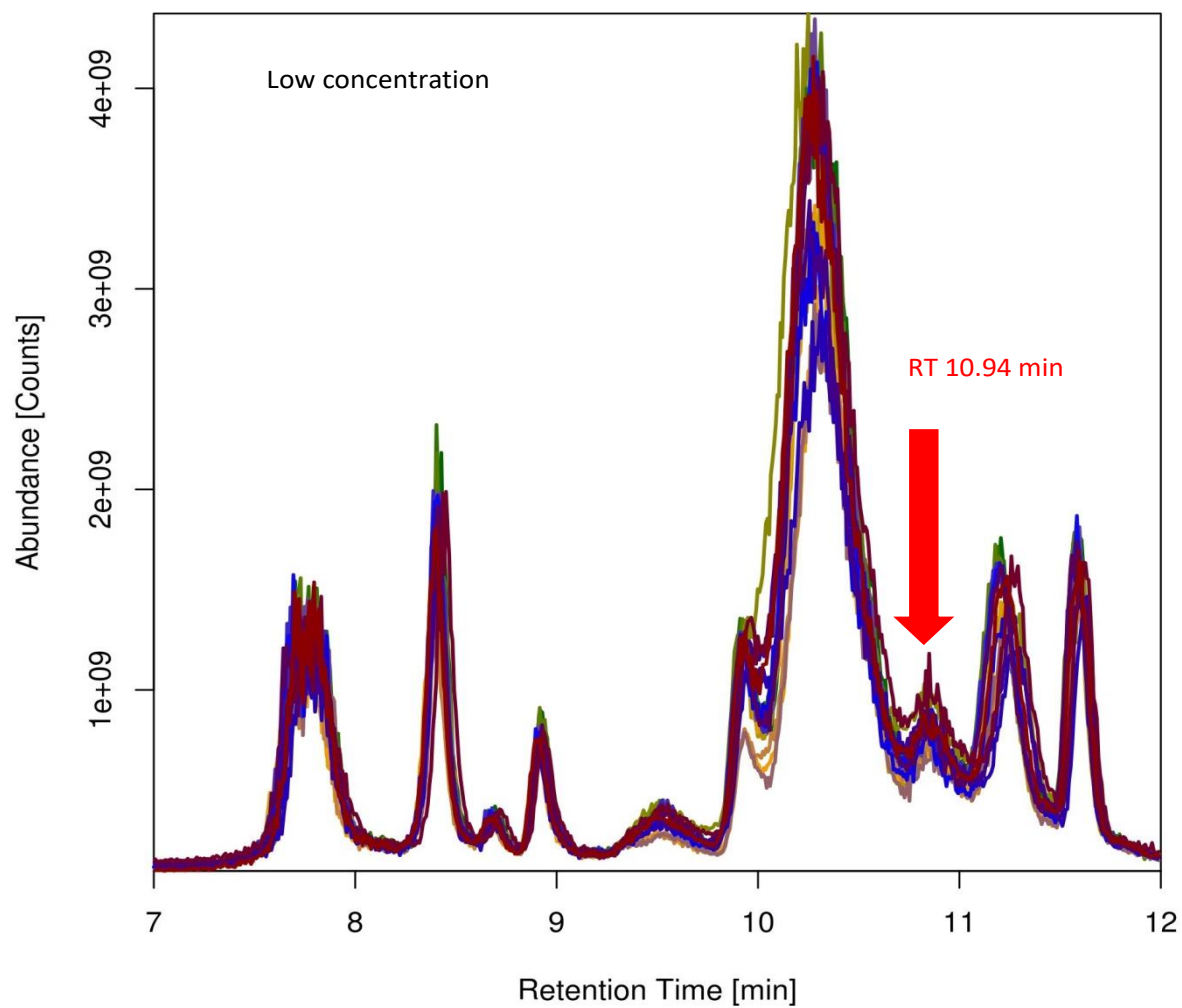


**Figure 58 C.** Detailed cut view (RT = 7-12) referring to the chromatograms presented above (cut view for the low concentration – cells treated with the mixture prepared at low concentration)

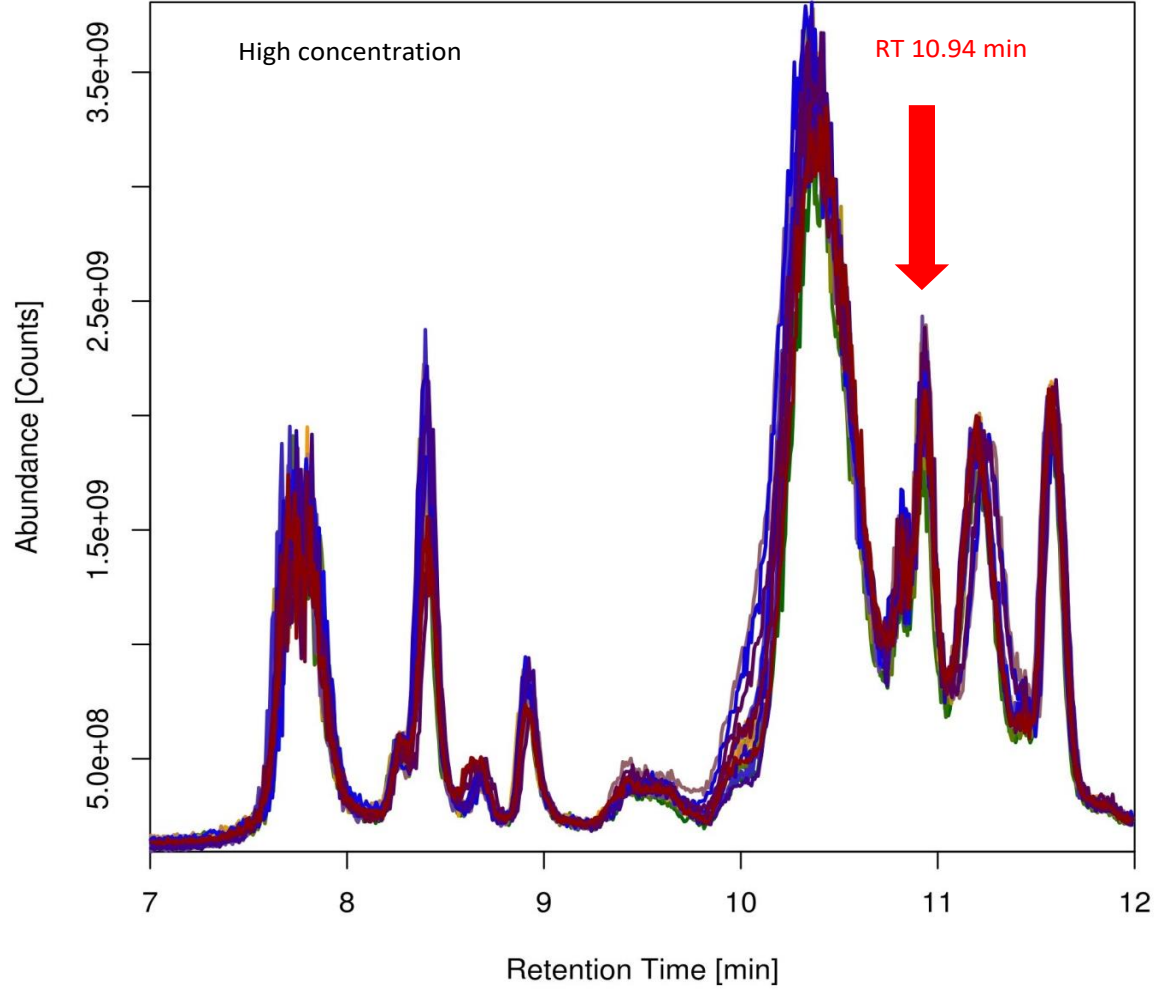


**Figure 58 D.** Detailed cut view (RT = 7-12) referring to the chromatograms presented above (cut view for the high concentration – cells treated with the mixture prepared at high concentration)

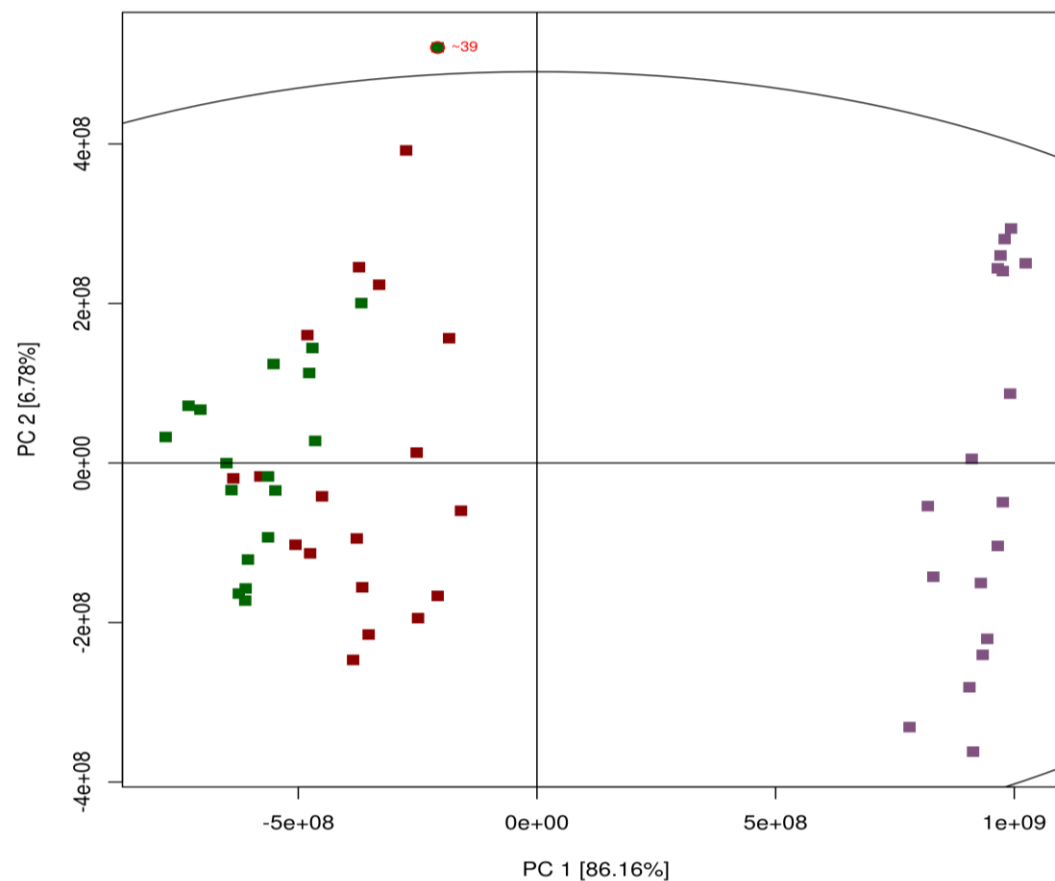


**Figure 58** Score plot of PC1 versus PC2 from principal component analysis of cellular extract after A549 treatment for 72 h with the mixture (significance of dot colours: green corresponds to the negative control, red corresponds to the samples treated with low mixture concentration where 1 % of cells lost their viability, purple corresponds to the samples treated with high mixture concentration, where 10 % of cells lost their viability)

The elaboration of LC-MS metabolomic data using the R/XCMS programme [450] is a very complex sequence of operations that includes 1) data pre-processing (peak finding, grouping and alignment), 2) data clean-up with elimination of technical outliers, chemical noise (contaminants), instrumental noise, and possible artefacts, 3) normalisation of the signal, 4) statistical analysis, and 5) tentative annotation of features/metabolite identification [449].

The basic output consists of a table of intensities for detected peaks in each sample with peaks labelled by  $m/z$  and  $rt$  values (where  $m/z$  is the mass-to-charge ratio and  $rt$  is the retention time in s). A univariate analysis, which is the simplest form of quantitative analysis, was carried out with the description of a single variable (in this case represented by the exposure dose) in terms of unit of analysis. A paired Student's t-test was applied in the whole experiment in pairwise comparison of high and low exposure concentrations versus control. This is possible when working with an *in vitro* system where most of the parameters are under control (e.g. time, temperature, composition of the culture medium, chemical exposure etc.). Metabolites were considered to be differentially expressed if they showed a fold-change of at least 2 and a  $p$  value  $< 0.05$  with the t-test.

Further peak redundancy removal (de-isotoping and de-adduction) was carried out by the CAMERA open source package [451], identifying adducts and isotopes occurring from the parent molecular ions. The  $m/z$  features retained after statistical analysis were then submitted to database search for annotations. Public database annotations were performed with putative metabolites matching these queries. The Human Metabolome Data Base (HMDB, <http://www.hmdb.ca>) [452] was used for annotation, by matching the measured accurate masses  $\pm 0.01$  amu with theoretical ones.

Reporting standards for metabolite annotation/identification are essential for data analysis. In 2007, the Metabolomics Standards Initiative (MSI) (<http://msi-workgroups.sourceforge.net>) of the Metabolomics Society reached a general consensus on reporting standards in metabolomics [453]. These standards recommend that authors should report the level of identification for all metabolites based on a four-level system ranging from MSI level 1 (identified compounds), via levels 2 and 3 (putatively-annotated compounds and compound classes) to level 4 (unidentified or unclassified metabolites which nevertheless can be differentiated based upon spectral data).

The system is currently under revision by the Metabolic Society to reassess current reporting standards. A first option would be to provide sub-levels within the four MSI levels which will provide greater distinctions within the existing level system. A second option is a quantitative scoring system [454, 455].

Going through the identification of all metabolites of interest is fastidious and time consuming. The identification challenge is immense and confident unambiguous assignments of observed metabolic features to a single compound are not always easy. Definitive (level 1) identification requires the comparison of two or more orthogonal properties (eg. RT, accurately measured  $m/z$ , fragmentation mass spectrum) of a chemical standard to the same properties observed for the metabolite of interest analysed under identical analytical conditions.

The application of accurate measurement of  $m/z$  provides putative annotations (the top 5 possibilities are considered). Starting from a peak list of ca. 4260 and ca. 2280 features ( $m/z$ ,  $rt$  values) in the cell culture medium and cell extract, we could reduce to 3365 and 1556 features after the clean-up step (eliminating noise, contaminants). The output is a short list of 798 and 214 statistically relevant de-regulated features affected by the exposure dose in the cell culture medium and cell extract, respectively. For metabolite identification the standard reporting system described by Sumner et al. has been used [453]. We reported level 2 (putatively annotated metabolites) identification.

In order to better understand the obtained results for the toxicological response of the A549 cells exposed to IPOH, 4-AMCH or 4-OPA, the possible metabolites for these functional groups were searched.

On one hand, both free radicals and epoxides formed during the metabolism of xenobiotics can pose an oxidative stress on the cells, and thus higher ROS signals can be expected. On the other hand, aldehydes are known to have irritating properties, thus inducing the formation of pro-inflammatory cytokines/chemokines [456].

As can be observed in figure below, IPOH is capable of forming radical compounds, epoxides and aldehydes. Most probably, the observed oxidative stress and inflammatory response of cells exposed to IPOH arise from such metabolites.

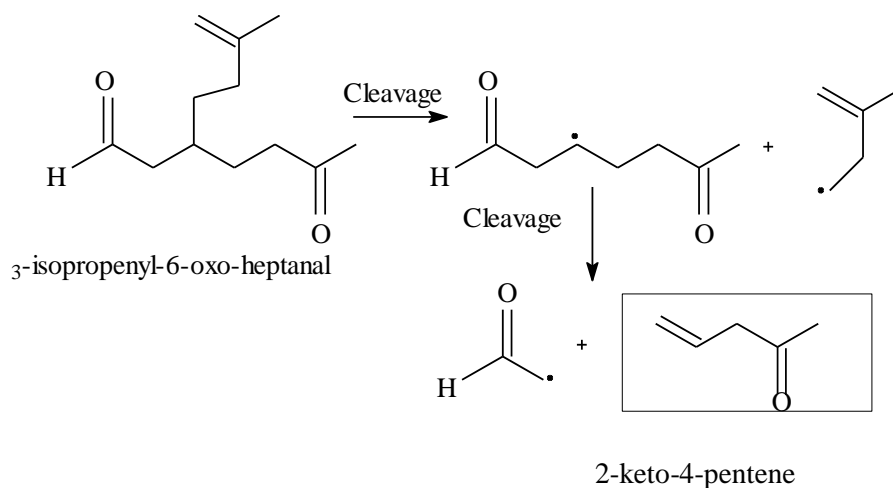


**Figure 59** Cleavage reaction of 3-isopropenyl-6-oxo-heptanal leading to epoxides and aldehydes

Radical reactions: Radicals can be recombined between them to form covalent bonds or add to the epoxide derived from oxidation of 2-keto-4-pentene (see **Figure 60**)

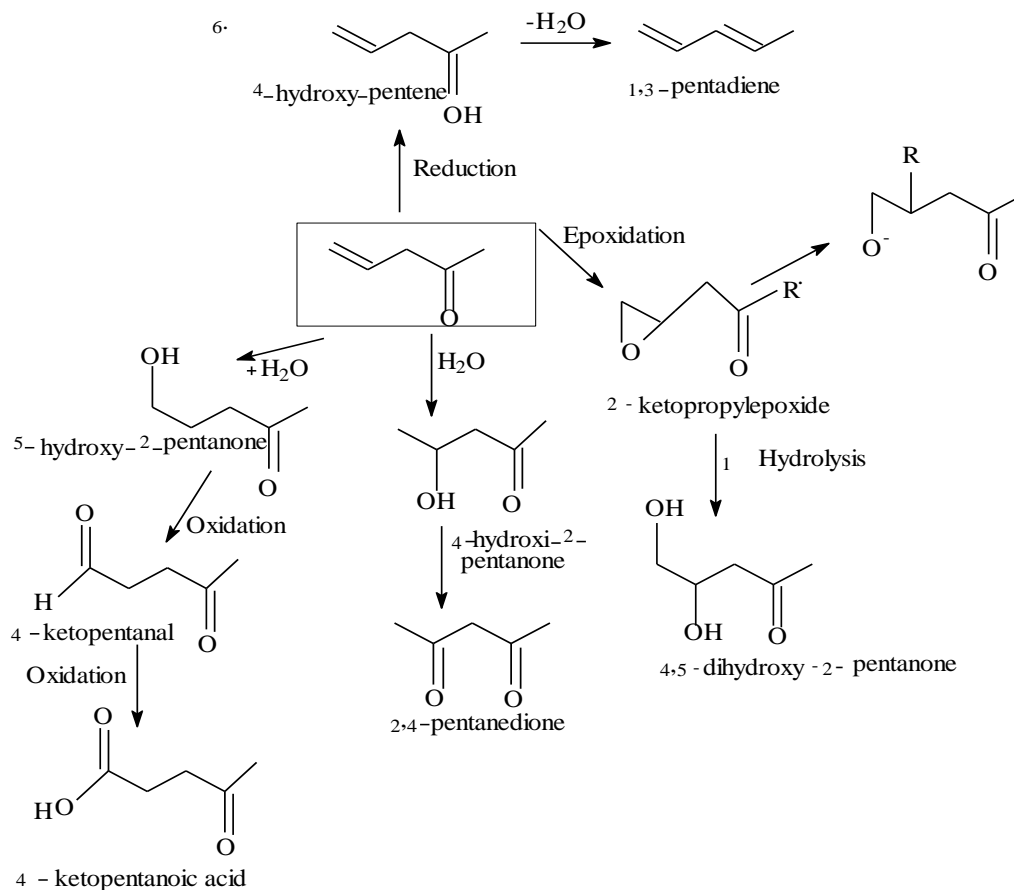


**Figure 60** Possible pathways of cellular reaction of IPOH leading to formation of radicals, epoxides and aldehydes

Based on a series of possible pathways of cellular reaction of 4-OPA when added to the selected human cells, various aldehydes, acids and alcohols are theoretically formed. Interestingly, 4-oxopentanoic acid (annotation based on the human metabolome database) determined in the cellular extract of the A549 cells treated with the mixture of 4-OPA, IPOH and 4-AMCH was observed as one of the most abundant metabolites (33-fold change) when compared to the untreated cells.

Most probably, the observed inflammatory response detected in A549 cells exposed to 4-OPA by increased levels of IL-6 (e.g. 1.4-fold higher) might be a consequence of the various acids formed during the pathway cellular reaction of 4-OPA. This hypothesis (that acids formed might be responsible of the inflammatory reaction) is based on some cytotoxic results reported in the literature, where A549 cells treated with compounds carrying an COOH group, caused the release of cytokines such as IL-8, IL-6, biomarkers responsible for the inflammation [457].

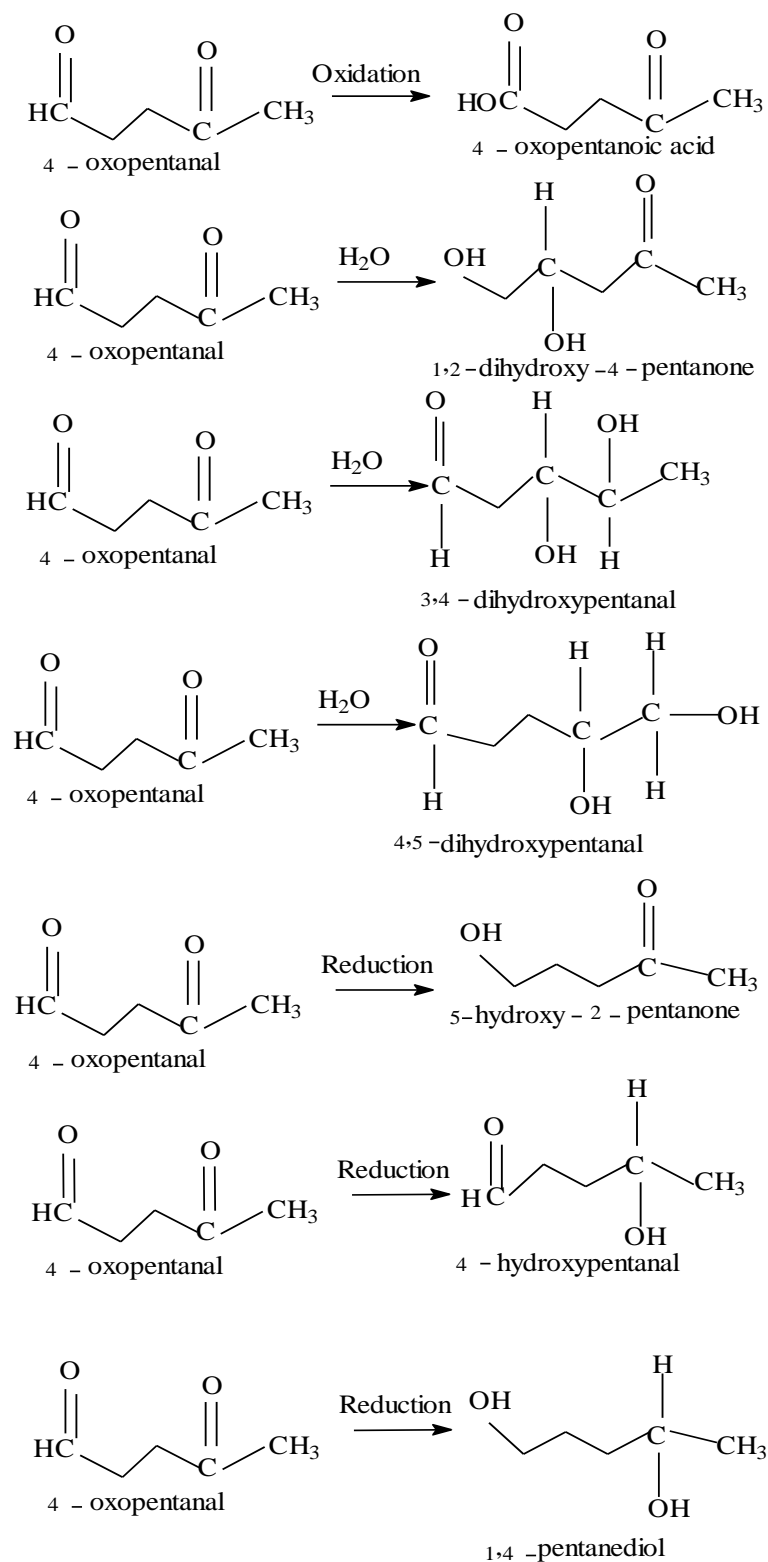
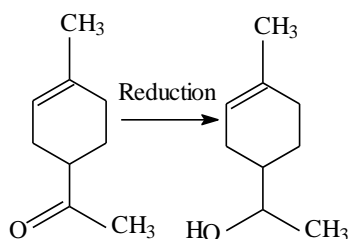
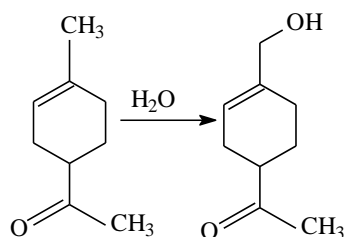


**Figure 61** Possible pathways of cellular reaction of 4-OPA leading to the formation of aldehydes, acids, alcohols

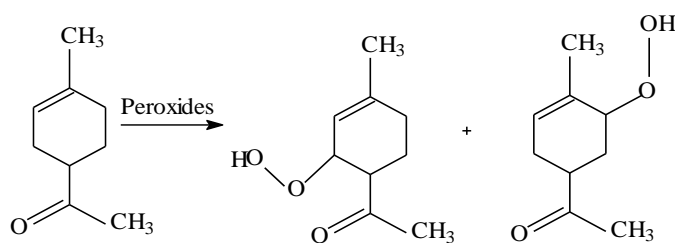
The formation of peroxides during the cellular pathway reaction of 4-AMCH in A549 cells might explain the potential effect of 4-AMCH to induce the oxidative stress in A549 cells that was determined by the presence of high intracellular ROS levels when compared to untreated cells (see results on the determination of ROS).



4-(2-hydroxyethyl)-1-methyl-1-cyclohexene



4-acetyl-1-hydroxymethyl-1-cyclohexene



4-acetyl-1-methyl-3-peroxyl-1-cyclohexene / 4-acetyl-1-methyl-5-peroxyl-1-cyclohexene

**Figure 62** Possible pathways of cellular reaction of 4-AMCH leading to the formation of peroxides, alcohols

De-regulated metabolites present in the cell culture medium and the cellular extract were listed, and their m/z features retained were further filtered based on the mass calculated of the new compounds obtained from the oxidation, hydration and reduction reaction that can occur with each individual test compounds (see reactions in the figure above). As presented in **Table 23**, metabolites in the cell culture medium and extract at high mixture

## Results and Discussion

---

concentration were selected as most abundant when compared to untreated cells and therefore annotated.

**Table 23** De-regulated metabolites present in the cellular medium and cellular extract [student t-test ( $p < 0.001$ ) and annotation using the human metabolome database (HMDB)]

m/z	rt	Cellular medium	Cellular extract	HMDB name
		Fold-change	Fold-change	
117	607.4	21	33	4-oxopentanoic acid
119	297.2	---	11.3	2,4-diaminobutanoic acid
131	545.5	---	2.7	---
153	656.5	18	6.2	Alpha-pinene-oxide
171	669.2	12	4.7	(6E)-8-methylnon-6-enoic acid
185	481.7	---	48.9	3,5-dihydroxy-4-methoxybenzoic acid
185	660.1	---	45.2	---
199	649.2	57.6	---	Guaifenesin
199	808.7	3.5	2.6	5-Dodecenoic acid
201	223.3	2.4	6.0	Ecgonine methyl ester

---

**Table 24** Cellular location indicated in the human metabolome database (HMDB) of the most significant de-regulated metabolites which were found in the cellular medium and cellular extract

HMDB name	Cellular location
4-oxopentanoic acid	Cytoplasm
2,4-diaminobutanoic acid	Cytoplasm
Alpha-pinene-oxide	Cytoplasm; extracellular; membrane
(6E)-8-methylnon-6-enoic acid	Extracellular; membrane
3,5-dihydroxy-4-methoxybenzoic acid	Not available
Guaifenesin	Not available
5-Dodecenoic acid	Cytoplasm; extracellular; membrane
Ecgonine methyl ester	Endoplasmic reticulum

Based on the consideration above, it is concluded that the mixture of 4-OPA, IPOH and 4-AMCH prepared at two concentrations (low and high) separated by a factor of 10, leads to a different cytotoxic effect (e.g. approximately 10 % loss of cell viability when cells were treated with the most concentrated mixture).

### 3.2.2 Potential inflammatory capacity of d-limonene and 4-OPA, 4-AMCH, IPOH in human blood evaluated by *In vitro* Pyrogen test (IPT)

Human fever reaction to chemicals was simulated *in vitro* by directly incubating the cryo-preserved blood with test compounds at various concentrations. Following 18 hours of incubation, the IL-1 beta released into blood samples was measured by *In vitro* Pyrogen test (IPT). However, different parameters such as the maximum time required for the blood distribution into samples after its thawing, and the optimal time incubation of blood with test compounds were considered in order to guarantee optimal execution of the test.

#### *Influence of blood distribution over time on the inflammatory response level (IL-1 beta)*

To identify the optimal time required to distribute the cryo-preserved blood into the culture medium containing the test compounds, different concentrations of lipopolysaccharide from *Escherichia coli* strain O113:H10 (LPS O113:H10) - used as positive control (WHO reference standard for fever-inducing contaminant) - were added to blood at various intervals of time (from 5 to 15 minutes counted after thawing the blood that is taken from the liquid nitrogen).

The IPT experiments were all run using the same lot of cryo-preserved blood, in order to avoid variability within different lots.

As can be seen in **Figure 63**, the quantity of the IL-1 beta expressed as optical density is decreasing over the blood time distribution. This trend of time is maintained for all the LPS concentrations expressed as Endotoxin Units (EU), which were tested in the range of 0.125 to 2 EU. Since time blood distribution is one of the sensitive parameters of this *in vitro* test, the time needed to distribute the blood over the samples was limited to 5 minutes for all the experiments.

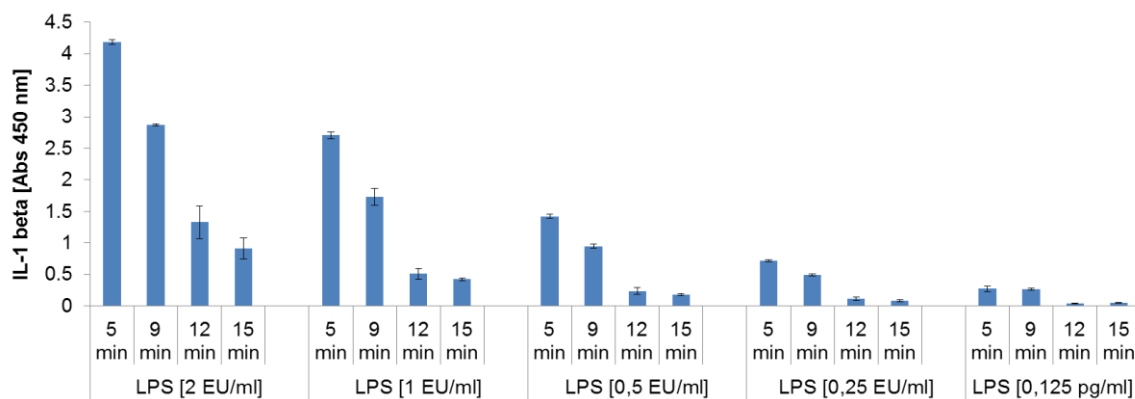


**Figure 63** Evaluation of time blood distribution on potential inflammatory capacity of various LPS concentrations [from 0.125 to 2 EU] added to blood (n=9 ± STD)

*Determination of optimal time for incubation of blood with LPS O113:H10 to produce maximum release of inflammatory response (IL-1 beta)*

The time course production of IL-1 beta release from cryo-preserved blood stimulated with three LPS concentrations was measured at 12, 15, 20 and 24 hours. The maximum release of IL-1 beta was observed at 15 hours after blood incubation with LPS within all concentrations tested (see **Figure 64**).

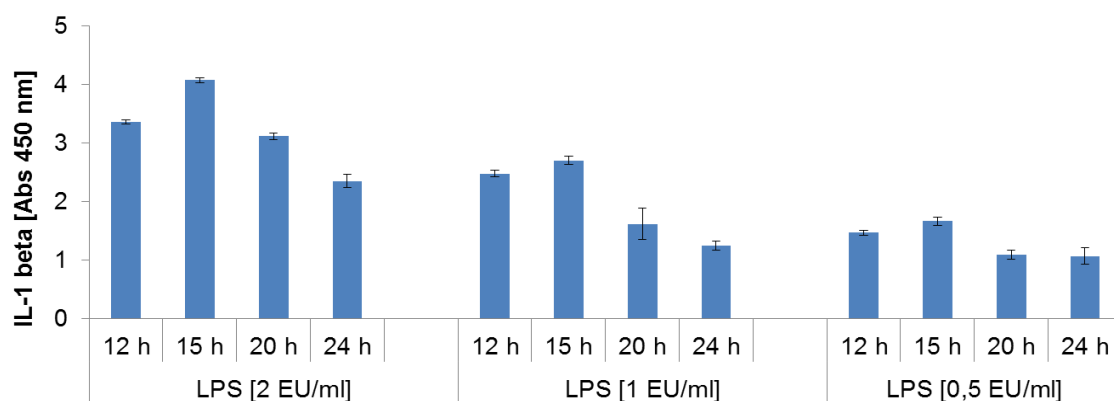


**Figure 64** Measurement of IL-1 beta release from blood incubated with LPS concentration in the range of 0.5-2 EU mL<sup>-1</sup> investigated at various incubation times

### *Evaluation of potential inflammatory capacity of d-limonene and 4-OPA, 4-AMCH, IPOH in human blood*

The single and the combined cytotoxic effects of 4-OPA, IPOH and 4-AMCH on human cell blood viability were assessed by optical microscopy. The morphological appearance of blood cells show that for single compounds less than 10 % of blood cells were damaged in the concentration range of 100 to 500  $\mu\text{M}$ , while the concentration of their mixture was tolerable (approximately 10 % reduction in blood cells) in the range of 10 and 100  $\mu\text{M}$ . Therefore, taking into consideration the blood cell counts, for an appropriate comparison between the potential inflammatory capacity of individual compounds and their mixtures, the inflammatory capacity of mixtures was tested in blood in the range of 0 to 100  $\mu\text{M}$ .

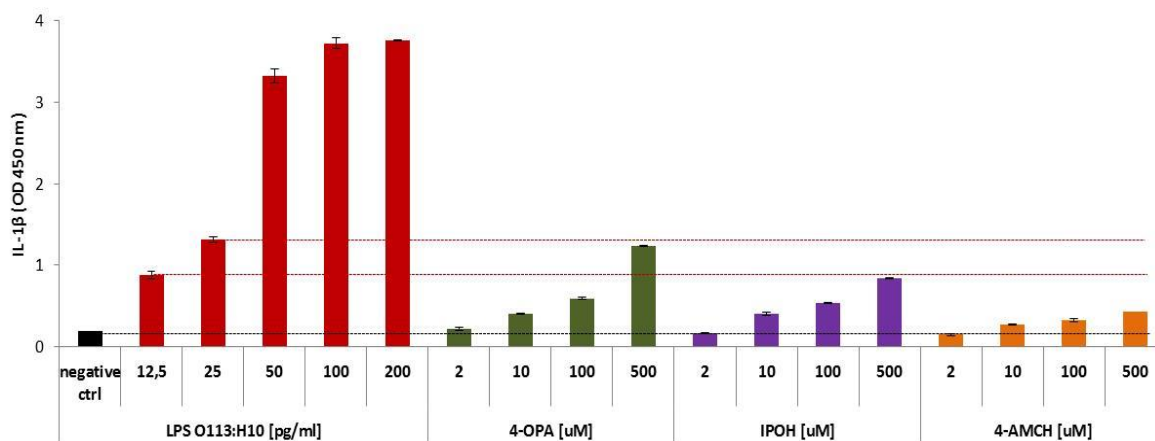


**Figure 65** IL-1 beta detected in human blood incubated with individual tested compounds at four concentrations (0-500  $\mu\text{M}$ ). Data represent mean  $\pm$  SD, n=3

As shown in **Figure 65**, human blood incubated with 4-OPA at 500  $\mu\text{M}$  released a higher amount of IL-1 beta when compared to the other compounds tested. The total amount of IL-1 beta induced into blood by 4-OPA at 500  $\mu\text{M}$  is comparable to the potential inflammatory capacity of the LPS O113:H10 at a concentration of 25  $\text{pg mL}^{-1}$ . The highest tested concentration (500  $\mu\text{M}$ ) of IPOH and 4-AMCH produced 1.5-times and 2.8-times respectively lower levels of IL-1 beta when compared to 4-OPA at 500  $\mu\text{M}$ .

At 10 and 100  $\mu\text{M}$ , both 4-OPA and IPOH induced similar amounts of IL-1 beta release in blood.

Human blood showed no significant production of IL-1 beta over the negative control levels at a concentration of 2  $\mu\text{M}$  for all tested individual compounds.

On the other hand, no IL-1 beta was released in the tested concentration range of 0 to 100  $\mu\text{M}$ , after 15 hours of blood incubated with binary (4-OPA + IPOH, 4-OPA + 4-AMCH and IPOH + 4-AMCH) or ternary mixtures (4-OPA + IPOH + 4-AMCH).

Nevertheless, according to literature, the threshold value of an endotoxin to induce fever is 0.5 EU. According to the inflammatory comparative results between the tested compounds, 4-OPA indicated the most potential inflammatory capacity in human blood. Added at a concentration of 500  $\mu\text{M}$  showed a higher IL-1 beta signal (3.1-fold) than the signal of IL-1 beta obtained to the other tested chemicals (IPOH – 2.7-fold, and 4-AMCH – 1.7), based on the comparison with the unexposed blood. However, total amount of IL-1 beta released by the human blood exposed to 4-OPA was lower than the total amount of IL-1 beta induced by 0.5 EU (50  $\text{pg mL}^{-1}$ ) of LPS O113:H10, which is a well-known fever inductor [458].

### **3.3 *In vitro* studies with human lung cells exposed to d-limonene and the mixture of 4-OPA, IPOH, 4-AMCH in presence/absence of ozone via Air-Liquid interface (CULTEX system)**

3.3.1 Assessment of cytotoxic effects induced by d-limonene, ozone and d-limonene/ozone gas mixtures on human lung cells

3.3.1.1 CULTEX exposure to d-limonene and ozone as individual compounds with A549 and THP-1 cells

To evaluate the potential cytotoxic effects of a chemical mixture (e.g. d-limonene – ozone mixture) on the pulmonary cultured cells, d-limonene and ozone were initially studied as individual compounds.

In order to assure that the concentration of compounds is reproducible between various exposure experiments, before and after each *in vitro* exposure runs, the target concentration of the test compounds was verified as follows: active sampling GC-MSD analysis for the quantification of d-limonene and for the determination of ozone and nitric dioxide values it was used an Ozone and NO/NO<sub>2</sub>/NO<sub>x</sub> analysers (see **Table 25**).

**Table 25** Concentrations of d-limonene, ozone and NO<sub>2</sub> (positive control) used to expose A549 cells in CULTEX exposure module coupled to the environmental test chamber. Target concentrations and chamber initial concentrations (measured in the chamber) during cell exposure are reported.

	$\mu\text{g m}^{-3}$	Run 1	Run 2	Run 3	Target [ $\mu\text{g m}^{-3}$ ]	Target [ppmv]
Positive control	NO <sub>2</sub>	11200	11200	11200	11200	6
	NO <sub>2</sub>	22500	22500	22500	22500	12
Initial Chamber concentrations	d-Limonene alone	250	240	240	200	0.02
	d-Limonene alone	5900	5700	5800	5000	0.5
	d-Limonene alone	15200	15100	15000	10000	2.5
	Ozone alone	137	137	139	137	0.07

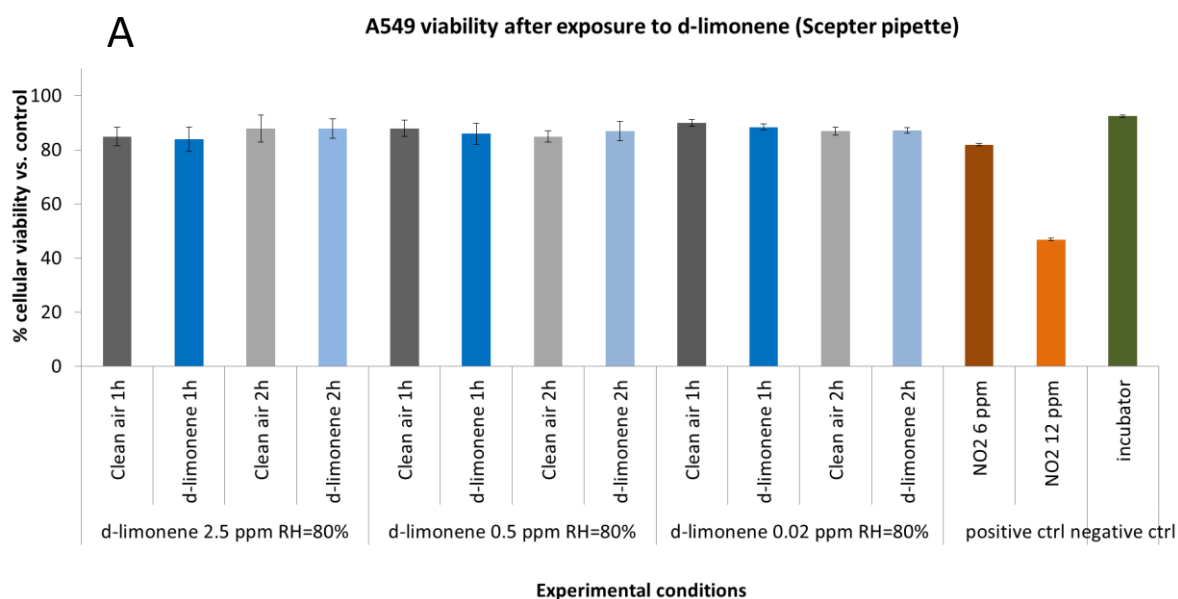
Dose-dependency of potential cytotoxic effects of d-limonene atmospheres covering the range from 0 to 15000  $\mu\text{g m}^{-3}$  (aprox. 2.5 ppmv) prepared at two relative humidity levels (50 and 80 % RH) was studied in human epithelial alveolar cells (A549). During each exposure, three transwell replicates of A549 cells were treated in parallel in the CULTEX system (under air-lifted conditions) with the target pollutants (d-limonene or ozone) at 2 mL min<sup>-1</sup> flow for 1 and 2 hours. After the indicated exposure times, cells were receiving fresh culture medium (with 1 % FBS) to both the apical and basal side, and were left to recover in the incubator until the assessment of the selected endpoints (e.g. recovery for 24 hours when cell viability, inflammatory response were evaluated while in case of glutathione assay, cells were immediately analysed after exposure).

As observed in **Figure 66 A** (measurement of cellular viability after exposure to d-limonene done by Scepter pipette) and **Figure 66 B** (cellular viability measured after exposure to ozone by Scepter pipette) there is a slight variation between the outcomes, but none of the exposure conditions applied induce a statistically significant biological response when compared to the control experiments, where cells were exposed only to humid Clean / Zero Air (e.g. p value was 0.11 for A549 cells exposed for 1 hour to 15000  $\mu\text{g m}^{-3}$  of d-limonene). No statistically significant cytokines release (no data shown) or variations in glutathione content (see **Figure 67**) were observed when cells were exposed to d-limonene or ozone alone. The use of LPS (10 ng mL<sup>-1</sup>) as positive control to induce cytokine secretion (IL-6 =

## Results and Discussion

$170 \pm 8.05 \text{ pg mL}^{-1}$ , IL-8 =  $1000 \pm 7.3 \text{ pg mL}^{-1}$ , MCP-1 =  $673 \pm 0.55 \text{ pg mL}^{-1}$ ) confirmed the suitability of the cell cultures to produce cytokines.

On the contrary to the data obtained when cells were exposed to d-limonene and ozone, exposure of the A549 cells to the positive control gas NO<sub>2</sub> (6 and 12 ppmv) showed significant loss of cell viability (around of 15 % at 6 ppmv and 50 % at 12 ppmv), LDH release (LDH activity measured in cellular medium had an increase of  $4 \% \pm 1.2$  compared to the control samples) and oxidative stress (GSNO / GSH ratio of A549 cells exposed for 1 hour to 12 ppmv NO<sub>2</sub> compared to the ratio of GSNO / GSH of the control biological samples increased more than 9-fold and 1,5-fold for the GSSG / GSH ratio), as can be observed in the graphs below. A higher formation of S-nitroso-glutathione with longer exposure time was observed when cells were exposed to 12 ppmv NO<sub>2</sub> for 2 hours (GSNO / GSH ratio of A549 cells exposed for 2 hours to 12 ppmv NO<sub>2</sub> compared to the ratio of GSNO / GSH of the control biological samples increased more than 21-fold and 2-fold for the GSSG / GSH ratio), which confirmed the technical validity of the exposure setup. The results obtained within this study regarding the toxic effect of NO<sub>2</sub> are in accordance with previous studies [459], which showed that at 10 ppmv NO<sub>2</sub>, cell viability of A549 cells was reduced to less than 50 %.



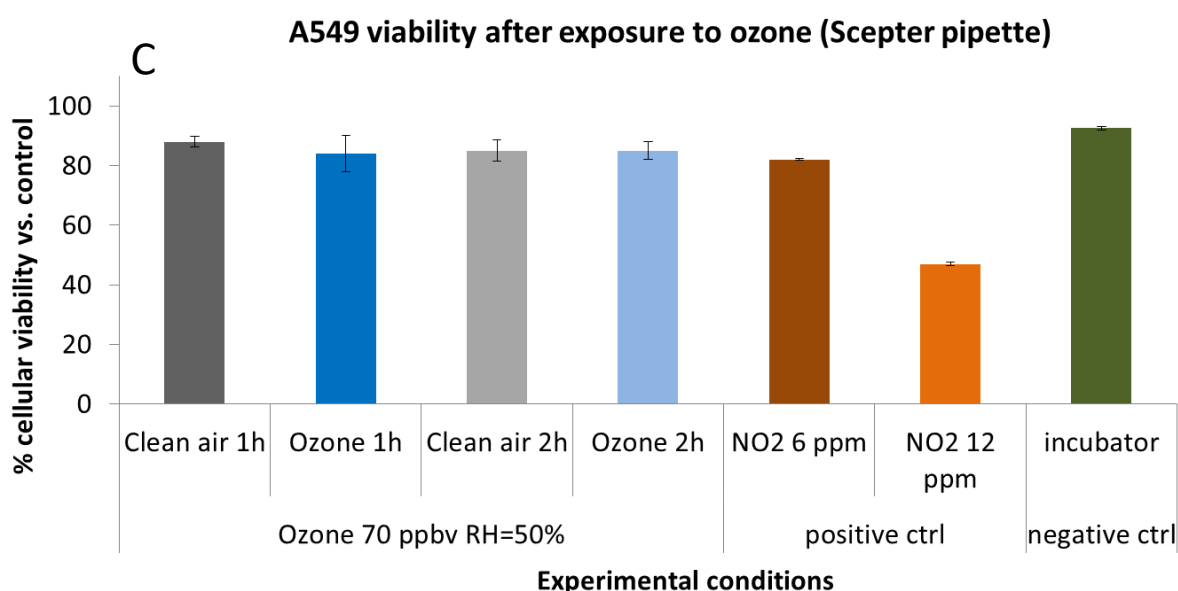
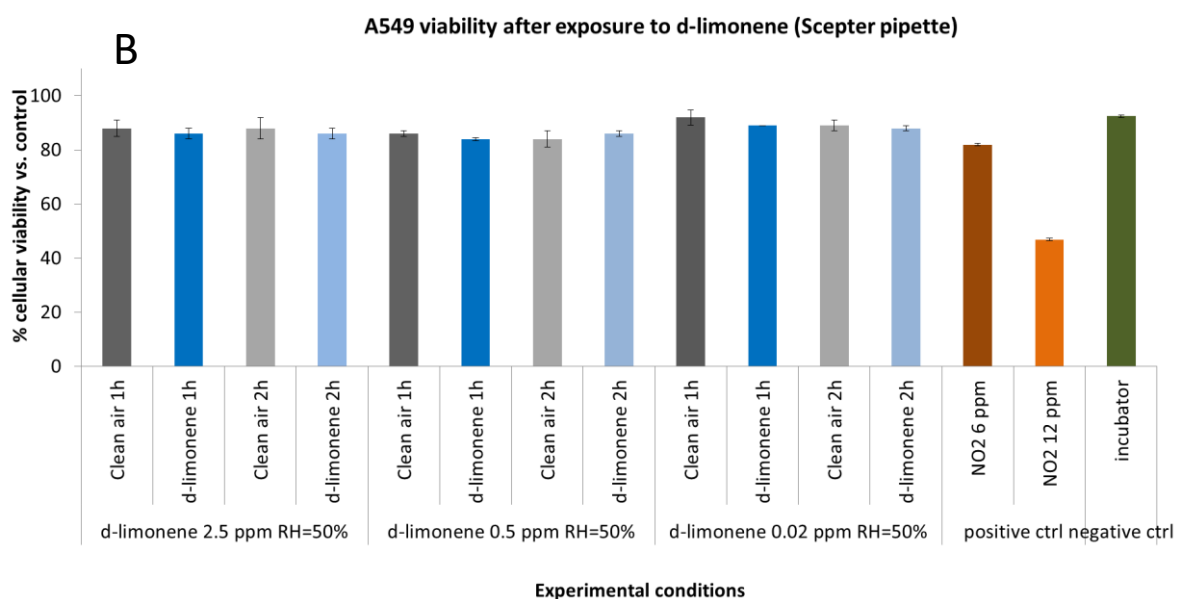


**Figure 66** Cellular viability results obtained after exposure of A549 cells in CULTEX for 1 and 2 hours to gas atmospheres containing **A.** d-limonene alone at various concentrations  $250 \mu\text{g m}^{-3}$  (approx. 0.02 ppmv),  $5800 \mu\text{g m}^{-3}$  (approx. 0.5 ppmv) and  $15000 \mu\text{g m}^{-3}$  (approx. 2.5 ppmv), relative humidity (RH)=80 % **B.** d-limonene alone at various concentrations  $250 \mu\text{g m}^{-3}$  (approx. 0.02 ppmv),  $5800 \mu\text{g m}^{-3}$  (approx. 0.5 ppmv) and  $15000 \mu\text{g m}^{-3}$  (approx. 2.5 ppmv), relative humidity (RH)=50 % **C.** ozone alone  $137 \mu\text{g m}^{-3}$  ( approx. 0.07 ppmv), RH=50 %. Mean ( $\pm$  STD) of at least three independent runs are presented. Carrier control (humid Clean/Zero air), negative (incubator) and positive ( $\text{NO}_2$ ) controls are also included in the figures.

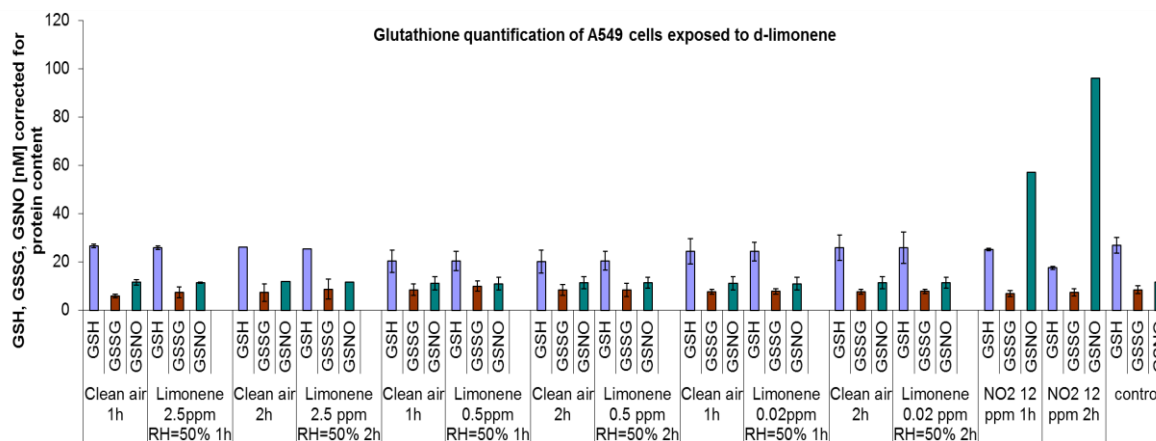


**Figure 67** Glutathione levels in A549 cells after exposure to d-limonene atmospheres (0.02, 0.5 and 2.5 ppmv). Positive control NO<sub>2</sub> (12 ppmv) and negative controls (clean air and incubator) are shown. The results are expressed as GSH, GSSG and GSNO equivalents, corrected for protein content. Mean ( $\pm$  STD) of three independent runs are presented.

The same series of exposure experiments have been carried out also for the differentiated THP-1 macrophage cell line (data not shown). However, even at the lowest d-limonene test concentration 250  $\mu\text{g m}^{-3}$  (approx. 0.02 ppmv) and exposure to ozone alone, no significant decrease in cell viability or increase in cytokines and glutathione levels was determined.

### 3.3.1.2 CULTEX exposure to d-limonene-ozone mixture with A549 and THP-1 cells

After testing d-limonene and ozone separately, a defined mixture of initial 250  $\mu\text{g m}^{-3}$  d-limonene and 137  $\mu\text{g m}^{-3}$  ozone (d-limonene-ozone ratio of 2:1) was also generated in the 0.45 m<sup>3</sup> environmental chamber, and initial compounds and reactions products were measured (see **Table 26**).

Before exposing the selected human lung cells to the d-limonene-ozone mixture, the reaction was allowed to proceed until the levels of key ozone initiated reaction products were stable (chemical reaction in the phase of steady state).

The cytotoxic effects of the mixture on the human lung cells were evaluated by applying the same endpoints as mentioned above.

The outcomes from both type of cells exposed to d-limonene-ozone mixture were compared to the results obtained with cells exposed to both positive (NO<sub>2</sub>) and negative (Clean / Zero Air and Incubator). Within these experimental conditions, the results obtained for both selected cell lines: alveolar (A549) and macrophages (THP-1) exposed to d-limonene-ozone mixture did not show a statistically significant increase in lactate

dehydrogenase (LDH) released into cellular medium when compared to controls (see **Figure 68**).

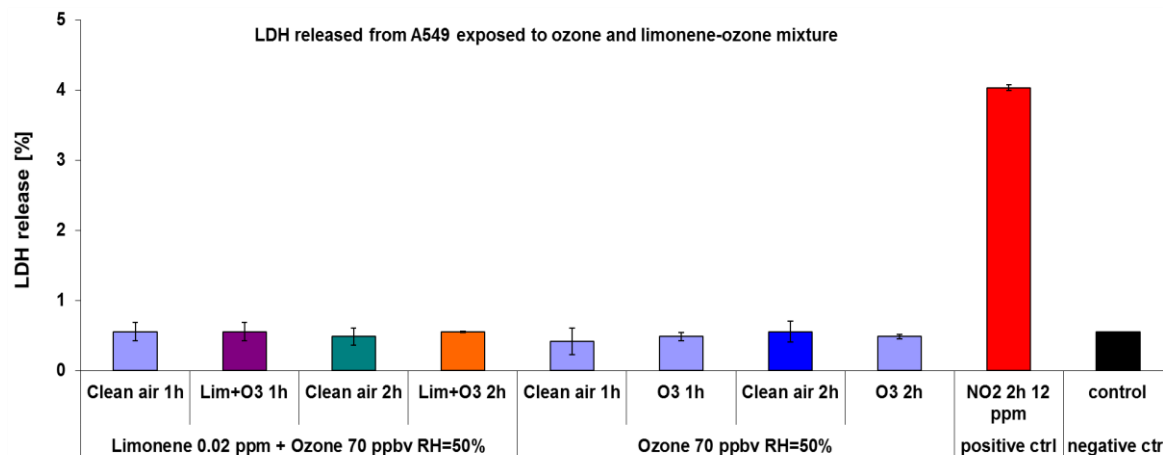


**Figure 68** Membrane damage measured in A549 cells after exposure in CULTEX for 1 and 2 hours to gas atmospheres containing only ozone (0.07 ppmv) and its mixture with 0.02 ppmv of d-limonene. Mean ( $\pm$  STD) of at least three independent runs are presented. Negative (black and light purple colors) and positive controls (red color) are shown.

Furthermore, no significant elevation in cytokines and intracellular glutathione levels nor loss of cellular viability were observed after 24 hours post exposure of both cell lines (A549 and THP-1) following exposure to d-limonene-ozone mixture when compared to Clean / Zero Air.

### 3.3.1.3 Chemical characterisation of generated atmosphere of d-limonene-ozone mixture and verification of target concentration of test compounds

The table below contains the target concentration of d-limonene and ozone as a mixture, showing that the generated atmospheres were well stabilized and reproducible between various exposure experiments. The table also contains the determined concentrations of the key secondary reaction products formed during d-limonene-ozone reaction.

**Table 26** Concentrations of d-limonene and ozone used to expose A549 and THP-1 cells in CULTEX exposure module coupled to their mixture generated in the 0.45 m<sup>3</sup> environmental test chamber. Target concentrations, chamber initial concentrations (measured in the chamber) and actual chamber concentrations during cell exposure are reported.

Chemicals	Run 1	Run 2	Run 3	Total amount [µg] delivered to cells	
	µg m <sup>-3</sup>	µg m <sup>-3</sup>	µg m <sup>-3</sup>	1 hour	2 hours
d-Limonene	230	220	210		
Ozone	134	128	131		
Formaldehyde	8.21	8.64	8.47	1.04 x 10 <sup>-3</sup>	2.07 x 10 <sup>-3</sup>
Acetaldehyde	1.58	1.56	1.84	0.22 x 10 <sup>-3</sup>	0.44 x 10 <sup>-3</sup>
Acetone	2.46	1.86	2.64	0.32 x 10 <sup>-3</sup>	0.63 x 10 <sup>-3</sup>
<b>IPOH</b>	7.58	--	9.91	1.19 x 10 <sup>-3</sup>	2.38 x 10 <sup>-3</sup>
<b>4-AMCH</b>	0.96	---	1.17	0.14 x 10 <sup>-3</sup>	0.28 x 10 <sup>-3</sup>
<b>4-OPA</b>	0.85	--	0.66	0.08 x 10 <sup>-3</sup>	0.15 x 10 <sup>-3</sup>
6-MHO	--	--	2.80	0.34 x 10 <sup>-3</sup>	0.67 x 10 <sup>-3</sup>

A series of *in vitro* exposure experiments to various concentrations of d-limonene, and a mixture of d-limonene-ozone has been carried out by using an air-lifted exposure module (CULTEX) along with the well-known A549 human lung cell line. Experiments with chemical concentrations expected in indoor environments have been included. Gas atmospheres have been generated, delivered to the CULTEX exposure system and the actual concentrations of substances have been measured. Cells were exposed for 1 and 2 hours for each condition (e.g. different relative humidities, time exposure etc.). A series of end points were measured (cell viability, membrane damage, cytokine secretion, oxidative stress) to assess potential lower airway effects. Positive (NO<sub>2</sub> and LPS) and negative controls (zero air and incubator) have been included in the study.

Target d-limonene concentrations covered a broad range including low - relevant to indoor environments - and high concentrations (0.02, 0.5 and 2.5 ppmv). Average concentrations of d-limonene 0 - 175.7 µg m<sup>-3</sup> have been measured during the AIRMEX project and reported in Geiss et al. [460]. Therefore, a defined mixture of 0.02 ppmv of d-limonene and 70 ppbv of ozone was generated; initial substances and reactions products were

measured. Before cell exposure, the reaction was allowed to proceed until the occurrence of key ozone initiated reaction products was stable.

Based on the selected measured endpoints, the exposure experiments performed in this study with d-limonene, ozone alone and d-limonene-ozone mixture did not produce cytotoxic effects on the cellular viability, nor did they induce inflammation or oxidative stress of A549 and differentiated THP-1 macrophage cells as compared to the control experiments. Since the formation of the secondary reaction products has been described to be highly dependent on the relative humidity at which the reaction takes place [461], the effect of the humidity was evaluated by exposing the cells to the reaction mixture obtained at both 50 and 80 % Relative Humidity (RH). Even if lower humidity levels (e.g. 20 %) have been observed to considerably increase the reaction yield [462], in the present study cells were not exposed to such a low relative humidity value due to the risk of affecting the cellular viability by the relative humidity itself.

In a recently published study, where the *in vitro* toxicological analysis of limonene-ozone mixture was carried out in A549 cells, it was found that at the same limonene:ozone ratio (5 : 1) but at various concentrations, the toxicological outcomes induced by the limonene-ozone reaction on A549 cells was different. A significant decrease in the secretion of MCP-1 and increase of IL-8 was produced when cells were exposed to 111 mg m<sup>-3</sup> (20 ppmv) of limonene in presence of 4 ppmv of ozone after 1 and 4 hours respectively, while no changes in IL-8 production were identified when A549 cells were exposed to 2.8 mg m<sup>-3</sup> (500 ppbv) of limonene in presence of 0.196 mg m<sup>-3</sup> (100 ppbv) of ozone. Based on Anderson's findings, different approaches in the experimental set-up were applied within this study. First of all, no synchronisation of A549 cell culture was considered in the present research, since this procedure does not reflect the real status of cells within the human body. Additionally, the serum-free medium could alter the cellular responses [463]. Cytotoxic effects of a different d-limonene-ozone ratio were tested on A549 cells and differentiated THP-1 cells, selecting d-limonene and ozone concentrations that were measured in real world settings. The selection of A549 cells was considered as a reference point for comparison with Anderson's studies, while macrophage differentiated THP-1 cells were chosen, since they are in direct contact with A549 cells in the human body, and aid in removing toxic compounds. However, more biological endpoints than in the Anderson study such as membrane damage and the anti-oxidant defence mechanism (variation of intracellular glutathione levels) were carried out. Additionally, the characterisation of the generated atmosphere was reported here, giving an idea of the secondary reaction product concentrations formed during d-limonene-ozone reaction when using a d-limonene : ozone ratio of 2:1.

### 3.3.2 Assessment of cytotoxic effects of the mixture of 4-OPA, 4-AMCH, IPOH in presence and absence of ozone on human lung cells (A549 and 16HBE14o-)

Due to the unavailability of commercially prepared gas cylinders containing the test chemicals as gas phase, an in-house preparation/volatilisation of the chemicals as gas phase was achieved in Tedlar bags. Thereafter, the human lung cells exposed to the gas mixture of 4-OPA, IPOH, 4-AMCH directly at the air/liquid interface was possible by adapting the *in vitro* CULTEX system to two Tedlar bags: one refilled with the chemical mixture and the other one refilled with Clean/Zero Air.

The chemical's concentration used in this *in vitro* exposure experiments was selected based on the chemicals ratio previously determined in a real world setting, where after the use of a cleaning kitchen products, IPOH was found to be the most predominant chemical (~86 %), followed by 4-OPA (~13 %) and 4-AMCH (~1 %).

Considering the presence of ozone in indoor environments (e.g. various types of electronic equipment), the mixture of 4-OPA, IPOH and 4-AMCH was tested both in presence and in the absence of ozone.

Thereafter, the human lung cells – alveolar (A549) and bronchial (16HBE14o-) – exposure to the gas mixture of 4-OPA, IPOH, 4-AMCH directly at the air/liquid interface was made possible by adapting the *in vitro* CULTEX system to two Tedlar bags: one filled with the chemical mixture and the other one was filled with Zero Air (called also Clean air), when cells were exposed to the mixture of 4-OPA, IPOH, 4-AMCH in absence of ozone. In the case of cells exposed to the mixture in presence of ozone, the reference Tedlar bag was filled with Clean / Zero Air containing ozone.

#### Verification of target concentration of test compounds

**Table 27** A and B shows the total amount of the individual d-limonene ozonolysis products, 4-OPA, 4-AMCH and IPOH to which cells were exposed at 2 mL min<sup>-1</sup> during 1 and 2 hours. As indicated by the ozone analyzer, the ozone concentration detected before running the *in vitro* exposure had a starting value between 50 to 60 ppbv, while post *in vitro* exposure the ozone concentration was between 20 to 30 ppbv.

**Table 27** Total amount [ $\mu\text{g}$ ] of target chemicals IPOH, 4-OPA and 4-AMCH in absence (**Table 27 A**) and presence (**Table 27 B**) of ozone which was delivered to both A549 and 16HBE14o- cells exposed within CULTEX for 1 and 2 hours ( $n = 3 \pm \text{SD}$ ). The data presented in this table were not corrected according to the results obtained with the recovery tests regarding the target chemicals.

**A.**

Mixture in absence of ozone (Tedlar bag)					
Chemicals	Concentration $\mu\text{g m}^{-3}$			Total amount [ $\mu\text{g}$ ] delivered to cells	
	Run 1	Run 2	Run 3	1 hour	2 hours
IPOH	27.500	27.000	27.500	$3.3 \pm 0.03$	6.6
4-AMCH	333	333	340	$0.04 \pm 0.0006$	0.08
4-OPA	4100	3900	4100	$0.49 \pm 0.01$	1

**B.**

Mixture in presence of ozone (Tedlar bag)					
Chemicals	Concentration $\mu\text{g m}^{-3}$			Total amount [ $\mu\text{g}$ ] delivered to cells	
	Run 1	Run 2	Run 3	1 hour	2 hours
IPOH	47.500	48.100	47.200	$5.7 \pm 0.05$	11.4
4-OPA	6667	6500	6700	$0.8 \pm 0.01$	1.6
4-AMCH	833	833	800	$0.1 \pm 0.002$	0.2

Based on the fact that a 70 kg adult is assumed to inhale  $20 \text{ m}^3$  of air per day [170], and considering the total amount of chemicals to which cells were exposed for 1 and 2 hours, the *in vivo* time necessary for an adult to inhale the same quantity of chemicals to which cells were exposed was predicted (by calculation). Therefore, when cells are exposed for 1 or 2 hours to the chemicals amount mentioned above, an adult inhales approximately the same quantity in 15 or 30 minutes.

### Recovery tests of 4-OPA, IPOH, 4-AMCH

As presented in **Table 28**, outcomes showed a good recovery for 4-OPA and 4-AMCH, 91.5 % respectively 82.5 %, while a slight sink effect has been observed for the chemical compound IPOH, which showed only a value of 55.9 % for the recovery test.

**Table 28** Recovery values obtained from Tenax tubes collected from the inlet line (the gas atmosphere was immediately sampled before being distributed to the human cells).

Compounds	Target concentration [ $\mu\text{g L}^{-1}$ ]	Recovery % (samples front)
<b>4-OPA</b>	6.8	91.5 $\pm$ 10.8
<b>4-AMCH</b>	1.6	82.5 $\pm$ 0.5
<b>IPOH</b>	43.7	55.9 $\pm$ 4.1

In order to understand the slight sink phenomenon observed in case of IPOH, future work should also include tests on film type (polyethylene terephthalate), film reactivity etc.

Cytotoxic effects induced by the mixture of the test compounds in absence of ozone, on both cell lines, were first measured in terms of loss of cell viability. The effects of the mixture on cellular viability were expressed as a percentage of cellular viability compared to the cells exposed to Clean air. Cell viability was significantly reduced in a time-dependent manner after exposure of bronchial cells (16HBE14o-) as follows: After 1 hour exposure of human bronchial cells to the mixture, significant cell viability reduction was observed of around 8 % (7.9  $\pm$  1.08), with a p value less than 0.05. A longer exposure (2 hours) of the bronchial cells to the mixture resulted in a higher reduction of cell viability to less than 20 % (20.23  $\pm$  1.25) compared to cells exposed to clean air (control), with a p value less than 0.01. On the contrary, the exposure of alveolar cells (A549) to the same mixture showed no significant difference versus control (see **Figure 69 A-B**).

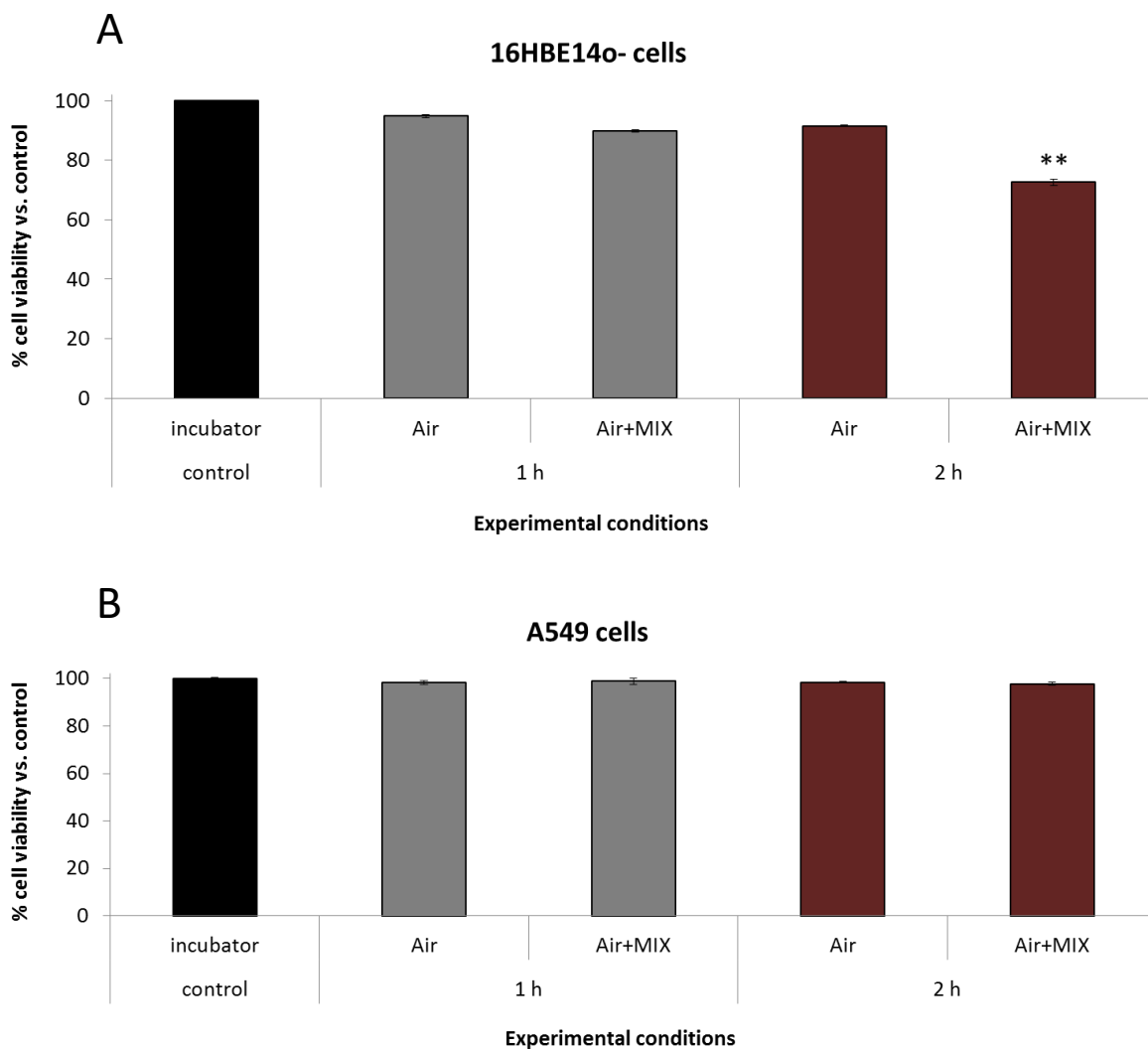


**Figure 69** Evaluation of cellular viability of pulmonary cells exposed to the mixture of 4-OPA + IPOH + 4-AMCH for 1 and 2 hours. **A.** 16HBE14o- cells; **B.** A549 cells (n = 9 ±SD, significance of t-test, \* p < 0.05, \*\* p < 0.01))

The effects of the mixture of 4-OPA + IPOH + 4-AMCH in presence of ozone produce slightly different results compared to the cytotoxic effects of the mixture alone.

As shown in **Figure 69**, the cellular viability of bronchial cells was altered only after 2 hours of exposure (20.6 % ± 0.21), while the mixture in presence of ozone had no effect on the cellular viability of A549 (**Figure 70 A-B**).

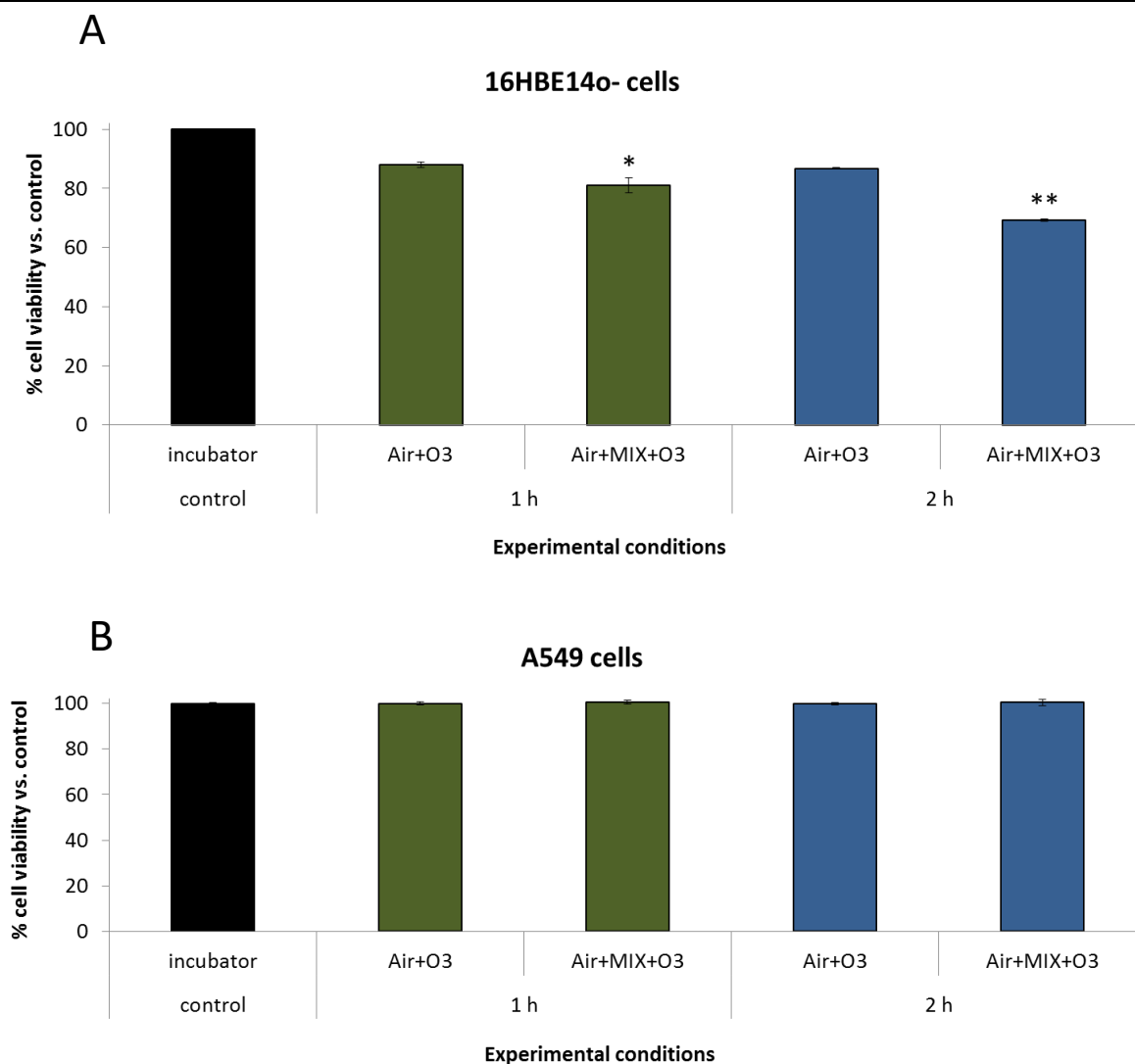
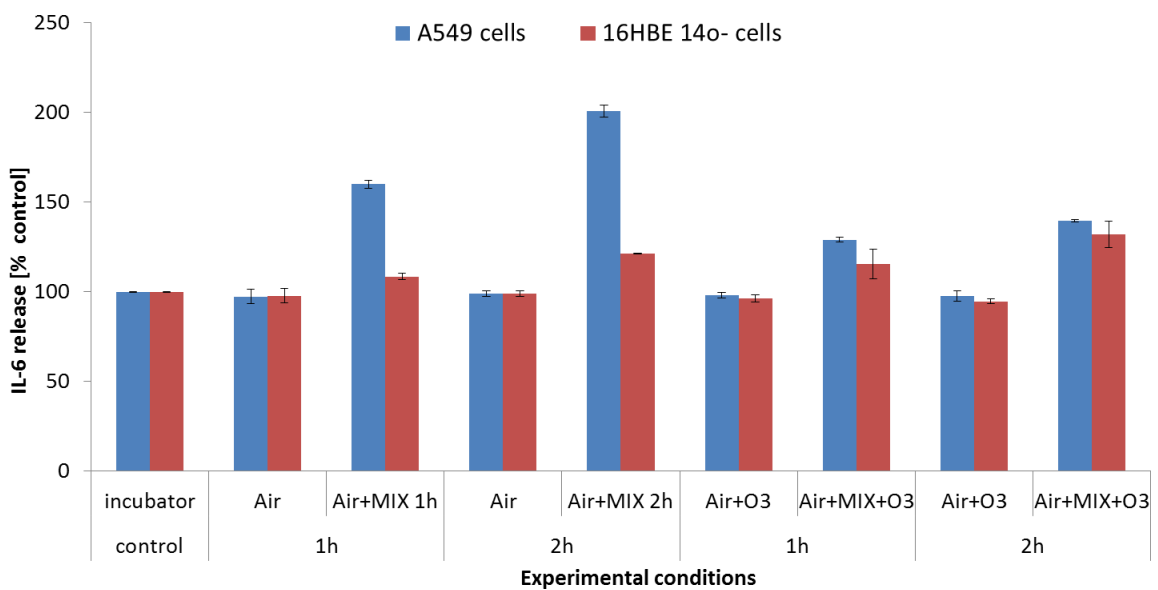
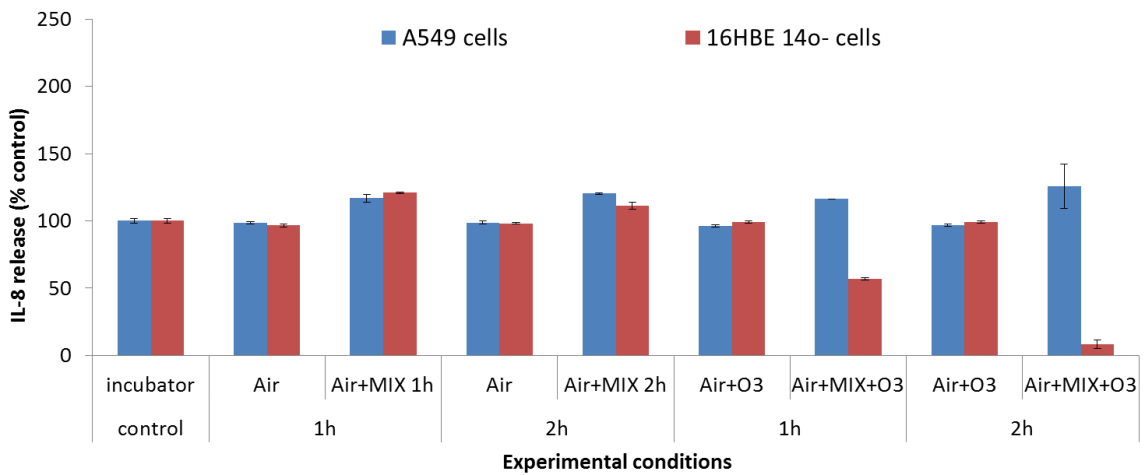
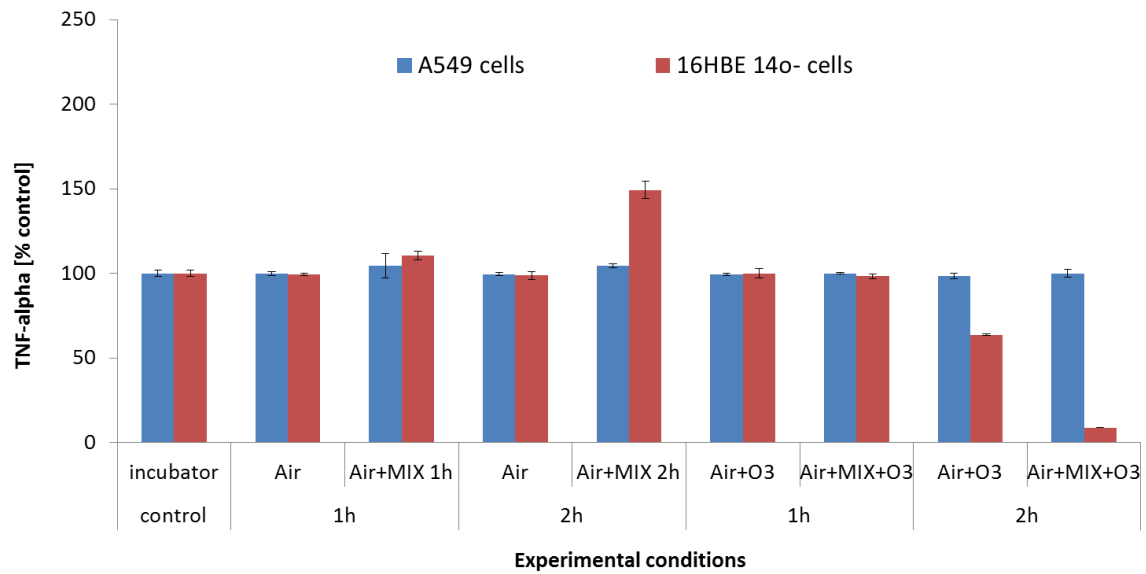


**Figure 70** Evaluation of cellular viability of pulmonary cells exposed for 1 and 2 hours to the mixture of 4-OPA + IPOH + 4-AMCH in presence of ozone. **A.** 16HBE14o- cells; **B.** A549 cells. The effects of (n=9 ± SD, significance of t-test, \*\* p < 0.01)

Different cytokines such as IL-6, IL-8, TNF-alpha, RANTES, IL-15, IL-4 were selected since they play a key role in the development of the allergic inflammatory responses at the pulmonary level [67].

**Figure 71** shows the percentage of the selected cytokines released 24 hours after both type of cells (A549 and 16HBE14o-) were exposed to the mixture of 4-OPA + IPOH + 4-AMCH in presence and in absence of ozone.

## Results and Discussion



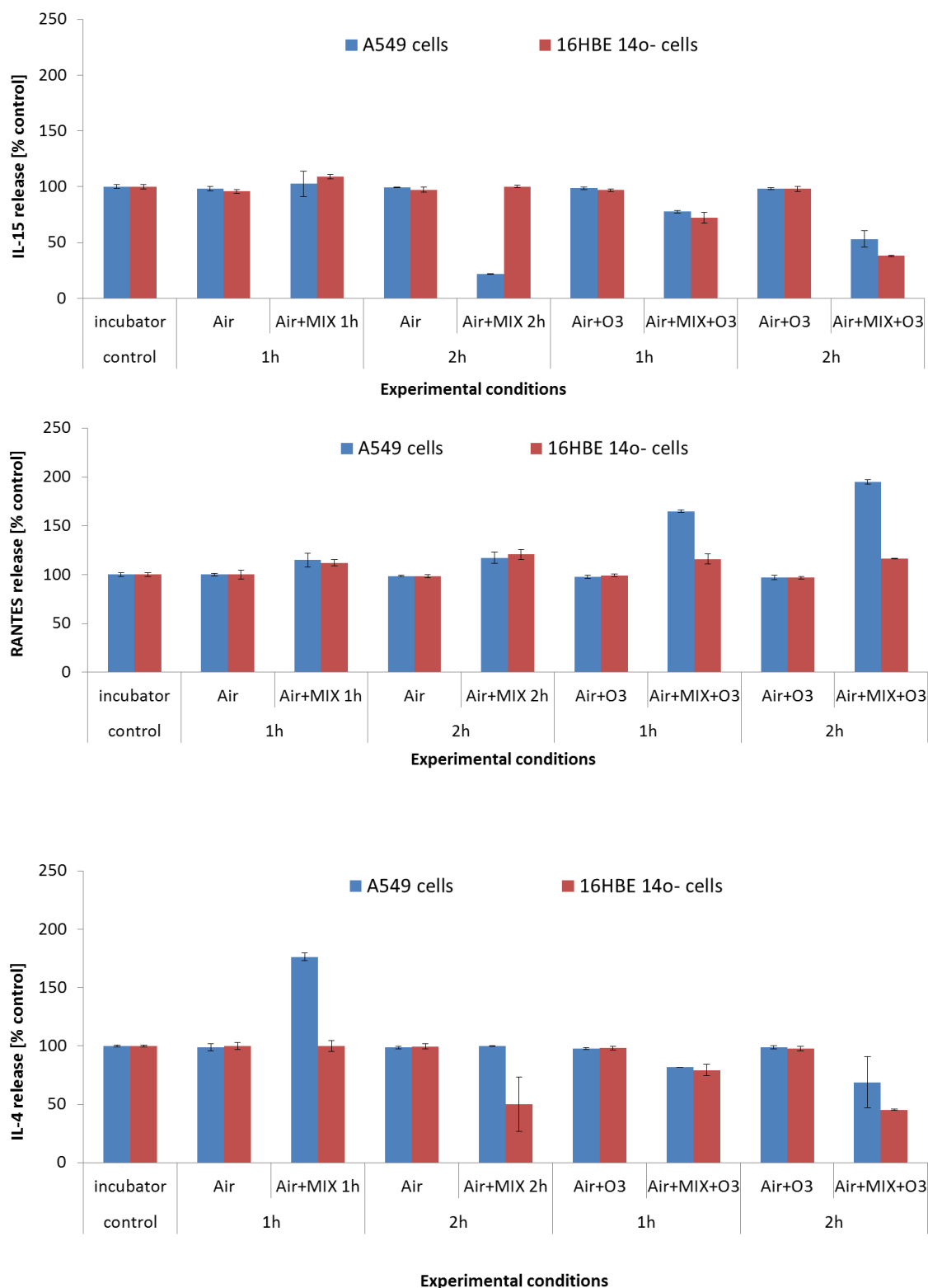


**Figure 71** Determination of IL-6, IL-8, TNF-alpha, RANTES, IL-15, IL-4 release in the medium of A549 and 16HBE14o- cells exposed to the mixture of 4-OPA + IPOH + 4-AMCH in absence and in presence of ozone (noted in the figure as Air+MIX + O3).

The results are expressed as the percentage  $\pm$  SD of each cytokine released into the culture medium compared to control cells. Each experiment was repeated at least three times and each exposure condition had three replicates.

A significant increase of IL-6 level was observed only for the alveolar cells exposed to the mixture of 4-OPA + IPOH + 4-AMCH. After 1 hour exposure, IL-6 released in the medium of A549 cells showed a minimum of 1.5-fold increase, while after 2 hours exposure, the IL-6 levels increased 2 times more than those found in the controls. The addition of ozone to the mixture determined a significant decrease in the level of IL-6 compared to the mixture alone. A549 cells exposed to the mixture in presence of ozone showed just a 1.2-fold increase after 1 hour and 1.4-fold after 2 hours. However, both exposure conditions (mixture alone and mixture in presence of ozone) produced a statistically significant amount of IL-6 in A549 cells ( $p < 0.05$ ). In contrast, the bronchial cells had an opposite effect. A significant decrease in IL-6 level was observed only after 2 hours exposure of 16HBE14o- to the mixture alone (1.3-fold  $\pm$  0.2) since after 1 hour exposure no statistically significant amount of IL-6 was secreted compared to control. In the case of cells exposed to the mixture with ozone, the exposure time effect showed a decreasing trend in IL-6 as follows: 1.7-fold and 8.2-fold decrease after 1, respectively 2 hours.

Quantification of IL-8 levels released in culture medium of A549 cells exposed to mixture in presence/absence of ozone, gave higher levels of IL-8 compared with those produced by cells exposed to Clean air. As shown in **Figure 71**, the amount of secreted IL-8 was 1.14-times higher when cells were exposed for 1 hour. A time dependent effect was observed also here since after 2 hours exposure, a statistically significant amount of IL-8 was released (from 1.14-fold to approximately 1.25-fold) with a value less than 0.05. Regarding the IL-8 amount secreted by bronchial cells, only after 1 hour's exposure to the mixture alone, the IL-8 level was increased to 1.2-times compared to control. A pronounced decrease in IL-8 was found when 16HBE14o- cells were exposed for 2 hours to the mixture in presence of ozone (8.2-fold  $\pm$  10.2). A similar trend, as in the case of IL-6 release, was obtained for IL-8, when cells were exposed for 1 and 2 hours to the mixture with ozone. However, the concentrations of these interleukines were different: IL-6 was found to be approximately  $319.5 \text{ pg mL}^{-1} \pm 10.3$  and  $69.65 \text{ pg mL}^{-1} \pm 10.2$  (1 and 2 hours to mixture with ozone); while IL-8 was  $1419.5 \text{ pg mL}^{-1} \pm 0.78$  and  $206.5 \text{ pg mL}^{-1} \pm 3.36$  (1 and 2 hours to mixture with ozone). Both IL-6 and IL-8 are often described in the literature as being involved in the inflammatory process at the lung level [208, 464]. Earlier studies have shown a correlation between elevated IL-8 and IL-6 when A549 was exposed to 4-OPA alone at air/liquid interface. After 4-hours of exposure of A549 cells to a concentration of  $61\ 420 \text{ } \mu\text{g m}^{-3}$  (15 ppmv) of 4-OPA induced a 32-fold change in IL-6 and 14-fold change in

IL-8 levels. Other *in vitro* studies carried out for 4-OPA suggest that its potential toxicity could lead to skin and lip dryness [165]. In reviewing the literature, no data was found on the association of cytokines released induced by the mixture of 4-OPA + IPOH + 4-AMCH in presence / absence of ozone in human pulmonary cells.

It is interesting to note that a statistically significant increase of TNF-alpha (aprox. 1.5-fold change) was determined in bronchial cells exposed to the mixture alone for 2 hours. These results could be associated with the results obtained with cellular viability assay, indicating that the increased release of TNF-alpha could induce cell death (apoptosis) in the bronchial cells. The results showed a decreased tendency when cells were exposed to mixture with ozone. The increases of TNF-alpha levels were not significant in A549 cells when compared to control in any of the exposure conditions. Data from different studies have demonstrated that TNF-alpha has pro-inflammatory and pro-oxidative actions [224]. Research carried out in transgenic mice has identified that TNF-alpha depleted cellular glutathione levels [224]. Additionally, it has been revealed in both *in vitro* and *in vivo* studies that TNF-alpha induced oxidative stress in cells by generating subcellular ROS formation followed by the activation of pro-inflammatory molecules [465]. Recent studies indicate that TNF-alpha treatment in neuronal cells induced cell death (apoptosis) [466].

The results showed that IL-15 levels in both alveolar and bronchial cells are slightly increasing after 1 hour exposure of cells to the mixture alone (1.2-fold change) while the amount of IL-15 is decreasing in a time-dependent manner when both type of cells were exposed to the mixture in presence of ozone and in the case of alveolar cells exposed for 2 hours to the mixture alone. It has been demonstrated that the overexpression of IL-15 in peritoneal adherent cells from mice inhibited apoptosis [467]. Contrary to the above mentioned study, the IL-15 levels were drastically decreasing (21-fold change for A549 cells exposed to the mixture for 2 hours and 77- and 53-fold change when A549 cells were exposed to the mixture in presence of ozone for 1 and 2 hours respectively). A down-regulation of IL-15 was observed in 16HBE14o- cells after their exposure only to the mixture in presence of ozone (72-and 38-fold change after 1 and 2 hours exposure). These findings might be a sign of cellular apoptosis, but further studies are needed to confirm this hypothesis.

The last chart of **Figure 71** shows an inhibition of IL-4 level in a time-dependent manner in bronchial cells exposed to mixture in presence/absence of ozone. Alveolar cells produced higher amounts of IL-4 only after 1 hour exposure to the mixture alone (approximately 1,8-fold), while after 2 hours no statistically significant effect on IL-4 release was noticed. A similar decreased tendency in IL-4 amount was obtained for both alveolar and bronchial cells after 1 hour exposure to the mixture with ozone. According to literature, IL-4 plays an

important role in the pathogenesis of allergic asthma [468] and it was also shown that at concentrations of  $8040 \text{ pg mL}^{-1}$  it induces apoptosis in A549 cells [469]. However, the concentrations found within this study, where A549 cells were exposed to the mixture alone, were lower ( $1.64 \text{ pg mL}^{-1}$ ) compared to the data literature and as indicated in the study above did not alter the cellular viability.

The difference between the A549 and 16HBE14o- cells to increase or inhibit the secretion of different selected cytokines could be explained by the fact that the A549 cell has a malignant phenotype (being a carcinoma cell line) while the phenotype of 16HBE14o- cells is similar to the normal bronchial epithelial cells.

The present study considered the relationship between oxidative stress and inflammation [470], therefore the oxidative stress was investigated by the quantification of intracellular glutathione content in both bronchial (16HBE14o-) and alveolar (A549) cells exposed to mixture in presence/absence of ozone.

Bronchial cells (16HBE14o-) exposed to the mixture of 4-OPA + IPOH + 4-AMCH showed a time-dependent marked decrease in GSH / GSSG ratio, as follows: 13.4 (decrease of 8 %, after 1 hour) and 12.6 (decrease of 13.7 %, after 2 hours), compared to 14.6 for GSH / GSSG ratio of untreated cells, while the GSH / GSNO ratio corresponded to 7.2 (after 1 hour) and 12 (after 2 hours) in relation to the GSH / GSSG and GSH / GSNO ratio of cells exposed to clean air.

Exposure of bronchial cells to the mixture in presence of ozone also caused a decrease in the GSH/GSSG ratio: 12.8 (decrease of 12.3 % after 1 hour) and 12.2 (decrease of 16.5 %, after 2 hours exposure), with fold-changes statistically different on time-exposure ( $p < 0.05$ ). In addition, a lower fold-change in the ratio of GSH / GSSG followed by an augmented fold change in the ratio of GSH / GSNO was noticed when compared to the fold change observed in cells exposed to the mixture alone ( $p < 0.05$ ).

Exposure of alveolar cells (A549 cells) to mixture in presence or absence of ozone did not lead to statistically significant changes in the intracellular reduced/oxidised (GSH / GSSG) and reduced/nitroso (GSH / GSNO) glutathione species ratios when compared to control values (cell exposed to clean air with/without ozone).

In this study, the potential oxidative stress impact of 4-OPA + IPOH + 4-AMCH in presence/absence of ozone on both bronchial (16HBE14o-) and alveolar (A549) cell lines was evaluated by measuring the intracellular levels of reduced, oxidised and nitroso-glutathione forms. These findings are significant as they suggest that bronchial cells exposed to both mixture alone and mixture with ozone, significantly decrease the GSH levels leading to the formation of GSSG and GSNO. No significant reduction in GSH levels was found in the alveolar cells post-exposure to mixture in presence or absence of ozone.

This is the first study which investigates the toxicological effects of 4-OPA, IPOH, 4-AMCH as a mixture in presence and absence of ozone on human pulmonary cell lines. Previously, only one *in vivo* study has been carried out, where the respiratory effects of 4-OPA, IPOH, 4-AMCH, as individual compounds, were investigated in a head out mouse bioassay [423]. Based on the different parameters investigated, such as time of brake (TB), time of inspiration / expiration (TI / TE) and mild expiratory flow rate, the authors reported that IPOH might be classified as a sensory irritant as observed by the elongation of TB, and with an estimated no observed (adverse) effect level (NO(A)EL) of around 1.6 ppmv, while for 4-AMCH, the NOEL for sensory irritation was established to be around 13 ppmv. Mice exposed to 4-OPA presented a complex cascade of effects such as airflow limitation, sensory and pulmonary irritation, with an estimate for sensory irritation of around 3.4 ppmv. Moreover, based on the sensory irritation thresholds determined in mice, the authors considered an assessment factor of 2 to calculate the NOAEL in humans by extrapolating the lowest-observed (adverse) effect level experimentally determined in mice. Thus, the calculated human reference values of IPOH, 4-AMCH and 4-OPA was found to be 1100  $\mu\text{g m}^{-3}$  (0.16 ppmv), 7350  $\mu\text{g m}^{-3}$  (1.3 ppmv) and 5320  $\mu\text{g m}^{-3}$  (1.3 ppmv) respectively. In conclusion, the authors highlight the need for indoor/ambient exposure data, especially for IPOH and 4-OPA, since measurements of these compounds in offices have not been reported.

The present study differs from the head out mouse bioassay in that: i) biological effects were investigated at two specific target lung sites: bronchial and alveolar region; ii) each cell line selected (A549 and 16HBE14o-) was analysed under controlled conditions; iii) both cell lines were exposed to the mixture of 4-OPA + IPOH + 4-AMCH in presence / absence of ozone within environmental relevant concentration levels. Based on the total amount of each compound that an adult could inhale per day (8 hours), and according to the 4-OPA, IPOH, 4-AMCH ratios identified in real world settings, human lung cells were exposed to the air/liquid interface within CULTEX for 1 and 2 hours. This time exposure corresponds to the total amount of chemicals that humans could inhale within 30 minutes (when cells were exposed to chemicals for 1 hour) and 1 hour (when cells were exposed to chemicals for 2 hours).

Although the toxicological effects of individual tested compounds have been studied *in vivo*, as mentioned in the above study, much less is known about their potential toxicity in the human lung. There have been a few studies in which the biological effects (in terms of inflammation potency) of 4-OPA on A549 cells was assessed by the use of an air/liquid *in vitro* device [164], but *in vitro* exposure-related biological effects for the mixture of the selected d-limonene ozonolysis is lacking.

The originality of the current study lays in the demonstration that the mixture of the tested compounds both in presence/absence of ozone induces a marked decrease in cell viability, statistically significant secretion of various pro-inflammatory cytokines and perturbation of the anti-oxidant mechanism defense in both human pulmonary cell lines. However, the cytotoxic effects observed in bronchial cells suggest that the mixture of these compounds has a great impact on the airway epithelium of the bronchi rather than on the airway epithelium of the alveoli.

## 4. CONCLUSION

For the present thesis, state-of-the-art experimental methods have been applied, new methods are developed and optimized to investigate *in vitro* cytotoxic effects on selected human lung cells: bronchial (16HBE14o- cells); alveolar (A549 cells) and activated macrophages (THP-1) and human cryopreserved blood after exposure to the common indoor air pollutants d-limonene, ozone and their reaction products 4-oxopentanal (4-OPA), 3-isopropenyl-6-oxoheptanal (IPOH) and 4-acetyl-1-methyl-1-cyclohexene (4-AMCH) as individual compounds and mixtures.

When tested on human bronchial and alveolar cell lines by direct dilution into the cell culture medium, d-limonene alone did not induce any alterations in the cell functions concerning cell viability (e.g. measurement of lysosome damage), inflammatory response (e.g. variation in pro-inflammatory cytokines secretion such as IL-6, IL-8) or oxidative stress (e.g. variation of intracellular reactive oxygen/nitrogen species (ROS / RNS) and intracellular glutathione levels). On the contrary, 4-OPA and IPOH, AMCH tested individually or as mixtures caused a wide range of cytotoxic effects such as: **(1)** damage of lysosomes observed in both bronchial and alveolar cells; **(2)** induction of higher levels of intracellular reactive oxygen/nitrogen species, especially in bronchial cells exposed to IPOH; **(3)** perturbation of the anti-oxidative defense balance between reduced glutathione form (GSH) and nitroso- glutathione form (GSNO) or oxidative glutathione form (GSSG), especially in alveolar cells when exposed to IPOH and in bronchial cells when exposed to both IPOH and 4-OPA; **(4)** induction of pro-inflammatory cytokines (e.g. IL-6, IL-8) which was predominant in bronchial cells than in alveolar cells when exposed to 4-OPA and IPOH.

Among the tested compounds, IPOH has proven to have the strongest potency for induction of ROS/RNS (e.g. the formation of ROS/RNS in bronchial cells exposed to 500  $\mu$ M of IPOH was approximately 2-times higher when compared to the ROS / RNS levels measured in bronchial cells exposed to 4-OPA and 5-times higher than the ROS / RNS levels measured in bronchial cells exposed to 4-AMCH) and for induction of the cytokines IL-6 and IL-8 whereas 4-OPA demonstrated the strongest cell viability destruction with a  $LC_{50}$  at 1.6 mM (compared to 3.5 mM for IPOH and at least 5.8 mM for 4-AMCH). Exposure of bronchial cells to high concentrations levels (50  $\mu$ M) of 4-OPA showed a down-regulation of IL-6 (80-fold change) and IL-8 (61-fold change) when compared to untreated cells. On the other hand, IPOH (50  $\mu$ M) induced an increase of both IL-6 and IL-8 secretion in bronchial cells (2.8-fold change and 7.0-fold change respectively), which indicates that the deleterious effect of IPOH is higher in the bronchial cells than in the

## Conclusion

---

alveolar cells. Concerning the inflammatory effects of 4-AMCH on bronchial cells, only at lower tested concentration (1.5  $\mu$ M), both IL-6 and IL-8 levels were up-regulated (2-fold change higher than the cells untreated), while at higher concentration (50  $\mu$ M) the effects observed were the opposite (e.g. both IL-6 and IL-8 were 5-times down-regulated).

The fast screening metabolomics analysis carried out on alveolar (A549) cells exposed to the mixture of IPOH, 4-OPA and 4-AMCH showed a significant perturbation on their survival cellular processes ( $p < 0.5$ ). The biological effects observed (e.g. 10% loss of the cellular viability when compared to untreated cells) are the consequence of cell treatments with the selected mixture and probably the formation of their related metabolites present in both cellular medium and cellular extracts.

After exposing the alveolar (A549) and the activated macrophages (THP-1) cells to a mixture of d-limonene (0.02, 0.5 and 2.5 ppmv) and ozone (70 ppbv) alone as well as d-limonene-ozone mixture at realistic concentrations (e.g. 0.02 ppmv and 70 ppbv) in the gas phase, the results indicated that no statistically significant differences in cell viability, inflammation and intracellular glutathione content occurred, neither in alveolar (A549) nor in the activated macrophage (THP-1) cell lines, when compared to cells exposed to clean air, used as control. Under these experimental conditions, when alveolar and macrophages cell lines were exposed for 1 and 2 hours to d-limonene and ozone mixture, it can be concluded that the d-limonene-ozone mixture at realistic concentration levels cannot be considered as a potential health concern when in contact with the human alveolar compartment or with the macrophages.

From research that was performed with the liquid/liquid exposure method and by comparing both the human pulmonary cell lines used (bronchial and alveolar), it can be concluded that:

- the bronchial cells showed a more sensitive reaction than the alveolar cells in terms of loss of cell viability, when comparing their lowest observable effect concentration (LOEC) which causes statistically significant loss of cellular viability from the untreated cells (e.g. LOEC observed for bronchial cells exposed to IPOH was approximately 0.5 mM, while for alveolar cells it was approximately 1 mM);
- it appears that in the bronchial cell line, the formation of intracellular reactive oxygen/nitrogen species (ROS / RNS) is 2-times higher than in alveolar cell line after their exposure to the targeted chemicals;
- a 3.3-fold change of oxidative- glutathione form was measured in bronchial cells exposed to IPOH when compared to the levels found in alveolar cells;
- early toxicity such as inflammation measured by various types of cytokines was identified to be greater in bronchial cells than in alveolar cells (e.g. levels of IL-6 were found to be 2

times higher in 16HBE14o- than in A549 cells treated with a mixture of compounds [1.5  $\mu\text{M}$ ]).

The possible cytotoxic effects of a gas mixture of IPOH, 4-OPA and 4-AMCH on human bronchial and alveolar cell lines were evaluated in both presence and absence of ozone. From the outcome of this investigation, it can be concluded that the mixture prepared at concentration ratios based on a realistic scenario (e.g. concentrations relevant indoors: IPOH [16  $\mu\text{g m}^{-3}$ ], 4-OPA [2.5  $\mu\text{g m}^{-3}$ ], 4-AMCH [0.2  $\mu\text{g m}^{-3}$ ]) was found to cause a time-dependent effect on bronchial cellular viability (e.g. around 8 % loss of cell viability after cells were exposed to this mixture in absence of ozone for 1 hour and approximately 20 % when cells were exposed for 2 hours to both experimental conditions: the mixture with and without ozone); in alveolar cells, after their exposure to the mixture in absence of ozone, a statistically significant increase in IL-8 (e.g. 1.3-fold change after 2 hours exposure,  $p < 0.05$ ) and IL-6 levels (e.g. 2-fold change after 2 hours exposure,  $p < 0.01$ ) which indicates an inflammatory potential; and in bronchial cells exposed to the mixture in absence of ozone, a time-dependent decrease of GSH/GSSG ratio [e.g. 13.4 (after 1 hour) and 12.2 (after 2 hours)], correlated with the capacity of the mixture to induce oxidative stress.

Based on the Air-Liquid exposure outcomes, major conclusions regarding the comparison of bronchial and alveolar cells are as follows:

- no significant difference on cell viability of A549 cells exposed to the gas mixture was noticed when compared to the untreated cells, while bronchial cells lost 20% of cellular viability, indicating that bronchial cells are more sensitive than the alveolar cells, in terms of cellular viability;

- concerning the IL-6, a biomarker predicting Chronic Obstructive Pulmonary Disease (COPD), an increase of IL-6 levels was determined (1.5-fold change) in alveolar cells exposed to the gas mixture, while in the case of bronchial cells no statistically significant amount of IL-6 was determined when compared to control (cells exposed to clean air);

- on the other hand, a 1.5-fold change increase in secretion of TNF-alpha (a biomarker that plays a role in apoptosis induction) was measured only in bronchial cells exposed for 2 hours to the gas mixture, while the TNF-alpha levels in alveolar cells were not statistically different from the control.

Results of the experiments carried out with human cryopreserved blood incubated with d-limonene at its highest soluble concentration in the cell culture medium (100  $\mu\text{M}$ ) did not show any increase of interleukin-1 beta (IL-1 beta) activity, known as a cytokine biomarker for human inflammatory capacity (e.g. fever induction). Similar findings were demonstrated for 4-OPA IPOH and 4-AMCH at a concentration of 2  $\mu\text{M}$ . On the contrary, at higher concentrations (up to 500  $\mu\text{M}$ ) the three tested d-limonene ozonolysis products induced a concentration-dependent increase of IL-1 beta.

## 5. Outlook

Following the results obtained, further studies on this issue would be of interest, as follows:

The application of new methodologies such as metabolomics and proteomics could be of benefit to gain knowledge about possible pathological processes that the selected d-limonene ozonolysis products IPOH, 4-OPA and 4-AMCH can induce at the molecular level.

Similarly to the present work, other common abundant terpenes present in consumer products (e.g. linalool) would be of interest to be tested not only as a single compound but also in combination with strong oxidants present in the environment such as ozone that might lead to formation of toxicologically relevant products.

Additionally, it would be interesting to monitor the concentration of IPOH, 4-OPA and 4-AMCH formed during normal use of a wide range of consumer products (e.g. air fresheners, detergents etc.) in order to evaluate their accumulation in indoor spaces and the potential health effects in humans after exposure.

## 6. BIBLIOGRAPHY

1. Robinson J.P., Converse P.E., Szalai A., „Everyday life in twelve countries”, In A. Szalai (Ed.), “The Use of Time: Daily Activities of Urban and Suburban Populations in Twelve Countries Mouton”, The Hague, 1972, pp. 112–144;
2. Klepeis N. E., Nelson W. C., Ott W. R., Robinson J. P., Tsang A. M., Switzer P., Behar J. V., Hern S. C., Engelmann W. H., „The national human activity pattern survey (NHAPS): A resource for assessing exposure to environment pollutants”, *J. Expo. Anal. Env. Epid.*, 2001, 11, 3, pp. 231-252;
3. U.S. Environmental Protection Agency, „The total exposure assessment methodology (TEAM) study: summary and analysis”, 1987, EPA/600/6-87/002a. Washington, DC;
4. Daisey J.M., Hodgson, A.T., Fisk W.J., Mendell M.J., Brinke J.T., „Volatile organic compounds in twelve California office buildings: classes, concentrations and sources”, *Atmospheric Environment*, 1994, 28, pp. 3557-62;
5. Daisey J.M., Angell W.J., Apte M.G., „Indoor air quality, ventilation and health symptoms in schools: an analysis of existing information”, *Indoor air*, 2003, pp. 53-64;
6. Bone A., Murray V., Myers I., Dengel A., Crump D., „Will drivers for home energy efficiency harm occupant health?”, *Perspectives in Public Health*, 2010, 130, 5, pp. 233-238;
7. Viegi G., Maio S., Pistelli F., Baldacci S., Carrozzi L., „Epidemiology of chronic obstructive pulmonary disease: Health effects of air pollution”, *Respiratory*, 2006, 11, pp. 523-532;
8. World Health Organisation, *World Health Statistics - full report*, 2008, ISBN 978 92 4 0682740 (electronic version), <http://www.who.int/whosis/whostat/2008/en/>;
9. Ko F. W. S., Hui D. S. C., „Air pollution and chronic obstructive pulmonary disease”, *Respirology*, 2012, 17, pp. 395-401;
10. Sundell J., Lindvall T., „Indoor Air Humidity and Sensation of Dryness as Risk indicators of Sbs”, *Indoor air*, 2004, 3, 4, pp. 382-390;
11. Norbäck D., „An update on sick building syndrome”, *Curr. Opin. Allergy Clin. Immunol.*, 2009, 9, 1, pp. 55-9;
12. Lu C. Y., Ma Y. C., Lin J. M., Li C. Y., Lin R.S., Sung F.C., „Oxidative stress associated with indoor air pollution and sick building syndrome-related symptoms among office workers in Taiwan”, *Inhalation Toxicology*, 2007, 19, pp. 57-65;
13. World Health Organization, „Prevention of Allergy and Allergic Asthma”, Geneva, 2003, [http://www.worldallergy.org/professional/who\\_paa2003.pdf](http://www.worldallergy.org/professional/who_paa2003.pdf);

14. European Environment and Health Information System, „Prevalence of asthma and allergies in children”, Fact sheet no. 3.1, 2007, [http://www.euro.who.int/\\_\\_data/assets/pdf\\_file/0012/96996/3.1.pdf](http://www.euro.who.int/__data/assets/pdf_file/0012/96996/3.1.pdf);
15. Jaakkola M.S., Jaakkola J.J.K., „Office Work Exposures and Adult-Onset Asthma”, *Environmental Health Perspectives*, 2007, 115, pp. 1007-1011;
16. Kephelopoulos S., Kotzias D., Koistinen K., Carslaw N., Carrer P., Fossati S., Hoffman T., Langer S., Larsen B., Monn C., Nicolas M., Salthammer T., Schlitt C., Winterhalter R., Wolkoff P., „European Collaborative Action Impact of ozone- initiated terpene chemistry on indoor air quality and human health”, Report no 26, 2007, ISBN 978-92-79-07844-6;
17. Bibi H., Shoseyov D., Feigenbaum D., Nir P., Shiachi R., Scharff S., Peled R., „Comparison of positive allergy skin tests among asthmatic children from rural and urban areas living within small geographic area”, *Ann Allergy Asthma Immunol.*, 2002, 88, 4, pp. 416-20;
18. Majkowska–Wojciechowska B., Pełka J., Korzon L., Kozłowska A., Kaczała M., Jarzebska M., Gwardys T., Kowalski M. L., „Prevalence of allergy, patterns of allergic sensitization and allergy risk factors in rural and urban children”, *Allergy*, 2007, 62, pp. 1044-1050;
19. Andersson K., „Indoor climate and health: What do we really know?”, *Indoor Air*, 2008, 17-22, Copenhagen, Denmark, Paper ID: We9K1, [https://www.ust.is/library/Skrar/Atvinnulif/Hollustuhaettir/Mygla/Indoor\\_climate\\_and\\_health\\_Kjell.pdf](https://www.ust.is/library/Skrar/Atvinnulif/Hollustuhaettir/Mygla/Indoor_climate_and_health_Kjell.pdf);
20. Jaakkola M.S., Jaakkola J.J.K., „Office Work Exposures and Adult-Onset Asthma”, *Environmental Health, Perspectives*, 2007, 115, pp. 1007-1011;
21. Marraccini P., Farioli L., Pagani A., Rossi L., Russignaga D., Parmiani S., „Indoor allergens in office. Evaluation of the work station”, *G Ital Med Lav Ergon.*, 2004, 26, 2, pp. 97-101;
22. Bibi H., Shoseyov D., Feigenbaum D., Nir P., Shiachi R., Scharff S., Peled R., „Comparison of positive allergy skin tests among asthmatic children from rural and urban areas living within small geographic area”, *Annals of Allergy, Asthma and Immunology*, 2002, 88, pp. 416-420;
23. Sundell J., Bornehag C.G., Weschler C.J., Sjsgaard T., Lundgren B., Hasselgren M., Hagerhed-Engmann L., „The association between asthma and allergic symptoms in children and phthalates in house dust: a nested case control study”, *Environmental Health Perspectives*, 2004, 112, pp. 1393-1397;

24. Uzoigwe J. C., Prum T., Bresnahan E., Garelnabi M., „The Emerging Role of Outdoor and Indoor Air Pollution in Cardiovascular Disease”, *N Am J Med Sci.*, 2013, 5, 8, pp. 445–453;
25. Pope C. A., Burnett R. T., Thurston G. D., Thun M. J., Calle E. E., Krewski D., Godleski J. J., „Cardiovascular mortality and long-term exposure to particulate air pollution: Epidemiological evidence of general pathophysiological pathways of disease”, *Circulation*, 2004, 109, pp. 71–7;
26. Pope C. A., Burnett R. T., Thun M. J., Calle E. E., Krewski D., Ito K., Thurston G. D., „Lung cancer, cardiopulmonary mortality, and long-term exposure to fine particulate air pollution”, *JAMA*, 2002, 287, 9, pp. 1132-41;
27. Jin Y., Zhou Z., He G., Wei H., Liu J., Liu F., Tang N., Ying B., Liu Y., Hu G., Wang H., Balakrishnan K., Watson K., Baris E., Ezzati M., „Geographical, spatial, and temporal distributions of multiple indoor air pollutants in four Chinese provinces”, *Environ Sci Technol.*, 2005, 15, 39, 24, pp. 9431-9;
28. Zhang J. J., Smith K. R., „Household air pollution from coal and biomass fuels in China: Measurements, health impacts, and interventions”, *Environ Health Perspect.*, 2007, 115, pp. 848–55;
29. Pryor W. A., Stone K., „Oxidants in cigarette smoke. Radicals, hydrogen peroxide, peroxyxynitrate, and peroxyxynitrite”, *Ann N Y Acad Sci.*, 1993, 686, pp. 12–28;
30. Brook R. D., Rajagopalan S., Pope C. A., Brook J. R., Bhatnagar A., Diez-Roux A. V., Holguin F., Hong Y., Luepker R. V., Mittleman M. A., Peters A., Siscovick D., Smith S. C Jr, Whitsel L., Kaufman J. D., „Particulate matter air pollution and cardiovascular disease: An update to the scientific statement from the American Heart Association”, *Circulation.*, 2010, 1, 121, 21, pp. 2331-78;
31. Delfino R. J., Sioutas C., Malik S., „Potential role of ultrafine particles in associations between airborne particle mass and cardiovascular health”, *Environ Health Perspect.*, 2005, 113, 8, pp. 934-46;
32. EnVIE Co-ordination Action on Indoor Air Quality and Heal the Effects (Project no. SSPE-CT-2004-502671);  
<http://paginas.fe.up.pt/~envie/documents/finalreports/Final%20Reports%20Publishable/EnVIE%20WP1%20Final%20Report.pdf>;
33. Rosenman K. D., Reilly M. J., Schill D. P., Valiante D., Flattery J., Harrison R., Reinisch F., Pechter E., Davis L., Tumpowsky C.M., Filios M., „Cleaning products and work-related asthma”, *J Occup Environ Med.*, 2003, 45, 5, pp. 556-63;
34. Zock J. P., Plana E., Jarvis D., Antó J. M., Kromhout H., Kennedy S. M., Künzli N., Villani S., Olivieri M., Torén K., Radon K., Sunyer J., Dahlman-Hoglund A., Norbäck D.,

- Kogevinas M., „The use of household cleaning sprays and adult asthma: an international longitudinal study”, *Am J Respir Crit Care Med.*, 2007, 15, 176, 8, pp. 735-41;
35. Vandenplas O., D'Alpaos V., Evrard G., Jamart J., Thimpont J., Huaux F., Renauld J.C., „Asthma related to cleaning agents: a clinical insight”, *BMJ Open*, 2013, 3, 9;
36. Bello A., Quinn M. M, Perry M. J, Milton D. K, „Characterization of occupational exposures to cleaning products used for common cleaning tasks-a pilot study of hospital cleaners”, *Environmental Health*, 2009, 8, 11;
37. Quirce S., Barranco P., „Cleaning Agents and Asthma, Cleaning Agents and Asthma”, *J Investig Allergol. Clin Immunol.*, 2010, 20, 7, pp. 542-550;
38. Pechter E., Azaroff L. S., López I., Goldstein-Gelb M., „Reducing Hazardous Cleaning Product Use: A Collaborative Effort”, *Public Health Rep.*, 2009, 124, 1, pp. 45–52;
39. Sherriff A., Farrow A., Golding J., The ALSPAC Study Team, Henderson J., „Frequent use of chemical household products is associated with persistent wheezing in pre-school age children”, *Thorax*, 2006, 60, pp. 45-49;
40. European Chemicals Agency (ECHA), Guidance on information requirements and chemical safety assessment chapter R.8:Characterisation of dose [concentration]-response for human health“, 2012, vs. 2.1, pp. 1-195, [https://echa.europa.eu/documents/10162/13632/information\\_requirements\\_r8\\_en.pdf](https://echa.europa.eu/documents/10162/13632/information_requirements_r8_en.pdf);
41. Kotzias D., Koistinen K., Kephelopoulos S., Schlitt C., Carrer P., Maroni M., Jantunen M., Cochet C., Kirchner S., Lindvall T., McLaughlin J., Molhave L., de Oliveira Fernandes E., Seifert B., „The INDEX project -Critical Appraisal of the Setting and Implementation of Indoor Exposure Limits in the EU”, Final report, 2005, EUR 21590 EN, <http://publications.jrc.ec.europa.eu/repository/bitstream/JRC31622/1622%20-%20INDEX%20%20EUR%2021590%20EN%20report%5B1%5D.pdf>;
42. Gordon C. J., Sasman T. E., Oshiro W. M., Bushnell P. J., „Cardiovascular effects of oral toluene exposure in the rat monitored by radiotelemetry”, *Neurotoxicology and Teratology*, 2007, 29, pp. 228-235;
43. Wolkoff P., Nojgaard J.K., Franck C., Skov P., „The modern office environment desiccates the eyes?”, *Indoor Air*, 2006, 16, 4, pp. 258-265;
44. Wolkoff P., Wilkins C. K., Clausen P. A., Nielsen G. D., „Organic compounds in office environment – sensory irritation, odor, measurements, and the role of reactive chemistry”, *Indoor Air*, 2006, 16, pp. 7–19;
45. World Health Organisation (WHO), „Health aspects of air pollution with particulate matter, ozone and nitrogen dioxide”, 2003, EUR/03/5042688, [http://www.euro.who.int/\\_\\_data/assets/pdf\\_file/0005/112199/E79097.pdf](http://www.euro.who.int/__data/assets/pdf_file/0005/112199/E79097.pdf);

46. European Collaborative Action (ECA), „Impact of ozone- initiated terpene chemistry on indoor air quality and human health”, Report 26, 2007, [http://www.inive.org/medias/ECA/ECA\\_Report26.pdf](http://www.inive.org/medias/ECA/ECA_Report26.pdf);
47. Kinney P. L., Lippmann M., „Respiratory effects of seasonal exposures to ozone and particles”, *Archives of Environmental Health*, 2000, 55, pp. 210-216;
48. Brown J. S., Bateson T. F., McDonnell W. F., „Effects of exposure to 0.06 ppm ozone on FEV1 in humans: a secondary analysis of existing data”, *Environmental Health Perspectives*, 2008, 116, pp. 1023-1026;
49. Chen X., Hopke P. K., „Secondary organic aerosols from alpha-pinene ozonolysis in dynamic chamber system”, *Indoor Air*, 2009, 19, 4, pp. 335-345;
50. Fakhri A. A., Llic L. M., Wellenius G. A., Urch B., Silverman F., Gold D. R., Mittleman M. A., „Autonomic effects of controlled fine particulate exposure in young healthy adults: Effect modification by ozone”, *Environmental Health Perspectives*, 2009, 117, pp. 1287-1292;
51. Hauck H., Berner A., Frischer T., Gomiscek B., Kundi M., Neuberger M., Puxbaum H., Preining O., „AUTHER - Austrian project on health effects of particulates- General overview”, *Atmospheric Environment*, 2004, 38, pp. 3905-3915;
52. Polichetti G., Cocco S., Spinali A., Trimarco V., Nunziata A., „Effects of particulate matter (PM10, PM2.5, PM1) on the cardiovascular system”, *Toxicology*, 2009, 261, pp. 1-8;
53. Ostro B. D., Feng W.-Y., Broadwin R., Malig B. J., Green R. S., Lipsett M. J., „The impact of components of fine particulate matter on cardiovascular mortality in susceptible subpopulations”, *Occupational and Environmental Medicine*, 2008, 65, pp. 750-756;
54. Weichenthal S., Dufresne A., Infante-Rivard C., „Indoor ultrafine particles and childhood asthma: exploring a potential public health concern”, *Indoor Air*, 2007, 17, pp. 81-91;
55. Molhave L., Schneider T., Kjaergaard S. K., Larsen L., Norn S., Jorgensen O., „House dust in Danish offices”, *Atmospheric Environment*, 2000, 34, pp. 4767-4779;
56. Janko M., Gould D. C., Vance L., Stengel C. C., Flack J., „Dust mite allergens in the office environment”, *American Industrial Hygiene Association Journal*, 1995, 56, pp. 1133-1140;
57. Cox-Ganser J. M., Rao C. Y., Park J. H., Shcumpert J. C., Kreiss K., „Asthma and respiratory symptoms in hospital workers related to dampness and biological contaminants”, *Indoor Air*, 2009, 19, 4, pp. 280-290;
58. D. Kotzias, The INDEX project (Critical appraisal of the setting and implementation of indoor exposure limits in the EU) , Summary on recommendations and management

- options, 2004,  
[http://ec.europa.eu/health/ph\\_projects/2002/pollution/fp\\_pollution\\_2002\\_exs\\_02.pdf](http://ec.europa.eu/health/ph_projects/2002/pollution/fp_pollution_2002_exs_02.pdf);
59. Zhang J., Smith K. R., „Indoor air pollution: a global health concern”, *British Medical Bulletin*, 2003, 68, 1, pp. 209-225;
60. Weschler C. J., „Ozone’s Impact on Public Health: Contributions from Indoor Exposures to Ozone and Products of Ozone-Initiated Chemistry”, *Environ Health Perspect.*, 2006, 114, 10, pp. 1489–1496;
61. Weschler C. J., „New directions: ozone-initiated reaction products indoors may be more harmful than ozone itself”, *Atmos Environ.*, 2004, 38, 33, pp. 5715–5716;
62. Nazaroff W. W., Weschler C. J., Corsi R. L., „Indoor air chemistry and physics”, *Atmos Environ.* 2003, 37, 39–40, pp. 5451–5453;
63. Fick J., Nilsson C., Andersson B., „Formation of oxidation products in a ventilation system”, *Atmos Environ.* 2004, 38, 35, pp. 5895–5899;
64. Morrison G. C., Nazaroff W. W., „Ozone interactions with carpet: secondary emissions of aldehydes”, *Environ Sci Technol.* 2002, 36, 10, pp. 2185–2192;
65. Delfino R. J., Staimer N., Tjoa T., Arhami M., Polidori A., Gillen D. L., George S.C., Shafer M. M., Schauer J. J., Sioutas C., „Associations of primary and secondary organic aerosols with airway and systemic inflammation in an elderly panel cohort”, *Epidemiology.*, 2010, 21, 6;
66. Laumbach R. J., Fiedler N., Gardner C. R., Laskin D. L., Fan Z. H., Zhang J., Weschler C. J., Liou P. J., Devlin R. B., Ohman-Strickland P., Kelly-McNeil K., Kipen H. M., „Nasal effects of a mixture of volatile organic compounds and their ozone oxidation products”, *J Occup Environ Med.*, 2005, 47, pp. 1182–1189;
67. van Eeden S. F., Tan W. C., Suwa T., Mukae H., Terashima T., Fujii T., Qui D., Vincent R., Hogg J. C., „Cytokines involved in the systemic inflammatory response induced by exposure to particulate matter air pollutants (PM(10))”, *Am J Respir Crit Care Med.*, 2001, 164, pp. 826–830;
68. Calogirou A., Larsen B. R., Kotzias D., „Gas-phase terpene oxidation products: a review”, *Atmospheric Environment*, 1999; 33, pp. 1423-1439;
69. Höpfe P., Praml G., Rabe G., Lindner J., Fruhmann G., Kessel R., „Environmental ozone field study on pulmonary and subjective responses of assumed risk groups”, *Environmental Research*, 1995, 71, pp. 109-121;
70. Groes L., Pejtersen J., Valbjørn O., „Atmospheric oxidation of selected terpenes and related carbonyls: gas-phase carbonyl products”, *Environmental Science and Technology*, 1996, 26, pp. 1526-1533;

71. Järnström H., Saarela K., Kalliokoski P., Pasanen A.-L., „Reference values for indoor air pollutant concentrations in new, residential buildings in Finland”, *Atmospheric Environment*, 2006, 40, pp. 7178-7192;
72. Singer B.C., Destailats H., Hodgson A.T., Nazaroff W.W., „Cleaning products and air fresheners: emissions and resulting concentrations of glycol ethers and terpenoids”, *Indoor air*, 2006, 16, pp. 179-191;
73. Rosell L., „Air quality and chemical emissions from construction material in houses adapted for allergic persons”, Technical report Sp Rapport, 1995, 54;
74. Sarwar G, Olson D. A., Corsi R. L., Weschler C. J., „Indoor fine particles: The role of terpene emissions from consumer products”, *J Air Waste Manage Assoc.*, 2004, 54, pp. 367-377;
75. Steinemann A. C., „Fragranced consumer products and undisclosed ingredients”, *Environ Impact Assess Rev*, 2009, 29, pp. 32-38;
76. Norgaard A. W., Jensen K. A., Janfelt C., Lauritsen F. R., Clausen P. A., Wolkoff P., „Release of VOCs and particles during use of nanofilm spray products”, *Environ Sci Technol*, 2009, 43, pp. 7824-7830;
77. Maupetit F., Squinazi F., „Caractérisation des émissions de benzène et de formaldéhyde lors de la combustion d'encens et de bougies d'intérieur: élaboration de scénarios d'exposition et conseils d'utilisation”, *Environ Risques Sante*, 2009, 8, 2, pp. 109-118;
78. Jo W. K., Lee J. H., Kim M. K., „Head-space, small-chamber and in-vehicle tests for volatile organic compounds (VOCs) emitted from air fresheners for the Korean market”, *Chemosphere*, 2008, 70, pp. 1827–1834;
79. Nazaroff W. W., Coleman B. K., Destailats H., Hodgson A. T., Liu D. L., Lunden M. M., Singer B. C., Weschler C. J., „Indoor Air Chemistry: Cleaning Agents, Ozone and Toxic Air Contaminants”, Final report: contract no. 01-336, 2006, <http://www.arb.ca.gov/research/apr/past/01-336.pdf>
80. Guenther A., Geron C., Pierce T., Lamb B., Harley P., Fall R., „Natural emissions of non-methane volatile organic compounds, carbon monoxide, and oxides of nitrogen from North America”, *Atmospheric Environment*, 2000, 34, 12-14, pp. 2205–2230;
81. Nazaroff W. W., Weschler C. J., „Cleaning products and air fresheners. Exposure to primary and secondary pollutants”, *Atmospheric Environment*, 2004, 38, pp. 2841-2865;
82. Plotto A., Margaria C. A., Goodner K. L., Goodrich E. A., „Odour and flavour thresholds for key aroma components in an orange juice matrix: Terpenes and aldehydes”, *Flavour Fragr J*, 2004, 19, pp. 491–498;
83. NIOSH, „Hazard evaluation and technical assistance report no. 92-0101, <http://www.cdc.gov/niosh/hhe/reports/pdfs/1992-0101-2341.pdf>

84. Boelens M. H., Boelens H., van Gemert L. J., „Perfumer & Flavorist”, 1993, 18, 6, pp. 1-15;
85. Nagda N. L., „Air quality and comfort in airliner cabins”, ASTM, 2000, Science, 290 pages;
86. World Health Organization (WHO), „Concise International Chemical Assessment Document 5, 1998, <http://www.who.int/ipcs/publications/cicad/en/cicad05.pdf>
87. Rastogi S. C., Heydorn S., Johansen J. D., Basketter D. A., „Fragrance chemicals in domestic and occupational products”, Contact Dermatitis, 2001, 45, pp. 221–225;
88. Massaldi H. A., King C. J., „Simple technique to determine solubilities of sparingly soluble organics: solubility and activity coefficients of d-limonene, n-butylbenzene, and n-hexyl acetate in water and sucrose solutions”, Journal of chemical and engineering data, 1973, 18, 4, pp. 393–397;
89. ENVIROFATE database, (calculated value), Office of Toxic Substances, US Environmental Protection Agency, and Syracuse Research Corporation [SRC], New York, NY, 1995)
90. Environmental Chemicals Data and Information Network (ECDIN), 1993, Ispra, Italy, CEC Joint Research Centre;
91. European Chemicals Agency (ECHA), publication dates: first published 17 March 2011; last modified 12 September 2014; [http://apps.echa.europa.eu/registered/data/dossiers/DISS-9eb16d5d-b83e-2831-e044-00144f67d031/DISS-9eb16d5d-b83e-2831-e044-00144f67d031\\_DISS-9eb16d5d-b83e-2831-e044-00144f67d031.html](http://apps.echa.europa.eu/registered/data/dossiers/DISS-9eb16d5d-b83e-2831-e044-00144f67d031/DISS-9eb16d5d-b83e-2831-e044-00144f67d031_DISS-9eb16d5d-b83e-2831-e044-00144f67d031.html)
92. Holcomb L. C., Seabrook B. S., „Indoor concentrations of volatile organic compounds: implications for comfort, health and regulation”, Indoor Environment, 1995, 4, pp. 7-26;
93. Li T. H., Turpin B. J., Shields H. C., Weschler, C. J., „Indoor hydrogen peroxide derived from ozone/d-limonene reactions”, Environ. Sci. Technol., 2002, 36, pp. 3295-3302;
94. Brown S. K., Sim M. R., „Concentrations of volatile organic compounds in indoor air – a review”, Indoor Air, 1994, 4, pp. 123-134;
95. Wainman T., Zhang J., Weschler C. J., Liou P. J., „Ozone and limonene in indoor air: a source of submicron particle exposure”, Environ. Health Perspect., 2000, 108, pp. 1139-1145;
96. Langer S., Moldanová J., Arrhenius K., Ljungström E., Ekberg L., „Ultrafine Particles Produced by Chemical Reactions in Indoor Air under Low/Closed Ventilation Conditions”, Atmospheric Environment, 2007, 42, pp. 4149-4159;

97. Ongwandee M., Moonrinta R., Panyametheekul S., Tangbanluekal C., Morrison G., „Investigation of volatile organic compounds in office buildings in Bangkok, Thailand: Concentrations, sources, and occupant symptoms”, *Building and Environment*, 2011, 46, pp. 1512-1522;
98. Viana M., Rivas I., Querol X., Alastuey A., Sunyer J., Álvarez-Pedrerol M., Bouso L., Sioutas C., „Indoor/outdoor relationships and mass closure of quasi-ultrafine, accumulation and coarse particles in Barcelona schools”, *Atmos. Chem. Phys.*, 2014, 14, pp. 4459–4472;
99. Bruin Y. Bruinen De, Koistinen K., Reina V., Geiss O., Tirendi S., Kephelopoulos S., Kotzias D., „The AIRMEX Project; Comparison of Indoor, Outdoor and Personal Exposure Concentrations of VOCs Across European Cities”, *Epidemiology*, 2006, Volume 17, 6, pp. S454-S455;
100. Jia C., Batterman S., Godwin C., Charles S., Chin J.Y., „Sources and migration of volatile organic compounds in mixed-use buildings, *Indoor Air*, 2010, 20, pp. 357-369;
101. Doty R. L., Brugger W.E., Jurs P. C., Orndorff M. A., Snyder P. J., Lowry L. D., „Intranasal trigeminal stimulation from odorous volatiles: psychometric responses from anosmic and normal humans”, *Physiol Behav.*, 1978, 20, 2, pp. 175-85;
102. Tamas G., Weschler C. J., Toftum J., Fanger P. O., „Influence of ozone-limonene reactions on perceived air quality”, *Indoor Air*, 2006, 16, pp. 168-178;
103. Knudsen H. N., Afshari A., Ekberg L., Lundgren B., „Impact of ventilation rate, ozone and limonene on perceived air quality in offices”, *Indoor Air 2002: Proceedings of the 9th International Conference on Indoor Air Quality and Climate, Monterey, California June 30-July 5, 2002.*: Vol. II, pp. 285-290;
104. Lee S. C., Lam S., Fai H. K., „Characterization of VOCs, ozone, and PM10 emissions from office equipment in an environmental chamber”, *Building and Environment*, 2001, 36, 7, pp. 837–842;
105. Destailats H., Maddalena R. L., Singer B. C., Hodgson A. T., McKone T. E., „Indoor Pollutants Emitted by Office Equipment: A Review of Reported Data and Information Needs”, *Atmospheric Environment*, 2008, 42, pp. 1371-1388;
106. Tuomi T., Engström B., Niemelä R., Svinhufvud J., Reijula K., „Emission of ozone and organic volatiles from a selection of laser printers and photocopiers, *Appl Occup Environ Hyg.*, 2000, 15, 8, pp. 629-34;
107. Niu, J. L., Tung, T. C. W., Burnett, J., „Quantification of dust removal and ozone emission of ionizer air-cleaners by chamber testing”, *J. Electrostat.*, 2001, 51, pp. 20–24;
108. Mullen N., Yu X., Zhao P., Corsi R.L., Siegel J.A., „Experimental characterization of portable ion generators”, *Indoor Air*, 2005: *Proceedings of the 10<sup>th</sup> International Conference on IAQ and Climate*, 4, pp. 2957–2961;

109. Waring M. S., Siegel J. A., Corsi R. L., „Ultrafine particle removal and generation by portable air cleaners”, *Atmos. Environ.*, 2008, 42, pp. 5003–5014;
110. Selway M. D., Allen R. J., Wadden R. A., „Ozone production from photocopying machines”, *Am Ind Hyg Assoc J.m*, 1980, 41, 6, pp. 455-9;
111. Phillips T. J., Bloudoff D. P., Jenkins P. L., Stroud K. R., „Ozone emissions from a "personal air purifier"”, *J Expo Anal Environ Epidemiol.*, 1999, 9, 6, pp. 594-601;
112. Castellano P., Canepari S., Ferrante R., L'Episcopo N., „Multiparametric approach for an exemplary study of laser printer emissions”, *J Environ Monit.*, 2012, 14, 2, pp. 446-54;
113. Brown S. K., „Assessment of pollutant emissions from dry-process photocopiers”, *Indoor Air*, 1999, 9, 4, pp. 259-67;
114. Allen R. J., Wadden R. A., Ross E. D., „Characterization of potential indoor sources of ozone”, *Am Ind Hyg Assoc J.*, 1978, 39, 6, pp. 466-71;
115. Sabersky R. H., Sinema D. A., Shair F. H., „Concentrations, decay rates, and removal of ozone and their relation to establishing clean indoor air”, *Environmental Science and Technology*, 1973, 7, pp. 347-353;
116. Weschler C. J., „Ozone in indoor environments: concentration and chemistry”, *Indoor Air*, 2000, 10, pp. 269-288;
117. Moriske H. J., Ebert G., Konieczny L., Menk G., Schöndube M., „Concentration and decay of ozone in indoor air in dependence on building and surface materials”, *Toxicol Letters*, 1998, 96-97, pp. 319-23;
118. Wisthaler A., Tamás G., Wyon D. P., Strøm-Tejse P., Space D., Beauchamp J., Hansel A., Märk T. D., Weschler C. J., „Products of ozone-initiated chemistry in a simulated aircraft environment”, *Environmental Science and Technology*, 2005, 39, pp. 4823-4832;
119. Nagda N. L., Fortmann M. D., Koontz M. D., Baker S. R., Ginevan M. E., „Airliner Cabin Environment: Contaminant Measurements, Health Risks, and Mitigation Options”, Prepared by GEOMET Technologies, 1989, Germantown, MD, for the U.S. Department of Transportation, Washington DC. DOT-P-15–89–5. NTIS/PB91–159384
120. Waters M. „Cabin Air Quality Exposure Assessment” National Institute for Occupational Safety and Health, Cincinnati, OH. Federal Aviation Administration Civil Aeromedical Institute. Presented to the NRC Committee on Air Quality in Passenger Cabins of Commercial Aircraft, 2001, National Academy of Science, Washington, DC;
121. EPA (U.S. Environmental Protection Agency), „Air Quality Criteria for Ozone and Related Photochemical Oxidants”, 1996, Vol. I-III. EPA/600/P-93/004aF, EPA/600/P-93/004bF, EPA/600/P-93/004cF, National Center for Environmental Assessment, Office of

- Research and Development, U.S. Environmental Protection Agency, Research Triangle Park, NC [online]. <http://cfpub.epa.gov/ncea/cfm/recorddisplay.cfm?deid=2831#Download>
122. Apte M. G., Buchanan, I. S. H., Mendell, M. J., „Outdoor ozone and building-related symptoms in the BASE study”, *Indoor Air*, 2008, 18, pp. 156-170;
  123. Bernhard C. A., Kirchner S., Knutti R., Lagoudi A., „Volatile organic compounds in 56 European office buildings”, In: Maroni, M. (Ed.), 1995, *Proceedings of the Healthy Buildings '95*, Milan. vol. 3, pp. 1347–1352;
  124. Jensen B., Wolkoff P., „VOCBASE–odor thresholds, mucous membrane irritation thresholds and physico-chemical parameters of VOCs”, 1996, A PC program, Version 2.1, National Institute of Occupational Health, Copenhagen;
  125. Glasius M., Lahaniati M., Calogirou A., Di Bella D., Jensen N. R., Hjorth J., Kotzias D., Larsen B. R., „Carboxylic acids in secondary aerosols from oxidation of cyclic monoterpenes by ozone”, *Environ Sci Technol.*, 2000, 34, pp. 1001–10;
  126. Carslaw N., „A new detailed chemical model for indoor air pollution”, *Atmospheric Environ*, 2007, 41, pp. 1164-1179;
  127. Crigee R., „Mechanismus der Ozonolyse”, *Angew. Chem. Int. Ed. Engl.*, 1975, 14, 745;
  128. Geletneky C., Berger S., „The mechanism of ozonolysis revisited by 17O-NMR spectroscopy”, *European Journal of Organic Chemistry*, 1998, 8, pp. 1625–1627;
  129. Paulson S. E., Chung M. Y., Hasson A. S., „OH radical formation from the gas-phase reaction of ozone with terminal alkenes and the relationship between structure and mechanism”, *The Journal of Physical Chemistry A*, 1999, 103, pp. 8125-8138;
  130. Weschler C. J, Shields H. C, „Indoor ozone/terpene reactions as a source of indoor particles”, *Atmospheric Environment*, 1999, 33, pp. 2301-2312;
  131. Fick J., Pommer L., Andersson B., Nilsson C., „A study of the gas-phase ozonolysis of terpenes: the impact of radicals formed during the reaction”, *Atmospheric Environment*, 2002, 36, pp. 3299–3308;
  132. Sarwar G., Corsi R., Kimura Y., Allen D., Weschler C. J., „Hydroxyl radicals in indoor environments”, *Atmospheric Environment*, 2002, 36, 24, pp. 3973–3988;
  133. Fan Z. H., Weschler C. J., Han I. K., Zhang J. F., „Co-formation of hydroperoxides and ultra-fine particles during the reactions of ozone with a complex VOC mixture under stimulated indoor conditions”, *Atmospheric Environment*, 2005, 39, 28, pp.5171–5182;
  134. Glasius M., Duane M., Larsen B. R., „Determination of polar terpene oxidation products in aerosols by liquid chromatography-ion trap mass spectrometry”, *J. chromatography A*, 1999, 833, 2, pp. 121-135;
  135. Wilkins C. K, Wolkoff P., Clausen P. A., Hammer M., Nielsen G. D, „Terpene/ozone reaction products (tops). Dependence of irritation on reaction time and

- relative humidity”, Proceedings: Indoor Air, 2002, <http://www.irbnet.de/daten/iconda/CIB6673.pdf>;
136. Grosjean D., Williams E. L., Grosjean E., Andino J. M., Seinfeld J. H., „Atmospheric oxidation of biogenic hydrocarbons: reaction of ozone with beta-pinene, d-limonene and trans-caryophyllene”, *Environ Sci Technol*, 1993, 27, pp. 2754-2758;
137. Hakola H., Arey J., Aschmann S., Atkinson R., „Product formation from gas-phase reactions of OH radicals and O<sub>3</sub> with a series of monoterpenes”, *Journal of Atmospheric Chemistry*, 1994, 18, pp. 75-102;
138. Hatakeyama S., Akimoto H., „Reactions of Criegee intermediates in the gas-phase”, *Research on Chemical Intermediates* 1994, 20, pp. 503-524;
139. Brared C. J., Matura M., Bäcktorp C., Börje A., Nilsson J. L., Karlberg A. T., „Hydroperoxides form specific antigens in contact allergy”, *Contact dermatitis*, 2006, 55, pp. 230-237;
140. Johanna B. C. , Johansson S., Hagvall L., Jonsson C., Börje A., Karlberg A. T., „Limonene hydroperoxide analogues differ in allergenic activity”, *Contact dermatitis*, 2008, 59, pp. 344-352;
141. Blanch G. P., „Determination of the enantiomeric composition of limonene and limonene 1,2 epoxide in lemon peel by multidimensional gas chromatography with flame ionization detection and selected ion monitoring mass spectrometry”, *Journal of chromatographic science*, 1998, 36, 1, pp. 37-43;
142. Leungsakul S., Kamens R. M., „Mechanistic detail and modelling of d-limonene with ozone in a darkness”, 2004, [http://www.researchgate.net/publication/239921052\\_Mechanistic\\_detail\\_and\\_modeling\\_of\\_d-limonene\\_with\\_ozone\\_in\\_a\\_darkness](http://www.researchgate.net/publication/239921052_Mechanistic_detail_and_modeling_of_d-limonene_with_ozone_in_a_darkness);
143. Leungsakul S., Jaoui M., Kamens R. M., „Kinetic mechanism for predicting secondary organic aerosol formation from the reaction of d-limonene with ozone”, *Environ Sci Technol*, 2005, 39, 24, pp. 9583–9594;
144. Thomas A. F., "Limonene", *Natural product reports*, 1989, <http://www.sciencemadness.org/scipics/Nicodem/Limonene.pdf>;
145. Atkinson R., Arey J., „Gas-phase tropospheric chemistry of biogenic volatile organic compounds: a review”, *Atmospheric Environment*, 2003, 37, pp. S197-S219;
146. Hardik Surendra Amin, „Speciation studies for biogenic volatile organic compounds and secondary organic aerosol generated by ozonolysis of volatile organic compounds mixtures”, dissertation 2012, <http://opensiuc.lib.siu.edu/cgi/viewcontent.cgi?article=1529&context=dissertations>;
147. Wells J. R., „Use of denuder/filter apparatus to investigate terpene ozonolysis”, *Journal of Environmental Monitoring*, 2012, 14, 3, pp. 1044-1054;

148. Rossignol S., Chiappini L., Perraudin E., Rio C., Fable S., Valorso R., Doussin J. F., „Development of a parallel sampling and analysis method for the elucidation of gas/particle partitioning of oxygenated semi-volatile organics: a limonene ozonolysis”, *Atmos. Meas. Tech.*, 2012, 5, pp. 1459-1489;
149. Jaoui M., Corse E., Kleindienst T. E., Offenberg J. H., Lewandowski M., Edney E. O., „Analysis of secondary organic aerosol compounds from the photooxidation of d-limonene in the presence of NO<sub>x</sub> and their detection in ambient PM<sub>2.5</sub>”, *Environ Sci Technol.* 2006, 40, 12, pp. 3819-28;
150. Xinlian Chang, „Module for simulating composition effects on secondary organic aerosol partitioning and evaluation in the southeastern united states”, dissertation 2006, [http://etd.library.vanderbilt.edu/available/etd-08242006-151955/unrestricted/Xinlian\\_Dissertation.pdf](http://etd.library.vanderbilt.edu/available/etd-08242006-151955/unrestricted/Xinlian_Dissertation.pdf);
151. Long M. C., Suh H. H., Koutrakis P., „Characterization of Indoor Particle Sources Using Continuous Mass and Size Monitors”, *Journal of Air & Waste Management Association*, 2000, 50, pp. 1236-1250;
152. Rohr A. C., Weschler C. J., Koutrakis P., Spengler JD, „Generation and quantification of ultrafine particles through terpene/ozone reaction in a chamber setting”, *Aerosol Science and Technology*, 2003, 37, pp. 65-78;
153. Sarwar G., Corsi R., Allen D., Weschler C., „The significance of secondary organic aerosol formation and growth in buildings: experimental and computational evidence”, *Atmos. Environ.*, 2003, 37, pp. 1365-1381;
154. Künzli N., Avol E., Wu J., Gauderman W. J., Rappaport E., Millstein J., Bennion J., McConnell R., Gilliland F. D., Berhane K., Lurmann F., Winer A., Peters J. M., „Health effects of the 2003 Southern California wildfires on children”, *American Journal of Respiratory and Critical Care Medicine*, 2006, 174, 11, pp. 1221-1228;
155. Lamorena R. B., Lee W., „Influence of ozone concentration and temperature on ultra-fine particle and gaseous volatile organic compound formations generated during the ozone-initiated reactions with emitted terpenes from a car air freshener”, *J Hazard Mater.*, 2008, 158, 2-3, pp. 471-7;
156. Weschler C. J., Wells J. R., Poppendieck D., Hubbard H., Pearce T. A., „Workgroup report: Indoor chemistry and health”, *Environmental Health Perspectives*, 2006, 114, pp. 442-446;
157. National Cancer Institute: „Health effects of exposure to environmental tobacco smoke: the report of the California environmental protection agency” Smoking and tobacco control monograph no.10 NIH pub. No. 99-4645. Bethesda, MD: U.S. Department of health and human services, National Institutes of health, National Cancer Institute, 1999;

158. Delfino, R. J., Sioutas, C., Malik S., „Potential Role of Ultrafine Particles in Associations between Airborne Particle Mass and Cardiovascular Health”, *Environmental Health Perspectives*, 2005, 113, pp. 934-946;
159. Clausen P. A., Wilkins C. K., Wolkoff P., Nielsen G. D., „Chemical and biological evaluation of a reaction mixture of R-(+)-limonene/ozone: Formation of strong airway irritants”, *Environment International*, 2001, 26, pp. 511-522;
160. Hakola H., Arey J., Aschmann S. M., Atkinson R., „Product formation from the gas-phase reaction of OH radicals and O<sub>3</sub> with a series of monoterpenes”, *Journal of Atmospheric Chemistry*, 1994, 18, pp. 75–102;
161. Forester C. D., Wells J. R., „Yields of carbonyl products from gas-phase reactions of fragrance compounds with OH radical and ozone”, *Environmental Science and Technology*, 2009, 43, pp. 3561–3568;
162. Fruekilde P., Hjorth J., Jensen N. R., Kotzias D., Larsen B., „Ozonolysis at vegetation surfaces: A source of acetone, 4-oxopentanal, 6-methyl-5-hepten-2-one, and geranyl acetone in the troposphere”, *Atmos. Environ.*, 1998, 32, pp. 1893–1902;
163. Matsunaga S., Mochida M., Kawamura K., „High abundance of gaseous and particulate 4-oxopentanal in the forestal atmosphere”, *Chemosphere*, 2004, 55, pp. 1143–1147;
164. Anderson S. E., Jackson L. G., Franko J., Wells J. R., „Evaluation of dicarbonyls generated in a simulated indoor air environment using an in vitro exposure system”, *Toxicological Sciences*, 2010, 115, pp. 453–461;
165. Anderson S. E., Franko J., Jackson L. G., Wells J. R., Ham J. E., Meade B. J., „Irritancy and allergic responses induced by exposure to the indoor air chemical 4-oxopentanal”, *Toxicological Sciences*, 2012, 127, pp. 371–381;
166. Franko J., Munson A. E., Ham J., Jackson L. G., Wells J. R., Butterworth L., Anderson S. E., „4-Oxopentanal identified as a potential indoor air irritant and allergen”, *Toxicologist.*, 2009, pp. 108-31;
167. Anderson S. E., Wells J. R., Fedorowicz A., Butterworth L. F., Meade B. J., Munson A. E., „Evaluation of the contact and respiratory sensitization potential of volatile organic compounds generated by simulated indoor air chemistry”, *Toxicol. Sci.*, 2007, 97, pp. 355–363;
168. Nørgaard A. W., Kudal J. D., Kofoed-Sørensen V., Koponen I. K., Wolkoff P., „Ozone-initiated VOC and particle emissions from a cleaning agent and an air freshener: risk assessment of acute airway effects”, *Environ Int.*, 2014, 68, pp. 209-18;
169. Nørgaard A. W., Kofoed-Sørensen V., Mandin C., Ventura G., Mabilia R., Perreca E., Cattaneo A., Spinazzè A., Mihucz V. G., Szigeti T., Y. de Kluizenaar, Cornelissen H. J. M., Trantallidi M., Carrer P., Sakellaris I., Bartzis J., Wolkoff P., „Ozone-initiated Terpene

Reaction Products in Five European Offices: Replacement of a Floor Cleaning Agent”, *Environ. Sci. Technol.*, 2014, 48, 22, pp. 13331–13339;

170. Chris Kent, *Basics of toxicology* (ebook), 1998, ISBN: 978-0-471-29982-0, 416 pages,

<https://books.google.it/books?id=VEUIWz4vQssC&pg=PA303&lpg=PA303&dq=a+70+kg+adult+is+assumed+to+inhale+20+m3+of+air+per+day&source=bl&ots=0rgylSRh-W&sig=E8TMLXsk-5OLCqIQfdypOzhEU30&hl=fr&sa=X&ei=PHVIVa7-K4XkUZjQgcAF&ved=0CCAQ6AEwADgK#v=onepage&q=a%2070%20kg%20adult%20is%20assumed%20to%20inhale%2020%20m3%20of%20air%20per%20day&f=false>;

171. BéruBé, K. A., Balharry, D., Sexton, K., Koshy, L., Jones, T. P., „Combustion-derived nanoparticles: mechanisms of pulmonary toxicity”, *Clinical Experimental Pharmacology Physiology*, 2007, 34, pp. 1044-1050;

172. Miller F. J., „Dosimetry of particles in laboratory animals and man” in *Toxicology of the Lung*, 1999, eds Gardner DE, Crapo JD, McClellan RO (Taylor and Francis, Washington, DC), 3, pp. 513–55;

173. Raabe O. G., „Respiratory exposure to air pollutants”, In: Swift DL and Foster WM, eds. *Air Pollutants and the Respiratory Tract* (ISBN 0824795210). New York, 1999, Marcel Dekker, pp. 39-73;

174. Kofi Asante-Duah, „Public Health Risk Assessment for Human Exposure to Chemicals” (ebook), *Environmental Pollution*, ISBN-13: 978-1402009211, [https://books.google.it/books?id=TUzVWBsL994C&pg=PA354&lpg=PA354&dq=Public+Health+Risk+Assessment+for+Human+Exposure+to+Chemicals+Kofi+Asante-Duah&source=bl&ots=5epVLeUT-D&sig=5yOWJOvcryAi05H5fmIDB890FgU&hl=fr&sa=X&ei=VMNIVdn\\_KMTzUt-PgcAN&ved=0CEUQ6AEwBA#v=onepage&q=Public%20Health%20Risk%20Assessment%20for%20Human%20Exposure%20to%20Chemicals%20Kofi%20Asante-Duah&f=false](https://books.google.it/books?id=TUzVWBsL994C&pg=PA354&lpg=PA354&dq=Public+Health+Risk+Assessment+for+Human+Exposure+to+Chemicals+Kofi+Asante-Duah&source=bl&ots=5epVLeUT-D&sig=5yOWJOvcryAi05H5fmIDB890FgU&hl=fr&sa=X&ei=VMNIVdn_KMTzUt-PgcAN&ved=0CEUQ6AEwBA#v=onepage&q=Public%20Health%20Risk%20Assessment%20for%20Human%20Exposure%20to%20Chemicals%20Kofi%20Asante-Duah&f=false);

175. Rozman K. K., Klaassen C. D., „Absorption, distribution and excretion of toxicants”, *Casarett and Doull's Toxicology: the basic science of poisons*, sixth edition, 2001, Klaassen, C.D. (Ed). McGraw-Hill, New York, pp. 105-132;

176. Hext P. M., „Inhalation toxicology”, *General and Applied Toxicology*, Second edition, 2000, vol 1. Ballantyne, B., Marrs, T.C. and Syversen, T. (Eds). Macmillan reference LTD, London, pp. 587-601;

177. National Heart, Lung, and Blood Institute (NIH), U.S. Department of Health & Human Services, <http://www.nhlbi.nih.gov/health/health-topics/topics/hlw/system>;

178. Rogers D. F., Jeffery P. K., „Inhibition by oral N-acetyl-cysteine of cigarette smoke-induced "bronchitis" in the rat”, *Exp Lung Res.*, 1986, 10, pp. 267–283;

179. Harkema J. R., Hotchkiss J. A., „In vivo effects of endo-toxin on intraepithelial mucosubstances in rat pulmonary airways”, *Quantitative histochemistry, Am J Pathol* 1992, 141, pp. 307–317;
180. Elaine Nicpon Marieb, „Essentials of Human Anatomy and Physiology”, 2005, ISBN 10: 0131934813, published by Old Tappan, New Jersey, U.S.A.: Pearson;
181. Ross M. H., Gordon K. I., Pawlina W., „Histology: A text and atlas”, 2002, Lippincott Williams and Wilkins: Philadelphia, Microscopic structures of the alveoli;
182. Ross M. H., Wojciech P., „Histology: A Text and Atlas”, 6th edition, 2010, published by Lippincott Williams & Wilkins: Wolters Kluwer, ISBN-13: 978-0781772006;
183. Adams D. O., Hamilton T. A., „The cell biology of macrophage activation”, *A. Rev. Immunol.*, 1984, 2, pp. 283-318;
184. Klaassen C. D., Watkins J. B., Casarett L. J., „Casarett & Doull's essentials of toxicology”, (ebook), 2010, ISBN-13: 978-0071622400, McGraw-Hill Medical;
185. Unanue E. R., Allen P. M., „The basis for the immunoregulatory role of macrophages and other accessory cells”, *Science*, 1987, 236, pp. 551-557;
186. BéruBé K., Prytherch Z., Job C., Hughes T., „Human primary bronchial lung cell constructs: the new respiratory models”, *Toxicology*, 2010, 278, 3, pp. 311-318;
187. Medinsky M. A., Bond J. A., „Sites and mechanisms for uptake of gases and vapors in the respiratory tract”, *Toxicology*, 2001, 160,1-3, pp. 165-172;
188. Haschek W. M., Rousseaux C. G., Wallig M. A., Bolon B., Ochoa R., „Handbook of toxicologic pathology”, ISBN: 978-0-12-330215-1;
189. Shultz M. A., Choudary P. V., Buckpitt A. R., „Role of murine cytochrome P-450 2F2 in metabolic activation of naphthalene and metabolism of other xenobiotics”, *The Journal of Pharmacology and Experimental Therapeutics*, 1999, 290, 1, pp. 281-288;
190. Anzenbacher P., Zanger U. M., „Metabolism of drugs and other xenobiotics”, 2012, ISBN: 9783527329038, Wiley-VCH Verlag GmbH & Co. KGaA;
191. Pittet J. F., Mackersie R. C., Martin T. R., Matthay M. A., „Biological markers of acute lung injury: prognostic and pathogenetic significance”, *American Journal of Respiratory & Critical Care Medicine*, 1997, 155, 4, pp. 1187-205;
192. Toews G.B., „Cytokines and the lung”, *Eur Respir J*, 2001, 34, pp. 3s-17s;
193. Robays L. J., Maes T., Lebecque S., Lira S. A., Kuziel W. A., Brusselle G. G., Joos G. F., Vermaelen K. V., „Chemokine receptor CCR2 but not CCR5 or CCR6 mediates the increase in pulmonary dendritic cells during allergic airway inflammation. *J Immunol*, 2007, 178, pp. 5305–5311;
194. Park S. J., Burdick M. D., Brix W. K., Stoler M. H., Askew D. S., Strieter R. M., Mehrad B., „Neutropenia enhances lung dendritic cell recruitment in response to

- Aspergillus via a cytokine-to-chemokine amplification loop”, *J Immunol*, 2010, 185, pp. 6190–6197;
195. Demedts I. K., Bracke K. R., Maes T., Joos G. F., Brusselle G. G., „Different roles for human lung dendritic cell subsets in pulmonary immune defense mechanisms. *Am J Respir Cell Mol Biol*, 2006, 35, pp. 387–393;
196. Waal Malefyt R., Abrams J., Bennett B., Figdor C. G., de Vries J. E., „Interleukin 10 (IL-10) inhibits cytokine synthesis by human monocytes: an autoregulatory role of IL-10 produced by monocytes”, *JEM*, 1991, 174, 5, pp. 1209-1220;
197. Barnes P. J., „Mechanisms in COPD: differences from asthma”, *Chest*, 2000, 117, 2, pp. 10S–14S;
198. Barnes P. J., „A new approach to the treatment of asthma”, *New Engl J Med*, 1989, 321, pp. 1517–1527;
199. Barnes P. J., The cytokine network in asthma and chronic obstructive pulmonary disease, *J Clin Invest.*, 2008, 118, 11, pp. 3546–3556;
200. Yoshimoto T., Yasuda K., Mizuguchi J., Nakanishi K., „IL-27 suppresses Th2 cell development and Th2 cytokines production from polarized Th2 cells: a novel therapeutic way for Th2-mediated allergic inflammation”, *J. Immunol.*, 2007, 179, pp. 4415–4423;
201. Berry M. A., Hargadon B., Shelley M., Parker D., Shaw D. E., Green R. H., Bradding P., Brightling C. E., Wardlaw A. J., Pavord I. D., „Evidence of a role of tumor necrosis factor alpha in refractory asthma. *N. Engl. J. Med.*, 2006, 354, pp. 697–708;
202. Keatings V. M., Collins P. D., Scott D. M., Barnes P. J., „Differences in interleukin-8 and tumor necrosis factor- $\alpha$  in induced sputum from patients with chronic obstructive pulmonary disease or asthma, *Am J Resp Crit Care Med*, 1996, 153, pp. 530–534;
203. Hupin C., Rombaux P., Lecocq M., Weynand B., Sibille Y., Pilette C., „Immune Defence Mechanisms: Comparing Upper and Lower Airways in Chronic Airway Diseases”, *Immun., Endoc. & Metab. Agents in Med. Chem.*, 2010, 10, pp. 123-141;
204. Lalani I., Bhol K., Ahmed A. R., „Interleukin-10: biology, role in inflammation and autoimmunity”, *Ann Allergy Asthma Immunol*, 1998, 80, 3, pp. A-6;
205. Liu Z., Lu X., Zhang X. H., Bochner B. S.; Long X. B., Zhang F., Wang H., Cui Y.H., „Clara cell 10-kDa protein expression in chronic rhinosinusitis and its cytokine-driven regulation in sinonasal mucosa”, *Allergy*, 2009, 64, 1, pp. 149-157;
206. O'Byrne P. M., „Cytokines or their antagonists for the treatment of asthma”, *Chest*, 2006, 130, 1, pp. 244-250;
207. Karadag F., Karul A. B., Cildag O., Yilmaz M., Ozcan H., „Biomarkers of systemic inflammation in stable and exacerbation phases of COPD”, *Lung*, 2008, 186, 6, pp. 403-409;

208. Rincon M., Irvin C. G., „Role of IL-6 in Asthma and Other Inflammatory Pulmonary Diseases”, *Int. J. Biol. Sci.*, 2012, 8, pp. 1281-1290;
209. Morjaria J. B., Babu K. S., Vijayanand P., Chauhan A. J., Davies D. E., Holgate S. T., „Sputum IL-6 concentrations in severe asthma and its relationship with FEV<sub>1</sub>”, *Thorax.*, 2011; pp. 66- 537;
210. Neveu W., Allard J. B., Dienz O., Wargo M. J., Ciliberto G., Whittaker L. A., Rincon M., „IL-6 is required for airway mucus production induced by inhaled fungal allergens”, *J Immunol.*, 2009; 183, pp. 1732-8;
211. Qiu Z., Fujimura M., Kurashima K., Nakao S., Mukaida N., „Enhanced airway inflammation and decreased subepithelial fibrosis in interleukin 6-deficient mice following chronic exposure to aerosolized antigen”, *Clin Exp Allergy.*, 2004, 34, pp. 1321-8;
212. Kleinjan, A., Dijkstra, M. D., Boks, S. S., Severijnen, L. A., Mulder, P. G., Fokkens, W. J., „Increase in IL-8, IL-10, IL-13, and RANTES mRNA levels (in situ hybridization) in the nasal mucosa after nasal allergen provocation”, *J. Allergy Clin. Immunol.*, 1999, 103, pp. 441-450;
213. Xiao W., Hsu Y. P., Ishizaka A., Kirikae T., Moss R. B., „Sputum cathelicidin, urokinase plasminogen activation system components, and cytokines discriminate cystic fibrosis, COPD, and asthma inflammation”, *Chest*, 2005, 128, 4, pp. 2316-2326;
214. Chung K. F., Marwick J. A., „Molecular mechanisms of oxidative stress in airways and lungs with reference to asthma and chronic obstructive pulmonary disease”, *Ann N Y Acad Sci.*, 2010, 1203, pp. 85–91;
215. Nocker R. E., Schoonbrood D. F., van de Graaf E. A., Hack C. E., Lutter R., Jansen H. M., Out T. A., „Interleukin-8 in airway inflammation in patients with asthma and chronic obstructive pulmonary disease”, *Int Arch Allergy Immunol.*, 1996, 109, 2, pp. 183-91;
216. Hsu-Chung Liu, Min-Chi Lu, Yi-Chun Lin, Tzu-Chin Wu, Jeng-Yuan Hsu, Ming-Shiou Jan, Chuan-Mu Chen, „Differences in IL-8 in serum and exhaled breath condensate from patients with exacerbated COPD or asthma attacks”, *Journal of the Formosan Medical Association*, 2014, 113, 12, pp. 908–914;
217. Yalcin A. D., Bisgin A., Gorczynski R. M., „IL-8, IL-10, TGF-, and GCSF Levels Were Increased in Severe Persistent Allergic Asthma Patients with the Anti-IgE Treatment”, *Mediators of Inflammation*, 2012, 8 pages;
218. Stemmler S., Arinir U., Klein W., Rohde G., Hoffjan S., Wirkus N., Reinitz-Rademacher K., Bufe A., Schultze-Werninghaus G., Epplen J. T., „Association of interleukin-8 receptor  $\alpha$  polymorphisms with chronic obstructive pulmonary disease and asthma”, *Genes and Immunity*, 2005, 6, pp. 225–230;

219. Norzila M. Z., Fakes K., Henry R. L., Simpson J., Gibson P. G., „Interleukin-8 secretion and neutrophil recruitment accompanies induced sputum eosinophil activation in children with acute asthma”, *Am J Respir Crit Care Med*, 2000, 161, pp. 769–774;
220. Rutgers S. R., Timens W., Kaufmann H. F., van der Mark T. W., Koeter G. H., Postma D. S. „Comparison of induced sputum with bronchial wash, bronchoalveolar lavage and bronchial biopsies in COPD”, *Eur Respir J.*, 2000, 15, pp. 109–115;
221. Matera M. G., Calzetta L., Cazzola M., „TNF-alpha inhibitors in asthma and COPD: we must not throw the baby out with the bath water”, *Pulm Pharmacol Ther.*, 2010, 23, 2, pp. 121-8;
222. Keatings V. M., Collins P. D., Scott D. M., Barnes P. J., „Differences in interleukin-8 and tumor necrosis factor-alpha in induced sputum from patients with chronic obstructive pulmonary disease or asthma”, *Am J Respir Crit Care Med.*, 1996, 153, 2, pp. 530-4;
223. Antoniu S. A., Mihaltan F., Ulmeanu R., „Anti-TNF-alpha therapies in chronic obstructive pulmonary diseases”, *Expert Opin Investig Drugs*, 2008, 17, 8, pp. 1203-11;
224. Mukhopadhyay S., Hoidal J. R., Mukherjee T. K., „Role of TNF $\alpha$  in pulmonary pathophysiology”, *Respiratory Research*, 2006, 7, 125;
225. Wouters E. F. M., „Chronic obstructive pulmonary disease • 5: Systemic effects of COPD”, *Thorax J.*, 2002, 57, pp. 1067-1070;
226. Wanderer A. A., „Interleukin-1beta targeted therapy in severe persistent asthma (SPA) and chronic obstructive pulmonary disease (COPD): proposed similarities between biphasic pathobiology of SPA/COPD and ischemia-reperfusion injury”, *Isr Med Assoc J.*, 2008, 10, 12, pp. 837-42;
227. Lappalainen U., Whitsett J. A., Wert S. E., Tichelaar J. W., Bry K., „Interleukin-1beta causes pulmonary inflammation, emphysema, and airway remodeling in the adult murine lung”, *Am J Respir Cell Mol Biol.*, 2005, 32, 4, pp. 311-8;
228. Caoa Y., Gong W., Zhang H., Liu B., Li B., Wu X., Duan X., Dong J., „A Comparison of Serum and Sputum Inflammatory Mediator Profiles in Patients with Asthma and COPD”, *Journal of International Medical Research*, 2012, 40, 6, pp. 2231-2242;
229. Asadullah K., Sterry W., Volk H. D., „Interleukin-10 therapy - review of a new approach”, *Pharmacol Rev.* 2003, 55, pp. 241–269;
230. Hacievliyagil S. S., Gunen H., Mutlu L. C., Karabulut A. B., Temel I., „Association between cytokines in induced sputum and severity of chronic obstructive pulmonary disease”, *Respir Med.*, 2006, 100, pp. 846–854;
231. Burgess J. L., Nanson C. J., Hysong T. A., Gerkin R., Witten M. L., Lantz R. C., „Rapid decline in sputum IL-10 concentration following occupational smoke exposure”, *Inhal Toxicol.*, 2002, 14, pp. 133–140;

232. Atamas S. P., Chapoval S. P., Keegan A. D., „Cytokines in chronic respiratory diseases”, *F1000 Biology Reports*, 2013, 5, 3;
233. Chung K. F., „Cytokines in chronic obstructive pulmonary disease”, *Eur Respir J* 2001, 18, 34, pp. 50s–59s;
234. Lim S., Roche N., Oliver B. G., Mattos W., Barnes P. J., Chung K. F., „Balance of matrix metalloprotease-9 and tissue inhibitor of metalloprotease-1 from alveolar macrophages in cigarette smokers: regulation by interleukin-10”, *Am J Respir Crit Care Med* 2000, 162, pp. 1355–1360;
235. McNamara P. S., Smyth R. L., „Interleukin-9 as a possible therapeutic target in both asthma and chronic obstructive airways disease”, *Drug News Perspect.* 2005, 18, 10, pp. 615-21;
236. Kambayashi T., Larosa D. F., Silverman M. A., Koretzky G. A., „Cooperation of adapter molecules in proximal signaling cascades during allergic inflammation”, *Immunol Rev.*, 2009, 232, pp. 99–114;
237. Panzner P., Lafitte J. J., Tsiopoulos A., Hamid Q., Tulic M. K., „Marked up-regulation of T lymphocytes and expression of interleukin-9 in bronchial biopsies from patients with chronic bronchitis with obstruction”, *Chest*, 2003, 124, pp. 1909–1915;
238. Romagnani S., „T-cell responses in allergy and asthma”, *Curr Opin Allergy Clin Immunol.*, 2001, 1, pp. 73–78;
239. Robinson D. S., Hamid Q., Ying S., Tsiopoulos A., Barkans J., Bentley A. M., Corrigan C., Durham S. R., Kay A. B., „Predominant TH2-like bronchoalveolar T-lymphocyte population in atopic asthma”, *N Engl J Med*, 1992, 326, pp. 298–304;
240. Panina-Bordignon P., Papi A., Mariani M., Di Lucia P., Casoni G., Bellettato C., Buonsanti C., Miotto D., Mapp C., Villa A., Arrigoni G., Fabbri L. M., Sinigaglia F., „The C-C chemokine receptors CCR4 and CCR8 identify airway T cells of allergen-challenged atopic asthmatics”, *J Clin Invest*, 2001, 107, pp. 1357–1364;
241. Grubek-Jaworska H., Papińska M., Hermanowicz-Salamon J., Białek-Gosk K., Dąbrowska M., Grabczak E., Domagała-Kulawik J., Stępień J., Chazan R., „IL-6 and IL-13 in induced sputum of COPD and asthma patients: correlation with respiratory tests”, *Respiration.*, 2012, 84, 2, pp. 101-7;
242. Beghé B., Hall I. P., Parker S. G., Moffatt M. F., Wardlaw A., Connolly M. J., Fabbri L. M., Ruse C., Sayers I., „Polymorphisms in IL-13 pathway genes in asthma and chronic obstructive pulmonary disease”, *Allergy*, 2010, 65, 4, pp. 474-81;
243. Wills-Karp M., Luyimbazi J., Xu X., Schofield B., Neben T. Y., Karp C. L., Donaldson D. D., „Interleukin-13: central mediator of allergic asthma *Science*”, 1998, 282, pp. 2258–2261;

244. Alcorn J. F., Crowe C. R., Kolls J. K., „TH17 Cells in Asthma and COPD”, *Annual Review of Physiology*, 2010, 72, pp. 495-516;
245. Kinyanjui M. W., Shan J., Nakada E. M., Qureshi S. T., Fixman E. D., „Dose-Dependent Effects of IL-17 on IL-13 Induced Airway Inflammatory Responses and Airway Hyperresponsiveness”, *J Immunol*, 2013, <http://www.jimmunol.org/content/early/2013/03/17/jimmunol.1200506.full.pdf>;
246. Shannon J. P., Yamauchi E. Y., Olivenstein R., Lemiere C., Foley S., Cicora L., Ludwig M., Hamid Q., Martin J. G., „Differences in airway cytokine profile in severe asthma compared to moderate asthma”, *Chest*, 2008, 133, pp. 420–426;
247. Vanaudenaerde B. M., Verleden S. E., Vos R., De Vleeschauwer S. I., Willems-Widyastuti A., Geenens R., Van Raemdonck D. E., Dupont L. J., Verbeken E. K., Meyts I., „Innate and Adaptive Interleukin-17–producing Lymphocytes in Chronic Inflammatory Lung Disorders”, *American Journal of Respiratory and Critical Care Medicine*, 2011, 183, 8, pp. 977-986;
248. Bullens D. M., Truyen E., Coteur L., Dilissen E., Hellings P. W., Dupont L. J., Ceuppens J.L. „IL-17 mRNA in sputum of asthmatic patients: linking T cell driven inflammation and granulocytic influx?”, *Respir Res.*, 2006, 7, 135;
249. Opal S. M., DePalo V. A., Anti-inflammatory cytokines, *Chest*, 2000, 117, 4, pp. 1162-72;
250. Ding-Lei Su, Zhi-Min Lu, Min-Ning Shen, Xia Li, Ling-Yun Sun, Roles of Pro- and Anti-Inflammatory Cytokines in the Pathogenesis of SLE, *Journal of Biomedicine and Biotechnology*, 2012, <http://www.hindawi.com/journals/bmri/2012/347141/>;
251. Sultani M., Stringer A. M., Bowen J. M., Gibson R. J., Anti-Inflammatory Cytokines: Important Immunoregulatory Factors Contributing to Chemotherapy-Induced Gastrointestinal Mucositis, *Chemotherapy Research and Practice*, 2012, <http://www.hindawi.com/journals/cherp/2012/490804/>;
252. Scheller J., Chalaris A., Schmidt-Arras D., Rose-John S., „The pro- and anti-inflammatory properties of the cytokine interleukin-6”, *Biochimica et Biophysica Acta (BBA) - Molecular Cell Research*, 2011, 1813, 5, pp. 878–888;
253. Petra Pietarinen-Runtti, „Regulation of antioxidant defense in cells derived from the human lung”, dissertation 2000, <http://ethesis.helsinki.fi/julkaisut/laa/kliin/vk/pietarinen-runtti/regulati.pdf>;
254. Quinlan T., Spivack S., Mossman B. T., „Regulation of antioxidant enzymes in lung after oxidant injury”, *Environ Health Perspect.*, 1994, 102, 2, pp. 79–87;
255. Auten R. L., Davis J. M., „Oxygen Toxicity and Reactive Oxygen Species: The Devil Is in the Details”, *Pediatric Research*, 2009, 66, pp. 121–127;

256. Suzy A., Comhair A., Bhathena P. R., Farver C., Thunnissen F. B. J. M., Erzurum S. C., „Extracellular glutathione peroxidase induction in asthmatic lungs: evidence for redox regulation of expression in human airway epithelial cells”, *The FASEB Journal*, 2001, 15, 1, pp. 70-78;
257. Sarsour E. H., Kumar M. G., Chaudhuri L., Kalen A. L., Prabhat C., Goswami P. C., „Redox Control of the Cell Cycle in Health and Disease”, *Antioxid Redox Signal*, 2009, 11, 12, pp. 2985–3011;
258. Rasik A. M., Shukla A. „Antioxidant status in delayed healing type of wounds”, *Int J Exp Pathol.*, 2000, 81, pp. 257–263;
259. Poljsak B., Šuput D., Milisav I., „Achieving the Balance between ROS and Antioxidants: When to Use the Synthetic Antioxidants”, *Oxidative Medicine and Cellular Longevity*, 2013, <http://www.hindawi.com/journals/omcl/2013/956792/>;
260. Kinnula V. L., Fattman C. L., Tan R. J., Oury T. D., „Oxidative Stress in Pulmonary Fibrosis”, *American Journal of Respiratory and Critical Care Medicine*, 2005, 172, 4, pp. 417-422;
261. Kinnula V. L., Crapo J. D., „Superoxide dismutases in the lung and human lung diseases”, *Am J Respir Crit Care Med*, 2003, 167, pp. 1600–1619;
262. Valko M., Leibfritz D., Moncol J., Cronin M. T. D., Mazur M., Telser J., Free radicals and antioxidants in normal physiological functions and human disease, *The International Journal of Biochemistry & Cell Biology*, 2007, 39, pp. 44–84;
263. Ahmad A., Shameem M., Husain Q., „Relation of oxidant-antioxidant imbalance with disease progression in patients with asthma”, *Annals of Thoracic Medicine*, 2012, 7, pp. 226-232;
264. Bast A., Haenen G. R., Doelman C. J., „Oxidants and antioxidants: state of the art”, *The American Journal of Medicine*, 1991, 91, pp. 2S-13S;
265. Carter J. D., Driscoll K. E., „The role of inflammation, oxidative stress, and proliferation in silica-induced lung disease: a species comparison”, *Journal of Environmental Pathology, Toxicology and Oncology*, 2011, 20, pp. 33-43;
266. Mohod K., Dhok A., Kumar S., „Status of oxidants and antioxidants in pulmonary tuberculosis with varying bacillary load”, *Journal of Experimental Sciences*, 2011, 2, pp. 35-37;
267. Sah N. K., Singh M., Singhal U., Gupta S., Pandey R., Aggarwal S. K., „Nitric oxide: current perspectives in health and disease”, *Current Trends in Biotechnology and Chemical Research*, 2012, 2, pp. 118-1;
268. Fransen M., Nordgren M., Wang B., Apanasets O., „Role of peroxisomes in ROS/RNS-metabolism: Implications for human disease”, *Biochimica et Biophysica Acta (BBA) - Molecular Basis of Disease*, 2012, 1822, 9, pp. 1363–1373;

269. Cooke M. S., Evans M. D., Dizdaroglu M., Lunec J., „Oxidative DNA damage: mechanisms, mutation, and disease”, *The FASEB Journal*, 2003, 17, 10 pp. 1195-1214;
270. Nediani C., Raimondi L., Borchi E., Cerbai E., „Nitric oxide/reactive oxygen species generation and nitroso/redox imbalance in heart failure: from molecular mechanisms to therapeutic implications”, *Antioxid Redox Signal*, 2011, 14, 2, pp. 289-331;
271. Hsieh H.-J., Liu C.-A., Huang B., Tseng A. H. H., Wang D. L., „Shear-induced endothelial mechanotransduction: the interplay between reactive oxygen species (ROS) and nitric oxide (NO) and the pathophysiological implications”, *Journal of Biomedical Science*, 2014, 21, 3;
272. Trachootham D., Lu W., Ogasawara M. A., Rivera-Del Valle N., Huang P., „Redox Regulation of Cell Survival”, *Antioxid Redox Signal.*, 2008, 10, 8, pp. 1343–1374;
273. Devasagayam T. P. A., Tilak J. C., Bloor K. K., Sane K. S., Ghaskadbi S. S., Lele R. D., „Free radicals and antioxidants in human health: current status and future prospects”, *The Journal association of physicians of India*, 2004, 52, pp. 794–804;
274. Filomeni G., De Zio D., Cecconi F., „Oxidative stress and autophagy: the clash between damage and metabolic needs”, *Cell Death and Differentiation*, 2015 22, pp. 377–388;
275. Kroemer G., Marino G., Levine B., „Autophagy and the integrated stress response”, *Mol Cell* 2010, 40, pp. 280–293;
276. Mardones L., Zúñiga F. A., Villagrán M., Sotomayor K., Mendoza P., Escobar D., González M., Ormazabal V., Maldonado M., Oñate G., Angulo C., Concha I. I., Reyes A. M., Cárcamo J. G., Barra V., Vera J. C., Rivas C. I., „Essential role of intracellular glutathione in controlling ascorbic acid transporter expression and function in rat hepatocytes and hepatoma cells”, *Free Radical Biology and Medicine*, 2012, 52, pp. 1874–1887;
277. Lushchak V. I., „Glutathione Homeostasis and Functions: Potential Targets for Medical Interventions”, *Journal of Amino Acids*, 2012, 26;
278. Sies H., „Glutathione and its role in cellular functions”, *Free Radical Biology and Medicine*, 1999, 27, 9-10, pp. 916–921;
279. Pastore A., Federici G., Bertini E., Piemonte F., „Analysis of glutathione: implication in redox and detoxification”, *Clinica Chimica Acta*, 2003, 1, pp. 19-39;
280. Jozefczak M., Remans T., Vangronsveld J., Cuypers A., „Glutathione Is a Key Player in Metal-Induced Oxidative”, *International Journal of Molecular Sciences*, 2012, 13, pp. 3145-3175;
281. Carmel-Harel O., Storz G., „Roles of the glutathione- and thioredoxin- dependent reduction systems in the *Escherichia coli* and *Saccharomyces cerevisiae* responses to oxidative stress”, *Annual Review of Microbiology*, 2000, 54, pp. 439-461;

282. Lipton A. J., Johnson M. A., Macdonald T., Lieberman M. W., Gozal D., Gaston B. „S-Nitrosothiols signal the ventilatory response to hypoxia”, *Nature*, 2001, 413, pp. 171-174;
283. Beeh K.M., Beier J., Haas I.C., Kornmann O., Micke P., Buhl R., „Glutathione deficiency of the lower respiratory tract in patients with idiopathic pulmonary fibrosis”, *Eur Respir J.*, 2002, 19, pp. 1119–1123;
284. Vlahos R., Bozinovski S., „Glutathione peroxidase-1 as a novel therapeutic target for COPD”, *Redox Report*, 2013, 18, 4;
285. Bentley A. R., Emrani P., Cassano P. A., „Genetic variation and gene expression in antioxidant related enzymes and risk of COPD: a systematic review”, *Thorax*, 2008, 63, 11, pp. 956–61;
286. Beeh K. M., Beier J., Koppenhoefer N., Buhl R., „Increased glutathione disulfide and nitrosothiols in sputum supernatant of patients with stable COPD”, *Chest.*, 2004, 126, 4, pp. 1116-22;
287. Geraghty P., Hardigan A. A., Wallace A. M., Mirochnitchenko O., Thankachen J., Arellanos L., Thompson V., D'Armiento J. M., Foronjy R. F., „The glutathione peroxidase 1-protein tyrosine phosphatase 1B-protein phosphatase 2A axis. A key determinant of airway inflammation and alveolar destruction”, *Am J Respir Cell Mol Biol.*, 2013, 49, 5, pp. 721-30;
288. Schmidt R., Luboinski T., Markart P., Ruppert C., Daum C., Grimminger F., Seeger W., Gunther A., „Alveolar antioxidant status in patients with acute respiratory distress syndrome”, *Eur Respir J.*, 2004, 24, pp. 994–999;
289. Bunnell E., Pacht E. R., „Oxidized Glutathione Is Increased in the Alveolar Fluid of Patients with the Adult Respiratory Distress Syndrome”, *American Review of Respiratory Disease*, 1993, 148, 5, pp. 1174-1178;
290. Smith L. J., Houston M., Anderson J., „Increased levels of glutathione in bronchoalveolar lavage fluid from patients with asthma”, *Am Rev Respir Dis*, 1993, 147, pp. 1461–1464;
291. Comhair S. A. A., Ricci K. S., Arroliga M., Lara A. R., Dweik R. A., Song W., Hazen S. L., Bleecker E. R., Busse W. W., Chung K. F., Gaston B., Hastie A., Hew M., Jarjour N., Moore W., Peters S., Teague W. G., Wenzel S. E., Erzurum S. C., „Correlation of Systemic Superoxide Dismutase Deficiency to Airflow Obstruction in Asthma”, *American Journal of Respiratory and Critical Care Medicine*, 2005, 172, 3, pp. 306-313;
292. Gaston B., Drazen J. M., Loscalzo J., Stamler J. S., „The biology of nitrogen oxides in the airways”, *Am J Respir Crit Care Med*, 1994, 149, pp. 538–551;
293. Reynaert N. L., „Glutathione biochemistry in asthma”, 2011, 1810, 11, pp. 1045-51;

294. Fitzpatrick A. M., Teague W. G., Burwell L., Brown M. S., Brown L. A. S., „Glutathione Oxidation Is Associated With Airway Macrophage Functional Impairment in Children With Severe Asthma”, *Pediatric Research*, 2011, 69, pp. 154–159;
295. Delfino R. J., „Epidemiologic evidence for asthma and exposure to air toxics: linkages between occupational, indoor, and community air pollution research”, *Environ Health Perspect.*, 2002, 110, 4, pp. 573–589;
296. Delfino R. J., Gong H. Jr, Linn W. S., Pellizzari E. D., Hu Y., Asthma symptoms in Hispanic children and daily ambient exposures to toxic and criteria air pollutants, *Environ Health Perspect.*, 2003, 111, 4, pp. 647–656;
297. Fuciu A., Gamulin M., Ferencic Z., Rokotov D. S., Katic J., Bartonova A., Lovasic I. B., Merlo D. F., „Lung Cancer and Environmental Chemical Exposure: A Review of Our Current State of Knowledge With Reference to the Role of Hormones and Hormone Receptors as an Increased Risk Factor for Developing Lung Cancer in Man”, *Toxicologic Pathology*, 2010, 38, pp. 849-855;
298. Schulte H. von A., Bernauer U., Madle S., Mielke H., Herbst U., Richter-Reichhelm H.-B., Appel K.-E., Gundert-Remy U., „Assessment of the Carcinogenicity of Formaldehyde [CAS No. 50-00-0]”, Bericht zur Bewertung der Karzinogenität von Formaldehyd, ISBN 3-938163-14-3, [http://www.bfr.bund.de/cm/350/assessment\\_of\\_the\\_carcinogenicity\\_of\\_formaldehyde.pdf](http://www.bfr.bund.de/cm/350/assessment_of_the_carcinogenicity_of_formaldehyde.pdf);
299. Salthammer T., Mentese S., Marutzky R., „Formaldehyde in the Indoor Environment”, *Chem Rev.*, 2010, 110, 4, pp. 2536–2572;
300. Leikauf G. D., „Hazardous air pollutants and asthma”, *Environ Health Perspect.*, 2002, 110, 4, pp. 505–526;
301. Rajan K. G., Davies B. H., „Reversible airways obstruction and interstitial pneumonitis due to acetic acid”, *Br J Ind Med.*, 1989, 46, 1, pp. 67–68;
302. Morris J. B., Symanowicz P. T., Olsen J. E., Thrall R. S., Cloutier M. M., Hubbard A. K., „Immediate sensory nerve-mediated respiratory responses to irritants in healthy and allergic airway-diseased mice”, *J. Appl. Physiol.*, 2003, 94, 4, pp. 1563-1571;
303. Ernstgard L., Iregren A., Sjogren B., Johanson G., „Acute effects of exposure to vapours of acetic acid in humans”, *Toxicol. Lett.*, 2006, 165, 1, pp. 22 -30;
304. Zuskin E., Mustajbegovic J., Schachter E. N., Pavicic D., Budak A., „A follow-up study of respiratory function in workers exposed to acid aerosols in a food -processing industry”, *Int. Arch. Occup. Environ. Health*, 1997, 70, pp. 413-418;
305. Fiedler N., Laumbach R., Kelly-McNeil K., „Health Effects of a Mixture of Indoor Air Volatile Organics, Their Ozone Oxidation Products, and Stress”, *Environmental Health Perspectives*, 2005, 113, 11, pp. 1542-1548;

306. Klenø J. G., Wolkoff P., „Changes in eye blink frequency as a measure of trigeminal stimulation by exposure to limonene oxidation products, isoprene oxidation products and nitrate radicals”, *Int Arch Occup Environ Health*, 2004, 77, pp. 235-243;
307. Koren H. S., Devlin R. B., House D., Steingold S., Graham D. E., „Exposure of humans to a volatile organic mixture”, III. Inflammatory Response. *Archives of Environmental Health*, 1992, 47, pp. 39–44;
308. Cometto-Muniz J., Cain W., Abraham M., Kumarsingh R., „Sensory properties of selected terpenes—thresholds for odor, nasal pungency, nasal localization, and eye irritation”, *Annals of the New York Academy of Sciences*, 1998, 855, pp. 648–651;
309. Nøjgaard K., Christensen J. G., Wolkoff P., „The effect on human eye blink frequency of exposure to limonene oxidation products and methacrolein“, *Toxicology Letters*, 2005, 156, pp. 241-251;
310. Laumbach R. J., Fiedler N., Gardner C. R., Laskin D. L., Fan Z. H., Zhang J., Weschler C. J., Liroy P. J., Devlin R. B., Ohman-Strickland P., Kelly-McNeil K., Kipen H. M., „Nasal Effects of a Mixture of Volatile Organic Compounds and Their Ozone Oxidation Products”, *Journal of Occupational & Environmental Medicine*, 2005, 47, 11, pp. 1182-1189;
311. Clausen P. A., Wilkins C. K., Wolkoff P., Nielsen G. D., „Chemical and biological evaluation of a reaction mixture of R-(+)-limonene/ozone: formation of strong airway irritants”, *Environ Int.*, 2001, 26, 7-8, pp. 511-22;
312. Rohr A. C., Wilkins C. K., Clausen P. A., Hammer M., Nielsen G. D., Wolkoff P., Spengler J. D., „Upper airway and pulmonary effects of oxidation products of (+)-alpha-pinene, d-limonene, and isoprene in BALB/c mice”, *Inhal Toxicol.*, 2002, 14, 7, pp. 663-84;
313. Wolkoff P., Clausen P. A., Wilkins C. K., Nielsen G. D., „Formation of strong airway irritants in terpene/ozone mixtures”, *Indoor Air*, 2000, 10, pp. 82–91;
314. Wilkins C. K., Wolkoff P., Clausen P. A., Hammer M., Nielsen G. D., „Upper airway irritation of terpene/ozone oxidation products (TOPS). Dependence on reaction time, relative humidity and initial ozone concentration”, *Toxicology Letters*, 2003, 143, pp. 109-114;
315. Sunil V. R., Laumbach R. J., Patel K. J., Turpin B. J., Lim H.-J., Kipen H. M., Laskin J. D., Laskin D. L., „Pulmonary effects of inhaled limonene ozone reaction products in elderly rats”, *Toxicology and Applied Pharmacology*, 2007, 222, pp. 211–220;
316. Wolkoff P., Clausen P. A., Larsen K., Hammer M., Larsen S. T., Nielsen G. D., „Acute airway effects of ozone-initiated d-limonene chemistry: importance of gaseous products”, *Toxicol Lett.*, 2008, 181, 3, pp. 171-6;

317. Wolkoff P., Clausen P. A., Larsen S. T., Hammer M., Nielsen G. D., „Airway effects of repeated exposures to ozone-initiated limonene oxidation products as model of indoor air mixtures”, *Toxicology Letters*, 2012, 209, pp. 166– 172;
318. Jeffrey A. M., Iatropoulos M. J., Williams G. M., „Nasal Cytotoxic and Carcinogenic Activities of Systemically Distributed Organic Chemicals”, *Toxicol Pathol*, 2006, 34, 7, pp. 827-852;
319. Roberts S. M., James R. C., Williams P. L., „Principles of Toxicology: Environmental and Industrial Applications”, 3rd Edition, ISBN: 978-0-470-90791-7, 496 pages;
320. Bond J. A., „Metabolism of xenobiotics by the respiratory tract”, Chapter 7, Gardner DE, editor *Toxicology of the lung*, 1993, New York: Raven Press Ltd., pp. 187-215;
321. Niemeier R. W., „The isolated perfused lung”, *Environ Health Perspect*, 1984, 56, pp. 35-41;
322. Tronde A., Norden B., Jeppsson A. B., Brunmark P., Nilsson E., Lennernas H., Bengtsson U. H., „Drug absorption from the isolated perfused rat lung--correlations with drug physicochemical properties and epithelial permeability”, *J Drug Target*, 2003, 11, pp. 61-74;
323. Saldias F. J., Comellas A., Guerrero C., Ridge K. M., Rutschman D. H., Sznajder J. I., „Time course of active and passive liquid and solute movement in the isolated perfused rat lung model”, *J Appl Physiol*, 1998, 85, pp. 1572-7;
324. Clemedson C., Mcfarlane-Abdulla E., Andersson M., Barile B., Calleja M. C., Chesné C., Clothier R., Cottin M., Curren R., Dierickx P. J., Ferro M., Fiskejö G., Garza-Ocañas, Gómez-Lechón M. J., Gülden M., Isomaa B., Janus J., Judge P., Kahru A., Kemp R. B., Kerszman G., Kristen U., Kunimoto M., Kärenlampi S., Lavrijssen K., Lewan L., Lilius H., Ma Imsten A., Ohno T., Persoone G., Pettersson R., Roguet R., Romert L., Sandberg M., Sawyer Th. W., Seibert H., Shrivastava R., Sjöström M., Stamatii A., Tanaka N., Torres-Alanis O., Voss J-U., Wakuri Sh., Walum E., Wang X., Zucco F., Ekwall B., „MEIC Evaluation of acute systemic toxicity, Part II. *In vitro* results from 68 toxicity assays used to test the first 30 reference chemicals and a comparative cytotoxicity analysis”, *ATLA*, 1996, 24, pp. 273-311;
325. Ekwall B., „Screening of Toxic Compounds in Mammalian Cell Cultures”, *Ann. New York Acad. Sci.*, 1983, 407, pp. 64-77;
326. Ekwall B., Clemedson C., Crafoord B., Ekwall Ba., Hallander S., Walum E., Bondesson I., „MEIC Evaluation of Acute Systemic Toxicity. Part V Rodent and Human Toxicity Data for the 50 Reference Chemicals”, *ATLA*, 1998a, 26, 2, pp. 569-615;

327. Lechner J. F., Haugen A., McClendon I. A., Shamsuddin A. K. M., „Induction of squamous differentiation of normal human bronchial epithelial cells by small amounts of serum”, *Differentiation*, 1984, 25, pp. 229–237;
328. Gray T. E., Guzman K., Davis C. W., Abdullah L. H., Nettesheim P., „Mucociliary differentiation of serially passaged normal human tracheobronchial epithelial cells”, *Am J Respir Cell Mol Biol.*, 1996, 14, pp. 104-112;
329. Davis A. S., Chertow D. S., Moyer J. E., Suzich J., Sandouk A., Dorward D. W., Logun C., Shelhamer J. H., Taubenberger J. K., „Validation of Normal Human Bronchial Epithelial Cells as a Model for Influenza A Infections in Human Distal Trachea”, *Journal of Histochemistry & Cytochemistry*, 2015, 63, 5, pp. 312–328;
330. Chemuturi N.V., Hayden P., Klausner M., Donovan M. D., „Comparison of human tracheal/bronchial epithelial cell culture and bovine nasal respiratory explants for nasal drug transport studies”, *J. Pharm. Sci.*, 2005, 94, pp. 1976–1985;
331. <http://www.mattek.com/epiAirway/features>;
332. <http://www.epithelix.com/>;
333. Foster K. A., Avery M. L., Yazdanian M., Audus K. L., „Characterization of the Calu-3 cell line as a tool to screen pulmonary drug delivery”, *Int. J. Pharm.*, 2000, 208, pp. 1 – 11;
334. Grainger C. I., Greenwell L. L., Lockley D. J., Martin G.P., Forbes B., „Culture of Calu-3 cells at the air–liquid interface provides a representative model of the airway epithelial barrier”, *Pharm. Res.*, 2006, 23, pp. 1482–1490;
335. Kinnula V. L., Yankaskas J. R., Chang L., Virtanen I., Linnala A., Kang B. H., Crapo JD., „Primary and immortalized (BEAS 2B) human bronchial epithelial cells have significant antioxidative capacity in vitro”, *Am J Respir Cell Mol Biol.*, 1994, 11, 5, pp. 568-76;
336. Forbes B., Shah A., Martin G. P., Lansley A. B., „ The human bronchial epithelial cell line 16HBE14o- as a model system of the airways for studying drug transport”, *Int J Pharm.*, 2003, 12, 257, 1-2, pp. 161-7;
337. Cozens A. L., Yezzi M. J., Kunzelmann K., Ohrui T., Chin L., Eng K., Finkbeiner W. E., Widdicombe J. H., Gruenert D. C., „CFTR expression and chloride secretion in polarized immortal human bronchial epithelial cells”, *Am. J. Respir. Cell. Mol. Biol.*, 1994, 10, pp. 38–47;
338. Elbert K. J., Schäfer U. F., Schäfers H. J., Kim K. J., Lee V. H., Lehr C. M., „Monolayers of human alveolar epithelial cells in primary culture for pulmonary absorption and transport studies”, *Pharm. Res.* 1999, 16, pp. 601–608;
339. Rehan V. K., Torday J. S., Peleg S., Gennaro L., Vouros P., Padbury J., Rao S., Satyanarayana R. G., „1Alpha, 25-dihydroxy-3-epi-vitamin D3, a natural metabolite of

- 1alpha, 25-dihydroxy vitamin D3: production and biological activity studies in pulmonary alveolar type II cells”, *Mol Genet Metab.*, 2002, 76, pp. 46-56;
340. Cottier M., Tchirkov A., Perissel B., Giollant M., Campos L., Vago P., „Cytogenetic characterization of seven human cancer cell lines by combining G- and R-banding, M-FISH, CGH and chromosome and locus-specific FISH”, *Int J Mol Med*, 2004, 14, pp. 483-95;
341. Hermanns M. I., Unger R. E., Kehe K., Peters K., Kirkpatrick C. J., „Lung epithelial cell lines in coculture with human pulmonary microvascular endothelial cells: development of an alveolo-capillary barrier in vitro”, *Lab. Invest. J. Tech. Methods Pathol.*, 2004, 84, pp. 736-752;
342. Tsuchiya S., Yamabe M., Yamaguchi Y., Kobayashi Y., Konno T., Tada K., „Establishment and characterization of a human acute monocytic leukemia cell line (THP-1)”, *Int. J. Cancer*, 1980, 26, pp. 171-176;
343. Littlefield M. J., Teboul I., Voloshyna I., Reiss A. B., Polarization of Human THP-1 Macrophages: Link between Adenosine Receptors, Inflammation and Lipid Accumulation, *Int J Immunol Immunother*, 2014, 1, 1, ISSN: 2378-3672;
344. Kwok A. K H, Yeung C-K., Lai T. Y. Y., Chan K-P., Pang C. P., „Effects of trypan blue on cell viability and gene expression in human retinal pigment epithelial cells”, *Br J Ophthalmol.*, 2004, 88, 12, pp. 1590–1594;
345. Rezai K. A., Farrokh-Siar L., Gasyna E. M., Ernest J. T., „Trypan blue induces apoptosis in human retinal pigment epithelial cells”, *Am J Ophthalmol.*, 2004, 138, 3, pp. 492-5;
346. Nielsen L. K., Smyth G. K., Greenfield P. F., „Hemocytometer Cell Count Distributions: Implications of Non-Poisson Behavior”, *Biotechnol. Progr.*, 1991, 7, 6, pp. 560–563;
347. Pappenheimer Alwin M., „Experimental studies upon lymphocytes. I. The reactions of lymphocytes under various experimental conditions”, *J. Exper. Med.*, 1917, 25, 633;
348. Neuman M. G., Malkiewicz I. M, Shear N. H., „A novel lymphocyte toxicity assay to assess drug hypersensitivity syndromes”, *Clin Biochem.*, 2000, 33, 7, pp. 517-24;
349. Freshney R., „Culture of Animal Cells: A Manual of Basic Technique”, New York: Alan R Liss Inc, 1987, pp. 117;
350. Smith J., Ongena K., „The new Scepter 2.0 Cell counter enables the analysis of a wider range of cell sizes and types with high precision”, *Merck Millipore Cellutions*, 2011, 1, pp. 19-22;
351. Lin Ming Xian, Hyun Kyung-A, Moon Hui-Sung, Sim Tae Seok, Lee Jeong-Gun, Park Jae Chan, Lee Soo Suk, Jung Hyo-II, „Continuous labeling of circulating tumor cells

- with microbeads using a vortex micromixer for highly selective isolation”, Elsevier, Biosensors and Bioelectronics, 2013, 40, pp. 63-67;
352. Bronzini Patruno M., Iacopetti I., Martinello T., „Influence of temperature, time and different media on mesenchymal stromal cells shipped for clinical application”, The Veterinary Journal, 2012, 194, pp. 121-123;
353. Ongena K., J. L., Gil S., Johnston G., „Determining Cell Number During Cell Culture using the Scepter Cell Counter”, Journal of Visualized Experiments, 2010, 45, pp. 1-5;
354. Houwen B., „Fifty years of hematology innovation: the Coulter principle, Medical Laboratory Observer”, BioTechniques, 2010, 48, pp. 325-327;
355. Nogueira D. R., Mitjans M., Infante M. R., Vinardell M. P., „Comparative sensitivity of tumor and non-tumor cell lines as a new approach for in vitro cytotoxicity screening of lysine-based surfactants with potential pharmaceutical applications”, <http://diposit.ub.edu/dspace/bitstream/2445/33815/1/598681.pdf>;
356. Moravec R., Riss T., „Assay system for detecting apoptosis and cell death”, Promega notes, 1998, 68, pp. 13-8;
357. Berridge M. V., Herst P. M., Tan A. S., Tetrazolium dyes as tools in cell biology: New insights into their cellular reduction, Biotechnology annual review, 2005, 11, ISSN: 1387-2656;
358. Fotakis G., Timbrell J. A., „In vitro cytotoxicity assays: Comparison of LDH, neutral red, MTT and protein assay in hepatoma cell lines following exposure to cadmium chloride”, Toxicology Letters, 2006, 160, pp. 171–177;
359. Babich H., Borenfreund E., „Neutral red assay for toxicology in vitro”, Watson, RR (Ed.), In Vitro Methods of Toxicology, 1992, CRC Press Inc, Boca Raton, pp. 237-252;
360. Borenfreund E., Babich H., „The neutral red cytotoxicity assay”, INVITTOX Protocol 64, 1992, <http://ecvam-sis.jrc.it/invittox/static/index.html>;
361. Bourdeau P., Sommers E., Mark Richardson G., Hickman J. R., International Council of Scientific Unions. Scientific Committee on Problems of the Environment, International Programme on Chemical Safety, „Short-term toxicity tests for non-genotoxic effects”, Chichester Wiley (Ed.), SCOPE report, 1990, 41, chapter 3;
362. Champion S., Aubrecht J., Boekelheide K., Brewster D. W., Vaidya V. S., Anderson L., Burt D., Dere E., Hwang K., Pacheco S., Saikumar J., Schomaker S., Sigman M., Goodsaid F., „The current status of biomarkers for predicting toxicity”, Expert Opin Drug Metab Toxicol., 2013, 9, 11;
363. Tarrant J. M., „Blood cytokines as biomarkers of in vivo toxicity in preclinical safety assessment: considerations for their use”, Review of the use of cytokines as biomarkers, Toxicol Sci., 2010, 117, 1, pp. 4–16;

364. Lee R., Margaritis M., Channon K. M., Antoniades C., „Evaluating Oxidative Stress in Human Cardiovascular Disease: Methodological Aspects and Considerations”, *Curr Med Chem.*, 2012, 19, 16, pp. 2504–2520;
365. Ho E., Galougahia K. K., Liu C-C., Bhindia R., Figtree G. A., „Biological markers of oxidative stress: Applications to cardiovascular research and practice”, *Redox Biology*, 2013, 1, pp. 483–491;
366. Palmieri B., Sblendorio V., „Oxidative stress detection: what for?” Part II, *European Review for medical and pharmacological sciences*, 2007, 11, pp. 27-54;
367. Liu L., Poon R., Chen L., Frescura A. M., Montuschi P., Ciabattini G., Wheeler A., Dales R., „Acute effects of air pollution on pulmonary function, airway inflammation, and oxidative stress in asthmatic children”, *Environ. Health perspect.*, 2009, 117, pp. 668-674;
368. Yang P., Ebbert J. O., Zhifu Sun Z., Weinshilboum R. M., „Role of the Glutathione Metabolic Pathway in Lung Cancer Treatment and Prognosis: A Review”, *Journal of Clinical Oncology*, 2006, 24, 11, pp. 1761-1769;
369. Sen S., Chakraborty R., Sridhar C., Reddy Y. S. R., De B., „Free radicals, antioxidants, diseases and phytomedicines: current status and future prospect”, *International Journal of Pharmaceutical Sciences Review and Research*, 2010, 3, 1, pp. 91–100;
370. Gomez-Amores L., Mate A., Revilla E., Santa-Maria C., Vazquez C. M., „Antioxidant activity of propionyl-L-carnitine in liver and heart of spontaneously hypertensive rats”, *Life Sciences*, 2006, 78, pp. 1945-1952;
371. Blanco R. A., Ziegler T. R., Carlson B. A., Cheng P-Y., Park Y., Cotsonis G. A., Accardi C. J., Jones D. P., „Diurnal variation in glutathione and cysteine redox states in human plasma”, *Am J Clin Nutr.*, 2007, 86, 4, pp. 1016-1023;
372. Senft A. P., Dalton T. P., Shertzer H. G., „Determining glutathione and glutathione disulfide using the fluorescent probe o-phthalaldehyde”, *Analytical Biochemistry*, 2000, 280, pp. 80-86;
373. Guvenc M., Cetintas B., Irtegun S., Tastan H., Sahin K, „A Practical HPLC Method to Measure Reduced (GSH) and Oxidized (GSSG) Glutathione Concentrations in Animal Tissues”, *Journal of Animal and Veterinary Advances*, 2009, 8, 2, pp. 343-347;
374. Anderson S. E., Khurshid S. S., Meade B. J., Lukomska E., Wells J. R., „Toxicological analysis of limonene reaction products using an in vitro exposure system”, *Toxicol In Vitro*, 2012, 27, 2, pp. 721-730;
375. ECA-Indoor Air Quality, „Guideline for the characterization of volatile organic compounds emitted from indoor materials and products using small test chamber”, *European Collaborated Action „Indoor Air Quality and its Impact on Man”*, report 8, EUR

13593 EN, 1991, European Commission, Luxembourg: Office for Official Publications of the European Communities;

376. Trabue S. L., Anhalt J. C., Zahn J. A., „Bias of Tedlar bags in the measurement of agricultural odorants”, *J Environ Qual.*, 2006, 35, 5, pp. 1668-77;

377. Koziel J. A., Spinhirne J. P., Lloyd J. D., Parker D. B., „Evaluation of same recovery of odorous VOCs and semi-VOCs from odor bags, sampling canisters, tenax TA sorbent tubes, and SPME”, *AIP Conf. Proc.*, 2009, 1137, 55;

378. HSDB, „Picric acid, in: Hazardous Substances Data Bank”, National Library of Medicine, Bethesda, MD, USA. <http://www.nlm.nih.gov> (Toxnet), accessed August 11, 2014;

379. Lieber M., Smith B., Szakal A., Nelson-Rees W., Todaro G., „A continuous tumor-cell line from a human lung carcinoma with properties of type II alveolar epithelial cells”, *Int J Cancer*, 1976, 17, 1, pp. 62–70;

380. Jiang J.-G., Fu X.-N., Chen C.-L., Wang D.-W., „Expression of cytochrome P450 arachidonic acid epoxygenase 2J2 in human tumor tissues and cell lines”, *Chinese Journal of Cancer*, 2009, 28, 2, pp. 93-96, <http://www.cjcsysu.com/ENpdf/2009/2/93.pdf>;

381. Gomez-Casal R., Bhattacharya C., Ganesh N., Bailey L., Basse P., Gibson M., Epperly M., Levina V., „Non-small cell lung cancer cells survived ionizing radiation treatment display cancer stem cell and epithelial-mesenchymal transition phenotypes”, *Molecular Cancer*, 2013, 12, 94;

382. Gazdar A. F., Girard L., Lockwood W. W., Lam W. L., Minna J. D., „Lung Cancer Cell Lines as Tools for Biomedical Discovery and Research”, *J Natl Cancer Inst.*, 2010, 102, 17, pp. 1310–1321;

383. Chen Q., Catharine R. A., „Retinoic acid regulates cell cycle progression and cell differentiation in human monocytic THP-1 cells”, *Exp Cell Res.*, 2004, 297, pp. 68–81;

384. Tsuchiya S., Kobayashi Y., Goto Y., Okumura H., Nakae S., Konno T., Tada K. „Induction of maturation in cultured human monocytic leukemia cells by a phorbol diester”, *Cancer Res.*, 1982, 42, pp. 530–6;

385. Schwende H., Fitzke E., Ambs P., Dieter P. „Differences in the state of differentiation of THP-1 cells induced by phorbol ester and 1,25- dihydroxyvitamin D3”, *J Leukoc Biol* 1996, 59, pp. 555–61;

386. Humeniuk-Polaczek R., Marcinkowska E. „Impaired nuclear localization of vitamin D receptor in leukemia cells resistant to calcitriol- induced differentiation”, *J Steroid Biochem Mol Biol*, 2004, 88, pp. 361–6;

387. Liang F., Seyrantepe V., Landry K., Ahmad R., Ahmad A., Stamatou N. M., Pshezhetsky A. V., „Monocyte Differentiation Up-regulates the Expression of the Lysosomal Sialidase, Neu1, and Triggers Its Targeting to the Plasma Membrane via Major

Histocompatibility Complex Class II-positive Compartments”, *The Journal of Biological Chemistry*, 2006, 281, pp. 27526-27538;

388. Adati N., Huang M.-C., Suzuki T., Suzuki H., Kojima T., „High-resolution analysis of aberrant regions in autosomal chromosomes in human leukemia THP-1 cell line”, *BMC Research Notes*, 2009, 2, 153;

389. Auwer J., *The human leukemia cell line, THP-1 : A multifaceted model for the study of monocyte-macrophage differentiation*, *Experientia* 47, 1991, BirkhS.user Verlag, CH-4010 Basel/Switzerland;

390. Harrison L. M., Christel van den Hoogen, Wilhelmina C. E. van Haaften, Tesh V. L., „Chemokine Expression in the Monocytic Cell Line THP-1 in Response to Purified Shiga Toxin 1 and/or Lipopolysaccharides”, *Infect Immun.*, 2005, 73, 1, pp. 403–412;

391. Ehrhardt C., Kneuer C., Fiegel J., Hanes J., Schaefer U. F., Kim K.-J., Lehr C.-M., „Influence of apical fluid volume on the development of functional intercellular junctions in the human epithelial cell line 16HBE14o-: implications for the use of this cell line as an in vitro model for bronchial drug absorption studies”, *Cell Tissue Res.*, 2002, 308, pp. 391–400;

392. Forbes B., Shah A., Martin G. P., Lansley A. B., „The human bronchial epithelial cell line 16HBE14o—as a model system of the airways for studying drug transport”, *International Journal of Pharmaceutics*, 2003, 257, pp. 161–167;

393. Forbes B., „Human airway epithelial cell lines for in vitro drug transport and metabolism studies”, *Pharm. Sci. Technol.*, 2000, 3, pp. 18–27;

394. Carroll T. P., Greene C. M., Taggart C. C., Bowie A. G., O'Neill S. J., McElvaney N. G., „Viral Inhibition of IL-1- and Neutrophil Elastase-Induced Inflammatory Responses in Bronchial Epithelial Cells”, *J Immunol*, 2005, 175, pp. 7594-7601;

395. Gersting S. W., Schillinger U., Lausier J., Nicklaus P., Rudolph C., Plank C., Reinhardt D., Rosenecker J., „Gene delivery to respiratory epithelial cells by magnetofection”, *J Gene Med.*, 2004, 6, 8, pp. 913-22;

396. Heijink I. H., Brandenburg S. M., Noordhoek J. A., Postma D. S., Slebos D.-J., van Oosterhout A. J. M., „Characterisation of cell adhesion in airway epithelial cell types using electric cell–substrate impedance sensing”, *ERJ*, 2010, 35, 4, pp. 894-903;

397. Heijink I. H., Kies P. M., Kauffman H. F., Postma D. S., van Oosterhout A. J., Vellenga E. „Down-regulation of E-cadherin in human bronchial epithelial cells leads to epidermal growth factor receptor-dependent Th2 cell-promoting activity”, *J Immunol*, 2007, 178, 12, pp. 7678-85;

398. Gruenert D. C., Finkbeiner W. E., Widdicombe J. H., „Culture and transformation of human airway epithelial cells”, *Am J Physiol.*, 1995, 268, pp. L347-60;

399. Bleck B., Tse D. B., Gordon T., Ahsan M. R., Reibman J., „Diesel exhaust particle-treated human bronchial epithelial cells upregulate Jagged-1 and OX40L in myeloid dendritic cells via TSLP”, *J Immunol.*, 2010, 185, 11, pp. 6636–6645;
400. Brzoska M., Langer K., Coester C., Loitsch S., Wagner T. O., Mallinckrodt C., „Incorporation of biodegradable nanoparticles into human airway epithelium cells—In vitro study of the suitability as a vehicle for drug or gene delivery in pulmonary diseases”, *Biochem. Biophys. Res. Commun.*, 2004, 318, pp. 562–570;
401. Rach J., Budde J., Möhle N., Aufderheide M., „Direct exposure at the air–liquid interface: evaluation of an in vitro approach for simulating inhalation of airborne substances”, *Journal of Applied Toxicology*, 2014, 34, pp. 506–515;
402. Schindler S., Asmus S., von Aulock S., Wendel A., Hartung T., Fennrich S., „Cryopreservation of human whole blood for pyrogenicity testing”, *Journal of immunological methods*, 2004, 294, 1-2, pp. 89-100;
403. Park E. K., Jung H. S., Yang H. I., Yoo M. C., Kim C., Kim K. S., „Optimized THP-1 differentiation is required for the detection of responses to weak stimuli”, *Inflamm Res*, 2007, 56, 1, pp. 45-50;
404. The National Toxicology Program (NTP) Interagency Center for the Evaluation of Alternative Toxicological Methods (NICEATM), „Test method protocol for the NHK neutral red uptake cytotoxicity assay”, 2003, <http://ntp.niehs.nih.gov/iccvam/methods/acutetox/invidocs/phiiiiprot/nhkphiii.pdf>;
405. Repetto G., del Peso A., Zurita J. L., „Neutral red uptake assay for the estimation of cell viability/cytotoxicity”, *Nat Protoc.*, 2008, 3, 7, pp. 1125-31;
406. Halliwell B., Whitemann M., „Measuring reactive species and oxidative damage in vivo and in cell culture: how should you do it and do the results mean?”, *British Journal of Pharmacology*, 2004, 142, pp. 231-255;
407. Danielsson R., Bylund D., Markides K. E., „Matched filtering with background suppression for improved quality of base peak chromatograms and mass spectra in liquid chromatography -mass spectrometry”, *Analytica Chimica Acta*, 2002, 454, pp. 167-184;
408. Patti G. J., Tautenhahn R., Siuzdak G., „Meta-analysis of untargeted metabolomic data from multiple profiling experiments”, *Nature Protocols*, 2012, 7, pp. 508–516;
409. Prince J. T., Marcotte E. M., „Chromatographic alignment of ESI-LC-MS proteomics data sets by ordered bijective interpolated warping”, *Anal Chem.*, 2006, 78, 17, pp. 6140-52;
410. Berg R. A., Hoefsloot H. C., Westerhuis J. A., Smilde A. K., Werf M. J., „Centering, scaling, and transformations: Improving the biological information content of metabolomics data”, *BMC-Genomics*, 2006, 7, 142;

411. Ruth J. H., „Odor Thresholds and Irritation Levels of Several Chemical Substances: A Review”, *AIHAJ*, 1986, 47, pp. A142-A151;
412. Hogg N., „The biochemistry and physiology of S-nitrosothiols”, *Annu Rev Pharmacol Toxicol*, 2002, 42, pp. 585–600;
413. Tsikas D., Sandmann J., Holzberg D., Pantazis P., Raida M., Frölich J. C., „Determination of S-nitrosoglutathione in human and rat plasma by high-performance liquid chromatography with fluorescence and ultraviolet absorbance detection after precolumn derivatization with o-phthalaldehyde”, *Anal Biochem.*, 1999, 273, 1, pp. 32-40;
414. Airaki M., Sanchez-Moreno L., Leterrier M., Barroso J. B., Palma J. M., Corpas F. J., „Detection and Quantification of S-Nitrosoglutathione (GSNO) in Pepper (*Capsicum annum* L.) Plant Organs by LC-ES/MS”, *Plant & Cell physiology*, 2011, 52, 11, pp. 2006-2015;
415. Afzal M., Afzal A., Jones A., Armstrong D., „A rapid method for the quantification of GSH and GSSG in biological samples”, *Methods Mol Biol.*, 2002, 186, pp. 117-22;
416. Rossi R., Milzani A., Dalle-Donne I., Giustini D., Lusini L., Colombo R., Di Simplicio P., „Blood glutathione disulfide : in vivo factor or in vitro artefact”, *Clinical Chemistry*, 2002, 48, 5, pp. 745-753;
417. Yap L-P., Sancheti H., Ybanez M. D., Garcia J., Cadenas E., Han D., „Determination of GSH, GSSG, and GSNO Using HPLC with Electrochemical Detection”, *Methods Enzymol.*, 2010, 473, pp. 137–147;
418. Pariselli F., Sacco M. G., Rembges D., „An optimized method for in vitro exposure of human derived lung cells to volatile chemicals”, *Exp Toxicol Pathol.*, 2009, 61, 1, pp. 33-9;
419. Calabrese E. J., „Hormesis: a revolution in toxicology, risk assessment and medicine”, *EMBO Rep.*, 2004, 5, 1, pp. S37–S40;
420. Rithidech K. N., Scott B. R., „Evidence for radiation hormesis after in vitro exposure of human lymphocytes to low doses of ionizing radiation”, *Dose-Response*, 2008, 6, pp. 252–271;
421. Calabrese V., Bates T. E., Mancuso C., Cornelius C., Ventimiglia B., Cambria M. T., Di Renzo L., De Lorenzo A., Dinkova-Kostova A. T., „Curcumin and the cellular stress response in free radical-related diseases”, *Mol Nutr Food Res.*, 2008, 52, pp. 1062–1073;
422. Calabrese E. J., „Cancer biology and hormesis: human tumor cell lines commonly display hormetic (biphasic) dose responses”, *Crit Rev Toxicol.*, 2005, 35, 6, pp. 463-582;
423. Wolkoff P., Larsen S. T., Hammer M., Kofoed-Sørensen V., Clausen P. A., Nielsen G. D., „Human reference values for acute airway effects of five common ozone-initiated terpene reaction products in indoor air”, *Toxicology Letters*, 2013, 216, pp. 54– 64;

424. Hernández-García A., Romero D., Gómez-Ramírez P., María-Mojica P., Martínez-López E., García-Fernández A. J., *In vitro* evaluation of cell death induced by cadmium, lead and their binary mixtures on erythrocytes of Common buzzard (*Buteo buteo*)", *Toxicology in Vitro*, 2014, 28, 2, pp. 300–306;
425. Deutsche Pharmakologische Gesellschaft, 1977, pp. 1-63, <https://books.google.it/books?id=bMf3CAAQBAJ&pg=PA18&lpg=PA18&dq=different+esterase+activity+in++various+cell+lines&source=bl&ots=M3hmVEAv1C&sig=KUUHDMZ5gp2THIfTz7aqEKPIgWs&hl=fr&sa=X&ei=vQxTVcvpFoGuswHwnYGoBA&ved=0CD8Q6AEwAw#v=onepage&q=different%20esterase%20activity%20in%20%20various%20cell%20lines&f=false> (eng.);
426. Robinson J. P., Bruner L. H., Bassoe C. F., Hudson J. L., Ward P. A., Phan S. H., „Measurement of intracellular fluorescence of human monocytes relative to oxidative metabolism”, *J Leukoc Biol.*, 1988, 43, 4, pp. 304-10;
427. Ertel A., Verghese A., Byers S. W., Ochs M., Tozeren A., „Pathway-specific differences between tumor cell lines and normal and tumor tissue cells”, *Molecular Cancer*, 2006, 5, 55;
428. Curtin J. F., Donovan M., Cotter T. G., “Regulation and measurement of oxidative stress in apoptosis”, *J Immunol Methods.*, 2002, 265, 1-2, pp. 49-72;
429. Robinson J. P., „Oxygen and Nitrogen Reactive Metabolites and Phagocytic Cells”, *Phagocyte Function: A Guide for Research and Clinical Evaluation*, J. Paul Robinson and George F. Babcock (ed.), ISBN O-47 1- 12364-1, <http://www.cyto.purdue.edu/archive/flowcyt/research/pdfs/oxygen%20and%20nitrogen%20oreactive%20ch9.pdf>;
430. Russo A., DeGraff W., Friedman N., Mitchell J. B., „Selective Modulation of Glutathione Levels in Human Normal versus Tumor Cells and Subsequent Differential Response to Chemotherapy Drugs”, *Cancer Res.*, 1986, 46, pp. 2845-2848;
431. Traverso N., Ricciarelli R., Nitti M., Marengo B., Furfaro A. L., Pronzato M. A., Marinari U. M., Domenicotti C., „ Role of Glutathione in Cancer Progression and Chemoresistance”, *Oxidative Medicine and Cellular Longevity*, 2013, article ID 972913;
432. Dalleau S., Baradat M., Guéraud F., Huc L., „Cell death and diseases related to oxidative stress: 4-hydroxynonenal (HNE) in the balance”, *Cell Death and Differentiation*, 2013, 20, pp. 1615–1630;
433. Klaunig J. E., Kamendulis L. M., Hoceva B. A., „Oxidative Stress and Oxidative Damage in Carcinogenesis”, *Toxicol Pathol.*, 2010, 38, 1, pp. 96-109;
434. Spadaro A., Ronsisvalle G., Pappalardo M., „Rapid Analysis of Glutathione in Human Prostate Cancer Cells (DU145) and Human Lung Adenocarcinoma Cells (A549)

- by HPLC with Electrochemical Detection”, *J. Pharm. Sci. & Res.*, 2011, 3, 12, pp. 1637-1641;
435. Serru V., Baudin B., Ziegler F., David J-P., Cals M-J., Vaubourdolle M., Mario N., „Quantification of Reduced and Oxidized Glutathione in Whole Blood Samples by Capillary Electrophoresis”, *Clinical Chemistry*, 2001, 47, 7, pp. 1321-1324;
436. Owen J. B., Butterfield D. A., „Measurement of oxidized/reduced glutathione ratio”, *Methods Mol Biol.*, 2010, 648, pp. 269-77;
437. Ahner B. A., Wei L., Oleson J. R., Ogura N., „Glutathione and other low molecular weight thiols in marine phytoplankton under metal stress”, *Marine Ecology Progress Series*, 2002, 232, pp. 93–103;
438. Hassan H. M., Fridovich I., „Mechanism of the antibiotic action pyocyanine”, *J. Bacteriol.*, 1980, 141, 1, pp. 156-163;
439. Zitka O., Skalickova S., Gumulec J., Masarik M., Adam V., Hubalek J., Trnkova L., Kruseova J., Eckschlager T., Kizek R., „Redox status expressed as GSH:GSSG ratio as a marker for oxidative stress in paediatric tumour patients”, *Oncol Lett.*, 2012, 4, 6, pp. 1247–1253;
440. Gogos C. A., Drosou E., Bassaris H. P., Skoutelis A., „Pro- versus Anti-inflammatory Cytokine Profile in Patients with Severe Sepsis: A Marker for Prognosis and Future Therapeutic Options”, *J Infect Dis.*, 2000, 181, 1, pp. 176-180;
441. Mukhopadhyay S., Hoidal J. R., Mukherjee T. K., „Role of TNF $\alpha$  in pulmonary pathophysiology”, *Respir Res.*, 2006, 7, 1, 125;
442. Miyazaki Y., Araki K., Vesin C., Garcia I., Kapanci Y., Whitsett J. A., Piguet P. F., Vassalli P., „Expression of a tumor necrosis factor-alpha transgene in murine lung causes lymphocytic and fibrosing alveolitis. A mouse model of progressive pulmonary fibrosis”, *J Clin Invest.*, 1995, 96, 1, pp. 250–259;
443. Corda S., Laplace C., Vicaut E., Duranteau J., „Rapid Reactive Oxygen Species Production by Mitochondria in Endothelial Cells Exposed to Tumor Necrosis Factor- $\alpha$  Is Mediated by Ceramide”, *Am J Respir Cell Mol Biol*, 2001, 24, pp. 762-768;
444. Armstrong L., Jordan N., Millar A., „Interleukin 10 (IL-10) regulation of tumour necrosis factor alpha (TNF-alpha) from human alveolar macrophages and peripheral blood monocytes”, *Thorax*, 1996, 51, pp. 143-149;
445. Avdiushko R., Hongo D., Lake-Bullock H., Kaplan A., Cohen D., „IL-10 receptor dysfunction in macrophages during chronic inflammation”, *Journal of Leukocyte Biology*, 2001, 70, pp. 4624-632;
446. Cavillon J.-M., „Pro- versus anti-inflammatory cytokines: myth or reality”, *Cellular and molecular biology* , 2001, 47, 4, pp. 695-702;

447. Marie C., Pitton C., Fitting C., Cavaillon J-M., „Regulation by anti-inflammatory cytokines (IL-4, IL-10, IL-13, TGF) of interleukin-8 production by LPS and/ or TNF-activated human polymorphonuclear cells”, *Mediators of Inflammation*, 1996, 5, pp. 334-340;
448. Muro S., Taha R., Tsiropoulos A., Olivenstein R., Tonnel A. B., Christodoulopoulos P., Wallaert B., Hamid Q., „Expression of IL-15 in inflammatory pulmonary diseases”, *J Allergy Clin Immunol.*, 2001, 108, 6, pp. 970-5;
449. Wilmes A., Bielow C., Ranninger C., Bellwon P., Aschauer L., Limonciel A., Chassaing H., Kristl T., Aiche S., Huber C. G., Guillou C., Hewitt P., Leonard M. O., Dekant W., Bois F., Jennings P., „Mechanism of cisplatin proximal tubule toxicity revealed by integrating transcriptomics, proteomics, metabolomics and biokinetics”, *Toxicol In Vitro*, 2014, 14, pp. S0887-2333;
450. Smith C. A., Want E. J., O'Maille G., Abagyan R., Siuzdak G., „XCMS: Processing Mass Spectrometry Data for Metabolite Profiling Using Nonlinear Peak Alignment, Matching, and Identification”, *Anal. Chem.*, 2006, 78, pp. 779–787;
451. Kuhl C., Tautenhahn R., Böttcher C., Larson T. R., Neumann S., „CAMERA: An Integrated Strategy for Compound Spectra Extraction and Annotation of Liquid Chromatography/Mass Spectrometry Data Sets”, *Anal. Chem.*, 2012, 84, pp. 283–289;
452. Wishart D. S., Knox C., Guo A. C., Eisner R., Young N., Gautam B., Hau D. D., Psychogios N., Dong E., Bouatra S., Mandal R., Sinelnikov I., Xia J., Jia L., Cruz J. A., Lim E., Sobsey C. A., Shrivastava S., Huang P., Liu P., Fang L., Peng J., Fradette R., Cheng D., Tzur D., Clements M., Lewis A., De Souza A., Zuniga A., Dawe M., Xiong Y., Clive D., Greiner R., Nazyrova A., Shaykhtudinov R., Li L., Vogel H. J., Forsythe I., „HMDB: a knowledgebase for the human metabolome”, *Nucleic Acids Res.*, 2009, 37, pp. D603–610;
453. Sumner L. W., Amberg A., Barrett D., Beale M. H., Berger R., Daykin C. A., Fan T. W.-M., Fiehn O., Goodacre R., Griffin J. L., Hankemeier T., Hardy N., Harnly J., Higashi R., Kopka J., Lane A. N., Lindon J. C., Marriott P., Nicholls A. W., Reilly M. D., Thaden J. J., Viant M. R., „Proposed minimum reporting standards for chemical analysis Chemical Analysis Working Group (CAWG) Metabolomics Standards Initiative (MSI)”, *Metabolomics*, 2007, 3, pp. 211–221;
454. Dunn W. B., Erban A., Weber R. J. M., Creek D. J., Brown M., Breitling R., Hankemeier T., Goodacre R., Neumann S., Kopka J., Viant M. R., „Mass appeal: metabolite identification in mass spectrometry-focused untargeted metabolomics”, *Metabolomics*, 2013, 9, pp. S44-S66;
455. Creek D. J., Dunn W. B., Fiehn O., Griffin J. L., Hall R. D., Lei Z., Mistrik R., Neumann S., Schymanski E. L., Sumner L. W., Trengove R., Wolfender J.-L., „Metabolite identification: are you sure? And how do your peers gauge your confidence?” *Metabolomics*, 2014, 10, pp. 350–353;

456. Babiuk C., Steinhagen W. H., Barrow C. S., „Sensory irritation response to inhaled aldehydes after formaldehyde pretreatment”, *Toxicol Appl Pharmacol.*, 1985, 79, 1, pp. 143-9;
457. Ursini C. L., Cavallo D., Fresegna A. M., Ciervo A., Maiello R., Buresti G., Casciardi S., Bellucci S., Iavicoli S., „Differences in Cytotoxic, Genotoxic, and Inflammatory Response of Bronchial and Alveolar Human Lung Epithelial Cells to Pristine and COOH-Functionalized Multiwalled Carbon Nanotubes”, *Biomed Res Int.*, 2014, 359506;
458. Kozak W., Conn C. A., Kluger M. J., „Lipopolysaccharide induces fever and depresses locomotor activity in unrestrained mice”, *Am J Physiol.*, 1994, 266, pp. R125-35;
459. Bakand S., Winder C., Khalil C., Hayes A., „An experimental in vitro model for dynamic direct exposure of human cells to airborne contaminants”, *Toxicology Letters*, 2006, 165, pp. 1–10;
460. Geiss O., Giannopoulos G., Tirendi S., Barrero-Moreno J., Larsen B. R., Kotzias D., „The AIRMEX Study-VOC measurements in public buildings and schools/kindergartens in eleven European cities: statistical analysis of the data”, *Atmos Environ.*, 2011, 45, pp. 3676–84;
461. Huang Yu, Ho Kin Fai, Ho Steven Sai Hang, Lee Shun Cheng, Yau P.S., Cheng Yan, „Physical parameters effect on ozone-initiated formation of indoor secondary organic aerosols with emissions from cleaning products”, *Journal of Hazardous materials*, 2011, 192, pp. 1787–1794;
462. Saathoff H., Naumann K.-H., Möhler O., Jonsson A. M., Hallquist M., Kiendler-Scharr A., Mentel Th. F., Tillmann R., Schurath U., „Temperature dependence of yields of secondary organic aerosols from the ozonolysis of  $\alpha$ -pinene and limonene”, *Atmos. Chem. Phys.*, 2009, 9, pp. 1551–1577;
463. Larsson O., Zetterberg A., Engstrom W., „Consequences of parental exposure to serum-free medium for progeny cell division”, *J. Cell Sci.*, 1985, 75, pp. 259-268;
464. Smith K. R., Veranth J. M., Hu A. A., Lighty J. S., Aust A. E., „Interleukin-8 levels in human lung epithelial cells are increased in response to coal fly ash and vary with the bioavailability of iron, as a function of particle size and source of coal”, *Chem Res Toxicol.*, 2000, 13, 2, pp. 118-25;
465. Goossens V., Grooten J., De Vos K., Fiers W., „Direct evidence for tumor necrosis factor-induced mitochondrial reactive oxygen intermediates and their involvement in cytotoxicity”, *Proc Natl Acad Sci U S A.*, 1995, 92, pp. 8115–8119;
466. Talley A. K., Dewhurst S., Perry S. W., Dollard S. C., Gummuluru S., Fine S. M., New D., Epstein L. G., Gendelman H. E., Gelbard H. A., „Tumor Necrosis Factor Alpha-

Induced Apoptosis in Human Neuronal Cells: Protection by the Antioxidant N-Acetylcysteine and the Genes bcl-2 and crmA”, *Molecular and cellular biology*, 1995, pp. 2359–2366;

467. Hiromatsu T., Yajima T., Matsuguchi T., Nishimura H., Wajjwalku W., Arai T., Nimura Y., Yoshikai Y., „Overexpression of Interleukin-15 Protects against Escherichia coli-Induced Shock Accompanied by Inhibition of Tumor Necrosis Factor- $\alpha$ -Induced Apoptosis”, *The Journal of Infectious Diseases*, 2003, 187, pp. 1442–51;

468. Bosnjak B., Stelzmueller B., Erb K. J., Epstein M. M., „Treatment of allergic asthma: Modulation of Th2 cells and their responses”, *Respiratory Research*, 2011, 12, 114;

469. Shankaranarayanan P., Nigam S., „IL-4 induces apoptosis in A549 lung adenocarcinoma cells: evidence for the pivotal role of 15-hydroxyeicosatetraenoic acid binding to activated peroxisome proliferator-activated receptor gamma transcription factor”, *J Immunol.*, 2003, 170, 2, pp. 887-94;

470. Sadowska A. M., van Overvelda F. J., Góreckab D., Zdralc A., Filewskac M., Demkowc U. A., Luytena C., Saenena E., Zielinskib J., De Backer W. A., „The interrelationship between markers of inflammation and oxidative stress in chronic obstructive pulmonary disease: modulation by inhaled steroids and antioxidant”, *Respiratory Medicine*, 2005, 99, pp. 241–249.